STUDIES OF GROWTH RATES OF SOME
FRESHWATER CRYPTOPHYTE ALGAE

by

Anne Ojala

A Doctoral Thesis

Submitted in partial fulfilment of the requirements
for the award of Doctor of Philosophy of the Loughborough
University of Technology

June 1991

ACKNOWLEDGEMENTS

ABSTRACT

STUDIES OF GROWTH RATES OF SOME FRESHWATER CRYPTOPHYTE ALGAE
Anne Ojala
Ph.D
June, 1991

Cryptophytes are free–living unicellular algae which are important for the productivity and food chain dynamics of temperate lakes. This study provides fundamental information on the ecophysiology of some freshwater cryptophytes of different cell size, mainly in terms of growth and related factors.This thesis comprises of six chapters, three of which describe light or light–and–temperature experiments with small–scale batch cultures (Chapters 2 to 4), one depicts a larger scale laboratory experiment simulating natural conditions (Chapter 5) and the two last (Chapters 6 and 7) are based on short–term investigations *in situ*.

The effects of light and temperature on nutrient–saturated growth and cellular composition (chlorophyll *a*, proteins, carbohydrates) were studied in batch cultures. With the help of mathematical models, the physiological basis for interspecific differences of growth response was determined (Chapter 2). The cryptophyte strain L315 appeared to be a cold–water species as its optimum temperature was *ca.* 19 °C. The strain L485 was more adapted to warm–water conditions with its optimum of *ca.* 24.5 °C. In respect of their growth response to irradiance, L485 can be said to be a stenotopic and L315 a eurytopic strain, as L485 shows photoinhibition soon after saturation point, whereas L315 tolerates a much wider range of irradiance. The role of changes in cellular composition is discussed. In order to explain the observed growth differences the effects of light and temperature on gross photosynthesis, respiration and hence net productivity were studied (Chapter 3). The observed respiration/photosynthesis ratios were high, as in L485 and L315 respiration accounted for 17–77 % and 14–81 % of gross photynthesis, respectively. Under optimum conditions the respiration/P_{max} for L485 was 17 % and for L315 58 %. The response of cryptophytes to chromatic light was studied by means of quantitative epifluorescence microscopy and it was found that in comparison to blue–green algae cryptophytes L485 and L315 do not gain such great adaptational advantages in terms of growth by chromatic adaptation (Chapter 4). The modest role of chromatic adaptation is discussed.

The role of diel vertical migrations (DVM) in the growth of cryptophytes was studied in 4 m tall experimental columns (Chapter 5). Results revealed that by migrating into cooler, nutrient rich hypolimnion flagellated cryptophytes can increase their growth rate under conditions where resources (light and nutrients) are spatially separated for prolonged time periods. This study also emphasizes the need for more detailed DVM studies *in situ*.

Finally, the pattern and timing of nuclear and cellular division in two *Cryptomonas* species *in situ* was studied by means of mitotic index technique (Chapter 6) and DNA quantification (Chapter 7). The nuclear division of *Cryptomonas* L485 (Chapter 6) appeared to be well phased, but as in this division pattern mitosis and cytokinesis were totally overlapping, it was impossible to calculate *in situ* growth rates. Field observations (Chapter 7) revealed that DNA quantification by means of epifluorescence microscopy is possible from a natural cryptophyte population, but as the *Cryptomonas* sp. population under scrutiny was not well phased, growth rate calculation could not be carried out.

The survival strategies of Cryptophytes L485 and L315 in terms of r vs. K strategies are discussed in Chapter 8. It is pointed out that, although the habitats occupied by these strains as well as some of their morphological and physiological features indicate that L485 is probably a r–strategist and L315 a K–strategist, it is not possible to draw final conclusions on the basis of this study. Light and temperature, i.e. the factors mostly studied in this thesis, are presumably not the environmental factors of greatest selective importance for these cryptophytes in natural competitive situations.

Keywords: Cryptohytes, growth, productivity, accessory pigments, vertical migrations, mitotic pattern

TABLE OF CONTENTS   Page

Chapter 1

INTRODUCTION

1 INTRODUCTION

The cryptophytes are a taxonomically well–defined group of free–living unicellular algae with a wide size range (*ca*. 3–50 µm in length). In botany they are assigned to class level (Cryptophyceae) or division level (Cryptophyta), whereas zoologists classify them into an order (Cryptomonadida) within the class Phytomastigophorea (Klaveness 1988 and references therein). Due to the two haired flagella of equal or subequal length (Lucas 1970, Hibberd et al. 1971, Klaveness 1981), they are highly motile, although non–motile palmelloid phases have also been recorded (Santore 1978, references in Klaveness 1985). Cells of cryptophytes are asymmetric in shape resembling a slipper or bean and often dorsiventrally flattened. Besides the general cell form, the ventral depression–furrow–gullet system and the periplast structure have been regarded as the most important features in species determination (Faust 1974, Santore 1977, Munavar & Bistricki 1979, Klaveness 1981, Hill & Wetherbee 1989). Unique morphological features also include specialized ex-trusive organelles called ejectosomes or trichocysts, which are presumed to be used for direct defence (Lucas 1970, Gantt 1980). The cryptophytes also possess lyso-some–type structures called Maupas' ovals ("Corps–de–Maupas") which have been suggested to have a phagocytic function (Lucas 1970, Gantt 1980, Anton & Duthie 1981).

It is widely accepted that cryptophytes have just one chloroplast, possibly with a narrow bridge between the two separate lobes (Pringsheim 1968, Gantt 1980), although Anton & Duthie (1981), Santore (1984) and, more recently, Hill & Wetherbee (1989) have been of the opinion that there are two chloroplasts at least in some species in the genera *Cryptomonas* and *Rhodomonas*. Figure 1.1 depicts the general morphology and outlook of a cryptophyte cell as decribed by Santore (1984). As in other algae, the major photosynthetic pigment is chlorophyll *a*, but the cryptophytes also possess chlorophyll c_2 and phycobiliproteins as accessory pigments. The phycobiliproteins are uniquely situated in the intrathylakoidal spaces of photosynthetic lamellae (Lichtlé et al. 1987). Absence or presence of pyrenoids
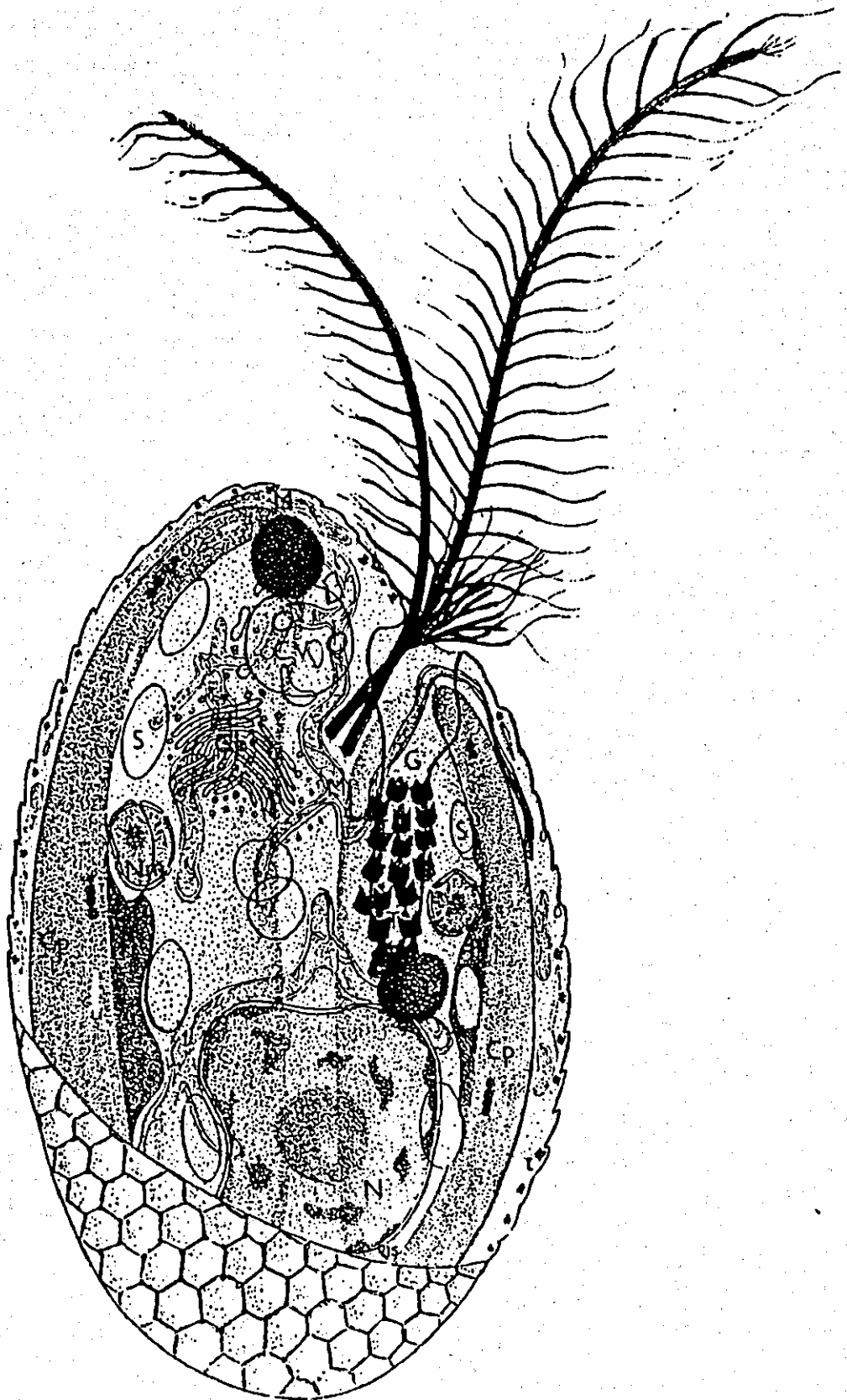
Fig. 1.1. Drawing of a member of the genus *Cryptomonas* (*Cryptomonas ovata*) by Santore (1984). Abbreviations: C$_p$, chloroplast; CV, contractile vacuole; G, gullet; Go, Golgi body; L, lipids; Ly, lysosomal vesicles; M, mitochondria; ni, microbody; N, nucleus; Nm, nucleomorph; P, pyrenoid; S, starch; T, gullet; t, peripheral trichocyst.

within the chloroplasts is of great value in generic taxonomy (Anton & Duthie 1981, Klaveness 1985).

Sexual stages have rarely been discovered (Wawrik 1980) and reproduction mainly occurs as a binary division of the vegetative cell (Oakley & Bisalputra 1977, Ward & Bowen 1979, Hill & Wetherbee 1989). Under unfavourable environmental conditions some cryptophytes can differentiate into a resistant form and turn into a cyst, which allows a survival period. When favourable conditions return, the excystment process occurs (Huber–Pestalozzi 1968, Heynig 1976, Lichtlé 1979, 1980, Lichtlé & Dubacq 1984, Klaveness 1985).

Despite their overall group homogeneity, the generic taxonomy of cryptophytes has not been satisfactorily resolved, and the boundaries between species are still ill–defined. Problems in identification arise often from the small cell size and the delicate nature of the cryptophyte cells, that make standard algal sampling and preservation procedures unsuitable for these organisms. The fundamental problem, however, is speciation in apparently asexual organisms. After a thorough reexamination of the cryptophyte genera, the total number of valid species is likely to drop from the present *ca*. 100 (Klaveness 1988), when dozens of ecotypes and local variants will find their right taxonomic place.

The lack of conspicuous morphological features applicable to practical species identification by routine light microscopy has led to numerous ecological studies in which cryptophytes are classified merely as undetermined flagellates. Despite this major inaccuracy the significance of these cosmopolitan algae for the productivity and food chain dynamics in freshwaters is now becoming more and more evident. At least intermittent dominance of phytoplankton communities by one or more species of cryptophytes is common, and especially frequent in temperate freshwater lakes regardless of their trophic status (e.g. Schnee 1976, Stewart & Wetzel 1986, Klaveness 1988 and references therein). Information on their importance in nothern European humic lakes has been accumulating quite recently (Ilmavirta 1983, Arvola 1984, Ahtiainen et al. 1985, Arvola et al. 1986, Eloranta 1986, Arvola et al. 1987). These algae often increase in numbers most rapidly immediately following declines of other dominant algal forms and a generalised phytoplankton seasonal successional

pattern, completed with the cryptophyte–microflagellate complex, has thus been presented as in Fig. 1.2 (Stewart & Wetzel 1986). Cryptophytes are also of high nutritive value to herbivorous zooplankton and the whole food chain (e.g. Skogstad et al. 1987). According to Stewart & Wetzel (1986) these special features give an essential role to cryptophytes and other microflagellates in dampening oscillations in energy transfer, diverting energy from detrital pathways and enhancing overall ecosystem efficiency. They have also stated that a system dominated by microflagellates is relatively unstructured and behaves in a very fluid manner, thus responding opportunistically to small alterations in the biota and abiotic environment.

Relative to the knowledge of morphology and ever–increasing information on synecology of cryptophytes, very little is known about their autecology and ecophysiology. Studies on pigmentation chemistry and physiology (MacColl et al. 1986, Thinh 1983, Kamiya & Miyachi 1984a, 1984b, Rhiel et al. 1989) as well as physiology and mechanisms of photoorientation (Watanabe & Furuya 1974, Watanabe et al. 1976, Uematsu–Kaneda & Furuya 1982a,b, Watanabe & Furuya 1982, Häder 1987, Rhiel et al. 1988, Häder & Häder 1989, 1990) have generally used cultured species, but autecological and ecophysiological studies, both *in situ* and *in vitro*, are still scarce (Morgan & Kalff 1975, 1979, Bowen & Ward 1977, Cloern 1977, 1978, Gavrieli 1984, Braunwarth & Sommer 1985, Pedrós-Alió et al. 1987). Klaveness (1988) indicated the gaps in knowledge of nutritional physiology and ecology, light and temperature adaptation, and in assessment of the nutritional value of cryptophytes for zooplankton.

This study provides fundamental information on the ecophysiology of ~~some~~ two freshwater cryptophytes, mainly in terms of growth and related factors. Because of the taxonomical difficulties, no attempt was made to identify the cryptophytes employed. However, they are here described and, where possible, designated by culture collection code numbers. This thesis comprises of six chapters, three of which describe light or light–and–temperature experiments with small–scale batch cultures, one depicts a larger scale laboratory experiment simulating natural conditions and the last two are based on short–term investigations *in situ*. A special effort was made to use recent or fairly recent isolates in laboratory experiments, as
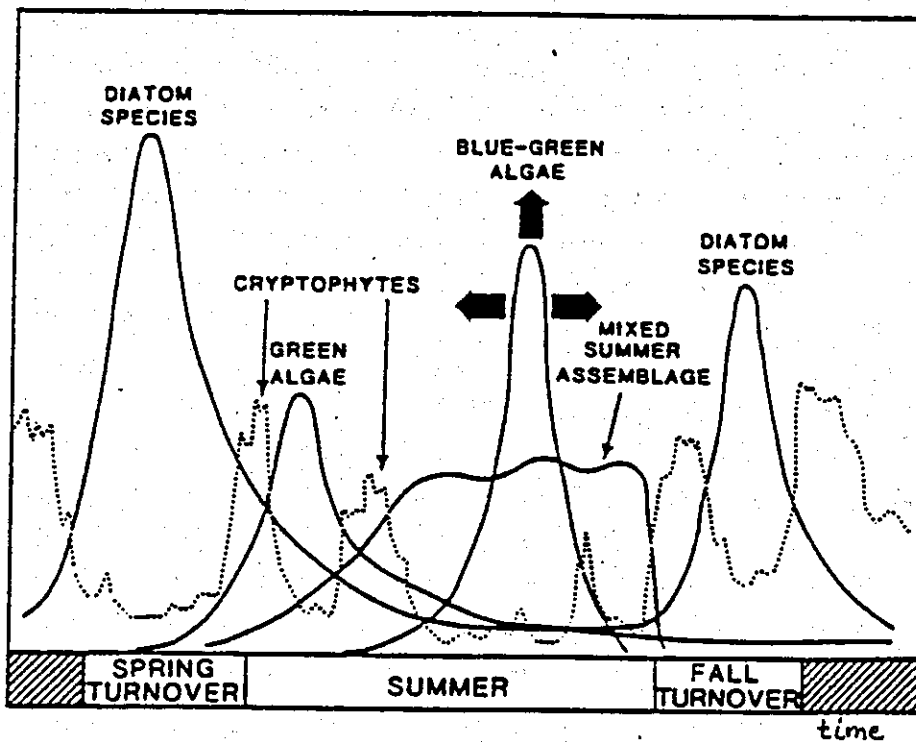
Fig. 1.2. A model of phytoplankton successional pattern incorporating seasonal fluctuations of the cryptophyte–microflagellate complex (Stewart & Wetzel 1986).

failure to do so has been regarded as a problem (Klaveness 1988). Arvola (unpubl. data) noticed that the cryptophyte *Rhodomonas minuta* var. *nannoplanctica* had lost its natural ability to grow at temperatures below 15 °C after being held in culture for 20 years.

Chapter 2

EFFECTS OF TEMPERATURE AND IRRADIANCE ON THE GROWTH OF TWO FRESHWATER CRYPTOPHYTES

2.1 INTRODUCTION

There has been a continual interest amongst phytoplankton ecologists in understanding physiological adaptations of algae to their environment, especially to irradiance and temperature. Judging merely from the amount of published data, light has been regarded as the more important factor of these two (e.g. reviews by Richardson et al. 1983 and Raven & Geider 1988). Phytoplankton growth has even been suggested to be predominantly light limited (Tett et al. 1985), since the cellular composition of slowly growing algae *in situ* has been found to be similar to ratios found in laboratory cultures under conditions of non–limiting nutrient concentrations (Goldman et al. 1979). The overriding importance of light has also been shown by accurately predicting primary production from information on light and pigment concentrations alone (Marra & Heinemann 1987).

Experiments carried out with unialgal cultures under controlled laboratory conditions have revealed substantial interspecific differences in the three parameters characterizing the typical μ *vs* I curves (Fig. 2.1). Maximum growth rates (μ_{max}) of algae range from the modest values of 0.30 divisions day^{-1}, or even lower, found in dinoflagellates to an amazing rate of 11.6 divisions day^{-1} recorded for a blue–green alga, *Anacystis nidulans* (for a review, see Reynolds 1984). Interspecific differences in light adaptation can be seen in varying compensation light intensities (I_c), (i.e. in the lowest photon flux densities supporting net growth), and in growth efficiencies (α_g), which characterize the slope of the μ *vs* I curve and hence the capability of the alga to exploit photons of light at suboptimal densities. For a dinoflagellate, *Gonyaulax tamarensis*, I_c has been recorded as 35 μmoles m^{-2}s^{-1} and for a diatom, *Phaeodactylum tricornutum*, as only 0.75 μmoles m^{-2} s^{-1} (Geider et al. 1986, Langdon 1987). The variability of α_g can be as high as 123– fold, ranging from 0.51 x 10^{-3} div. day^{-1} (μmoles m^{-2} s^{-1})$^{-1}$ for a dinoflagellate, *Prorocentrum micans* to 63 x 10^{-3} div. day^{-1} (μmoles m^{-2} s^{-1})$^{-1}$ for a chlorophyte, *Chlorella pyrenoidosa* (Bannister 1979, Falkowski et al. 1985b, Langdon 1988).

The effects of temperature have not gained such a widespread research interest as irradiance, as traditionally temperature has not been regarded as a major determinant
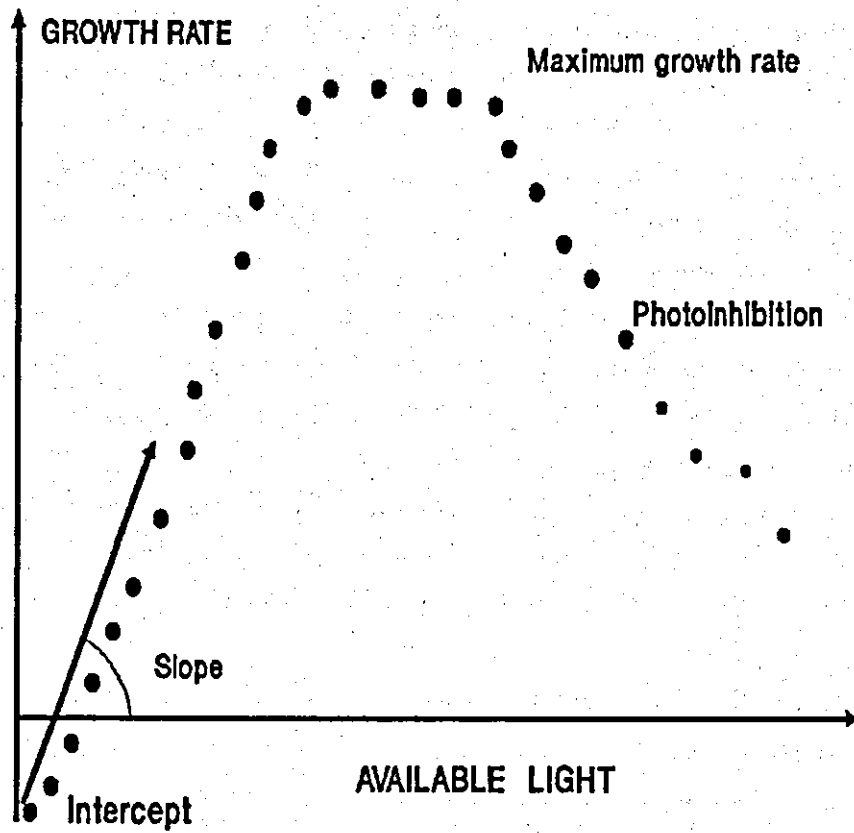
Fig. 2.1. A generalized growth vs. irradiance (μ vs. I) curve and the parameters characterizing it.

of phytoplankton growth in oceans and lakes (Steemann Nielsen 1960). However, almost two decades ago Eppley (1972) showed that temperature is important to phytoplankton production ecology as, if no other factors are limiting, temperature sets an upper limit for growth and photosynthesis. Eppley's (1972) famous temperature envelope demonstrates that for unicellular photosynthetic algae as a group, growth rate increases with temperature up to 40 °C and the upper limit of algal growth rate at a given temperature can be described with a logistic curve. Studies on temperature and irradiance as independent variables have been made (e.g. Sakshaug & Andresen 1986, Langdon 1987) but are of limited value in efforts to reveal the complementary interactions of both factors on algal growth. These interactions cannot be satisfactorily explained simply by multiplying independent temperature and irradiance functions (cf. Nicklisch & Kohl 1983, Feuillade & Feuillade 1987); a mathematical model based on combined temperature–irradiance experiments is needed.

This chapter describes the effects of light and temperature on nutrient–saturated growth and cellular composition (chlorophyll a, proteins, carbohydrates) of two freshwater cryptophytes of different cell size. This comparison seeks to determine, with the help of a mathematical model, the physiological basis for interspecific differences of growth response in relation to light and temperature. There have only been three previous comprehensive studies on light and temperature interactions on growth of some cryptophytes (Cloem 1977, Morgan & Kalff 1979, Gavrieli 1984) and the otherwise thorough reviews by Richardson et al. (1983) and Raven & Geider (1988) on the effects of irradiance and temperature on planktonic algae almost completely lack information on cryptophytes.

2.2 METHODS

Figs 6.3; 7.3

The experimental organisms (Fig. 2.2) obtained from the Culture Collection of Algae and Protozoa (CCAP), UK. were isolated by Mr. G. Jaworski. These two clonal *Cryptomonas* strains were unialgal, but not axenic. However, microscopical examination of exponentially growing cultures revealed few bacterial cells. The

a)

b)

Fig. 2.2. SEM micrographs of (a) L485 and (b) L315. Scale bar = 1.0 μm. Micrographs were taken by K. Clarke (cf. Arvola et al. 1991).

larger *Cryptomonas* strain L315 (volume *ca.* 5 000 –9 000 μm³) was isolated from Priest Pot, a hypertrophic pond in the English Lake District, and has been in culture since 1979. The smaller *Cryptomonas* strain L485 (volume *ca.* 500 – 900 μm³) was isolated in 1987 from Vähä–Valkjärvi, a clearwater acidic forest lake in southern Finland. Both of the strains were grown in a modification of Diatom Medium (DM) (Beakes et al. 1988; Table 2.1). The original pH 7.5 of the medium suited L315 well, but for the acidophilic L485 pH was lowered to 3.8–4.0 with 0.1 N HCl. The experimental cultures were grown in 150 ml of medium in cotton wool or foamed plastic– stoppered 250 ml conical flasks without continuous shaking or aeration, as experience showed that these strains would not thrive under artificial stirring (cf. Ahlgren 1987, Langdon 1987). At the beginning of experiments flasks were inoculated from stock cultures (T = 20–21 °C) in log growth to give a cell density of *ca.* 400 cells ml⁻¹ for L485 and *ca.* 40 cells ml⁻¹ for L315 and were thereafter placed in experimental conditions. As the maximum cell densities sustained in DM medium were 10^5 cells ml⁻¹ and 10^4 cells ml⁻¹ for L485 and L315 respectively, cultures of both species could undergo 8 divisions before reaching stationary phase. Experiments were conducted either in growth cabinets or water–filled glass tanks (temperatures ≤10 °C). The light source was provided by cool–white fluorescent tubes. Light intensities as photon flux densities (PFD) were measured at the base of the cultures either with a 2π planar (Li–Cor Inc., model LI–185 B) or a 4π spherical digital scalar quantum meter (Biospherical Instruments Inc., model number QSP–170, probe QSP–200). In the case of the 2π design probe, both the downward flux and the upward flux were measured and the readings summed to give a better estimate of total available PFD. The use of a quantum meter and the expression of light in quanta (μmoles) (and not in units of illumination or energy) in investigations of phytoplankton photoadaptation is recommended (Richardson et al. 1983). The PFDs received by the algae were modified when necessary with neutral density screening.

For the light–temperature experiments, cultures were incubated under a 16:8 h light–dark (LD) cycle at a range of PFDs (5 different photon flux densities at each temperature) at 26, 21, 16, 12, 10, 8 (L485 only) and 5 °C. Light–dark periodicity was chosen as cryptophytes have been shown to grow better under a photoperiod

Table 2.1. Composition of modified DM culture medium

Substance	$g\ l^{-1}$ in stock solution/ $mg\ l^{-1}$ in final culture medium
1. $Ca(NO_3)_2 * 4H_2O$	20
2. KH_2PO_4	6.2
3. $MgSO_4 * 7H_2O$	25
4. $NaHCO_3$	15.88
5. K_2SiO_3	35
6. $EDTA.Fe.Na$	2.27
7. H_3BO_3	2.48
$MnCl_2.4H_2O$	1.39
$(NH_4)_6Mo_7O_{24} *4H_2O$	1.00
8. Cyanocobalamin (B_{12})	0.02
Thiamine (B_1)	0.02
Biotin	0.02
9. $EDTA\ Na_2$	2.24

One ml of stocks were added to 1 litre deionised water for the required concentration. The medium was sterilized by autoclaving. Filter sterilized (0.2 μm) $NaHCO_3$ (4) and vitamins (8) were added to the sterilized medium.

(Bowen & Ward 1977). Such a long light period was chosen to simulate the long spring and summer days of the temperate zone and especially the boreal region, a procedure regarded as especially important for L485 of Finnish origin. All experiments were carried out with 4–5 parallel cultures and population growth was measured by periodically taking samples of 3–4 ml to estimate cell density, either by sedimenting 0.3 ml subsamples in small plastic cuvettes or by using Lund chambers (Lund 1959). Samples were always taken during the light period and preserved with Lugol's iodine solution. In order to reduce the effects of slightly varying environmental conditions in different parts of growth cabinets and tanks, the locations of flasks were changed randomly at every sampling. Microscopes used in counting of sedimented samples were Zeiss IM 35 Photo–Invertoscope (40x) and Leitz Diavert Inverted Microscope (40x); for counts with Lund chambers Wild M20 EB (20x) and Zeiss Standard 16 (10 x) microscopes were used.

The effects of the length of photoperiod on growth was determined in one experiment with a 12:12 LD cycle at 21 °C using L485. In addition an experiment with different light and dark period temperatures (22 °C during light period and 12 °C during dark period) was undertaken with L315 to reveal the growth response under thermal conditions more closely resembling the natural environment.

In all experiments growth was followed from the very beginning, including the possible lag phase of the acclimation period, till the end of the exponential growth phase. Growth rates were calculated by a least–square fit of a straight line to logarithmically transformed data as described by Guillard (1973). Cell concentrations determined on at least three separate sampling occasions 1–3 days apart were used for the regression calculations. The slope of the regression line (the regression coefficient), is the mean cell division rate. Results were expressed as divisions day^{-1}.

Cell volumes at each temperature–irradiance combination were determined with an ocular micrometer attached either to Leitz Diavert Inverted Microscope (40x) or Wild M20 microscope (40x). Calculations were based on the geometric formula $V = (\pi * l * b^2)/6$, where b is breadth and l length of the cell (Sicko–Goad et al. 1977). These parameters were determined for 25 cells from each flask giving an average

total of 100–125 measured cells for every treatment. Measurements were made on samples taken at the end of the exponential growth phase; in some cases these samples were accidentally destroyed before volume measurements could be made, in which case the second last samples were used. Volumes were not converted to carbon (see e.g. Strathmann 1967), as results by Morgan & Kalff (1979) revealed *Cryptomonas* cell carbon to vary with environmental conditions. The use of a conversion factor would only add an extra element of uncertainty to the results.

For chlorophyll *a*, protein and carbohydrate analyses, samples were taken at the end of the exponential growth phase; earlier harvesting would have resulted in samples not containing enough cells for quantitative analysis. However, in some experiments samples were too sparse for analysis. To avoid problems from possible phasing of cell division or from differences between light and dark cells, all samples were taken a couple of hours after the onset of the light period and frozen if not analyzed immediately. Two different methods of harvesting were used. In experiments with *Cryptomonas* L315 at temperatures 12, 16, 21 °C and 22 °C/12 °C and L485 at temperature 16 °C, cells were harvested by centrifuging 30 ml of cell suspension at 3 500 rpm for 5 min and carefully siphoning off the supernatant so that only the pellet and 5 ml of medium was left. This 5 ml concentrate was then used for analysis. In all the other experiments cells were harvested by filtering a known volume (10–15 ml) of culture on to a pre–ashed Whatman GF/F filter (450 °C, at least 3 h). Regardless of the harvesting methods protein and carbohydrate samples from every flask were replicated.

Protein was measured with the Folin–Ciocalteu reagent (Herbert et al. 1971), but sodium potassium tartrate was replaced with sodium citrate in order to avoid precipitation (Oliver & Walsby 1984). Optical density, after centrifugation in case of samples filtered on to GF/F filters, was measured at 750 nm with either a PYE Unicam spectrophotometer or a Shimadzu UV–150–02 double beam spectrophotometer. Blanks were subtracted from each sample value. Proteins used in preparing the standard curve were either casein (experiments with L315 at 12, 16, 21 °C and 22 °C/12 °C, and with L485 at 16 °C) or bovine albumin (all the other experiments) so that results are casein or albumin equivalents.

Particulate carbohydrate was measured by the phenol–sulphuric acid method (Herbert et al. 1971). This is more sensitive than the widely used anthrone method. Optical density, after centrifugation in case of samples filtered on to GF/F filters, was measured spectrophotometrically at 480 nm, which gave higher readings than the other possible wavelength of 488 nm. The former is said to measure pentoses and the latter hexoses (Dubois et al. 1956). The inclusion of 480 nm readings means that the carbohydrate concentrations are maximum values. Blanks were subtracted from each sample value. D–glucose was used as a standard so that carbohydrates are glucose equivalents.

For chlorophyll a determination at least 50 ml of sample was filtered onto a 4.7 cm Whatman GF/C glass fibre filter. Pigments were extracted using 90% alkaline acetone (Wetzel & Likens 1979) and the procedure was completed by grinding the cells with a pestle and mortar. Extinction coefficient of pigment extracts were measured spectrophotometrically and results calculated using the trichromatic equations of Strickland & Parsons (1968).

2.3 RESULTS

2.3.1 Growth rates and light requirements

Of the 35 light–temperature combinations at the 16:8 LD cycle tried with L485, 34 resulted in significant growth. One combination, $I = 26$ µmoles m^{-2} s^{-1}, $T = 5$ °C, produced no growth at all and the inoculated cells finally died. Calculated growth rate, or mortality rate, was a mean of four replicates -0.1025 halvings day^{-1}. With L315, 25 of the 30 experimental light–temperature treatments tested resulted in growth. None of the chosen photon flux densities at $T = 26$ °C gave significant growth and the cells actually died so quickly that sufficient sampling for growth or mortality measurements was impossible. Repetition of this experiment confirmed that 26 °C is lethal to L315.

The growth results presented here are first analyzed as described by Cloern (1977) for *Cryptomonas ovata* var. *palustris*, Gavrieli (1984) for *Rhodomonas lacustris* and Feuillade & Feuillade (1987) for *Oscillatoria rubescens* using Steele's (1965) empirical relation between growth rate and irradiance:

$$\mu = \mu_{max} * I/I_{opt} * \exp(1 - I/I_{opt}), \qquad (1)$$

where μ is observed growth rate at photon flux density I, μ_{max} is maximum growth rate, I_{opt} is the PFD at which $\mu = \mu_{max}$. As this relation assumes that μ is zero only at zero photon flux density, no experiments giving negative growth rates could be included in this analysis.

The ability of algal cells to change their light requirements in response to temperature is taken into account by assuming that the two parameters μ_{max} and I_{opt} both vary with temperature:

$$\mu = \mu_{max}(T) * I/I_{opt}(T) * \exp[1 - I/I_{opt}(T)], \qquad (2)$$

Temperature dependence of these parameters was described by a function derived by, Logan et al. (1976):

$$\gamma(T) = \alpha * [\exp(\beta * T) - \exp(\beta * T_m - t)], \qquad (3)$$
$$t = (T_m - T)/\Delta T, \qquad (4)$$

where α is a rate of the temperature–dependent process at some basal temperature, β can be intepreted as a composite Q_{10} value for critical biochemical reactions, T_m is a thermal maximum or an upper lethal temperature, ΔT is the temperature range over which, according to Logan et al. (1976), 'thermal breakdown' becomes the overriding influence.

To overcome the possible drawbacks caused from the assumption of Steele's (1965) curves passing through the origin, another well known empirical function, the hyperbolic tangent function of Platt & Jassby (1976), was fitted to the data. This enables the estimation of species specific compensation points (I_c) and growth

efficiencies (α_g). Due to the less restrictive assumptions of this model, the negative growth rates of L485 at 5 °C could be included in this analysis. The function is as follows:

$$\mu = \mu_{max} * \text{Tanh} \, [\alpha_g * (I - I_c)/\mu_{max}], \qquad (5)$$

where μ is observed growth rate at photon flux density I, μ_{max} is the maximum growth rate, α_g is the initial slope (i.e. growth efficiency), I_c is the X–axis intercept or the compensation irradiance and Tanh is the hyperbolic tangent function.

These models were fitted to the experimental data using a computer program written by Dr. I.Hakala (University of Helsinki, Lammi Biological Station) based on the geometrical and iterative Simplex algorithm (Caeci & Cacheris 1984), whereby the parameters of the functions were estimated.

Observed growth rates as a function of irradiance for each experimental temperature are shown in Figs 2.3 and 2.4. Also shown are the fitted Steele's (1965) and hyperbolic tangent functions. Coefficients of variation (c.v.) of the growth rates were usually well below 10 %, but at the lowest PFDs and at 5 °C there was a tendency to increasing c.v. values up to 30 %. Values of maximum growth rates (μ_{max}) and the corresponding optimum PFD (I_{opt}) are displayed in Tables 2.2 and 2.3 for L485 and L315, respectively. Maximum growth rates were estimated by using both of the models, whereas optimum PFD was given only by Steele's (1965) function.

Fig. 2.3 shows that for L485 the relationship between growth rate and irradiance at all temperatures is well described by Steele's (1965) equation, as this species exhibits light inhibition of growth at higher PFDs. At lower temperatures this inhibition was more pronounced and the saturation curve had a stronger flexure. However, at temperatures 26, 21 and 12 °C it is obvious that the assumption of the curve going through origin is not a correct one as at these temperatures the observed growth rates at lowest PFDs always fell below the fitted curve. Thus, the hyperbolic tangent function gives a better adjustment at limiting PFDs, i.e. in the ascending part of the growth *vs* irradiance curve. At low temperatures the adjustment to the hyperbolic

e)

Growth rate (div. day^{-1})

PFD (μmoles m^{-2}s^{-1})

f)

Growth rate (div. day^{-1})

PFD (μmoles m^{-2}s^{-1})
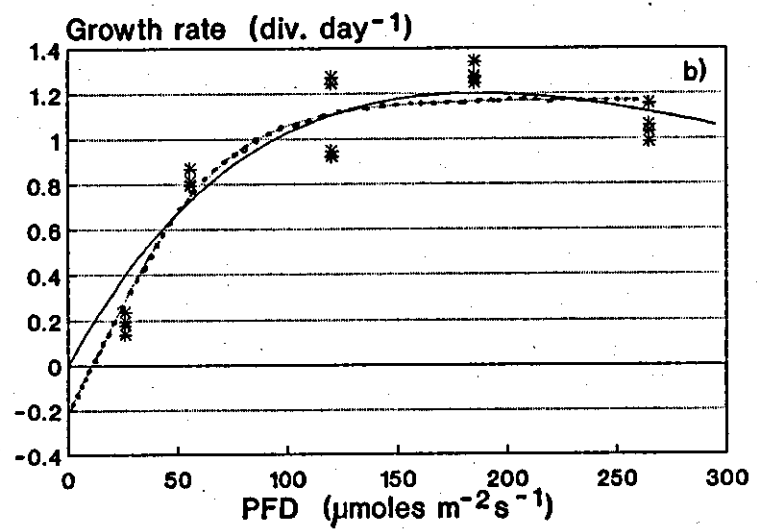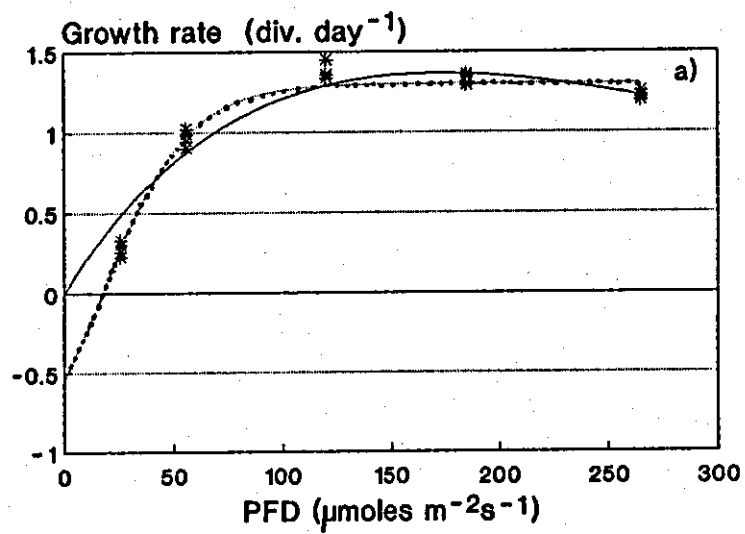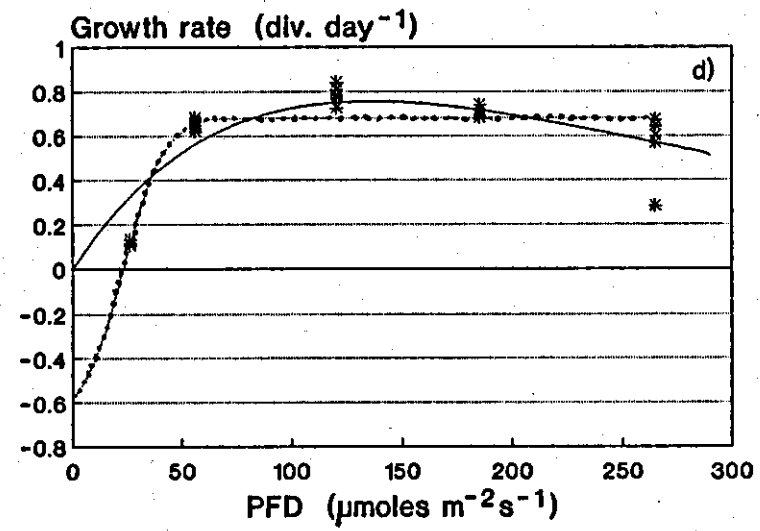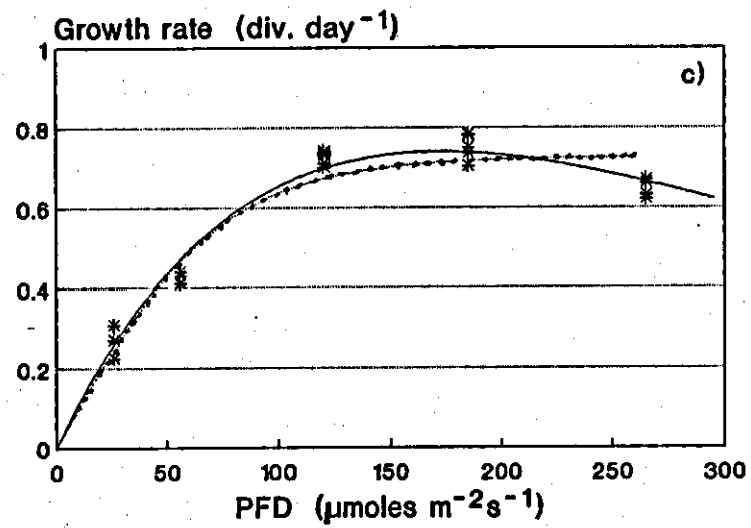
Fig. 2.3. Growth vs. irradiance relationship in L485 at different temperatures. a = 26 °C, b = 21 °C, c = 16 °C, d = 12 °C, e = 10 °C, f = 8 °C, g = 5 °C. The observed growth rates are displayed with asterisks (*). The solid line shows the fitted Steele's (1965) function and the dashed line the hyperbolic tangent function.

23

Table 2.2. Maximum growth rates and corresponding photon flux densities (PFD) for L485 estimated from Steele's (1965) and hyperbolic tangent functions

Temperature (°C)	μ_{max} (div. day^{-1})		I_{opt} (μmoles m^{-2} s^{-1})
	Steele	Tanh	Steele
26	1.37	1.30	172
21	1.20	1.17	186
16	0.74	0.73	172
12	0.76	0.68	136
10	0.49	0.43	128
8	0.33	0.24	110
5	0.18 ')	0.15	114 ')

') Negative growth rates at the lowest photon flux density not included in curve fitting

tangent function was not so reliable as there were not enough experimental observations in the light limited part of the curves. In general, the estimates of μ_{max} given by the models are consistent with each other, but the values from the hyperbolic tangent function are slightly lower.

For L315 Steele's (1965) function is less suitable (Fig. 2.4), as it cannot take into account the ability of this species to sustain its maximum growth rate over a wider range of irradiance. This phenomenon is most marked at temperatures 16, 10 and 5 °C, when the hyperbolic tangent function clearly gives a better fit. The growth response of L315 at 12 °C was peculiar, as the growth was saturated at only 86 μmoles m^{-2} s^{-1} and thereafter photoinhibition was marked. These unexpectedly low growth rates at higher PFDs were confirmed when the experiment was repeated. As with L485, the μ_{max} estimates from both of the models were consistent, but the hyperbolic tangent function seemed to slightly underestimate the maximum growth rates of L315.

The basic assumption of $I_c=0$ in Steele's (1965) model holds better for L315 than for L485, as can be seen from the compensation points estimated from the hyperbolic tangent function (Table 2.4). L315 seems more capable of growth at low PFDs, as only at T= 21 °C was its compensation point clearly different from zero. L485 is less adapted to grow at low irradiances. Nevertheless care must be taken in drawing detailed conclusions as the fit of L485 data to the hyperbolic tangent function at low temperatures was poor.

Table 2.5 summarizes the species–specific growth efficiencies (α_g, div. day^{-1} (μmoles m^{-2} s^{-1})$^{-1}$), i.e. slopes of growth vs irradiance curves at different temperatures. In general, L485 was more efficient in exploiting suboptimal photon flux densities. The means of values were 33 * 10^{-3} and 18 * 10^{-3} div. day^{-1} (μmoles m^{-2} s^{-1})$^{-1}$ for L485 and L315, respectively. The very high value 136 x 10^{-3} at 8 °C for L485 is not included in this consideration, as comparison with Langdon's (1988) review on interspecific differences in α_g (α_g = 0.51–63 x 10^{-3}) indicates this value to be an artefact. Efficiencies were not constant over the temperature range 5 – 26 °C, but no relationship with temperature was evident.
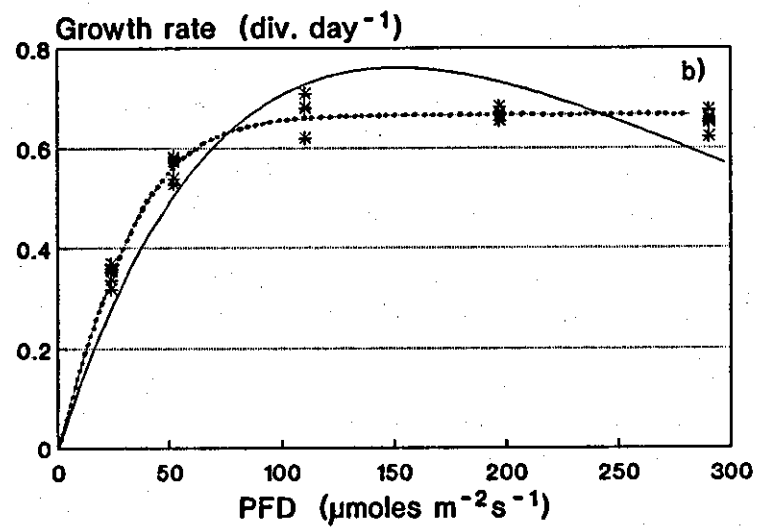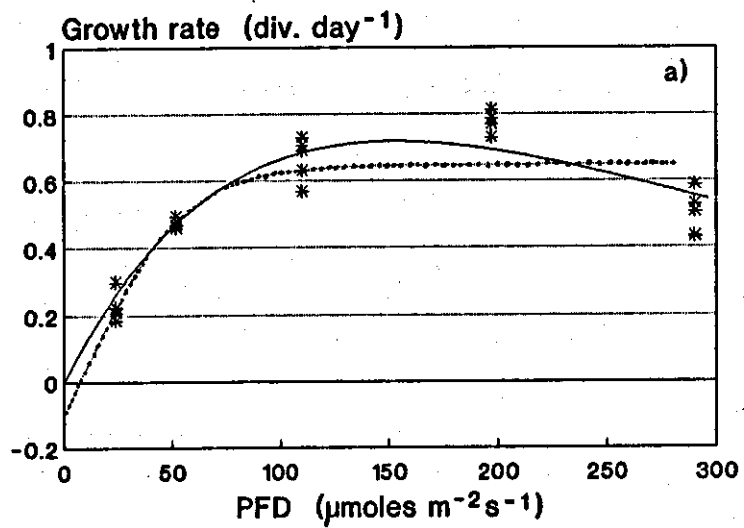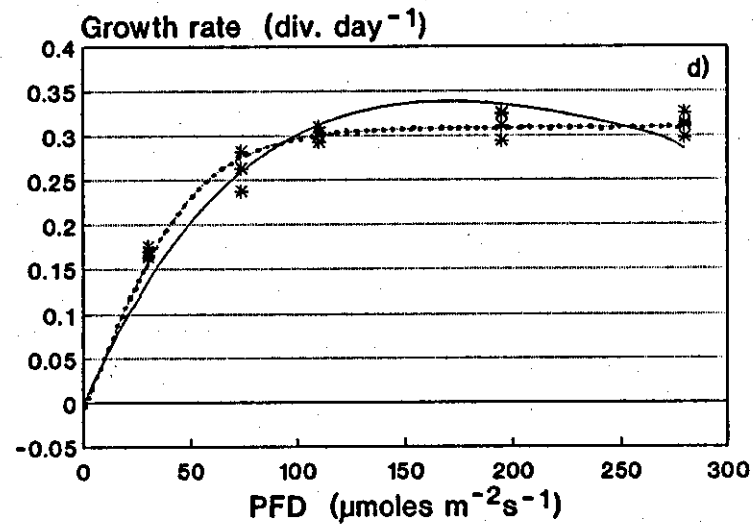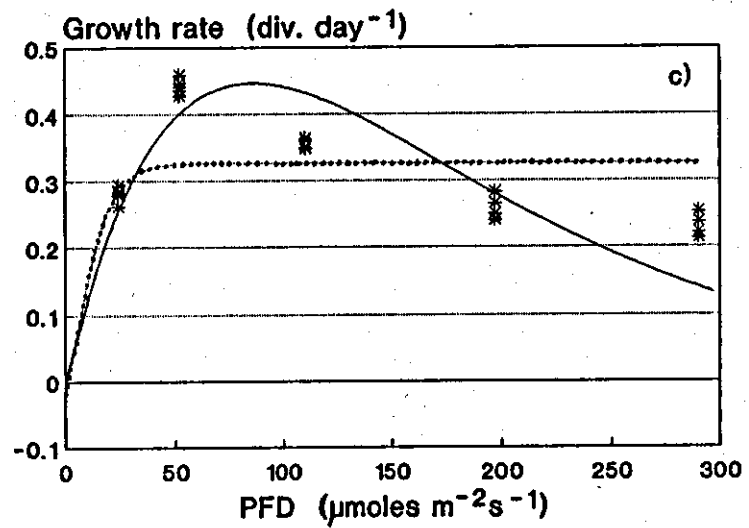
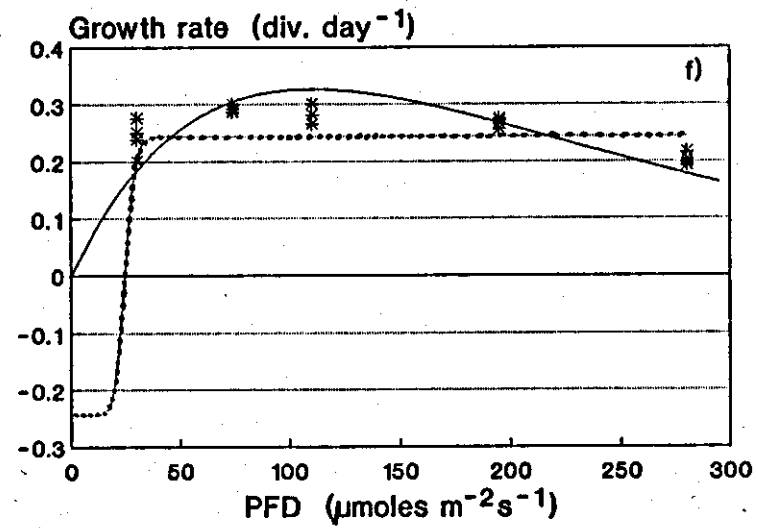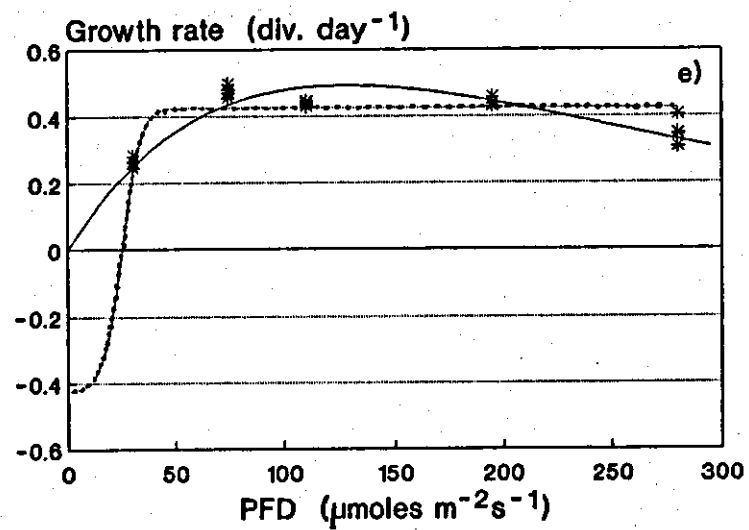**Fig. 2.4.** Growth vs. irradiance relationship in L315 at different temperatures. a = 21 °C, b = 16 °C, c = 12 °C, d = 10 °C, e = 5 °C. The observed growth rates are displayed with asterisks (*). The solid line shows the fitted Steele's (1965) function and the dashed line the hyperbolic tangent function.
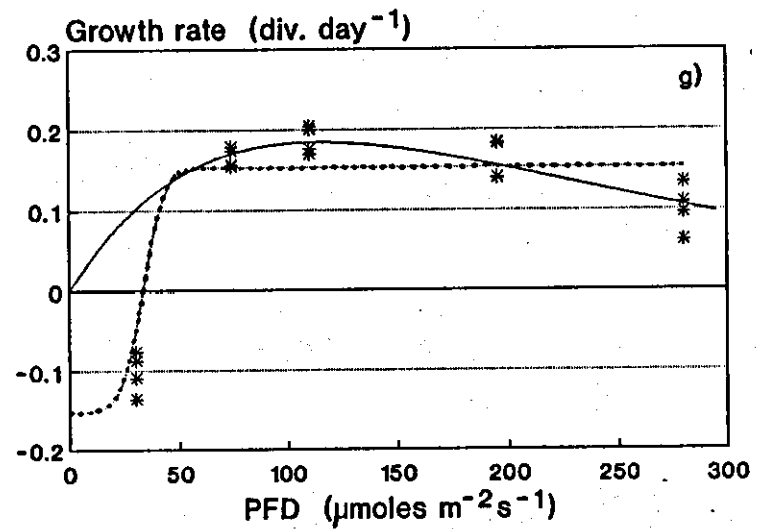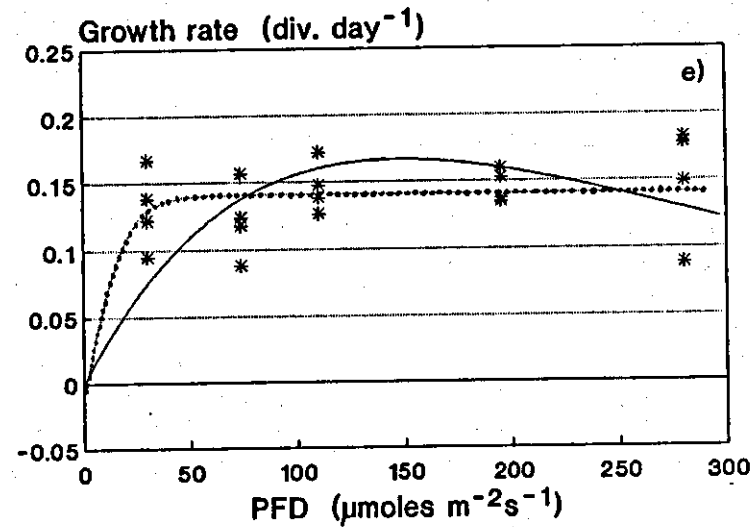
Table 2.3. Maximum growth rates and corresponding photon flux densities (PFD) for L315 estimated from Steele's (1965) and hyperbolic tangent functions.

Temperature (°C)	μ_{max} (div. day^{-1})		I_{opt} (μmoles m^{-2} s^{-1})
	Steele	Tanh	Steele
21	0.72	0.65	153
16	0.76	0.67	151
12	0.45	0.33	86
10	0.34	0.31	170
5	0.17	0.14	148

Table 2.4. Compensation points I_c (PFD, μmoles m^{-2} s^{-1}) for L485 and L315 estimated from hyperbolic tangent function

Temperature (°C)	Compensation point, I_c (μmoles m^{-2} s^{-1})	
	L485	L315
26	17.64	–
21	11.07	7.42
16	0.00	0.35
12	23.03	1.20
10	6.84	1.21
8	25.22	–
5	34.17	1.21

Table 2.5. Growth efficiencies (α_g) (div day^{-1}(μmoles m^{-2} s^{-1})$^{-1}$) of L485 and L315

Temperature °C	α_g div. day^{-1} (μmoles m^{-2} s^{-1})$^{-1}$ * 10^{-3}	
	L485	L315
26	33	–
21	20	14
16	10	16
12	39	20
10	64	1
8	(136 ?)	–
5	30	8

Maximum growth rates (estimated from Steele's (1965) function) fitted to temperature dependence equations (3) and (4) are presented in Fig. 2.5. The general feature of this type of curve is that at temperatures in excess of the optimum for growth the decline in growth rate is much steeper than at suboptimal temperatures, and this is also clearly seen for L485 and L315. The iteration process with Simplex algorithm gave the following temperature dependence functions:

$$\mu_{max} (T) (L485) = 0.1227 * \{\exp(0.1639 * T) - \exp(4.9780 - [(30.3646 - T)/5.9709)]\} \quad (6)$$

$$\mu_{max} (T) (L315) = 0.0949 * \{\exp(0.2119 * T) - \exp(4.9040 - [(23.1430 - T)/3.9175)]\} \quad (7)$$

Thus, the lethal temperature for L485 was 30.4 °C and for L315 23.1 °C. The latter upper limit is in agreement with the experimental observation of L315 populations dying at 26 °C. The optimum temperatures were ca 24.5 °C and 19.0 °C for L485 and L315 respectively. The corresponding maximum potential growth rates deduced from the curves were 1.38 div. day^{-1} for L485 and only 0.87 div. day^{-1} for L315. There were no distinct interspecific differences in temperature response rates as can be deduced from values of parameter β (0.16 and 0.21 for L485 and L315, respectively). The same conclusion can be drawn from estimated Q_{10} values of 4.1 and 3.8 for μ_{max} in the temperature range 0-10 °C. No effort was made to determine the real X-axis intercept (i.e. biological zero) of the μ_{max} (T) curve and hence the Y-axis intercept in Fig. 2.5 must be regarded as an artefact.

The temperature dependences of optimum photon flux densities are shown in Fig. 2.6. For L315 curve fitting could not be carried out, as in this case optimum values and temperature were not related in the way assumed by the model. Fig. 2.6 shows that when temperature increases there is a shift in optimum PFDs for L485 towards higher values until a certain temperature is reached after which there is a rapid decline. This temperature estimated from the curve is ca. 23 °C, which is lower than the optimum temperature for growth deduced from Fig. 2.5. The corresponding PFD is approximately 185 μmoles m^{-2} s^{-1}. The ascending part of the curve is less steep than in the maximum growth rate vs temperature curve, i.e. temperatures below the
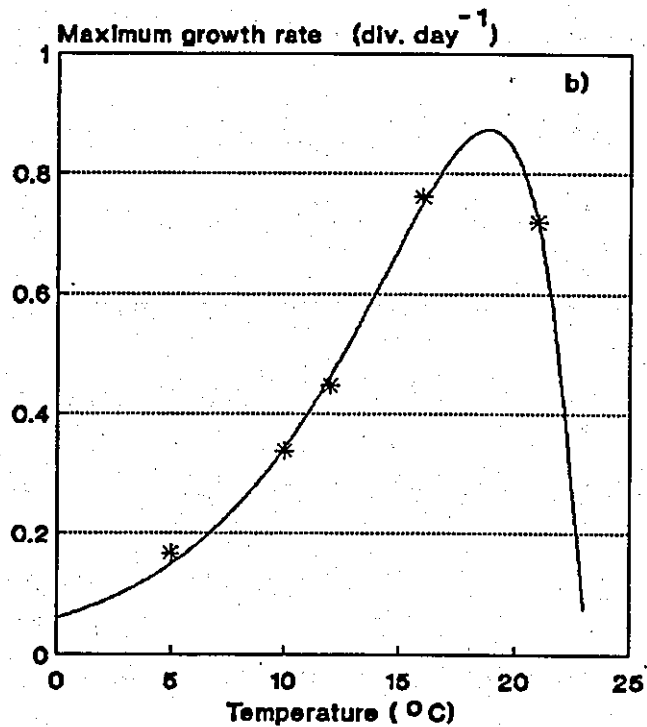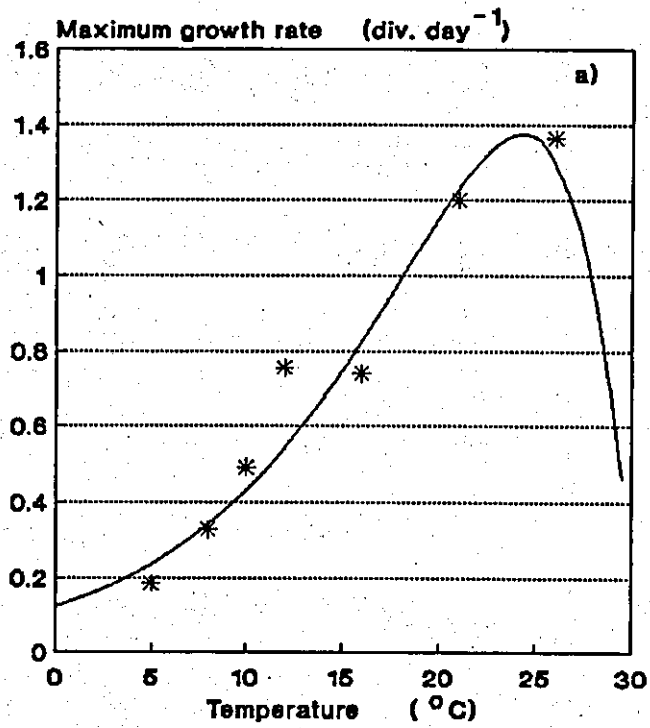
Fig. 2.5. Maximum growth rates of L485 (a) and L315 (b) in relation to temperature. The observed values are shown with asterisks (*) and the fitted functions of Logan et al. (1976) with solid lines.
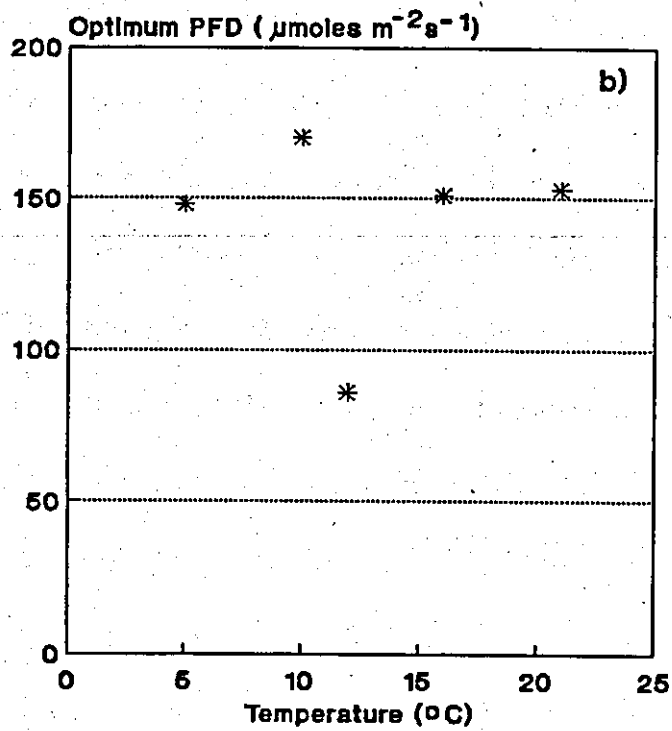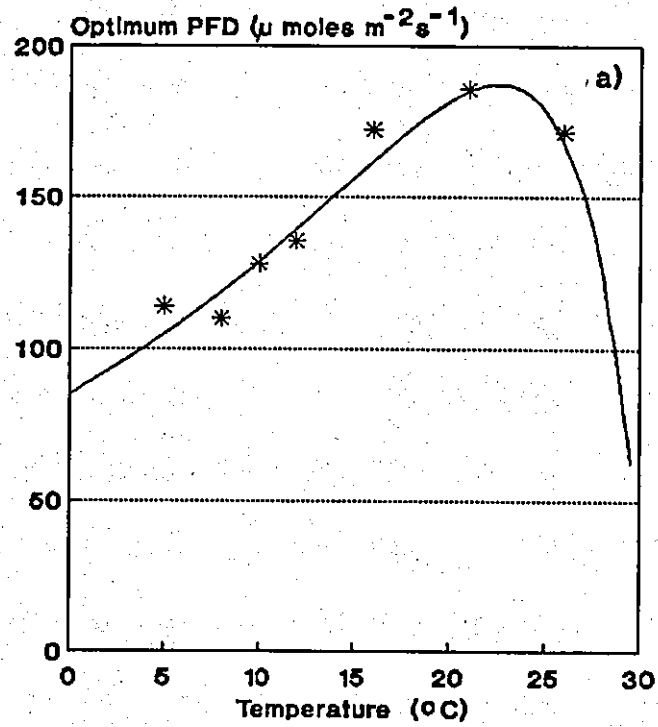
Fig. 2.6. Temperature dependence of I_{opt} in L485 (a) and L315 (b). The fitted function of Logan et al. (1976) for L485 is shown with a solid line. The observed values are shown with asterisks (*).

optimum cannot influence the light requirements of L485 as much as maximum growth rate.

2.3.2 Effects of shortened photoperiod on growth of L485

The growth response of L485 under a shortened 12 hour light period compared to that at the same temperature but with a 16 hour light period is illustrated in Fig. 2.7. The curves shown in the figure were fitted using Steele's (1965) model. The unambiguous result was that L485 grows better under 16:8 LD cycle. The estimated maximum growth rates for 12:12 LD and 16:8 LD regimes were 1.00 and 1.20 div. day^{-1} and growth under shorter photoperiod was always lower irrespective of incident PFD. The PFDs corresponding to maximum growth rates were quite similar, i.e. 186 and 174 μmoles m^{-2} s^{-1} for shortened and longer photoperiod, respectively. However, if irradiance is expressed as a light dose (i.e. moles m^{-2} d^{-1}), a difference in photoadaptation can be found, as optimum light dose under the 16:8 LD regime was 10.71 moles m^{-2} day^{-1} but under the 12:12 LD regime only 7.53 moles m^{-2} d^{-1}. Thus, under shorter photoperiod growth was saturated with a smaller dose of light. A shorter light period was also beneficial to growth at PFDs close to compensation points I_c, as the observed growth rates at 25 μmoles m^{-2} s^{-1} were approximately the same but the corresponding light doses were 1.08 and 1.44 moles m^{-2} day^{-1}.

2.3.3 Effects of lowered dark period temperature on growth of L315

The effects of a lowered dark period temperature on growth of L315 are shown in Fig. 2.8. Results from the T=22 °C/12 °C experiment are compared to those results from cultures grown at a constant 21 °C and for both data sets the fit to Steele's (1965) function is presented. The actual temperature cycle measured inside an experimental flask, and thus experienced by the algae, is also shown. The light cycle
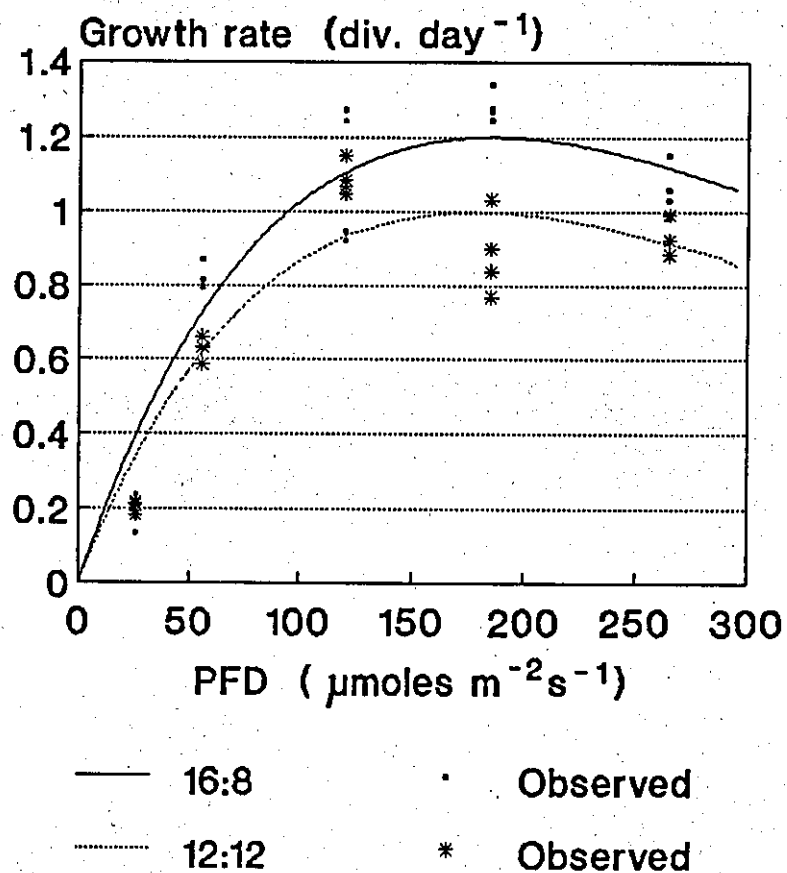
Fig. 2.7. Growth response of L485 under 16:8 LD and 12:12 LD regimes. Dashed and solid lines show fitted Steele's (1965) functions. Observed growth rates are shown with black squares and asterisks.
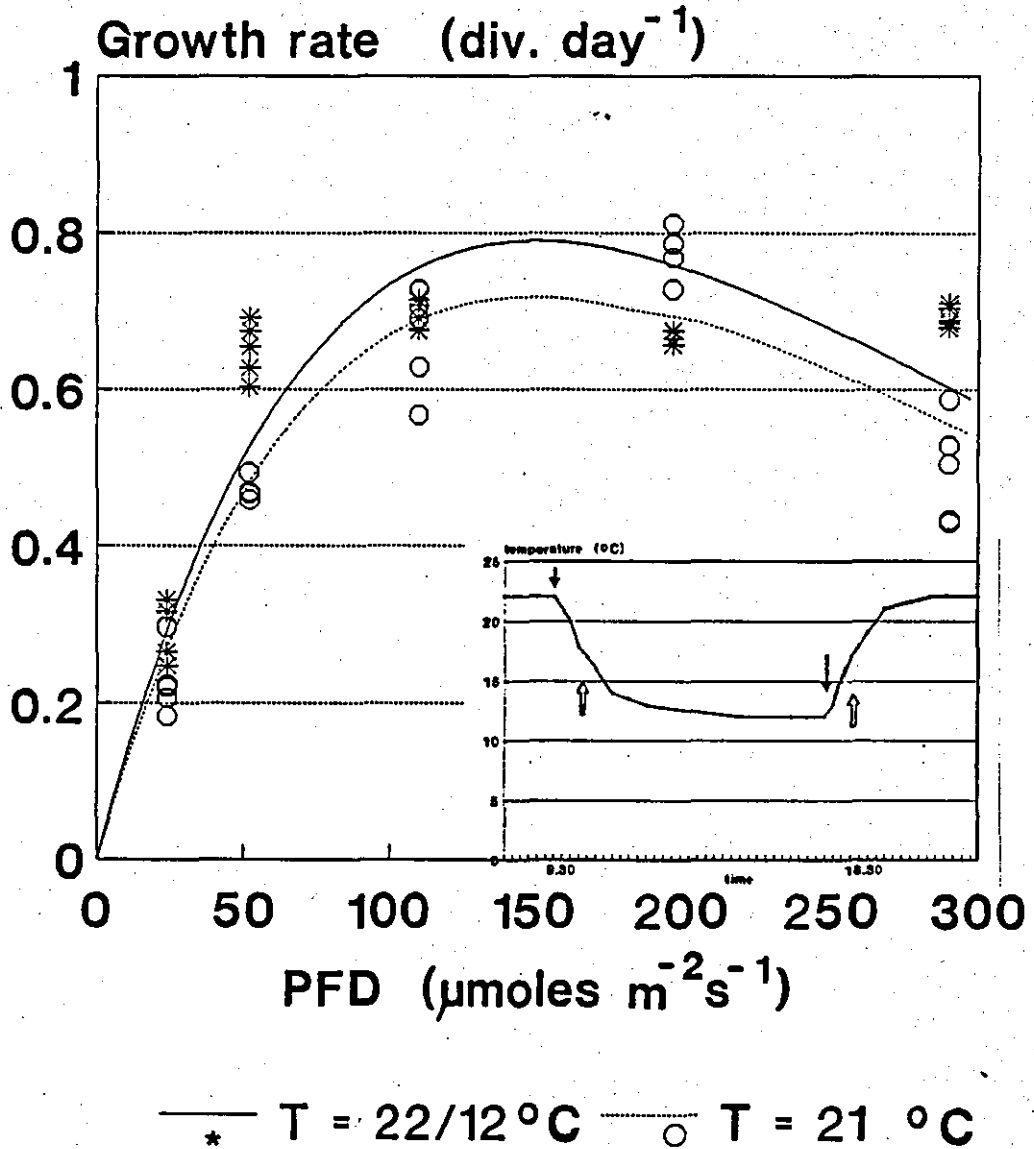
Fig. 2.8. Growth response of L315 at lowered dark period temperature (T=22/12 °C) compared to that at constant temperature (T=21 °C). The fitted Steele's (1965) functions are shown with a solid and dashed line and the observed values with asterisks and circles. The 24 h temperature cycle is displayed in the insert with the black arrows indicating the timing of the temperature cycle and the white arrows the timing of the LD cycle.

was reversed and there was a one hour difference in timing of the temperature and light cycles. Fig. 2.8 shows that by lowering temperature during the dark period extra growth could be gained as maximum growth rates estimated from Steele's (1965) function were 0.79 and 0.69 div. day^{-1} for lowered and constant temperature experiments respectively. In order to verify the result, part experiments at PFDs 290, 197 and 110 μmoles m^{-2} s^{-1} were repeated. These gave a similar trend but the growth rates (not shown) were slightly lower. Lowering temperature did not change the photoadaptation pattern of L315 expressed in terms of optimum irradiance. Estimated values of this parameter were 150 and 153 μmoles m^{-2} s^{-1} for T=22 °C/12 °C and T=21 °C experiments, respectively.

2.3.4 Variation in cell sizes

Cell sizes as a function of PFD at different temperatures are displayed in Fig. 2.9. The values shown are means of measurements from at least 75 individual cells. Coefficients of variation (c.v.) of mean cell sizes remained in general low (<10 %) throughout the experiments, but for L485 in a couple of treatments the c.v. reached a value of c. 27 %. Comparison of Fig. 2.9a and 2.9b shows that neither of the species had a constant cell size but that the size varied with temperature and light intensity. The interspecific differences in cell size response are also obvious. For L485 the cell size vs PFD curves are sigmoidal. However, at 10, 8 and 5 °C flexures of the curves are not so distinct indicating that at lower temperatures cell size is more independent of irradiance. At each temperature the smallest cells were recorded at the lowest experimental irradiance. The smallest L485 cells measured had an average volume of 232 μm^{-3} (T=16 °C, I=26 μmoles m^{-2} s^{-1}) and the largest ones 920 μm^{-3} (T=12 °C, I=120 μmoles m^{-2} s^{-1}) giving a 4-fold size difference within this single clone.

The tendency to more constant cell size at low temperatures can also be seen in L315. Cell size vs PFD curves at 5 and 10 °C are linear compared to those at higher temperatures; at 21 °C cells appear to be largest at the lowest and highest PFDs. This observation is quite different from the response of the cell size of L485. The
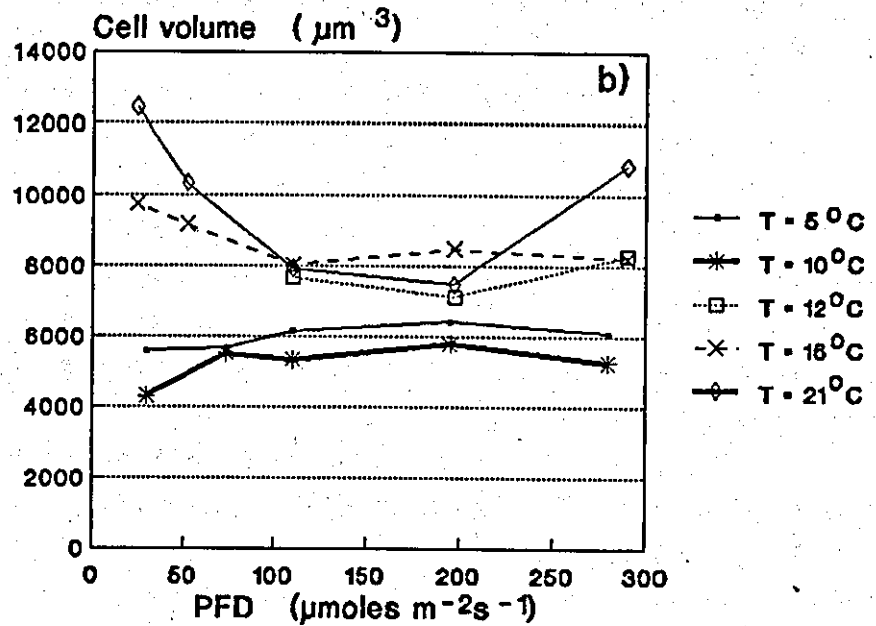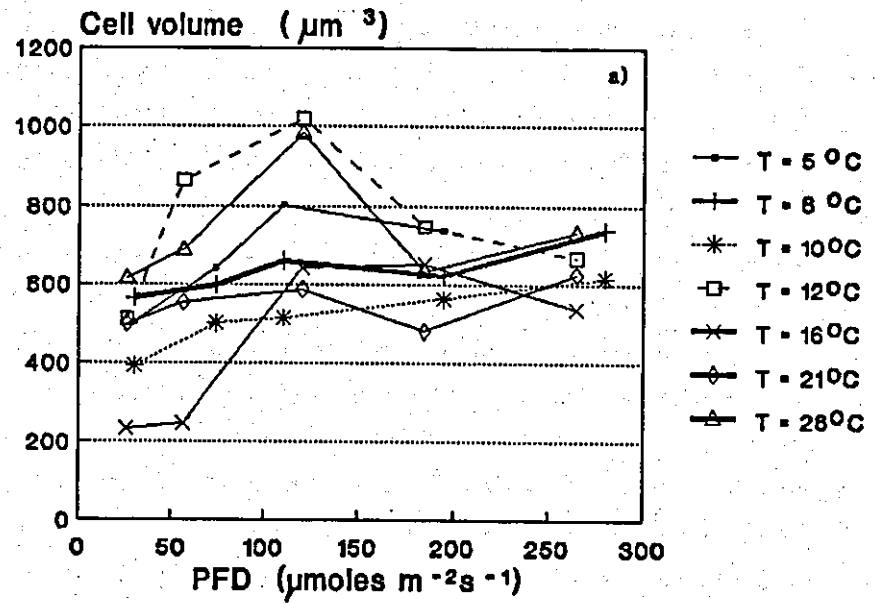
Fig. 2.9. Cell volumes of L485 (a) and L315 (b) in relation to irradiance and temperature

smallest and largest L315 cells measured had average volumes of 4 306 μm^{-3} (T=10 °C, I=280 $\mu moles. m^{-2} s^{-1}$) and 12 450 μm^{-3} (T=21 °C, I=197 $\mu moles. m^{-2} s^{-1}$), respectively, thus giving an 18-fold size difference between the smallest cells of these two species and a 12-fold difference between the largest ones. Within the L315 clone the cell size variability was considerably lower than in L485 varying by only 2.9-fold.

2.3.5 Chlorophyll *a* content

The species specific relationships of chlorophyll *a vs* irradiance are illustrated in Fig. 2.10. Each value is the mean of the replicated chlorophyll per cell results and expressed as per unit cell volume. The general response of microalgae to reduced photon flux densities (below *ca.* 110-120 $\mu moles\ m^{-2}s^{-1}$) is to increase the cellular pigment content and this response can clearly be seen in L485 and L315. No distinct species-specific differences in relative chlorophyll contents could be observed. However, for L315 the effects of reduced irradiance seemed to be temperature dependent, as the response curves have more flexure at 5 and 10 °C and the chlorophyll contents at these temperatures were higher than otherwise. For L485 no temperature dependence could be found. The change in chlorophyll content in response to the light environment was slightly greater ~~for L485 than for L315~~ L315, as within one temperature treatment ~~the first~~ could alter its relative chlorophyll content L485 by a factor of ca. 5 and ~~the latter~~ by a factor of 3.5.

2.3.6 Protein and carbohydrate content

The protein and carbohydrate results are displayed in Figures 2.11 and 2.12. For both species the protein pool remained quite stable at PFDs higher than 110-120 $\mu moles\ m^{-2} s^{-1}$, but at lower ~~densities~~ PFDs the protein pool increased. In L485 this increase was most remarkable at 16 and ~~12~~ 10 °C. In L315 the increase, as well as the overall protein content, was highest at 5 °C. There was no clear correlation with temperature, but
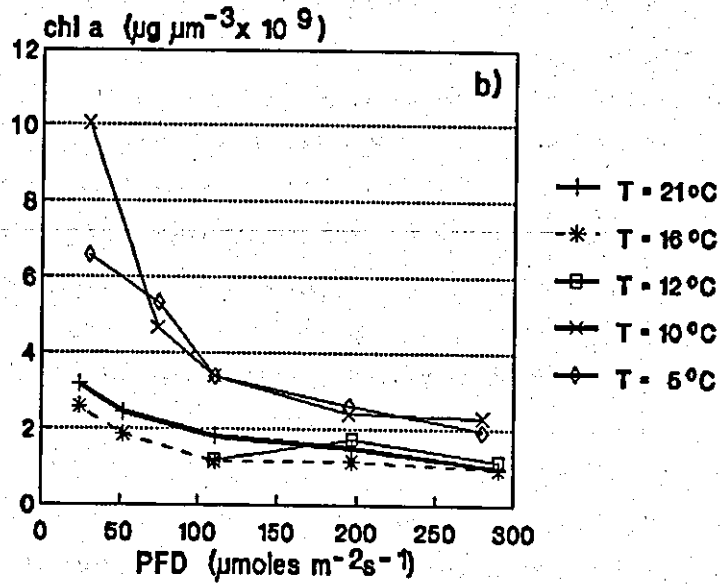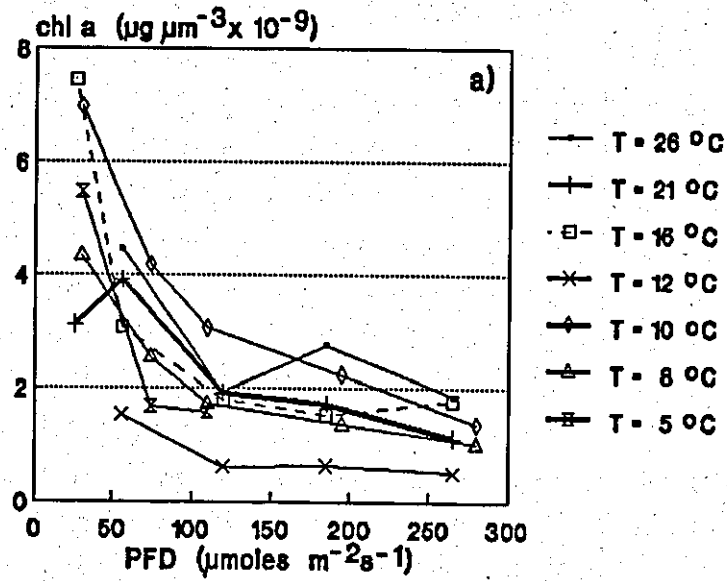
Fig. 2.10. Chlorophyll *a* (µg µm⁻³) vs. PFD relationship in L485 (a) and L315 (b) at different temperatures.

Protein $(\mu g\ \mu m^{-3} \times 10^{-7})$

a)

T = 26 C
T = 21 C
T = 16 C
T = 12 C
T = 10 C
T = 8 C

PFD $(\mu moles\ m^{-2}s^{-1})$

Protein $(\mu g\ \mu m^{-3} \times 10^{-7})$

b)

T = 21 C
T = 16 C
T = 12 C
T = 10 C
T = 5 C

PFD $(\mu moles\ m^{-2}s^{-1})$
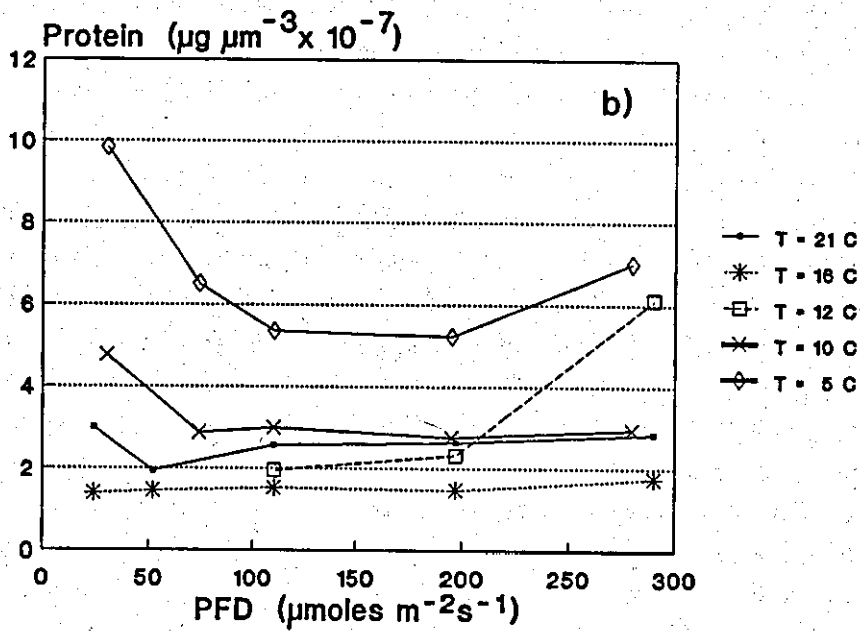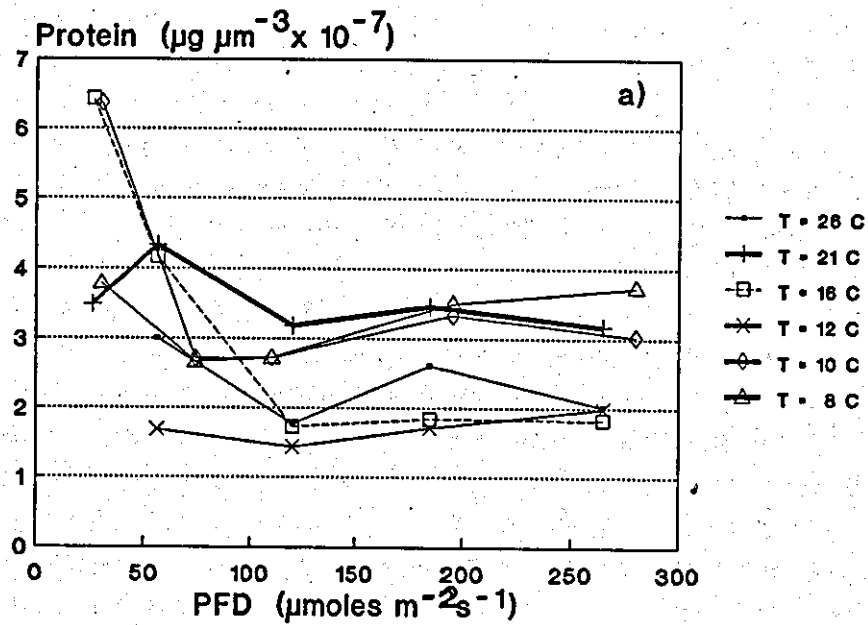
Fig. 2.11. Protein pool $(\mu g\ \mu m^{-3})$ in L485 (a) and L315 (b) in relation to irradiance and temperature.
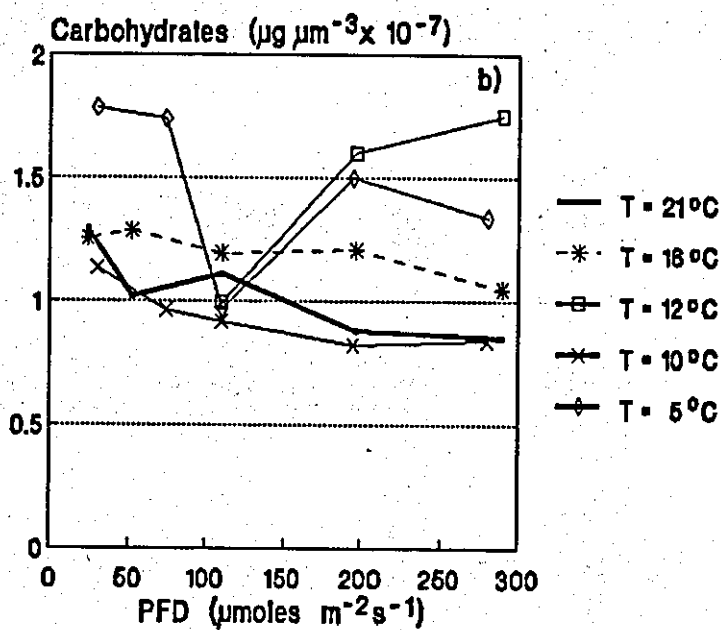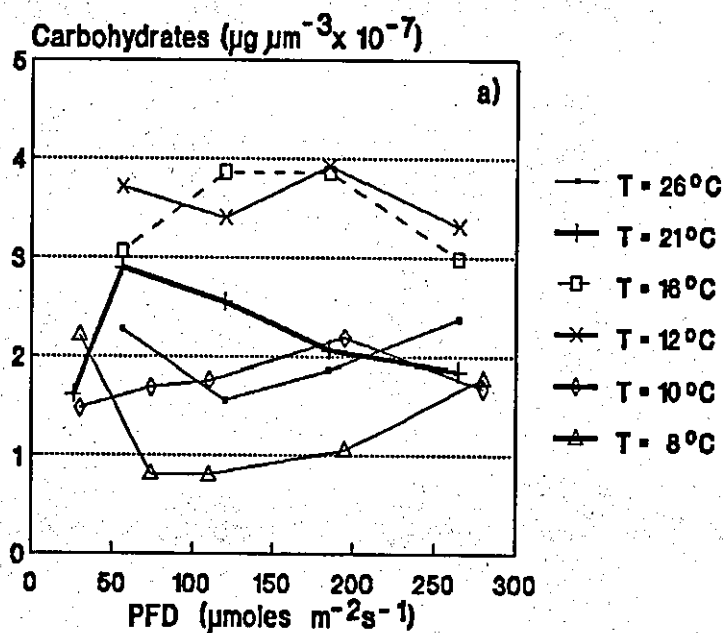
Fig. 2.12. Carbohydrate pool ($\mu g \ \mu m^{-3}$) in L485 (a) and L315 (b) in relation to irradiance and temperature.

there was a slight tendency for higher protein pool at the lowest experimental temperatures.

The carbohydrate results were less illustrative than the results for the protein pool, especially as in L485 no obvious pattern either in response to changing irradiance or to temperature, could be found. In L315 carbohydrate contents tend to decrease slightly at higher photon flux densities, but this pattern was reversed at 12 °C and 5 °C. The carbohydrate content in L315 was in general lower than in L485.

The protein and carbohydrate ratios are displayed in Tables 2.6 and 2.7. According to Myklestad (1974) these ratios can be considered as a convenient indicator of the physiological state of the cells. As a general rule, these ratios were well above 1.0 – 1.2, which is suggested to be the limit between nutrient sufficient and hence rapidly growing algae, and nutrient depleted cells with retarded growth (e.g. Healey 1975, Myklestad 1977). At temperatures 12 and 16 °C with L485 the ratios were clearly below 1.0, despite the fact that algae in these treatments were growing at a moderate rate. Some of these cultures might have been harvested too close to the stationary phase, thus resulting in decreased ratios (cf. Fogg 1965), but this explanation is certainly not valid in all cases. For L485 no obvious temperature dependence of ratios could be found, but for L315 ratios were higher at lower temperatures. The response to changing irradiance was also species specific, as in L315 the ratios slightly increased towards higher photon flux densities and in L485 the tendency seemed to be opposite. However, none of these results was distinct enough for definite conclusions.

2.4 DISCUSSION

Several types of empirical and semi-empirical equations have been presented as ideal models for describing the complex response of algal growth to variations in light and temperature. These models range from a simple rewritten Monod equation (Post et al. 1985) and more complicated functions combining existing equations

Table 2.6. Protein to carbohydrate ratios of L485

Irradiance (μmoles m^{-2} s^{-1})	Temperature (°C)						
	26	21	16	12	10	8	5
26		2.10					
30					4.30	1.72	2.10
56	1.32	1.50	1.36	0.46			
74					1.60	3.27	1.35
110					1.54	3.38	2.30
120	1.13	1.25	0.45	0.42			
185	1.40	1.68	0.48	0.44			
195					1.53	3.30	
265	0.85	1.71	0.61	0.60			
280					1.80	2.10	

Table 2.7. Protein to carbohydrate ratios of L315

Irradiance (μmoles m^{-2} s^{-1})	Temperature (°C)				
	21	16	12	10	5
24	2.32	1.12			
30				4.19	5.51
52	1.90	1.14			
74				2.99	3.74
110	2.32	1.28	1.97	3.28	5.52
195				3.36	3.48
197	3.00	1.23	1.45		
280				3.53	5.22
290	3.34	1.67	3.50		

(e.g.Nicklisch & Kohl 1983), to highly sophisticated models using up to nine para-meters and values just to describe the growth *vs* irradiance relationship (Falkowski et al. 1985b). The algal species to which these models have most often been applied are marine diatoms and bloom-forming blue-green algae. In the study presented here, no attempt was made to develop a new equation for the μ *vs* I relationship; instead two existing models were applied to the data. Steele's (1965) empirical model and the hyperbolic tangent function by Platt & Jassby (1976) were chosen for growth *vs* irradiance description. The first had previously been used for cryptophytes (Cloern 1978, Gavrieli 1984), thus making interpretation of the data presented here more comparable and the latter, despite originally being developed for photosynthesis *vs* irradiance curves, had succesfully been fitted to similar data by Yoder (1979), Verity (1982) and Langdon (1987). However, it must be concluded that neither of these models alone was able to fully describe the growth responses of the two cryptophyte species over a wide temperature range. In general, the hyperbolic tan-gent function was better suited for L315, as it describes the dependence of growth rate on light by means of a saturation curve, i.e. with no flexure in the curve after optimum light intensity. For L485 this function was superior in describing the light-limited part of the μ *vs* I curves, especially at higher temperatures, but Steele's (1965) exponent function could better take into account the light- inhibition of growth typical of this species. At lower temperatures neither of them gave a really satisfactory fit to the data. Hence, it is obvious that a combined model possessing the best characteristics of Steele's (1965) model and the hyperbolic tangent function would have given a more universal fit. The inability of a single model to adequately describe growth response at different temperatures has also been reported by Cloern (1977) and Nicklisch & Kohl (1983).

Comparison of the maximum growth rates, and hence the growth potential of L485 and L315, with the published values for other cryptophytes is hampered by the different temperature and light regimes used in various experiments as well as the rather restricted approach of most of the studies. Only Cloern (1977), Gavrieli (1984) and in some respects Morgan & Kalff (1979) have striven for a more generalized growth description, while others have been content with experiments conducted only at few temperature – irradiance combinations (Morgan & Kalff 1975, Bowen & Ward 1977, Thinh 1983) or else the data are solely a minor by-product of a study

aiming at something other than growth description (Wehr et al. 1986). The list of species used in these studies consists of *C. erosa* (Morgan & Kalff 1975, 1979), *C. ovata* (Bowen & Ward 1977, Cloern 1977, Wehr et a. 1986), *Rhodomonas lacustris* (Gavrieli 1984) and one unidentified strain (Thinh 1983). The maximum observed growth rates recorded for these species varied from 0.6 to 1.65 div. day^{-1}, but as they were not necessarily measured under optimum conditions, they cannot automatically be regarded as maximum potential values. Roukhijajnen (1977) recorded a very high growth rate of 2.8 div. day^{-1} for a marine *C. vulgaris*, but as the result was obtained with a natural population grown in an uncontrolled environment, its authenticity can be questioned. *C. erosa*, which in terms of size is most comparable to L485, has been observed to grow under continuous light at 1.23 div. day^{-1} (Morgan & Kalff 1979). This is only slightly lower than the estimated μ_{max} of 1.38 div. day^{-1} for L485. However, if these growth rates are expressed as divisions per hour of light, L485 turns out to be superior to *C. erosa* with its rate of 0.086 div. hour^{-1} of light against that of 0.051 div. hour^{-1} of light for *C. erosa*. Even *Rhodomonas lacustris*, with a daily growth rate 1.65 div. day^{-1} achieved under continuous light, appears to be a slower grower when viewed in this way ($\mu = 0.069$ div. hour^{-1} of light). Growth of L315 has to be compared with that of *C. ovata*, as no strains with closer resemblance in size to L315 have been used in experiments. On the basis of cell size this is not much a problem, as *C. ovata* is known to have widely varying cell size, the largest cells can have cell volumes even in excess of L315 (Huber–Pestalozzi 1968, Starmach 1974). The maximum growth rate of 0.87 div. day^{-1} for L315 estimated in this study was ca 40 % lower than that of L485, but quite comparable with the observed rates of 0.72 div. day^{-1} and 0.60 div. day^{-1} for *C. ovata* observed by Cloern (1977) and Bowen & Ward (1977) respectively. Uniformity of these growth rates is even more pronounced when they are expressed as div. hour^{-1} of light (0.054 for L315 and 0.048 and 0.05 for *C. ovata*, respectively). However, compared to the potential μ_{max} value (estimated from μ_{max} (T) curve) of 1.15 div. day^{-1} for *C. ovata* (Cloern 1977), L315 appears to grow more slowly.

The reason why it is reasonable to compare growth rates of species of comparable size is because it is generally known that growth rate is a decreasing function of cell size, i.e. smaller species tend to have higher growth rates and shorter gene–

ration times than larger ones. This 'law' applies to all organisms, not only to unicellular algae, and it gives a general explanation for the difference in estimated maximum growth rates of L485 and L315; the allometric relationship between growth and cell size has even been claimed to be the most promising explanation of interspecific differences in maximum growth rates (Langdon 1988). According to Banse (1976) there is evidence that this degree of size dependence is highest under optimal conditions of growth and less pronounced under suboptimal conditions. However, the estimated maximum growth rates of L485 and L315 could not be fitted into the allometric equation by Banse (1976), as instead of using cell volume data it requires results in cell carbon. Laws's (1975) allometric equation, based on the marine algal data of Eppley & Sloan (1966), uses cell volumes and thus enables comparison of the growth of cryptophytes, in respect of cell size, with other species. This empirical model predicts that algae having maximum growth rates of 1.4 and 0.9 div. day^{-1} would have cell volumes of ca 4 000 μm^{-3} and 340 000 μm^{-3}, respectively. These are 5-30 times higher than the greatest volumes ever measured for L485 and L315. Even the equation by Reynolds (1984), based only on freshwater data, gives differences of the same magnitude between the predicted and observed cell volumes. Thus, these cryptophytes appear similar to dinoflagellates, which have been said to have substantially lower specific growth rates than diatoms of the same mass (Banse 1982). Raven & Geider (1988) have explained this kind of under-achievement with the observations by Sicko-Goad (1977) indicating that dinoflagellates and cryptophytes have a smaller fraction of their catalytic volume occupied by photosynthetic apparatus.

The photon flux densities for saturation for L485 and L315 are high compared to observations on algae in other classes. This anomaly is most pronounced with blue-green algae, which is another group of algae besides cryptophytes and red algae possessing biliproteins as light harvesting accessory pigments (see e.g. MacColl 1982). According to Brown & Richardson (1968) algae with accessory pigments should have lower optimal PFDs for growth. Blue-green algae fulfill these expectations, as amongst the main taxonomic groups of algae their average optimum irradiance, 38.8 μmoles m^{-2} s^{-1}, is the lowest of all algal groups (Richardson et al. 1983). This is considerably lower than the estimated saturation intensities for L485 and L315 ranging from 86 to 186 μmoles m^{-2} s^{-1}. However, high optimum

irradiances have also been recorded for other cryptophytes. Gavrieli (1984) measured a value of 214.5 μmoles m^{-2} s^{-1} for *Rhodomonas lacustris* and the model by Cloern (1977) gives an estimate of 9.5 ly h^{-1} for the optimum irradiance of *C. ovata* var. *palustris* which, using a conversion factor given by Richardson et al. (1983), can be converted to give the remarkably high PFD value of *ca*. 550 μmoles m^{-2} s^{-1}. Despite at first sight being unbelievably high, the value is in agreement with the results of Javornicky (1970), who did not record light saturation of a natural population of cryptophytes until ca 540 μmoles m^{-2} s^{-1}. Thus, based on laboratory observations, cryptophytes can be said to resemble chlorophytes which, according to Richardson et al. (1983), have an I_{opt} of 211 $\pm$ 58 μmoles m^{-2} s^{-1}; neither do they show a strong photoinhibition (Harris 1978), a characteristic also found in L315.

The other light parameter, besides optimum/saturation irradiance, characterizing μ *vs* I curves is compensation point I_c, which in L485 and L315 showed more variability between species. The I_c values for L315 of close to zero are comparable with the results of Morgan & Kalff (1979) for *C. erosa*, indicating that both of these species are capable of growing at very low photon flux densities. Due to this capability of growth at low irradiances as well as depth regulation through swimming the contribution of cryptophytes to phytoplankton in ice–covered lakes can be important (Wright 1964, Ilmavirta & Kotimaa 1974). The minimum light requirement for growth of L485 seems considerably higher, being in the same range as for chlorophytes (Richardson et al. 1983).

The third parameter of the growth *vs* irradiance curve, α_g, also showed interspecific variability. Growth efficiency of L485 is comparable to e.g. *Nannochlorus atomus* (Chlorophyceae) and *Thalassiosira fluviatilis* (Bacillariophyceae), whereas L315 had α_g values consistent with those of *Thalassiosira weissflogii* and *Leptocylindrus danicus* (Bacillariophyceae) (Langdon 1988).

By combining the results on light saturation, compensation points and growth efficiencies at suboptimal irradiances, it can be concluded that there are great interspecific differences between L485 and L315 in their strategies of light utilization. L485 requires relatively high light intensities to be able to show net growth, but when the threshold irradiance is exceeded, it proves to be effective in photon

capture. L315 grows at very low levels of irradiance, but never reaches such a high growth rate as L485, and the growth efficiency is in general lower than for L485. However, L485 shows photoinhibition soon after saturation point, whereas L315 tolerates a much wider range of irradiance. The interspecific differences in genotypic photoadaptation strategies of these two cryptophytes are summarized diag‐ rammatically in Fig. 2.13. From their growth responses to light, L485 can be said to be a stenotopic and L315 a eurytopic strain.

From the triumvirate ~~taxonomy~~ species-size-temperature having effects on maximum growth rates, temperature was the most thoroughly investigated variable in this study and its effects were found to be well described by the analytical model of Logan et al. (1976). The model has provided a suitable fit for experimental data for *C. ovata* (Cloern 1977), *C. erosa* (Morgan & Kalff 1979) and *R. lacustris* (Gavrieli 1984) and now also for L485 and L315. The μ_{max} (T) function derived for L485 gave an excellent fit for *C. erosa*, and *R. lacustris* showed an overall μ_{max} (T) response similar to other cryptophytes. The temperature dependence rates of L485 and L315 (i.e. parameter β values) were consistent with the estimated value for *C. ovata* (Cloern 1977), and especially good was the agreement between L315 ($\beta=0.21$) and *C. ovata* ($\beta=0.20$), which were counterparts in the cell size/maximum growth rate comparison. For neither of the strains was a biological zero determined (i.e. that temperature where growth rate equals zero), but for cryptophytes it could be close to 0 °C, as Morgan & Kalff (1975) managed to grow *C. erosa* at 1 °C and Wright (1964) recorded cryptophytes in an ice‐covered lake at temperatures below 4 °C.

Growth experiments with different temperatures during light and dark periods are uncommon; the only reference found was Davis et al. 1953 in Borowitzka & Borowitzka 1988. Their results from *Chlorella* culture were similar to the results in this study, i.e. extra growth can be achieved by lowering the temperature during the dark period. These results can be explained by the known temperature dependence of dark respiration, e.g. in the diatom *Skeletonema costatum* (Geider & Osborne 1989). However, there is an obvious need for extra studies with more species and wider temperature ranges before any definite conclusions can be drawn, as it is known that cryptophytes undertaking diurnal vertical migrations *in situ* can experience temperature differences in excess of 10 °C (Salonen et al. 1984).
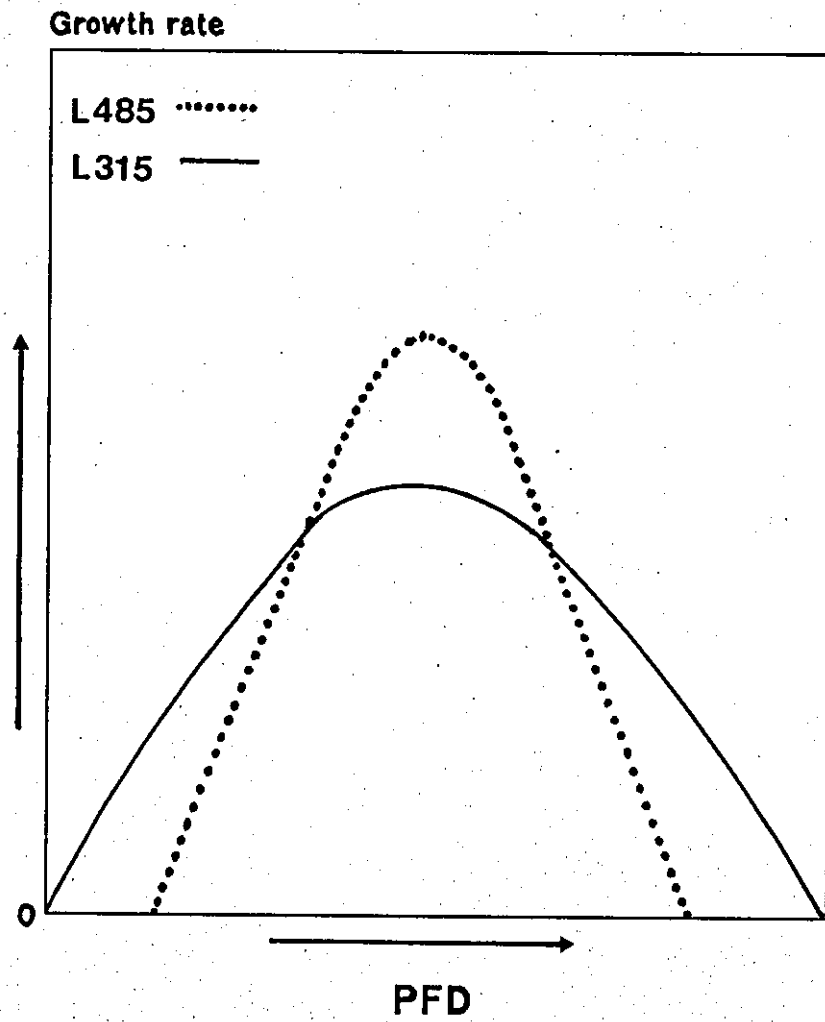
Fig. 2.13. A diagrammatic view of the genotypic photoadaptation of L485 and L315.

Amongst cryptophytes a decrease in optimum irradiance for growth at low temperatures has been seen for *C. ovata* var. *palustris* (Cloern 1977) and *C. erosa* (Morgan & Kalff 1979) as well as in the present study with L485. However, the rate of response of *C. ovata* var. *palustris* and *C. erosa* is clearly higher than that of L485; parameter β values for *C. ovata* var. *palustris* and L485 were 0.389 and ~~0.043~~ 0.16, respectively. A sharp increase in optimum irradiance in response to rising temperature has also been recorded for *R. lacustris* (Gavrieli 1984). Thus, the light saturation of L485, and especially of L315, is exceptionally insensitive to temperature.

In L485 and L315 there were no substantial intraspecific temperature effects on light-limited growth rate, i.e. on the initial slope of the μ vs. I curve. This observation agrees with Raven & Geider (1988) who, based on their review on temperature effects on catalysed and uncatalysed chemical transformation and transport processes, concluded that the expected effect of temperature on light-limited growth is much less than on resource-saturated (i.e. light-saturated) growth. However, in some cases growth rates at limiting PFDs are relatively temperature sensitive. For example, Verity (1982) has shown that the initial slope of the growth *vs* irradiance curve for a diatom, *Leptocylindrus danicus*, is temperature dependent. This dependence can be described by an exponential relationship and the resulting curve resembles the ascending part of the μ_{max} (T) and I_{opt}(T) curves derived from Logan et al. (1976).

The differences observed in mean cell volumes for L485 (i.e. tendency for cell volumes to increase with increasing growth irradiance) have also been recorded for some other cryptophytes, as well as for numerous other algae from different classes (e.g. Falkowski et al 1985b, Claustre & Gostan 1987, Langdon 1987). Morgan & Kalff (1975, 1979) reported a positive correlation for *C. erosa* between cell volume and growth irradiance. They also observed cells grown at low temperatures being 50–400 % larger than cells at high temperatures, but this was not recorded with either of the cryptophytes in this study, the opposite being true for L315. Extrapolating to the field their cell size results for *C. erosa*, Morgan & Kalff (1979) predicted cells of maximum size being found in the surface waters of lakes when the water temperature is low and the light flux high, i.e. in spring or in autumn. This

prediction does not hold for L485 and L315, and actually cells of L315 are largest at high temperatures and at low or high PFDs. This variability of cell size indicates that cryptophytes use size as a tool in the photoadaptation process. A wide range of cell volumes amongst one clonal strain also shows that cell size as a taxonomic criterion is of limited utility. The dimensions of L485 measured at the lowest PFDs were probably close to the genetically fixed minimum for this species, as these cells were grown very close to the compensation point and did not possess energy reserves for anything other than basic metabolism and vital cell structures.

Phenotypic adaptation of microalgae to different PFDs occurs through changes in amounts of photosynthetic pigments; at decreased PFDs either the size or the number of photosynthetic units is increased (Prezelin & Sweeney 1979, Falkowski & Owens 1980, Perry et al. 1981, Langdon 1987). By light–shade adaptation the effects of irradiance on growth can be attenuated, but the compensation is naturally incomplete, as otherwise growth rate would remain virtually constant over a wide range of light intensities. Cryptophytes L485 and L315 adapted by changing their relative chlorophyll a content maximally by a factor of 5 and 3.5, respectively. Thus, at low PFDs, when availability of energy limited growth, cells concentrated on light harvesting and were packed with chlorophyll. This kind of chlorophyll packing in *Cryptomonas* has also been observed by Thinh (1983), who measured chloroplasts of low and high light cells of *Cryptomonas* sp. occupying 41 % and 18 % of cell volume, respectively. The importance of packing of chlorophyll for growth efficiency of microalgae is also demonstrated by the non–linear relationship $\alpha_g = 4.303\ \theta_o^{1.754}$ (θ_o=ratio of chlorophyll a to particulate carbon at $\mu=0$) by Langdon (1988), suggesting that a doubling in θ_o results in a 3.4–fold increase in α_g.

Amongst cryptophytes *Rhodomonas lacustris* (Gavrieli 1984) and *C. erosa* (Morgan & Kalff 1979) have been shown to be capable of changing their chlorophyll content in a manner consistent with that found for L485 and L315, although the comparison of different data is somewhat hampered by the expression of the results for *R. lacustris* and *C. erosa* on a per cell rather than biovolume or carbon basis. Responses of the same magnitude have also been recorded for a chlorophyte, *Dunaliella tertiolecta*, (3.5) (Falkowski & Owens 1980), a diatom, *Thalassiosira weissflogii*, (3.2) and a chrysophyte, *Isochrysis galbana*, (4.1) (Falkowski et al.

1985b), thus indicating that cryptophytes are not particularly inefficient in phenotypic photoadaptation.

In essence, microscopic algae are protein–synthesizing organisms with a capacity for metabolic diversity in different environmental conditions (Morris 1981). High PFD is said to be one of the conditions enhancing synthesis of non–nitrogen–containing storage products, such as carbohydrates, at the expense of protein synthesis, and this has also been proven with some haptophycean species (Claustre & Gostan 1987). Thinh (1983) found this with an unidentified *Cryptomonas*, where cells grown at 260 µmoles $m^{-2} s^{-1}$ contained four times more carbohydrates than cells at 10 µmoles $m^{-2} s^{-1}$. However, both of the cryptophyte species in this present study actually showed a slight decrease in carbohydrates at high PFDs. According to Morimoto & James (1969), larger cells under certain conditions can result from an increase in carbohydrate synthesis relative to protein synthesis, with carbohydrate being accumulated by the cell. No evidence to support this was found for L485 and L315, although in some treatments (e.g. L485, T=16 & T=21 °C) the maximum cell size coincided with maximum carbohydrate content. For a more conclusive analysis a mathematical relationship between carbohydrate content, growth rate and environmental parameters is required.

The protein pool can be used as a tool in photoadaptation in suboptimal light environment, as by decreasing it algae can reduce the energy required for cell division (Richardson et al. 1983). This has been proven, e.g. with *Euglena gracilis*, showing a lowered protein content close to compensation point (Cook 1963). However, the cryptophytes in this study did not seem to employ this strategy but instead they increased their protein pool at lower PFDs. They may have employed an alternative strategy of lowering rates of protein breakdown and resynthesis at low irradiance or the high protein pool could be explained by biliprotein accessory pigments brought into use in suboptimal light environments (cf. Gibson 1985). However, with the data available in this present study these hypotheses can neither be accepted nor denied.

Chapter 3

RATES OF PHOTOSYNTHESIS AND RESPIRATION OF TWO
CRYPTOPHYTES IN RELATION TO IRRADIANCE AND
TEMPERATURE

3.1 INTRODUCTION

The photosynthesis–irradiance curves similar in appearance to the curves describing the algal growth response in respect to changing light climate (cf. Chapter 2) play a central role in theoretical studies of algal production ecology, both in the field with natural phytoplankton assemblages and in the laboratory with unialgal cultures. In laboratory experiments they have been used in attempts to determine the photoadaptation strategies of algae, i.e. whether the adaptation happens through changing the number or the size of the photosynthetic units (PSUs) (for a review, see Richardson et al. 1983). In field studies limnologists have often striven for a mathematical formulation of this response in order to facilitate the calculation of primary production from some simple measurements instead of using laborious and time–consuming incubation techniques; according to Coté & Platt (1984) there is a good correlation between *in situ* production rates and production values computed from P vs. I curves. Mathematical formulations may also provide parameters with biological meaning, thus making intra– and interspecific comparisons possible. These formulations have been creditably reviewed by Jassby & Platt (1976), Iwakuma & Yasuno (1983) and Cosby et al. (1984).

The photosynthesis concept referred to in P vs. I studies is gross or net photosynthesis when photosynthetic rates have been determined by oxygen exchange (Cook 1963, Dunstan 1973, Humphrey 1975, Burris 1977, Falkowski & Owens 1980, Langdon 1987) or the more ambiguous ^{14}C productivity if measurements have been based on radioisotope incorporation (Platt & Jassby 1976, Taguchi 1976, Feuillade & Feuillade 1987, Neale & Richerson 1987). The first approach – even though regarded as an old–fashioned method– makes determination of respiration rate and hence net productivity possible, but compared to the interest in photosynthesis and production, algal respiration has received little attention. The reason for this neglect may be an impression that respiration is only a correction to be made when meas-uring photosynthesis. Also measuring the very small changes in dissolved oxygen creates severe practical problems. As a result, no feasible mathematical formulations describing net photosynthesis or respiration in respect of irradiance are available at

the moment, but all the equations have been designed either for gross photosynthesis or ^{14}C productivity.

The aim of this chapter is to describe the effects of light on gross photosynthesis, respiration and hence net productivity of the two cryptophytes, L485 and L315, used earlier in the growth experiments (Chapter 2). Thus, this study seeks to determine physiological explanations for the inter- and intra-specific growth differences of these two species. The interest is not directed towards the description of the effects immediately following a change in irradiance but effects obtained if the algae are allowed to adjust to the experimental conditions. As in the growth experiments in Chapter 2, temperature effects are also scrutinized and an attempt is made to describe mathematically the temperature response of photosynthetic capacity (i.e. maximum of gross photosynthetic rate) and optimum light intensity. Usually temperature has been ignored in experimental productivity studies (e.g. Cook 1963, Dunstan 1973, Humphrey 1975, Burris 1977, Langdon 1987). Taking into account the lack of existing net production and respiration models, mathematical formulation is only applied to the gross photosynthesis data; introduction of novel mathematical descriptions of net photosynthesis and respiration in relation to changing light environment was considered to be beyond the scope of this study.

3.2 METHODS

3.2.1 Phytoplankton cultures and experimental culture conditions

The experimental organisms were the two clonal, non-axenic *Cryptomonas* strains (L485 and L315) used in the growth experiments and they were grown in the same medium and under the same light-dark cycle (16:8) as in the previous experiments (Chapter 2). The light source in growth cabinet or water filled glass tanks (temperatures $\leq °10\ C$) was provided from below by cool-white fluorescent tubes and light intensities as photon flux densities (PFD) were measured with a 4π spherical digital scalar quantum meter (Biospherical Instruments Inc., model number QSP-170, probe

QSP–200) at the base of the cultures, as explained in Chapter 2. Cultures were incubated at temperatures 26 °C, 21 °C, 16 °C, 10 °C and 5 °C (L315 only) at a range of five different PFDs achieved with neutral density screening. Production and respiration measurements were always carried out with diluted cultures well below their maximum cell density, as it has been shown that respiration increases when cultures reach stationary phase (Ryther 1954).

3.2.2 Production and respiration measurements

Production and respiration measurements were based on oxygen concentration changes in incubated enclosed cultures. The ^{14}C uptake method could not be applied as the low pH in L485 cultures made the determination of total inorganic carbon by Gran titration impossible. A Rank oxygen–electrode (Rank Brothers, Cambridge, U.K.) was also tried, but found to be impracticable as fragile cryptohytes could not be heavily concentrated without changing their physiological state and thus lessening the relevance of the results. So, the concentrations of dissolved oxygen were measured by titrating with the Winkler (1888) method as described by Mackereth (1963). Titrations were carried out with a Metrohm Herisau Multi–Burette E 485 connected to a Metrohm Herisau E 549 automatic stirrer system. For the experiments, cultures were acclimatized for 2–3 days in the same irradiance–temperature conditions under which incubations were due to be carried out. The growth experiments had revealed this time period to be sufficient for the cultures to pass the possible time lag and enter the exponential growth phase. To start incubations, six glass stoppered Pyrex bottles of 100 ml for each PFD were filled with the acclimatized algal suspension. Two of the bottles were initials and were fixed immediately, while two were tightly wrapped in aluminium foil and incubated together with the two remaining light bottles. The incubation time varied with the experimental temperature, but was in the range of 2–5.5 hours. However, in the experiment carried out at 5 °C cultures were incubated for 16 hours, i.e over the whole light period. After incubation all the dark and light bottles were fixed and titrations were carried out immediately. Calculations of oxygen concentrations were based on means of duplicate measurements.

In experiments with L315, incubations always started at the onset of the light period. With L485 this arrangement was not possible, as due to the low pH (pH < 4.0) and thus the small inorganic carbon pool – all of which was in the form of CO_2 – cultures enclosed in the bottles exhausted carbon in a couple of hours, making production measurements unreliable (cf. Johnson et al. 1970, Schindler & Fee 1973, Burris et al. 1981, Olaveson & Stokes 1989). To avoid this, bottles were filled with the algal suspension at the beginning of the preceding dark period and left overnight to respire and produce CO_2, which was then used during the light incubation. These bottles were not opened until the end of the light incubation.

Results were calculated as mg O_2 h^{-1} g^{-1} C and mg O_2 h^{-1} mg^{-1} chl *a*. Samples for chlorophyll *a* and particulate carbon (POC) determinations were taken from the acclimatized algal suspensions prior to incubations. Concentrations of chlorophyll *a* were calculated with trichromatic equations (Strickland & Parsons 1968) from the absorbance of pigments extracted with 90 % alkaline acetone (Wetzel & Likens 1979) from particulate material separated from the water by vacuum filtration onto 4.7 cm Whatman GF/C glass fibre filters. The procedure was completed by grinding the cells with a pestle and mortar. Absorbances of pigment extracts were measured with a Shimadzu UV–150–02 double beam spectrophotometer.

For the POC determinations, 5–10 ml of algal suspension was filtered onto a pre–combusted Whatman GF/F glass fibre filter and stored in a desiccator before analysis with a Unicarb Universal Carbon Analyzer. In this method POC is determined as CO_2 with an infrared gas analyser after high temperature (900 °C) combustion (Salonen 1979, 1981). Samples were run in duplicate and averaged at the end.

Mathematical equations were fitted to the experimental data using a computer program written by Dr I. Hakala (University of Helsinki, Lammi Biological Station) based on the Simplex algorithm (Caeci & Cacheris 1984).

3.3 RESULTS

3.3.1 Gross photosynthesis

The mathematical equations fitted to the gross photosynthesis data were the hyperbolic tangent function (Platt & Jassby 1976), Steele's (1965) empirical model, Parker's (1973) modification of Steele's (1965) model and the Michaelis– Menten equation. The hyperbolic tangent function and Michaelis–Menten equation are saturation models, whereas the models of Steele (1965) and Parker (1973) can also be applied to data showing photoinhibition at higher PFDs. The equations and parameters of these models are displayed in Table 3.1.

None of these equations was superior in describing the photosynthetic performance of L485 or L315. Models designed for saturation curves must be rejected as although they in general provided a good description, they could not be fitted to the L485 data at 21 °C and L315 data at 10 °C which both clearly showed photoinhibition at higher PFDs. Steele's (1965) and Parker's (1973) empirical models both gave a reasonably good fit, but the first one was preferred as it relies only on two parameters both of which are ecologically meaningful. The observed gross photosynthetic rates (mg O_2 h^{-1} mg^{-1} chl a) as a function of irradiance for each experimental temperature are illustrated in Figs. 3.1 and 3.2. Besides the observed rates, the fitted Steele's (1965) functions and the estimated slopes, i.e. photosynthetic efficiencies (mg O_2 h^{-1} mg^{-1} chl a (μmoles m^{-2} s^{-1})$^{-1}$), of the light–limited parts of the curves are shown. The maximum gross photosynthetic rates P_{max}, expressed as mg O_2 h^{-1} g^{-1} C and mg O_2 h^{-1} mg^{-1} chl a, and estimated from the model are presented in Table 3.2. Also shown are the corresponding optimum PFDs computed on a carbon as well as on a chlorophyll a basis (Table 3.3).

Figs. 3.1 and 3.2 show that Steele's (1965) empirical model could satisfactorily describe the gross photosynthetic rate of both of the species in respect of changing PFDs. However, the peculiar response of L315 at 10 °C could not be adequately described with this model. To verify this unexpected response curve the whole

Table 3.1. Mathematical equations fitted to the gross photosynthesis data. P_{max} is the maximum rate of gross photosynthesis, I_k (saturation onset parameter) is the photon flux density at which the initial slope line reaches the photosynthetic rate of P_{max}, I_{opt} is the saturating PFD, and m is a shape parameter for the curve.

Equation	Author
$P=P_{max}*Tanh(I/I_k)$	Platt & Jassby (1976)
$P=P_{max}*I/I_{opt}*exp(1-I/I_{opt})$	Steele (1965)
$P=P_{max}*\{I/I_{opt}*exp(1-I/I_{opt})\}^m$	Parker (1973)
$P=P_{max}*I/(k+I)$	Michaelis–Menten equation
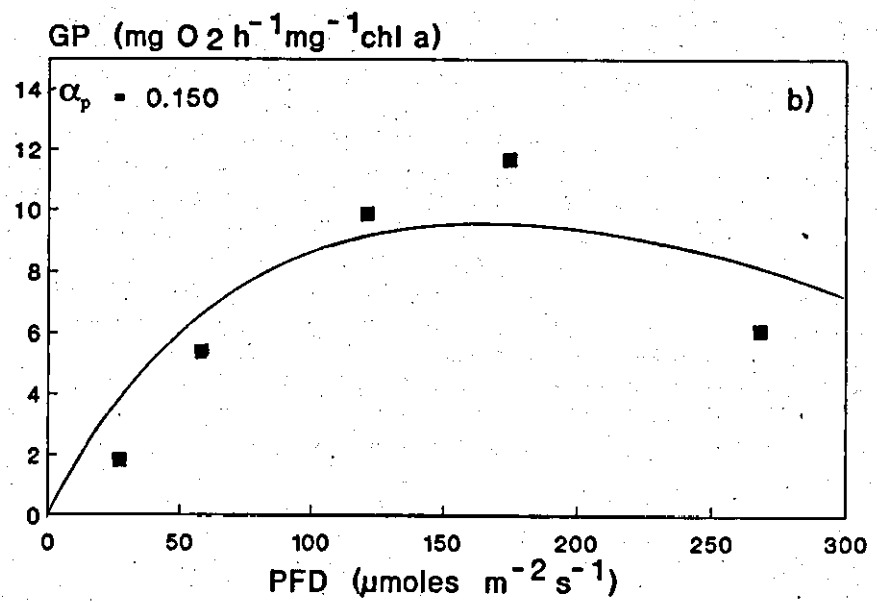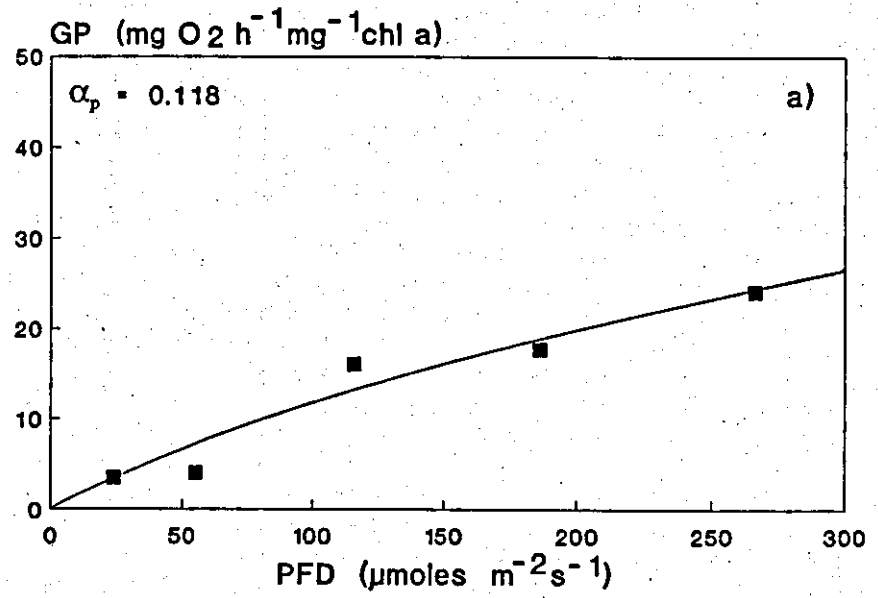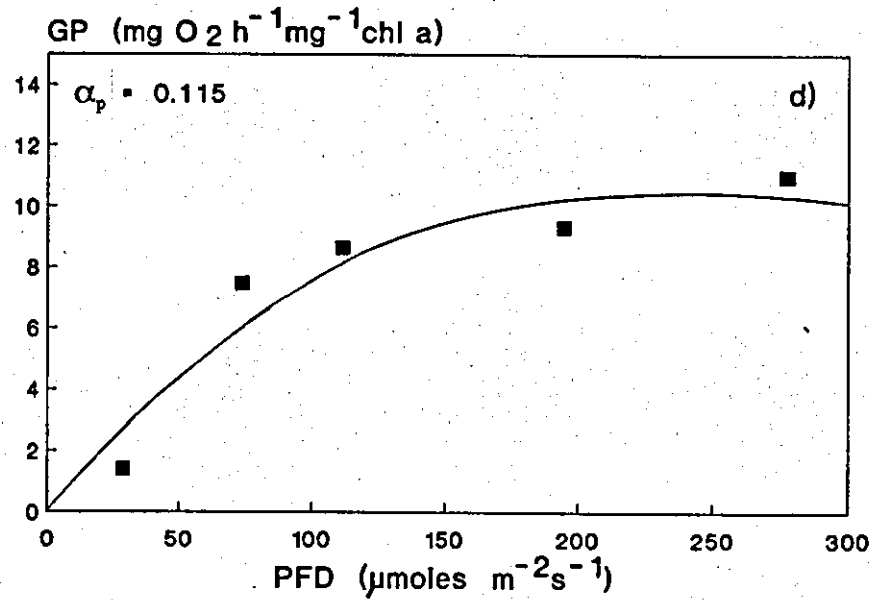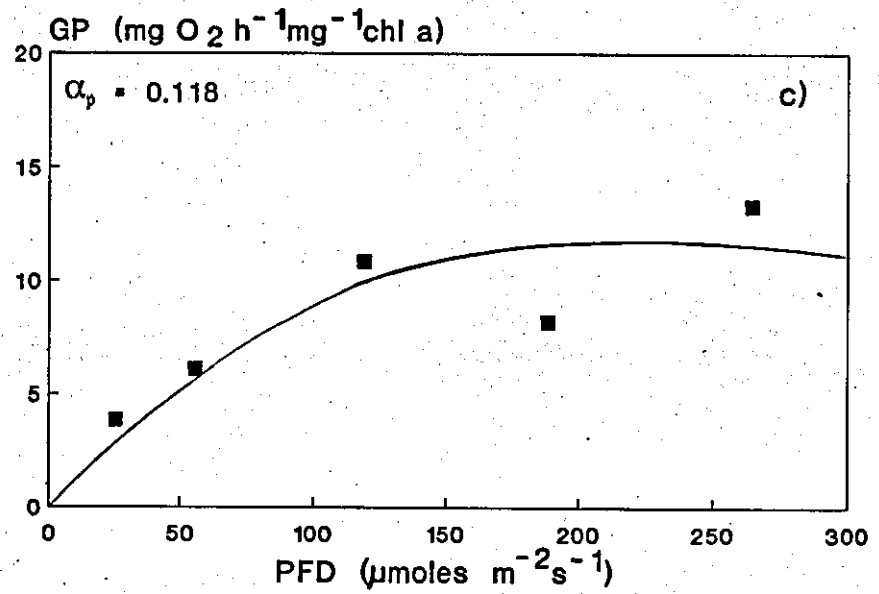
Fig. 3.1. Gross photosynthesis (GP) vs. irradiance relationship in L485 at different temperatures. a=26°C, b=21°C, c=16°C, d=10°C.

GP (mg O$_2$ h^{-1}mg^{-1}chl a)

α_p = 0.077

c)

PFD (μmoles m^{-2}s^{-1})

GP (mg O$_2$ h^{-1}mg^{-1}chl a)

α_p = 0.100

d)

PFD (μmoles m^{-2}s^{-1})
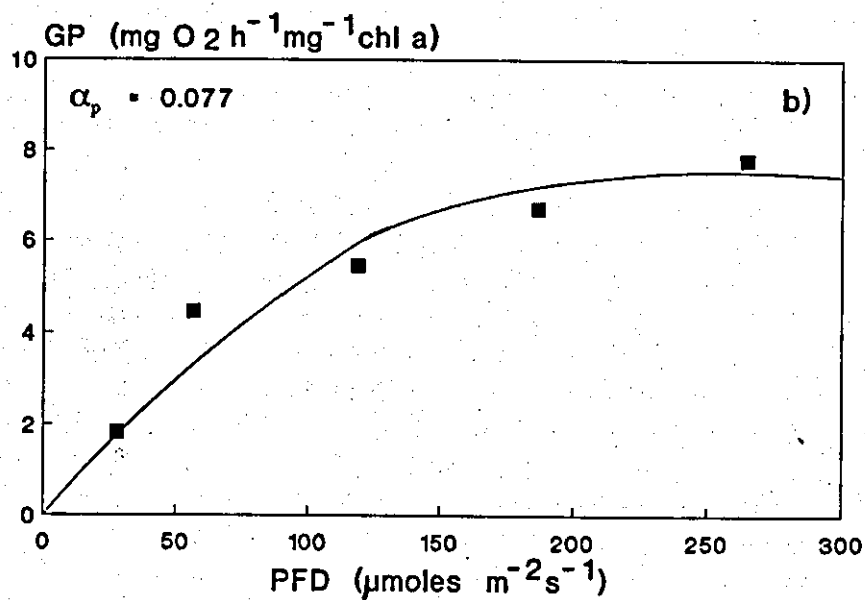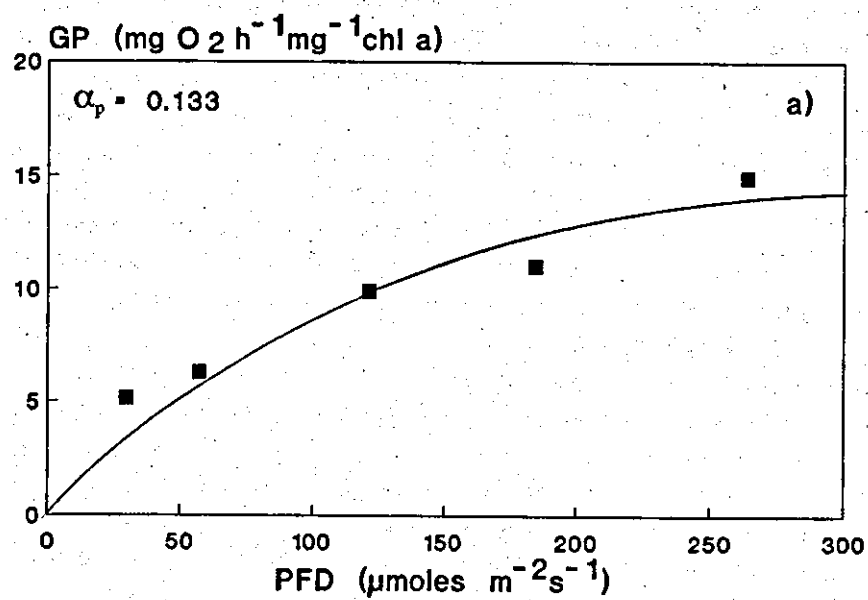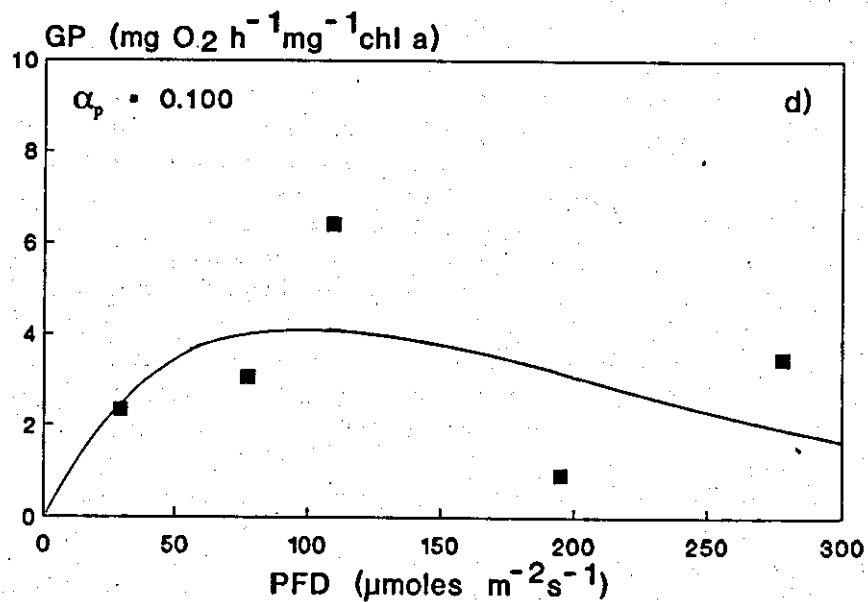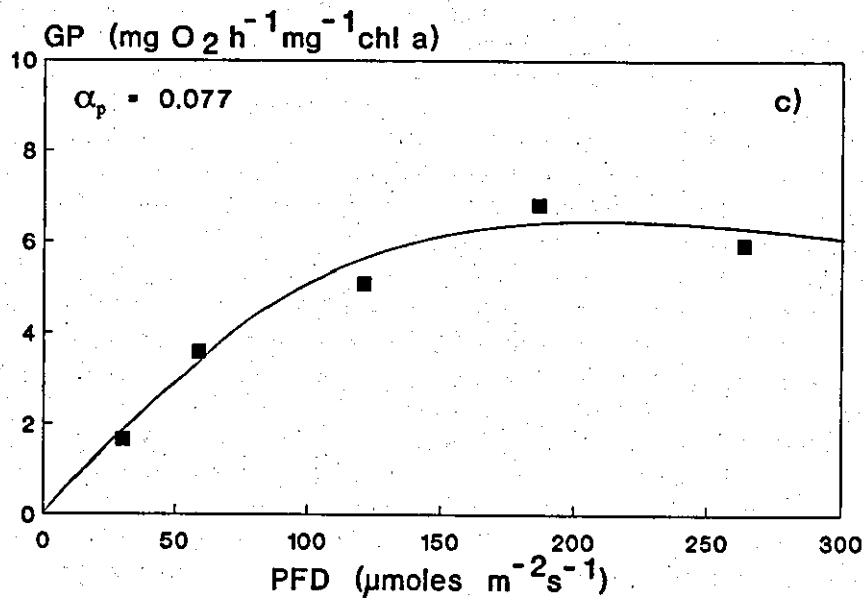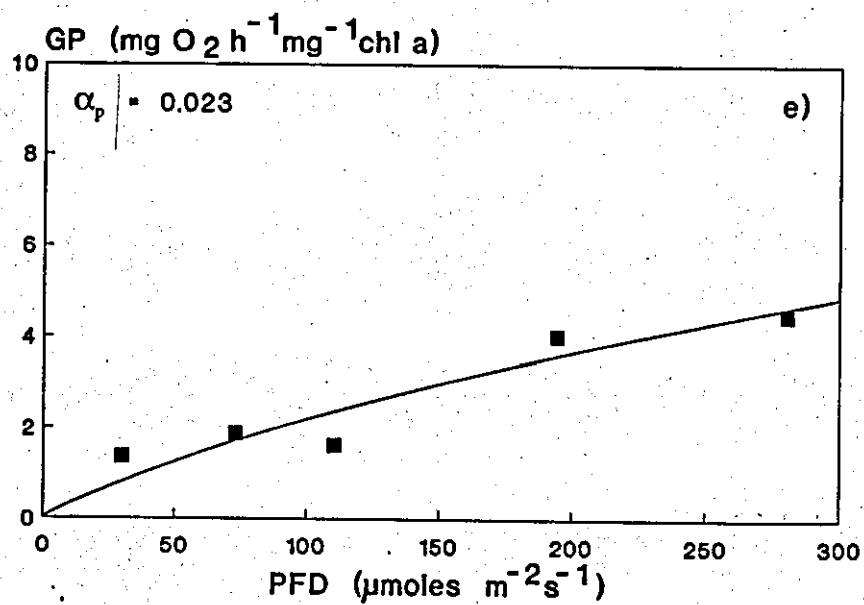
Fig. 3.2. Gross photosynthesis (GP) vs. irradiance relationship in L315 at different temperatures. a=26°C, b=21°C, c=16°C, d=10°C, e=5°C.

Table 3.2. Maximum gross photosynthetic rates (P_{max}, mg $O_2\,h^{-1}g^{-1}$ C and mg $O_2\,h^{-1}mg^{-1}$ chl *a*) of L485 and L315 estimated from Steele's (1965) equation.

Temperature (°C)	P_{max}, mg $O_2\,h^{-1}g^{-1}$ C		P_{max}, mg $O_2\,h^{-1}mg^{-1}$ chl *a*	
	L485	L315	L485	L315
26	128.7	53.9	31.7	14.1
21	81.0	110.1	9.5	7.5
16	80.8	55.5	11.5	6.3
10	66.9	16.9	10.7	3.9
5		6.9		6.4

Table 3.3. Optimum photon flux densities (I_{opt}, μmoles m^{-2}s^{-1}) of L485 and L315 estimated from Steele's (1965) equation.

Temperature (°C)	I_{opt}, carbon (μmoles m^{-2}s^{-1})		I_{opt}, chl a (μmoles m^{-2}s^{-1})	
	L485	L315	L485	L315
26	299	155	653	301
21	89	284	154	253
16	180	151	239	222
10	192	99	259	96
5		218		707

experiment was repeated but with the same final result (results not shown). Table 3.2 reveals that the photosynthetic performance of L485 was usually better than that of L315 irrespective of the basis on which the results were calculated. It also shows the tendency of optimum PFDs to be higher when computed from chlorophyll based data than from data expressed per unit carbon. This is especially clear with L485 and is caused by the inconstancy of carbon to chlorophyll ratios (Tables 3.4 and 3.5), which tend to increase towards higher PFDs. In L315 ratios were generally higher than in L485 and high ratios were ~~especially~~ recorded at extreme temperatures.

The effects of the changing temperature were analyzed using the temperature response model of Logan et al. (1976) which describes the temperature dependence of maximum gross photosynthetic rate and optimum PFD with the following equation:

$$A(T) = \alpha * \{\exp(\beta * T) - \exp(\beta * T_m - t)\}, \qquad (1)$$
$$t = (T_m - T)/\Delta T, \qquad (2)$$

where α is the rate of a temperature-dependent process at some basal temperature, β can be interpreted as a composite Q_{10} value for critical biochemical reactions, T_m is a thermal maximum or an upper lethal temperature, ΔT is the temperature range over which thermal breakdown becomes the overriding influence. This same model was also applied in the analysis of the growth rate data in Chapter 2. Fig. 3.3 illustrates the temperature optimum function of the maximum photosynthetic performance of L315 calculated on carbon basis. The data at 5 °C were not included in the fitting procedure as they were clearly different from data at other temperatures, and the carbon to chl a ratios indicated cells in a physiologically different state (Table 3.5). For L485 the temperature data could not be fitted as the data did not follow the assumptions of the model. Fig. 3.3 reveals that the chosen model could well describe the change in the photosynthetic maximum performance of L315 in relation to increasing temperature. It predicts that the optimum and lethal temperatures for L315 are ca 23.2 °C and 26.8 °C, respectively. The parameters of this equation and those of the optimum PFD vs. temperature equation (Fig. 3.4) are displayed in Table 3.6. The results reveal that when the temperature increases there is a shift in optimum PFDs of L315 towards higher values until a certain temperature

Table 3.4. Carbon to chlorophyll a (C:chl a) ratios of L485 at different PFD (μmoles $m^{-2}s^{-1}$) and temperature (°C) combinations.

PFD/Temperature	10	16	21	26
280	174			
265		163	133	197
195	149			
185		116	201	130
120		136	161	178
110	152			
74	125			
56		117	65	81
30	108			
26		141	42	110
Mean	150	133	141	146

Table 3.5. Carbon to chlorophyll *a* (C:chl *a*) ratios of L315 at different PFD (μmoles m^{-2}s^{-1}) and temperature (°C) combinations.

PFD/Temperature	5	10	16	21	26
280	633	207			
265			162	60	312
195	659	175			
185			135	94	217
120			91	78	195
110	294	268			
74	383	234			
56			77	58	181
30	441	178			
26			60	46	186
Mean	482	212	105	67	218
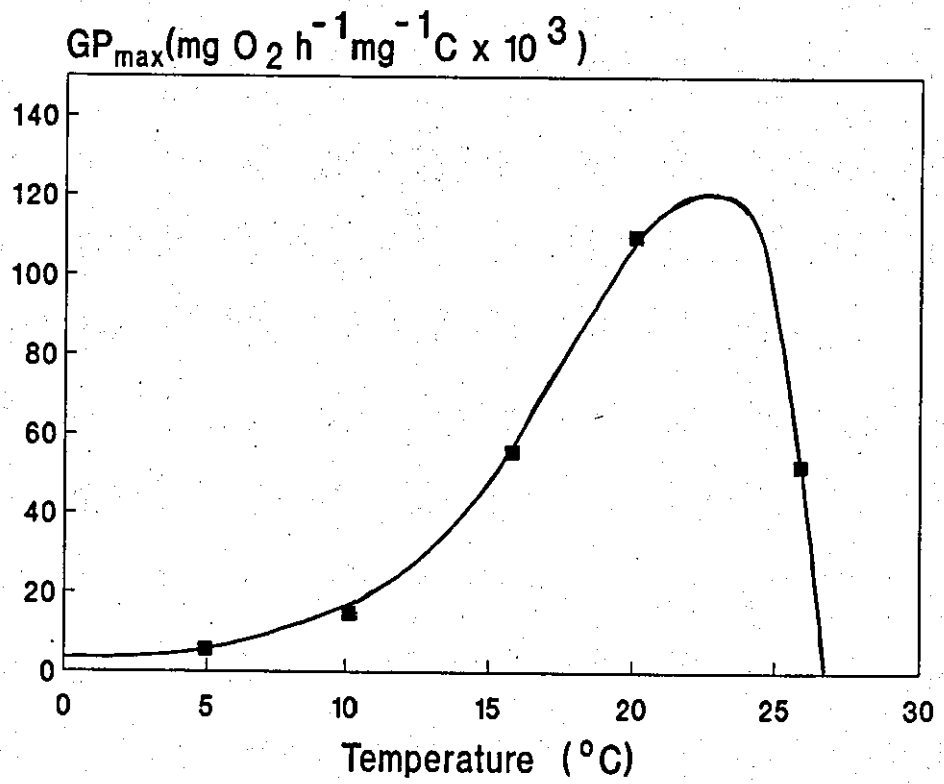
Fig. 3.3. Maximum photosynthetic performance (GP_{max}) of L315 in relation to temperature. The fitted temperature optimum function of Logan et al. (1976) is shown with a solid line.
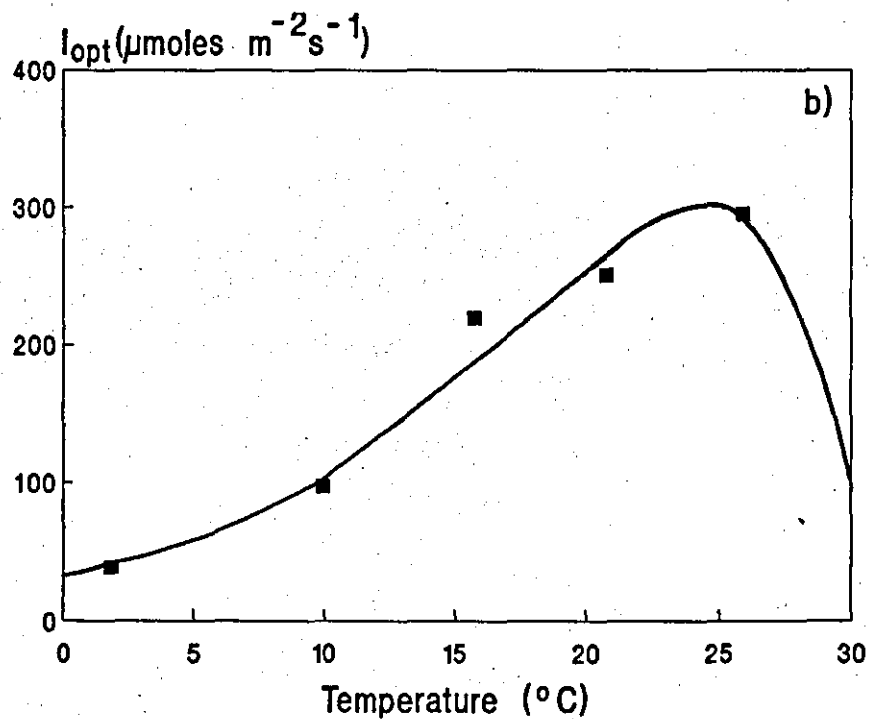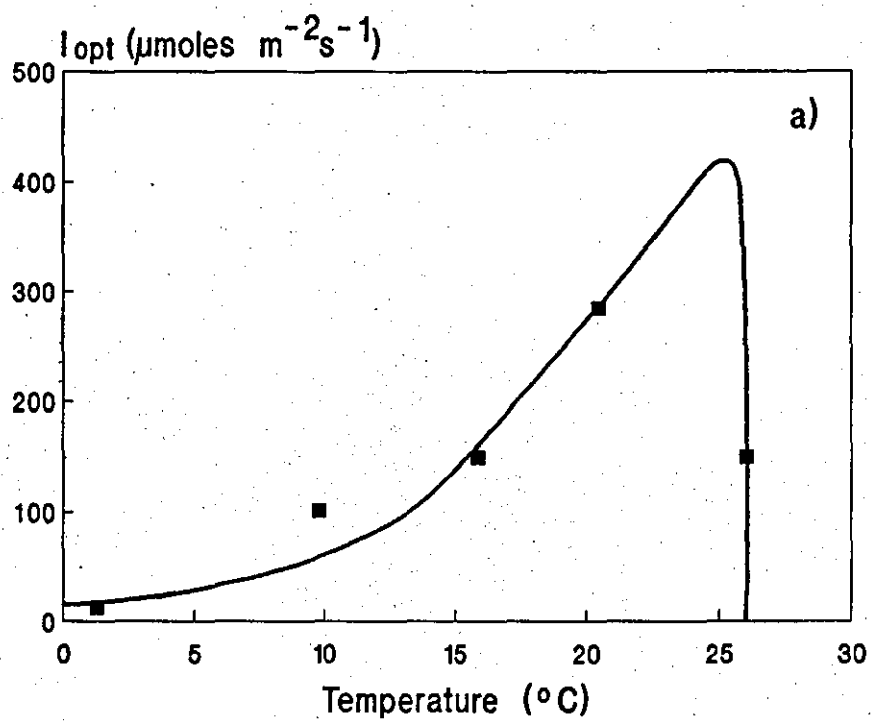
Fig. 3.4. Optimum irradiance (I_{opt}) of L315 in relation to temperature. Results are based on both on gross photosynthesis data on a carbon (a) and on a chl a (b) basis. The fitted temperature optimum functions of Logan et al. (1976) are shown with solid lines.

Table 3.6. Parameters of temperature dependence functions for the gross maximum photosynthesis (P_{max}) and the optimum light intensity (I_{opt}) of L315. Parameters for the gross maximum photosynthesis have been calculated from the data expressed per unit carbon, for optimum PFD from the data expressed both per unit carbon as well as chl *a*.

	P_{max}	I_{opt}	
		Carbon	Chl *a*
α	3.314	2.418	6.259
β	0.236	0.117	0.149
T_m	26.80	26.18	30.74
ΔT	3.554	0.479	5.852

is reached. After that, a rapid decline follows. This optimum estimated from the curves is ca 24–25 °C, i.e. somewhat higher than deduced from the photosynthetic performance curve. There are minor discrepancies also in the lethal temperature estimates. Parameter β values reveal that the gross maximum photosynthesis is more sensitive to temperature changes than the optimum PFD.

3.3.2 Respiration

Respiration rates of L485 and L315 at different PFD–temperature combinations are shown in Tables 3.7 and 3.8. Results are expressed as oxygen uptake per unit carbon as respiration rates are more closely related to the plasma content of cells than to their chlorophyll content (Jones 1977). Compared to the results on the gross photosynthetic rates, those of dark respiration are more ambiguous. With L485 especially, the lowest dark respiration rates were measured at the lowest PFDs, but after an 8 h exposure to total darkness the effects of light history on respiration were small. The temperature dependence of both species show the classical response of higher dark respiration rates at higher temperatures. The rates of L315 measured at 26 °C were usually lower than those measured at 21 °C and indicated the existence of a temperature 'optimum' (T_{opt}) at which the maximum respiration occurs. To determine whether this temperature optimum differs from the optimum for gross photosynthetic rate, the temperature dependence function of Logan et al. (1976) was fitted to data from five temperature experiments at a constant PFD, and the optimum temperature was computed. Results from these fittings are shown in Fig. 3.5 excluding the data from 185/195 μmoles m^{-2} s^{-1} as in this case fitting was not successful due to the low respiration rate at 21 °C. Estimated optimum temperatures vary from 23 to 25 °C giving an average of 24 °C. Thus, the temperature optimum of respiration can be said to coincide with the temperature optimum of the gross photosynthesis. The composite Q_{10} (β) values showed that the overall respiration rates depend on the light history of algae, as algae grown under 26/30 and 56/74 μmoles m^{-2} s^{-1} had lower β values (0.09 and 0.22, respectively) than algae at 110/120 and 185/195 μmoles m^{-2} s^{-1} (0.43 and 0.41, respectively).

Table 3.7. Respiration rates (mg $O_2h^{-1}g^{-1}$ C) of L485 at different PFDs (μmoles $m^{-2}s^{-1}$) and temperature (°C) combinations.

PFD/Temperature	10	16	21	26
280	37.28			
265		44.44	7.75	65.90
195	21.57			
185		16.38	22.44	23.44
120		38.96	17.45	43.91
110	29.59			
74	46.17			
56		21.24	42.14	21.65
30	7.07			
26		5.43	27.29	14.85
Mean	28.34	25.29	23.41	33.95
SD	14.98	16.15	12.72	20.90

Table 3.8. Respiration rates (mg $O_2h^{-1}g^{-1}$ C) of L315 at different PFDs (μmoles $m^{-2}s^{-1}$) and temperature (°C) combinations.

PFD/Temperature	5	10	16	21	26
280	5.39	13.92			
265			11.93	75.73	20.46
195	2.10	13.42			
185			24.93	17.37	17.96
120			5.98	44.38	11.58
110	2.85	15.18			
74	1.42	9.33			
56			28.46	43.36	24.03
30	8.03	12.14			
26			17.45	32.86	16.37
Mean	3.96	12.80	17.75	32.74	18.08
SD	2.73	2.22	9.20	21.41	4.64

Respiration (mg $O_2 h^{-1} g^{-1} C$)
a) 280/265

Temperature ($^\circ$C)

Respiration (mg $O_2 h^{-1} g^{-1} C$)
b) 110/120
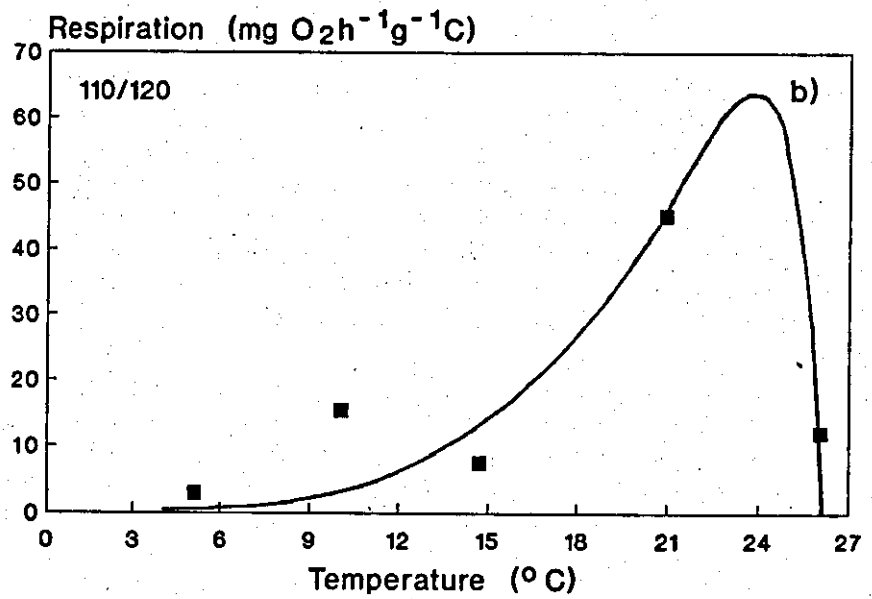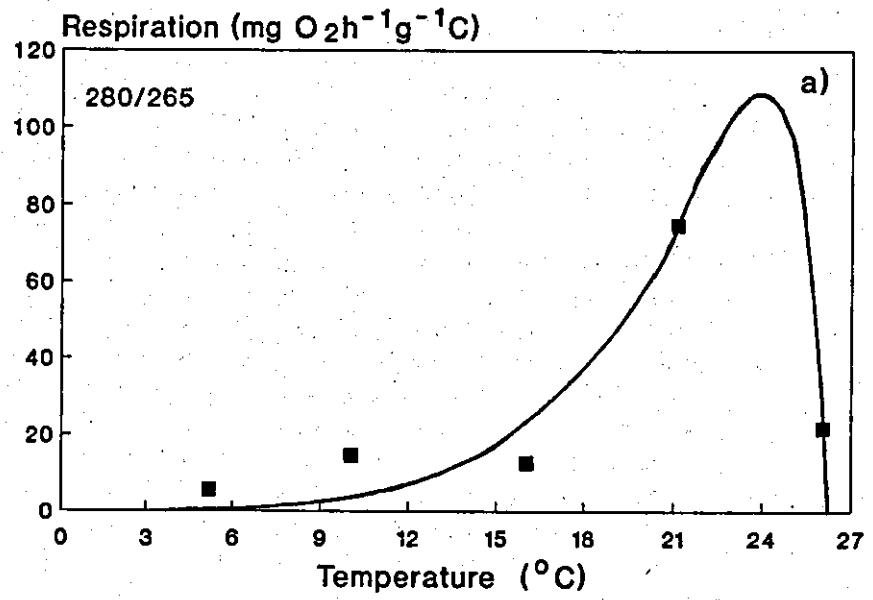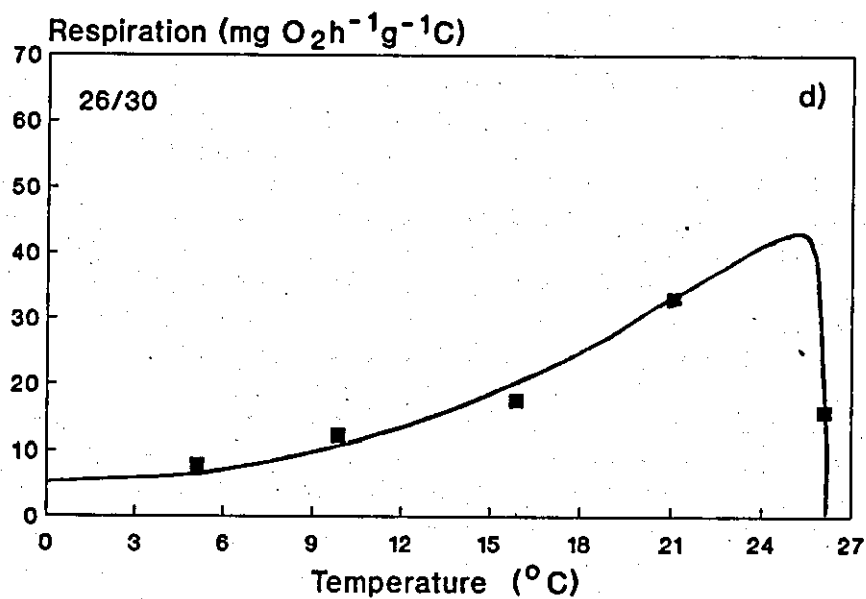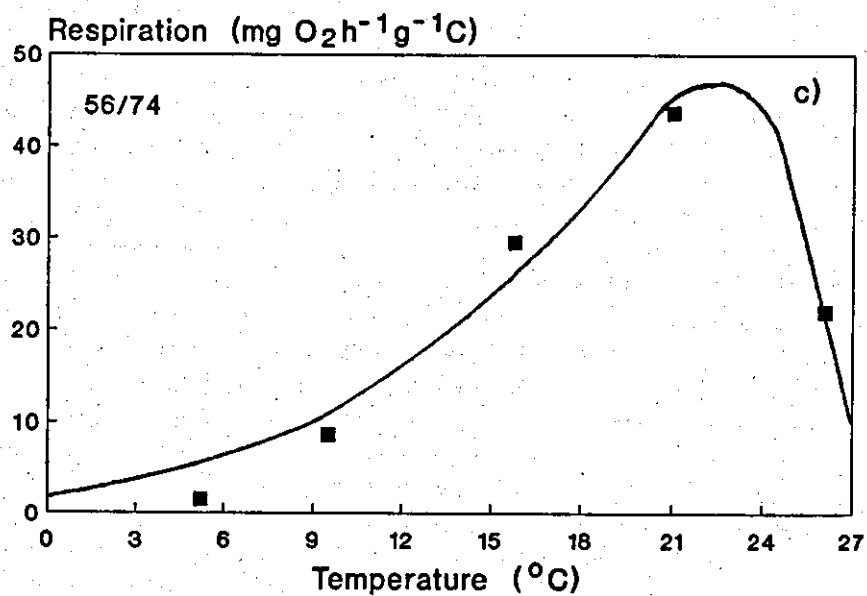
Temperature ($^\circ$C)

Fig. 3.5. Respiration (mg O_2 h^{-1} g^{-1} C) of L315 in relation to temperature at different PFDs (μmoles $m^{-2}s^{-1}$) indicated in the left top corner. Solid black lines show the fitted functions of Logan et al. (1976).

There were species–specific differences in carbon–specific oxygen uptake rates as shown in the means at different temperatures. The respiration rates of L485 were in general higher than those of L315, although the difference in overall respiration rates (27.7 mg O_2 h^{-1} g^{-1} C and 22.8 mg O_2 h^{-1} g^{-1} C for L485 and L315, respectively) – calculated as a mean at the temperature range 10–26 °C – was not statistically significant ($p > 0.05$). The rates of L315 at 5 °C were lower than in any other treatment, but as no experiments with L485 at 5 °C were carried out, it cannot be concluded whether this reduction in rates at low temperature is a common feature amongst cryptophytes or whether it is a species–specific phenomenon. Species–specific differences and a size–dependence could be seen in respiration rates calculated on per cell basis as is shown in Fig. 3.6. Linear regression of respiration/cell volume from the logarithmically transformed data gives a correlation coefficient of 0.86 and a slope of 0.76. Cell volumes for this analysis have been taken from the growth experiment data and respiration results were converted to carbon by an RQ value of 1. The lower and upper clusters of points in Fig. 3.6 represent L485 and L315, respectively and show the ca 10–fold size difference of these species (cf. Chapter 2).

3.3.3 Net photosynthesis

Net production as a percentage of gross photosynthesis is illustrated in Fig. 3.7. L485 showed positive net production at every temperature/PFD combination, but with L315 net production was negative, i.e. cells were utilizing storage products, in the treatments T=5 °C/PFD=30 μmoles m^{-2} s^{-1}, T=10 °C/PFD=74, 195 and 280 μmoles m^{-2} s^{-1}. These results are at odds with the growth results presented in Chapter 2 as L315 exhibited a positive net growth in all these conditions. A net production in this strain was also observed at all PFDs tried at T=26 °C, which is suprising as according to the growth experiments in Chapter 2, T=23 °C is lethal to this species. At 26 °C this species respires 22–79 % of its gross production and the rest must therefore be excreted. The proportion of excreted production is higher at higher PFDs. The largest proportion (83 %) of the L485 gross photosynthesis going to net production was observed at 26 °C and 185 μmoles m^{-2} s^{-1}. In L315 the optimum for net
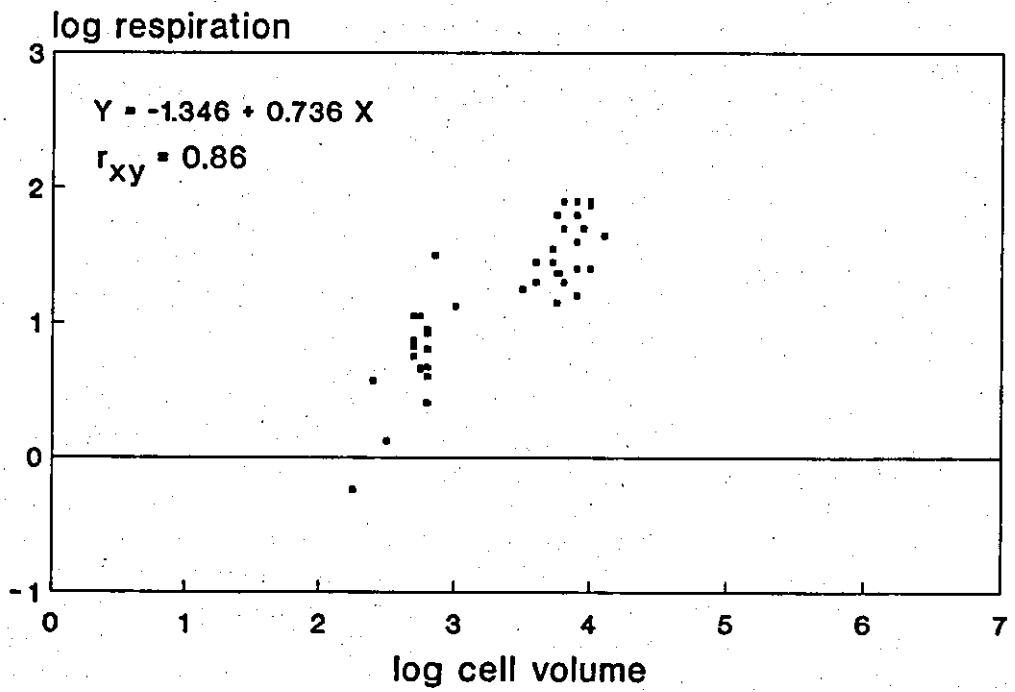
Fig. 3.6. Size–dependence of respiration in L485 and L315. Cell volume was expressed as μm^3 and respiration as mg C $h^{-1}/10^9$ cells.
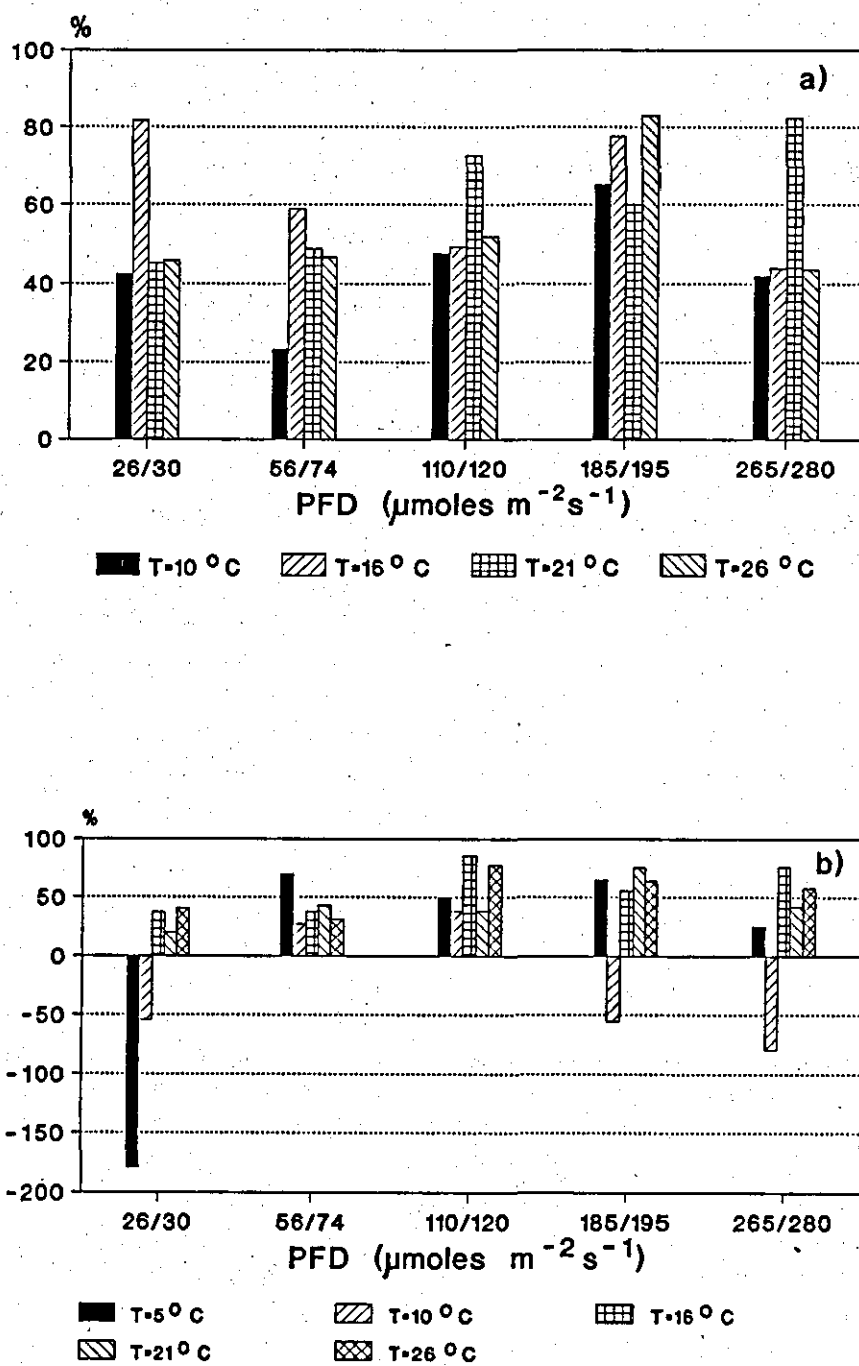
Fig. 3.7. Net production of L485 (a) and L315 (b) in different irradiance/temperature conditions as a percentage of gross photosynthesis.

production (86 %) was recorded at $\overset{16}{\cancel{10}}$ °C and $\overset{110/120}{\cancel{74}}$ µmoles m^{-2} s^{-1}. The maximum absolute values for L485 and L315 were recorded at 26 °C and 185 µmoles m^{-2} s^{-1} (114.0 mg O$_2$ h^{-1} g^{-1} C) and 21 °C and 265 µmoles m^{-2} s^{-1} (54.7 mg O$_2$ h^{-1} g^{-1} C), respectively.

3.4. DISCUSSION

The exponential inhibition equation of Steele (1965) was found to be the most practicable model to describe the photosynthetic performance – irradiance relationship of cryptophytes L485 and L315, has been widely used in simulation studies for its ease of integration and few parameters (e.g. Takahashi et al. 1973). It has also been successfully applied in growth studies (e.g. Cloern 1977, Gavrieli 1984) and proved to be a powerful tool in growth vs. irradiance analysis of the cryptophytes used in the present study (Chapter 2). However, it cannot be regarded as a universal solution to problems like this, as models found suitable for growth description are not necessarily useful for photosynthesis vs. light relationships and vice versa. Photosynthetic rate and growth rate can have quite different responses to light and temperature, the first being an immediate one and the second the delayed one. There are reports showing Steele's (1965) equation sometimes giving the most inappropriate fits amongst several models (Iwakuma & Yasuno 1983) and some P vs. I relationships of the cryptophytes L485 and L315 are not perfectly described by this model. The best model would have been a combined saturation– inhibition model – a more sophisticated version of the combination of ascending and descending regression lines (e.g. Knoechel & Kalff 1978). Neale & Richerson (1987) have made a proposal for such a model by combining the hyperbolic tangent function and an inhibition function. However, this approach was here rejected as their function is descrete at the point where the saturation model is changed to a photoinhibition model.

It has been demonstrated with diatoms that growth rates are determined primarily by maximum photosynthetic rates (Knoechel & Kalff 1978). This was also evident with the cryptophytes as L485, which was shown to have a greater growth ability (Chapter 2), exhibited higher rates of maximum gross photosynthetis. In addition to temperat-

ure, photosynthetic performance is said to be controlled by nutrients (which in these experiments were available in excess) and photosynthetic efficiency, α_p. This efficiency has been claimed to be equivalent amongst microalgae (e.g. Dunstan et al. 1973), but Platt & Jassby (1976) and Taguchi (1976) have disputed this view and showed α_p to be variable, as in large cells shading by the chloroplast itself decreases the efficiency of light–utilization. Results supporting the latter observations were also obtained with cryptophytes. The smaller L485, which had lower carbon to chl a ratios and higher growth efficiencies, had in general higher α_p values. Because the experiments with L485 and L315 were carried out under near steady–state conditions, estimates of α_p should be more reliable than if they were derived from conventional P vs. I experiments in which species grown at one PFD is rapidly exposed to a range of irradiances for short periods of time (Langdon 1988). In steady–state conditions α_p of the cryptophytes, especially that of L485, seemed to be independent of temperature (cf. Post et al. 1985).

The observed increase in the optimum PFD of L315 in respect of rising temperature was unexpected, as in the growth experiments the light saturation of this strain was exceptionally insensitive to temperature (Chapter 2). In this respect results for L485 were different as its optimum PFD could not be fitted into the model of Logan et al. (1976), unlike the data for growth. These contradictory results differ from the observations of Morgan & Kalff (1979) and Gavrieli (1984) who showed that the optimum PFD for carbon uptake and growth of *C. erosa* and *R. lacustris* responded in a similar way to changing temperature. The results for L315 obtained at 10 °C, i.e. strong photoinhibitory reaction at higher PFDs, possibly had a contributory influence on fitting, but this P vs. I curve with a sharp inflection could not simply be excluded as the result was confirmed by repeating the experiment and L315 was also the species showing a strong photoinhibition at 12 °C in the growth experiments. It cannot be certain whether the deviation from the pattern of other experiments was due to experimental errors or real physiological changes at 10–12 °C; anomalous photosynthesis results at 10 °C have also been recorded for natural algal assemblages (Megard et al. 1984).

As shown in the growth experiments with L485 and L315 in Chapter 2, the physiological state, even in exponentially growing cultures, varies with growth

conditions. This can be seen in the biochemical composition of algal cells and, vice versa, should also be reflected in their energy requirements. Richardson et al. (1983) have postulated that a higher protein content of cells implies a higher maintenance energy requirement related to protein degradation and resynthesis so that low–protein cells could economize on maintenance as well as capital costs.The importance of protein turnover in maintenance metabolism has also been emphasized by Penning de Vries (1975). According to a simplified growth energetics model $\mu_r = \mu_0 + S\mu$, where μ_r is the biomass–specific energy consumption rate, μ_0 is the maintenance metabolic rate, S is the dimensionless cost of synthesis and μ growth rate (Geider & Osborne 1989), this economizing could then be seen in lower respiration rates. These ideas can be examined with this study combined with the protein/carbohydrate results of Chapter 2. Amongst the 45 treatments tried with L485 and L315 there were 7 showing clearly lower respiration rates, i.e. all treatments with L315 at 5 °C and treatments of T=16 °C, I=26 μmoles m^{-2} s^{-1} and T=10 °C, I=30 μmoles m^{-2} s^{-1} with L485. However, in all of the corresponding treatments in the growth experiments protein/carbohydrate ratios were high, and not low as would be expected according to the arguments of Richardson et al. (1983). High protein contents were evident in relative (μg μm^{-3}) as well as in absolute units (μg cell^{-1}). Taking into account the results from the growth experiments showing that growth rates were low and cells small in these treatments, these results can be intepreted to show that high maintenance requirements of protein pool were compensated with low overall growth costs. They can also be seen as supporting Gibson's (1975) results on a positive correlation between algal respiration rate and carbohydrate content.

Besides the physiological state and biochemical composition, maintenance energy requirements have been said to be dependent on the contact area between the algal cell and environment, and thus on cell size. This so–called surface law also predicts that the exponent of the allometric equation for respiration approximates a value of 0.67, and Laws (1975) has come very close to this estimate by using the recalculated data of Eppley & Sloan (1965). The exponent for the allometric equation obtained in this study is somewhat higher, but is still in agreement with Laws's (1975) state-ment that large single phytoplankton cells catabolize a smaller fraction of their biomass than do small cells. Banse (1976) has suggested a value of 0.75 for this exponent, which is very similar to the value (0.76) obtained in this study.

Since Steemann Nielsen & Hansen (1959) suggested a value of 10 % for the respiration/photosynthesis ratio it has commonly been used in productivity models (e.g. Laws 1975). Compared to this value the observed respiration/photosynthesis ratios in this study are high, as in L485 and L315 respiration accounted for 17–77 % and 14–81 % of gross photosynthesis, respectively, if treatments showing negative net growth were not included. Under optimum conditions the respiration/P_{max} ratio for L485 was 17 % and for L315 58 %. However, in addition to the present study there are other observations indicating that the value of 10 % is an underestimate, as natural phytoplankton communities have been shown to respire > 30 % of photoas-ssimilated carbon (e.g. Devol & Packard 1978) and in unialgal cultures respiration usually accounts for ca. 25 % of gross photosynthesis (Falkowski & Owens 1978). The respiration/photosynthesis ratio has been shown to vary with taxon, being highest in dinoflagellates, which have been recorded to have ratios of dark respiration to light–saturated photosynthesis from 11 % to 59 % (Geider & Osborne 1989). It has also been noticed that some species as identified being genotypically adapted to high light exhibit considerably higher respiration ratios overall (Richardson et al. 1983). Apart from the present data on L485 and L315 there are no published data available on cryptophytes and thus no comparisons are possible, but the role of dark respiratory processes in cell metabolism seems to be as important in cryptophytes as in dinoflagellates. The overall respiration ratio of L485, calculated as a mean at the temperature range 10–26 °C and excluding the ratios higher than 100 %, was lower (41 %) than that of L315 (50 %), i.e. L485 was more efficient in assimilation, but the difference is very small. Including all the data at 10–26 °C the ratio of L315 would be 67 %. Thus, even though L485 with higher compensation PFDs for growth had higher absolute respiration rates it seemed to be more efficient in energy transfer than L315.

Falkowski & Owens (1978) have suggested that the high respiration rates of flagellates is related to their motility, but Raven & Beardall (1981) and Raven & Richardson (1984) have showed that the respiration associated with motility is only a small fraction of the maintenance respiration. However, Raven (1980) has pointed out that flagellate cells are effectively wall–less with respect to osmoregulation even when they possess a wall, as the flagellar membrane is always wall–less and volume

regulation in this type of cell requires an extra expenditure of energy. Nevertheless, flagellates do not always show exceptionally high respiration rates. Ryther (1954) measured a respiration ratio of only 5-10 % for an exponentially growing *Chlamydomonas* sp. culture although Harris & Piccinin (1983) demonstrated that *Chlamydomonas reinhardtii* uses 1/3 of its gross production in respiration. Ryther's (1954) study also emphasized the importance of culture conditions for respiration, as he showed respiration ratios to increase to 50 % as the population maximum was reached and equalling photosynthesis in ageing cultures. However, the age of culture cannot explain the high respiration ratios of this study as only diluted cultures in exponential growth phase were used in these experiments.

As the "light-and-dark" bottle technique measures photosynthetic production of oxygen instead of carbon incorporation, it does not discriminate between the net production used in growth or alternatively excreted. Thus, with this method it is possible to get positive net production results in extreme conditions, where growth of cells has ceased, as was the case with L315 at temperature 26 °C. Healthy cells usually excrete less than 10 % of assimilated carbon (e.g. Sharp 1977, Mague et al. 1980, Zlotnik & Dubinsky 1989), but because the realease of DOC is closely related to the photosynthetic rate, in conditions unfavourable to photosynthesis as much as 95 % of the assimilated carbon can be lost in this way (Fogg 1977, 1983). Zlotnik & Dubinsky (1989) concluded light to have a dominant role in determining excretion percentages, but also admitted the importance of sub- and supraoptimal temperatures as did Watanabe (1980). On the basis of this study it is impossible to conclude for cryptophytes which one of these environmental variables was of greater importance for the excretion fixed carbon. Even though it can be deduced that L315 cells at 26 °C were excreting, nothing definite can be said about the fate of "excess" gross photosynthesis between 19 °C (i.e. the optimum temperature for growth) and 23 °C (i.e. the optimum for gross photosynthesis). At least part of it was respired as the optimum for respiration was estimated to be ca 24 °C. The effects of temperature on gross photosynthesis and growth of L315 are summarized in Fig. 3.8.

The "light-and-dark bottle" technique applied in this study is based on the assumption that the rate of respiration measured in the dark also occurs during the light period. However, this assumption has been seriously challenged, as Falkowski

Gross photosynthesis/Growth
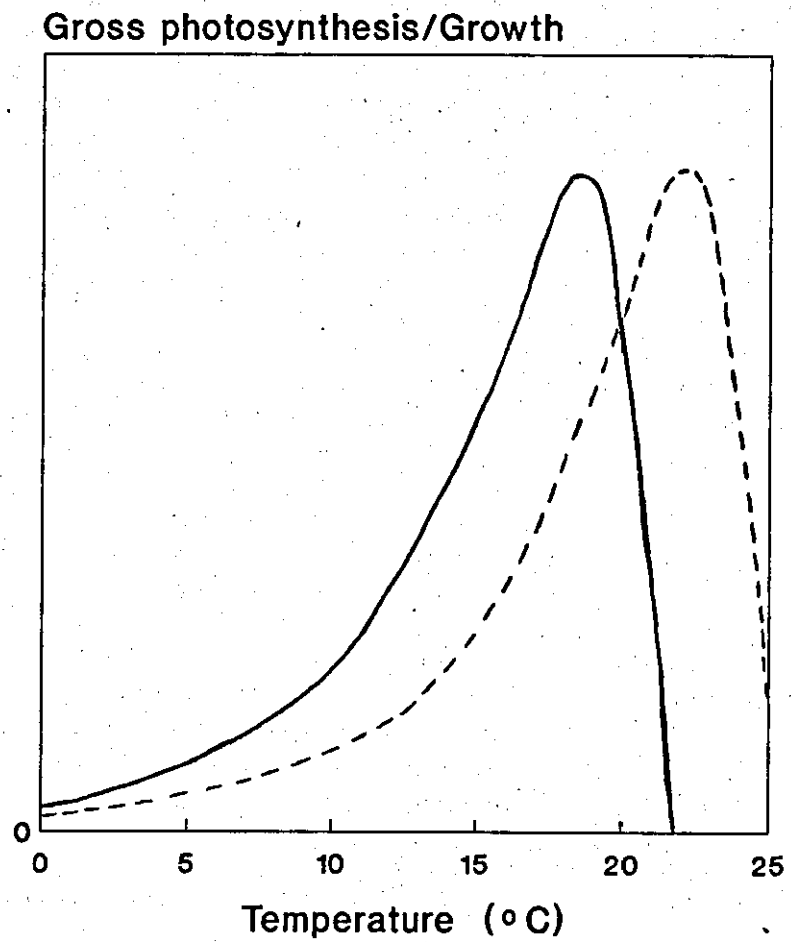
Fig. 3.8. A diagrammatic view of the effects of temperature on gross phtosynthesis and growth of L315. The solid line refers to growth and the dashed line to gross photosynthesis.

& Owens (1978) have reported a marked hysteresis between oxygen production and uptake at varying PFDs and Falkowski et al. (1985a) have described the so-called EPIR, i.e. enhanced post–illumination respiration phenomenon lasting up to 2.5 hours. It is also a well–known fact that respiration activity depends on the time spent in the dark, reaching a plateau after about 8 hours (Gibson 1975, Grobbelaar & Soeder 1985). One explanation offered for these observations is the light–intensity depen-dence of mitochondrial respiration and Weger et al. (1989) have managed to show that in *Thalassiosira weissflogii* the increased oxygen consumption during photosynthesis resulted from the mitochondrial respiration enhanced by an increase in substrate supply from photosynthesis. This type of oxygen consumption can also be caused from photoreduction of oxygen and photorespiration. In the present experiments no EPIR could have taken place as incubations started after the dark period, but photorespiration might have been of importance as oxygen concen-trations in sealed bottles were high – usually in excess of saturation – and in L485 experiments there was no bicarbonate in the growth medium, conditions shown to be favourable to photorespiration (Burris 1977, 1981). The primary use of newly made photosynthate in respiration could also have affected the results as during the course of dark incubations cells had to rely on older compounds, whereas in light they could utilize recently produced synthates. Thus, these confinements mean that the gross production values presented in this study are only approximates and probably undere-stimates, but as measurements based on oxygen exchange can account for respiratory losses (Weger et al. 1989) net production estimates are more correct. The reliability of net production estimates in terms of photorespiration emphasizes the need for practicable models of net production.

Thus, the problems of this study relate to the fact that the acidophilic L485 precluded the application of the more sensitive methods for production measurements and forced the use of enclosed cultures and prolonged incubation periods. A solution to all these problems would have been a sensitive method for direct measurements of dissolved inorganic carbon as described by Salonen (1981) and Bergström & Salonen (1984). The low pH in the L485 growth medium would not have caused any problems as this method has successfully been applied in primary production measurements in an acidic humic lake with an epilimnetic pH of 4.2–4.4. (Rask et al. 1986). Unfortunately this method has not yet become widely accessible.

Chapter 4

THE EFFECTS OF LIGHT QUALITY ON GROWTH AND CELLULAR PIGMENTATION OF TWO CRYPTOPHYTES IN COMPARISON WITH A GREEN AND A BLUE-GREEN ALGA

4.1. INTRODUCTION

The photic environment of planktonic algae is not vertically uniform as light is attenuated by water itself, dissolved organic compounds, plankton and other particulate matter (Kirk 1983). This attenuation takes place at different rates in different parts of the spectrum, thus creating gradients in total photon flux density as well as in the distribution of spectral energy of the downwelling light. In clear waters blue and blue–green light penetrate furthest, validating the remark of Jeffrey (1984) who called the oceans a giant blue–green filter. In coastal areas and freshwaters the maximum penetration is shifted more towards longer wavelengths due to increased amounts of dissolved organic compounds. Lakes can be classified in three types by their optical properties and each type is separated by the depth to which red (R), green (G) and blue (B) wavebands penetrate (Talling 1971). In class 1 the relative depths to which individual wavebands of light penetrate are $R < B < G$. In classes 2 and 3 the sequencies are $B < R < G$ and $B < R \leq G$, respectively. This classification also corresponds to the nutrient status of lakes so that lakes in class 1 are oligotrophic, in 2 mesotrophic and in 3 eutrophic. Brown–water lakes can be said to form the 4th class as high humic content creates a light environment strongly dominated by orange–red and red wavebands (e.g. Elomaa 1977, Eloranta 1978).

In order to adapt and thrive in such a light environment dominated by certain wavebands, algae have to posses a variety of pigment systems capable of harvesting available light. The chromatic adaptation, involving the preferential synthesis of that pigment which effectively absorbs the available light, has especially been studied in blue–green algae (cyanobacteria) and it was first described in *Oscillatoria rubescens* by Gaidukov (1902, cited in Kirk 1983) who observed that algal cells are red in colour when grown in green light and blue–green when grown in orange light. The pigments involved in chromatic adaptation are called phycobiliproteins (PBPs) and these accessory pigments, consisting of a bile pigment chromophore and an apoprotein unit linked to it, are found in rhodophytes and cryptophytes as well as in blue–greens (e.g MacColl 1982). There are three principal classes of PBPs, i.e.

phycoerythrin (PE), phycocyanin (PC) and allophycocyanin (APC), which differ in their absorption and fluorescence maxima (e.g. Bogorad 1975). They are immunochemically related to each other (MacColl et al. 1976), but differ in the way in which they are organized within cells. In blue–green algae and rhodophytes they form phycobilisomes on thylakoid lamellae, whereas in cryptophytes PBPs are located in the thylakoid lumen (e.g. Lichtlé et al. 1987). Cryptophytes can also be distinguished from other PBP-containing algae by the accessory pigment composition, as only one type of PBP per species tends to occur in cryptophytes and allophycocyanin has never been found in these algae (Gantt 1980). However, despite the existence of PBPs, the main photosynthetic pigments in cryptophytes are chl a and chl c_2 which, even in the reddish *Cryptomonas rufescens*, account for ca 80 % of pigment molecules (Lichtlé et al. 1987). All the energy trapped by accessory pigments is finally transferred to chlorophyll with transfer efficiencies close to 100 % (MacColl 1982, Lichtlé et al. 1987).

Compared to blue–green and red algae (e.g. Levy & Gantt 1988, Prezelin et al. 1989, Vernet et al. 1990) little is known about the PBPs and complementary chromatic adaptation and its ecological role in cryptophytes. Information on freshwater species is particularly meagre as the majority of the published records are from marine cryptophytes (Kamiya & Miyachi 1984a, 1984b, Lewitus & Caron 1990). The chromatic adaptation via changes in accessory pigmentation is said to provide organisms with advantages in adapting to the environment and even enable the over–wintering of algal populations under ice–cover (Skulberg 1978, MacColl 1982). Bearing in mind the importance of cryptophytes in aquatic ecosystems (e.g. Jones & Ilmavirta 1988, Stewart & Wetzel 1986), the need for more detailed information is obvious. The use of cryptophytes as experimental organisms is also necessitated by the differences in PBPs of cryptophytes and other biliprotein–containing algae, thus making the compatibility of data on different algae questionable.

The present investigation examines the response of isolates of some cryptophytes to chromatic light and describes the effects of qualitative variation in light climate on their growth and pigment composition. In this work pigment measurements were carried out by means of epifluorescence microscopy giving results only in relative values. A comparative study was made using cultures of a cryptophyte, a bloom–

forming blue–green alga *Oscillatoria bourellyi* known to be capable of chromatic adaptation (Skulberg 1978, Holtan 1979, Hilton et al. 1989, Ganf et al. 1991) and a green eglenoid without PBP and which served as a reference.

4.2. MATERIAL AND METHODS

The cryptomonas strains used in this study were the same as in the previous growth and photosynthesis experiments and they as well as their culture media, have been described in Chapters 2 and 3. L315 originates from a lake which can be said to belong to type 3 in Talling's (1971) classification, as green and red wavebands penetrate deepest and the lake is regarded as hyper–eutrophic in nutrient status (see Chapter 6). The lake from which L485 was isolated, fulfills the spectral characteristics of an oligotrophic lake (see Chapter 5, cf. Eloranta 1978). The reference organism *Oscillatoria bourellyi* (CCAP code number L159) was isolated by Mr G. Jaworski from Windermere (Cumbria, England, group 2 in Talling's (1971) classification) in 1967. It is being kept in Jaworski's Medium (JM) (Table 4.1) in the Culture Collection of Algae and Protozoa (CCAP), UK. and the same medium without any modifications was used in this study. The other reference organism, *Euglena* sp., was isolated from the same acidic clearwater Finnish lake as *Cryptomonas* L485 (see Chapter 5) and it was also cultured in the same medium (pH adjusted to 3.7–4.0) except that to obtain good growth of *Euglena*, EDTA FeNa and EDTA Na_2 had to be added in excess.

Algal stocks and experimental cultures were incubated in a constant temperature growth cabinet (19 °C, ± 0.1 °C) where continuous light was provided from below by a bank of cool–white fluorescent tubes. In order to diminish the PBP content of algae, stock cultures (including *Euglena* sp.) were kept at high photon flux density (260 μmoles m^{-2} s^{-1}) for four days prior to the experiments. For the experiments, light quantity (white light) was controlled with neutral density screening and quality with Lee celluloid filters (Lee Colortram Ltd., UK.) numbers 124 (green), 182 (red) and 183 (blue). Spectral transmittances of the colour filters are shown in Fig. 4.1. The red filter transmits mostly light > 600 nm, the green filter

Table 4.1. Composition of Jaworski's Medium (JM)

Stock solutions:	per 200 ml
1. $Ca(NO_3)_2.4H_2O$	4.0 g
2. KH_2PO_4	2.48 g
3. $MgSO_4.7H_2O$	10.0 g
4. $NaHCO_3$	3.18 g
5. EDTA.FeNa	0.45 g
EDTA.Na$_2$	0.45 g
6. H_3BO_3	0.496 g
$MnCl_2.4H_2O$	0.278 g
$(NH_4)_6Mo_7O_{24}.4H_2O$	0.2 g
7. Cyanocobalamin (Vitamin B$_{12}$)	0.008 g
Thiamine HCl (Vitamin B$_1$)	0.008 g
Biotin	0.008 g
8. $NaNO_3$	16.0 g
9. $Na_2HPO_4.12H_2O$	7.2 g

Final solutions:
Stock solutions 1–9
   1 ml of each
Deionised water   1.0 l
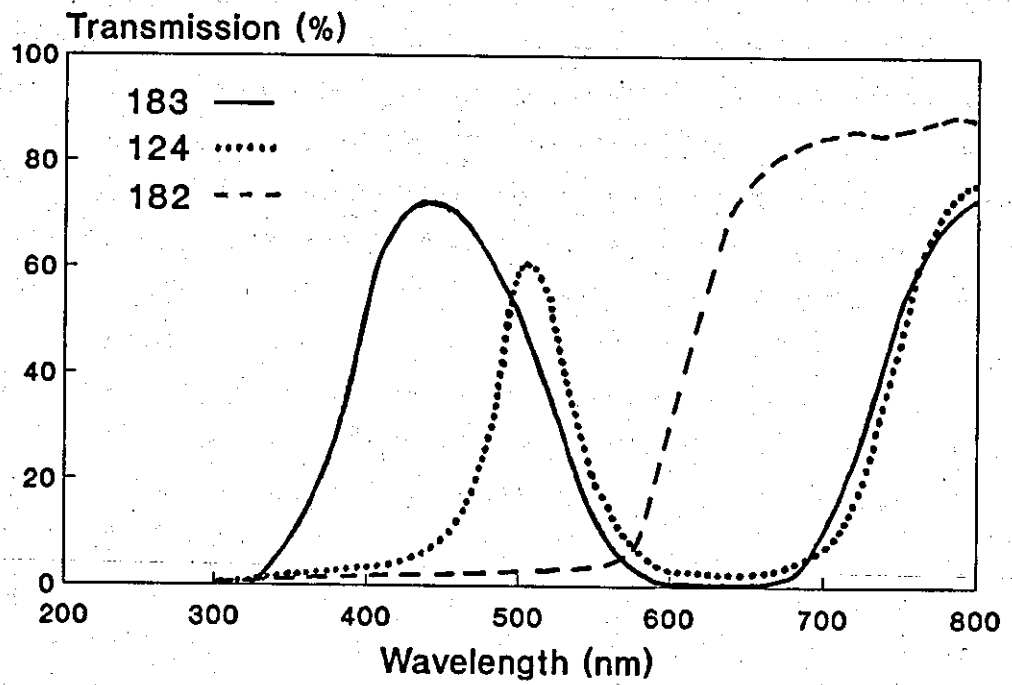
Fig. 4.1. Spectral transmittances of the blue (183), green (124) and red (182) filters used in light quality experiments.

between 480 and 550 nm, and > 700 nm. The blue filter transmits mostly between 400 and 550 nm, and > 700 nm. The photon flux densities (PFD) (for measurements and equipment, see Chapter 3) in white, red, green and blue light treatments were 28, 31, 31 and 27 μmoles m^{-2} s^{-1}, respectively. According to Kamiya & Miyachi (1984b) and Wyman & Fay (1986a) these PFDs are low enough to keep the cellular PBP concentration high. As the different treatments were conducted side by side, the culture flasks were placed in covered cylinders made of the appropriate filter material and were taken out only for sampling. The reported PFDs were measured inside these cylinders.

To start the experiments, batch cultures (150 ml cotton wool stoppered conical flasks filled with 125 ml of medium) were inoculated with 5 ml of exponentially growing cells to low initial densities (*ca.* 1 600, 85, and 515 cells ml^{-1} for L485, L315 and *Euglena*, respectively and 95 mm of filaments ml^{-1} for *Oscillatoria*). All experiments were carried out with two parallel cultures. Samples for growth measurements were taken six times during the 18 day incubation period, preserved with Lugol's iodine and counted in small plastic cuvettes (low cell counts) with an inverted microscope (Leitz Diavert Inverted Microscope, 500x magnification for L485, L315 and *Euglena*, 100x for *Oscillatoria*) or in Lund chambers (Lund 1959) with a bench microscope (Wild M20 EB, 250x) (high cell counts). Filament length of *Oscillatoria* was estimated with an eyepiece grid in the inverted microscope. Growth rates were calculated from the linear portion of the growth curves as described by Guillard (1973) and expressed as divisions day^{-1}.

Samples for pigment composition analysis were taken four times (1st, 4th, 11th and 18th day) during the experiments. They were fixed with 4 % glutaraldehyde buffered to pH 7.0 with 0.1 M sodium cacodylate buffer and measurements made immediately for chlorophyll *a* and PBP content of individual cells with a Leitz Fluovert epifluorescence microscope equipped with a photometer unit. Glutaraldehyde as a preservative for epifluorescence microscopy has also been used by Booth 1987, Booth et al. 1988 and Barbosa et al. (unpublished data) and glutaraldehyde combined with paraformaldehyde by Tsuji et al. 1986. Fluorescence measurements were made immediately as Barbosa et al. (unpublished data) found a drastic decrease in fluorescence yield soon after preservation. Filter blocks used for incident-light

fluorescence were I 2/3 with an excitation filter BP 450–490 (blue), dichroic mirror RKP 510 and suppression filter LP 520 and N2 with an excitation filter BP 530–560 (green), dichroic mirror RKP 580 and suppression filter LP 580. The size of the photometer measuring rectangle was kept as 18.7 μm x 17.4 μm for L485 and *Oscillatoria* and 34.7 μm x 37.4 μm for L315 and *Euglena*. For each photic regime 22 randomly chosen cells or parts of *Oscillatoria* filaments were measured and the results were expressed as relative fluorescence yields, i.e. as ratios of F_g/F_b where g refers to green light (PBPs) and b for blue light (chlorophyll) excitation, respectively.

The significance of the different treatments was evaluated by an ANOVA F–test in Statgraphics statistical package (Statistical Graphics Corporation). As an *a priori* test it tests for significance assuming a complete null hypothesis, but not for significance under a partial null hypothesis. As an *a posteriori* test the HSD (honestly significant difference) test was applied.

4.3. RESULTS

4.3.1. Growth

Growth responses of the reference algae and experimental *Cryptomonas* strains are illustrated in Fig. 4.2. The growth response of *Euglena* sp. varied with light quality in the following manner: blue > white > red > green and the division rates in the exponential phase – expressed as means of the duplicate cultures – were 0.484, 0.348, 0.264 and 0.257 div. day^{-1}, respectively (Fig. 4.2a). This pattern of growth response is consistent with the observations in *Cyclotella nana*, a marine diatom and *Dunaliella tertiolecta*, a marine green alga (Wallen & Geen 1971a). None of the *Euglena* cultures reached the stationary growth phase during the experiment but signs of retarded growth could already be seen. A short time lag in growth was also evident at the start of the experiment.

cell density (cells ml^{-1})

a)

- white light
+ red light
* green light
□ blue light

time, days

cell density (mm ml^{-1})

b)

- white light
+ red light
* green light
□ blue light

time, days
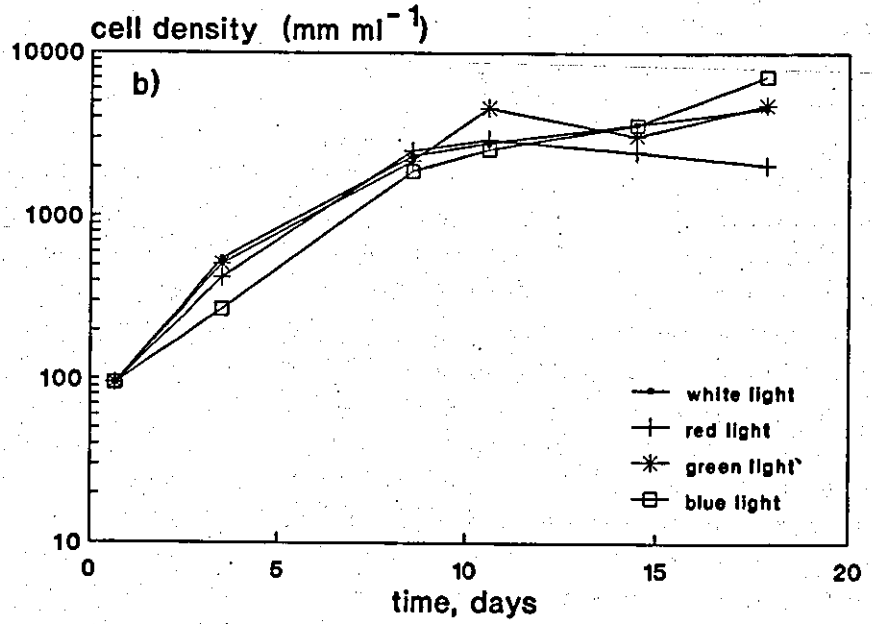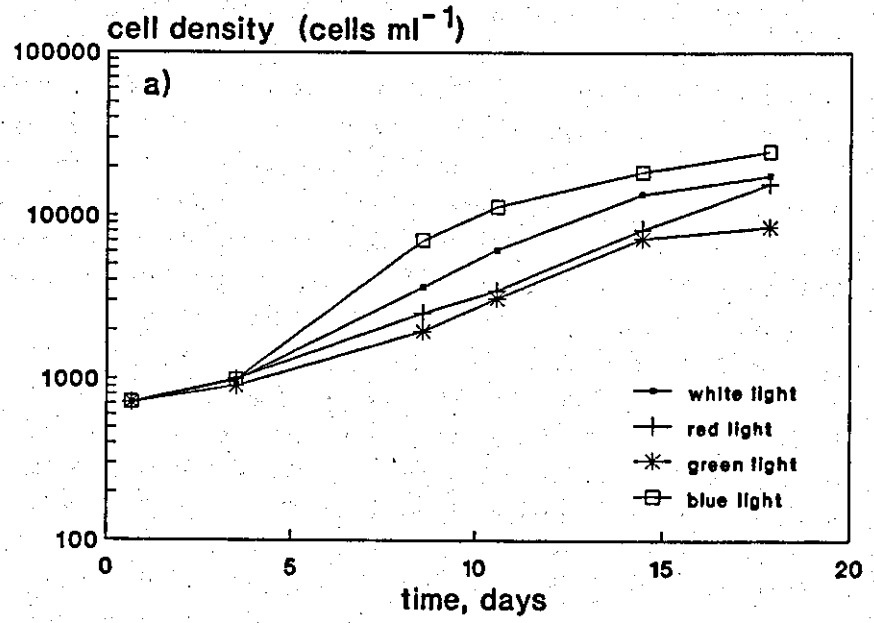
Fig. 4.2. Growth response of *Euglena* sp. (a), *Oscillatoria bourellyi* (b), *Cryptomonas* L485 (c) and L315 (d) under white, red, green and blue light.

In contrast to *Euglena* sp., the blue–green alga *O. bourellyi* showed a remarkable consistency of growth rates under different light qualities (Fig. 4.2b). The division rates in white, green, red and blue light were 0.565, 0.531, 0.507 and 0.498 div. day^{-1}, respectively. However, there was a 40 % difference in measured rates of duplicate cultures in red light, which gave individual growth rates of 0.634 and 0.380 div. day^{-1}. In all other treatments with *O. bourellyi* the difference was < 10 %. Thus, if the low growth rate of 0.380 div. day^{-1} is neglected, *O. bourellyi* can be said to show its best growth in red light. The suitability of red light for growth of blue–green algae has also been recorded by Wyman & Fay (1986b), but the eight species they employed showed comparatively higher growth rates in red light than *O. bourellyi* in this study. In green and red light, growth ceased after 10 days and cultures entered the stationary phase of growth. In white and blue light, growth continued till the end of the experimental period although in white light finally at a slower pace. Adaptation of *O. bourellyi* to different light regimes was immediate, as no time lag could be detected.

The growth response of *Cryptomonas* L485 was superior in blue light, with the estimated mean rate of 0.757 div. day^{-1} being 40 % higher than that in green light, which gave the second best growth response, 0.445 div. day^{-1} (Fig. 4.2c). The mean growth rate in white light was only slightly lower (0.429 div. day^{-1}) than that in green light. The poorest growth response was observed in red light where only a rate of 0.344 div. day^{-1} could be measured. A time lag of growth at the beginning of the experiment could be seen in every treatment, but the carrying capacity of growth medium was only reached in blue light where the cultures entered the stationary phase after 10 days.

The most suitable light quality for *Cryptomonas* L315 was the white light, which gave a growth rate of 0.406 div. day^{-1}. Growth rates in other light qualities varied as follows: blue > red > green and the calculated growth rates were 0.322, 0.184 and 0.164 div. day^{-1}, respectively (Fig. 4.2d). Thus, the overall growth rates were generally lower than in L485 and the response pattern resembled that of the green euglenoid in that poorest growth was observed in green light. Even this strain responded differently to the green light and blue light in terms of growth, despite their spectral overlap (Fig. 4.1). The variation in growth results between the duplicate

cultures was higher than with other strains varying from 9.6 % to 28.3 %. A time lag was only detected in green light and growth slowed in blue light although these cultures were not close to the maximum yield of L315 supported by the medium, which is approximately 10,000 cells ml^{-1} (Chapter 2).

4.3.2 Pigment composition

Pigment compositions measured as a F_g/F_b ratio, are shown in Fig. 4.3. Results from *Euglena* sp. confirmed the suitability of the method, as differences between the photic regimes were not statistically significant (ANOVA, $p = 0.05$) (Fig. 4.3a) and ratios remained stable throughout the experiment. The suitability of the method was also revealed by the distinct pattern of response in *O. bourellyi*. As soon as the *Oscillatoria* cultures were removed from high PFD and placed in the experimental conditions, the F_g/F_b ratios started to increase regardless of the light quality used for exposure. The highest ratio (15.4) was measured in green light after 3 days exposure and did not start to decline until the 10th day of the experiment. The cultures then entered the stationary growth phase (Fig. 4.2b) and a rapid collapse in the pigment ratio followed. The pattern observed in white light was similar, but the numerical values of the ratio stayed lower, and when the rapid decline happened, cultures were not in such an obvious stationary growth phase. This similarity between the white and green treatments could also be statistically verified by a two step analysis combining ANOVA ($p=0.05$) and HSD test ($p=0.05$), as paired comparisons revealed statistically significant differences only at the end of the experiment (Table 4.2). In blue light the highest ratio (13.8) was observed after 10 days of exposure. The decline in ratio coincided with that in green and white light, but at this time cultures were still actively growing. The dissimilarity (Table 4.2) of pigment ratios in green and blue light shows that *O.bourellyi* was able to differentiate green and blue light despite their apparent spectral overlap (Fig. 4.1). In red light the ratio started to decline much sooner, after only three days, and the minimum pigment ratio (1.8) was measured at the end of the experiment. This decline of the ratio started in the middle of the exponential growth phase, several days before the growth started to slow
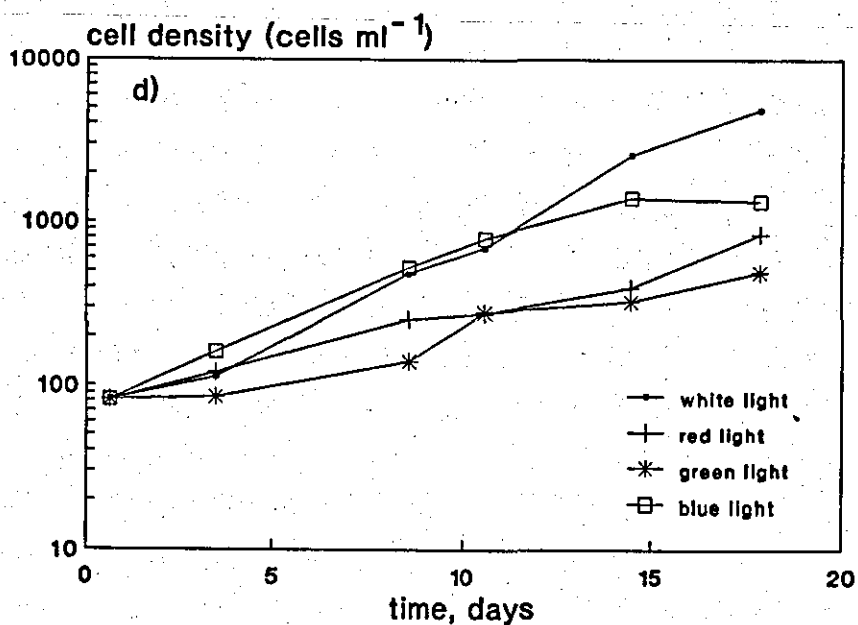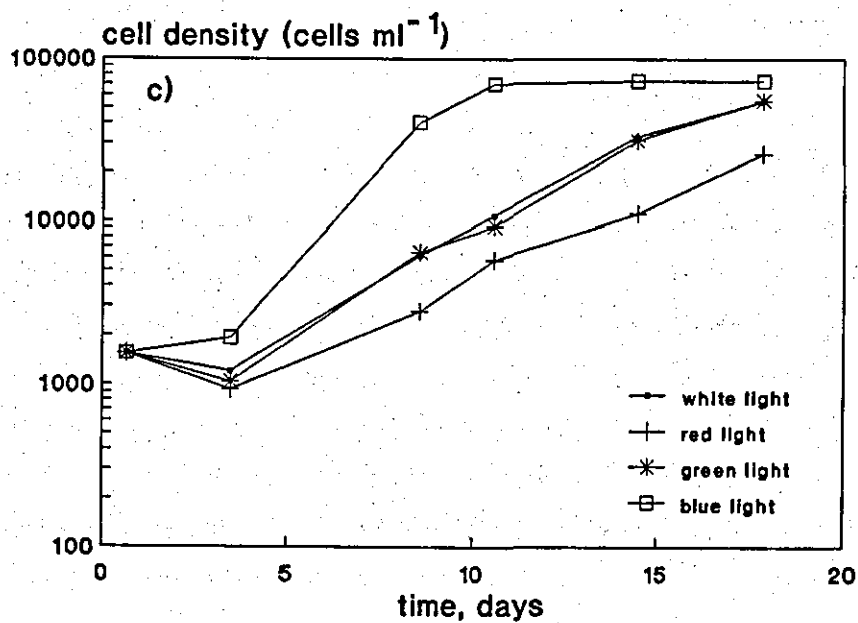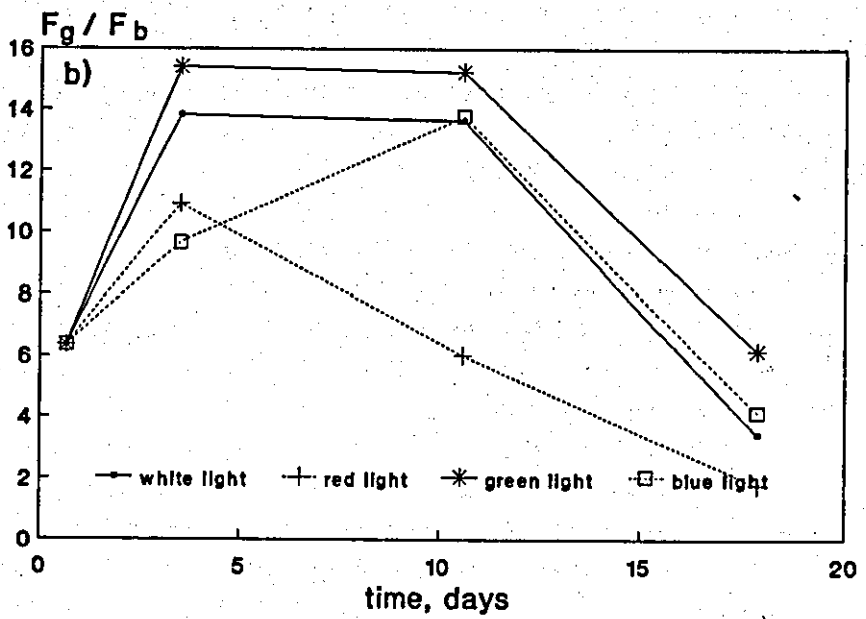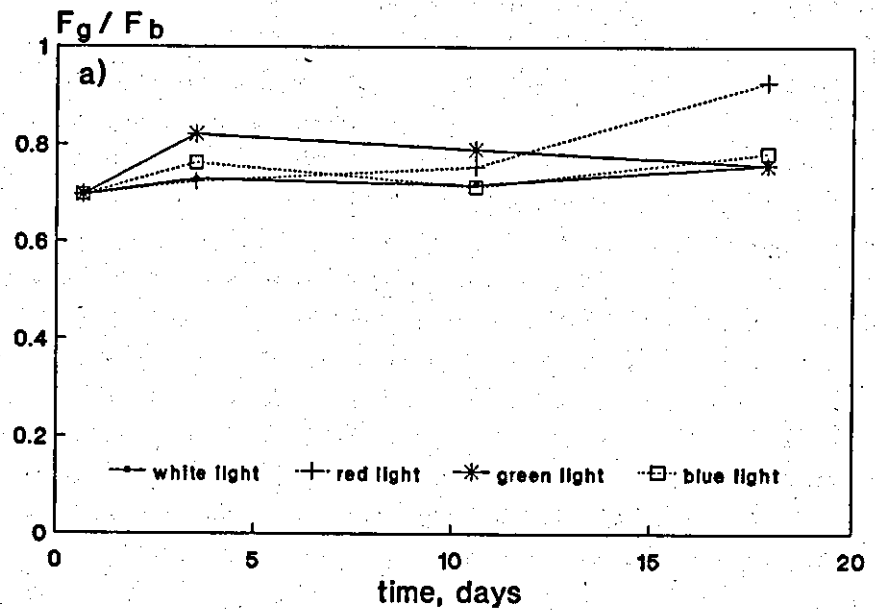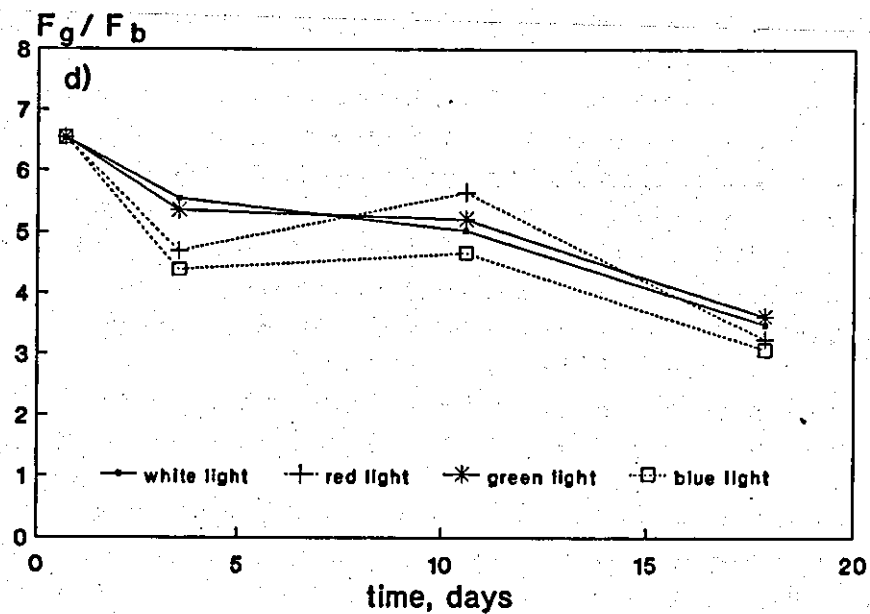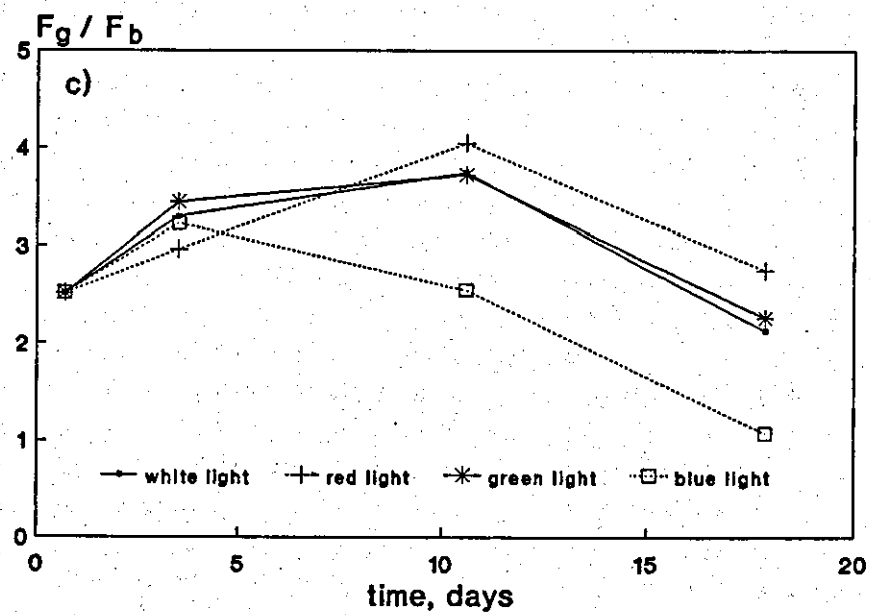
Fig. 4.3. Pigment ratios (F_g/F_b) of *Euglena* sp. (a), *Oscillatoria bourellyi* (b), *Cryptomonas* L485 (c) and L315 (d) under white, red, green and blue light.

Table 4.2. Differences in pigment composition ratios in *Oscillatoria bourellyi*. Paired comparisons based on HSD (i.e honestly significant difference) test, p = 0.05. + = significant difference, − = no significant difference.

Pair	3rd day W_3=2.98	10th day W_3=1.91	18th day W_3=1.85
white vs. red	2.90(−)	7.60(+)	1.64(−)
white vs. blue	4.18(+)	0.14(−)	0.70(−)
white vs. green	1.57(−)	1.61(−)	2.73(+)
red vs. blue	1.28(−)	7.74(+)	2.35(+)
red vs. green	4.48(+)	9.21(+)	4.38(+)
blue vs. green	5.75(+)	1.47(−)	2.03(+)

down. The pigment composition in red light was statistically different from that in green light from the beginning of the experiment.

In comparison with *O.bourellyi* and *Euglena* sp. the fluorescence ratios of cryptophytes L485 and L315 were intermediate; they were not so apparent as in the blue–green alga but not so stable as in the green alga. In L485 there was an increase in F_g/F_b ratio soon after the onset of the experiment. This first increase was most obvious in green light but then levelled off and only a value 3.7 was reached. After the 10th day there was a sharp decline and the ratio dropped to 2.3. As in *O. bourellyi*, the response pattern in white light was similar to that in green light, which could also be seen from the results of the paired comparison with the HSD test (Table 4.3). The combined composition of white light was shown in the similarity of pigment ratios in white light compared to those in other photic regimes; in 6 out of 9 cases there were no statistically significant differences. In red light the increase of the ratio continued longer, i.e till the 10th day when a ratio of 4.0 could be measured. This peak ratio was followed by a sharp decline. The response in blue light resembled the response of *O.bourellyi* in red light, as the declining trend of the ratio could already be seen after the 3rd day and the overall minimum (1.1) was observed at the end of the experiment. In 10 days L485 developed statistically significant pigmentation differences in green and red light compared to those in blue light (Table 4.3). Unlike *O.bourellyi*, *Cryptomonas* L485 was always in exponential growth phase when the decline in F_g/F_b ratio started.

In experiments with L315 there were no statistically significant differences between fluorescence ratios under different light qualities (ANOVA, p = 0.05) and in this respect the results resembled those for *Euglena* sp. There was a peculiar decline in the F_g/F_b ratios after the cultures were transferred from high PFD to low one and this response could clearly be seen in all treatments. In white light the decline continued throughout the whole experiment. In green and blue light there was a stable period from the 3rd to the 10th day after which the declining trend continued. As with L485, the highest ratio of L315 (5.6) was detected in red light and the overall response in red light was similar to that of L485. The lowest ratios were measured in blue light, as with L485. No relationship between the timing of retarded growth and onset of the decline in the F_g/F_b ratio could be detected.

Table 4.3. Differences in pigment composition ratios in *Cryptomonas* LA85. Paired comparisons based on HSD test, p = 0.05. + = significant difference, − = no significant difference.

Pairs	3rd day $W_3=0.81$	10th day $W_3=0.73$	18th day $W_3=0.47$
white vs. red	0.33(−)	0.30(−)	0.62(+)
white vs. blue	0.07(−)	1.20(+)	1.06(+)
white vs. green	0.15(−)	0.02(−)	0.13(−)
red vs. blue	0.26(−)	1.50(+)	1.67(+)
red vs. green	0.48(−)	0.33(−)	0.49(+)
blue vs. green	0.22(−)	1.17(+)	1.18(+)

4.4. DISCUSSION

The present study extends the observations of chromatic adaptation of marine cryptophytes (Jeffrey & Vesk 1977, Kamiya & Miyachi 1984a, 1984b) to two well-defined freshwater species of the same phylum. As the method applied in pigment composition measurements was a simple one and the determinations were made from intact cells without extraction procedures, some comments on sources of error are appropriate before evaluation of the results. The fluorescence emitted by the cells could have been affected by glutaraldehyde fixation, as Tsuji et al. (1986) have shown with natural phytoplankton species that preservation with glutaraldehyde or paraformaldehyde can have an impact on the wavelength location and intensity of phycoerythrin emission. In order to avoid the unwanted effects of fixation, fluorescence measurements were carried out immediately after sampling but the ideal of *in vivo* measurements was impracticable due to the motility of cryptophytes and *Euglena* sp. The yield of the phycoerythrin fluorescence could also have been affected also by the excitation and suppression filters. The filterblock used was in general suitable for the cryptophyte phycoerythrin excitation, as out of the three phycoerythrins listed by Bogorad (1975) two have absorption maxima between 530–560 nm. However, as *Cryptomonas* phycoerythrin has sometimes been recorded to have emission maxima below or just at 580 nm (e.g. Bogorad 1975, Yentsch & Phinney 1985) the use of the 580 nm suppression filter might have led to an underestimate of the total cellular phycoerythrin content. The underestimation could also have taken place in *O. bourellyi* measurements as Alberte et al. (1984) have reported the fluorescence maximum of *Synechococcus* spp. phycoerythrin to lie at 560 nm. However, the shapes of the emission spectra of cryptophyte PBPs are asymmetric with shoulders in the long wavelength regions thus leaving the majority of fluorescence emission unblocked even in the case of a 580 nm suppression filter (MacColl et al. 1976). Inaccuracy in pigment composition results could also have been caused by the response of chlorophyll to green light (Vesk & Jeffrey 1977, Kamiya & Miyachi 1984b) which was probably the underlying factor for the detected non–zero *Euglena* fluorescence yield after green excitation. However, according to

Yentsch & Phinney (1985) in green unicells excitation spectra are almost complete-
ly below 500 nm.

Despite the above-mentioned reservations and the relative units of pigment
measurements, the F_g/F_b ratios of *O. bourellyi* as well as the cryptophytes were
similar to those obtained using quantitative extraction methods in pigment analysis.
Alberte et al. (1984) found ratios of 18.0 and 22.55 for PE-containing
Synechococcus spp. and Wyman & Fay (1986b) reported PBP/chl ratios of 6.7–14.3
for several blue-green species in different chromatic light. Vesk & Jeffrey (1977)
reported, for a marine *Chroomonas* grown at 20 μmoles $m^{-2}s^{-1}$, PE/chl *a* ratios of
4.76 in white light and 6.25 in blue-green light, which are in the same range as the
ratios obtained with L315 and only slightly higher than those of L485. However,
neither of the freshwater cryptophytes showed such a great increase (*ca.* 25 %) in
relative phycobiliprotein content in blue or green light compared to that in white
light of the same PFD. In both species the highest ratios were actually found in red
light and in blue light the ratios were always lower than those in white light; in
green light the biggest relative inreases in comparison with white light in L485 and
L315 were only 3.7 % and 5.7 %, respectively. The interaction of blue and green
light in the *Chroomonas* study of Vesk & Jeffrey (1977) cannot totally explain this
difference in results, as in the present study also green light was a combination of
blue and green wavebands (Fig. 4.1). The lowest F_g/F_b ratio (1.1) in L485
corresponds to the PE/(chl a+c) ratios of freshwater *Cryptomonas rufescens* measured
in the encystment phase (Lichtlé 1979). However, there was no indication of
encystment in this study, as the appearance of cells remained unchanged and no cysts
were ever observed in the growth experiments and maintenance of the stock cultures
(Chapter 2). In white light at low PFD (*ca.* 20 μmoles $m^{-2}s^{-1}$) *C. rufescens* was
reported to have a PE/(chl a+c) ratio of 3.6, which is similar to those obtained for
L485 in white light.

The weak complementary chromatic adaptation of L485 and L315 was also reflected
in their modest or even poor growth in green light. In *O. bourellyi* the chromatic
adaptation seemed to be of use, since this blue-green alga was able to maintain a
constant growth rate regardless of the chromatic light available. However, the results
for L485 and L315 are quite consistent with those obtained by Glover et al. (1987)

with a marine cryptophyte called ID2. This strain showed the best growth response in blue-violet light. In both blue and green light the growth was depressed, but the growth rates in these photic regimes were equivalent. Thus, at first sight this is a result different from those obtained with L485 and L315, but a closer look at the chromatic filters used in these two studies revealed that the blue-violet filter of Glover et al. (1987) resembles the blue filter of this study as the maximum band transmittance of both filters is ca 450 nm. The results of these two studies are thus compatible. The weak chromatic adaptation of cryptophytes was also revealed by Wall & Briand (1979) who, based on their *in situ* manipulation experiments, reported cryptophytes not to show up as green light specialists, but instead to be relatively favoured by blue light. A stimulation of growth under blue light has frequently been found e.g in green algae (Wallen & Geen 1971a, Senger 1987) and was also recorded in this study with the *Euglena*. The stimulated growth is the ultimate response of algae to the prevailing light and is an interaction of light utilization in photosynthesis and photomorphogenetic processes, several of which have been shown to be controlled by blue light (Steup 1975,1977, Vesk & Jeffrey 1977, Ruyters et al. 1984, Kowallik 1987, Dring 1988, Grotjohann & Kowallik 1989, Rivkin 1989). For example, there is a large number of photosynthetic and carbohydrate-degrading enzymes reported to be affected by blue light wavebands (Ruyters 1987).

Evidence for the existence of complementary chromatic adaptation in cryptophytes has been presented by Kamiya & Miyachi (1984b), who studied the formation of amino-levulinic-acid (ALA) – assumed to be a precursor for the biosynthesis of phycobilin chromophores – in a marine *Cryptomonas* and recorded enhancement under green light compared to that under blue or red light. Photosynthesis results supporting the hypothesis of complementary chromatic adaptation in cryptophytes have also been published. Jeffrey (1984) and Kamiya & Miyachi (1984b) investigated the photosynthetic activity of a marine *Chroomonas* sp. and *Crypto-monas* sp. and reported them to be most active in blue/green and green light, respectively. The sensitivity of these strains to green light is consistent with their origin, since *Chroomonas* sp. is an alga found in deeper water environments and *Cryptomonas* sp. was actually isolated from an oceanic subsurface chlorophyll maximum and probably already adapted to a blue/green environment. However, with this type of reasoning L315 could be said to be adapted to red/green chromatic light

but no signs of this ccould be seen in growth experiments. In L485 the question of the natural light environment is complicated by the tendency of these algae *in situ* to congregate amongst the benthic *Drepanocladus* vegetation (Chapter 6), but the slightly better growth response of this strain in green light might be indicative of some adaptation.

The modest role of PBPs in chromatic adaptation in cryptophytes is hardly suprising as Raven (1984) has pointed out that PBPs are ineffective in terms of photon absorption and expensive in terms of energy and material to synthesize. He concluded that in the blue–green waveband, characteristic of aquatic shade, the light–harvesting machinery of chlorophytes and chromophytes is generally superior to that of algae containing PBPs.

So, what is the role of PBPs for cryptophytes if they do not provide an adaptational advantage in terms of enhanced growth in chromatic light? Some blue–green algae have been reported to use PBPs as a nitrogen reserve, as blue–green algae react to nitrogen depletion by decreasing the rate of PBP production and maintaining constant rates of growth and chlorophyll *a* production (Wyman et al. 1985, review in Lewitus & Caron 1990). Besides the decreasing accessory pigment production, nitrogen–stressed blue–green algae are able to degrade PBP already present in the cell. Analogous information on the effects of nitrogen availability on the pigment concentration of cryptophytes is rare but it is known that phycoerythrin can account for *ca.* 50 % of the total protein in cryptophytes (Lichtlé et al. 1987) and Lewitus & Caron (1990) have found that in the marine cryptophyte *Pyrenomonas salina* PBP content declines before cell division stops. Lichtlé (1979) has also pointed out that starved *C. rufescens* cells may use PE as a proteinic substrate. A similar exploitation of PBPs could have been the underlying cause for the declining F_g/F_b a ratios in L485 and *O. bourellyi*, as the decline took place already in the exponential phase of the growth. However, no direct evidence, such as information on intracellular nutrient concentrations, was gathered and the method for PBP measurements, based on emitted fluorescence, actually measures the amount of chromophore, not the attached apoprotein.

In summary, this study demonstrated that at least some freshwater cryptophytes are capable of chromatic adaptation, but this adaptation is probably weaker than in blue–green algae. However, the possession of accessory pigments did not seem to provide cryptophytes with any distinct advantages in terms of growth in chromatic light and as no experiments on PBPs as nutrient reserves were carried out, the ultimate reason for the existence of cryptophyte PBP remained obscure.

Chapter 5

GROWTH AND NUTRITIONAL STATE OF TWO CRYPTOPHYTES IN THERMALLY AND CHEMICALLY STRATIFIED EXPERIMENTAL COLUMNS

5.1 INTRODUCTION

In most aquatic environments growth of photosynthetic phytoplankton, although dependent on numerous physical and chemical variables, is primarily determined by the availability of light and nutrients. In temperate water bodies during thermal stratification these resources can be spatially separated for prolonged time periods as the availability of nutrients is restricted in adequately illuminated upper water column, but at the same time nutrients can be available in excess in the light–limited hypolimnion (Salonen et al. 1984).

Under these conditions motile flagellates, possessing an effective and responsive way of propulsion, can undertake diel vertical migrations (DVM). Such motile flagellates may then gain several decided advantages over their non–motile counterparts whose chances to control their position in the water column are more limited and mostly restricted to buoyancy and sinking rate control by means of photosynthate production and accumulation/mobilisation (Reynolds 1984, Heaney & Butterwick 1985, Klemer 1985). Motility provides migrating algae with access to a much larger portion of the water column and thus a potentially greater overall nutrient supply which, due to migrations, is utilized in pulses. Flagellates may also benefit from migrations by reducing their sinking losses, eliminating hydraulic washout and diminishing losses by predation (e.g. Eppley et al. 1968, Salonen et al. 1984, Jones 1988, Suttle et al. 1988, Jones 1991).

Although appreciable diel vertical migrations have been proven with raphidophytes (e.g. Watanabe et al. 1988), cryptophytes (Tilzer 1973, Happey–Wood 1976, Frempong 1981, Sommer 1982, Arvola 1984, Sommer 1985, Arvola et al. 1987, Smolander & Arvola 1988, Jones 1988, Arvola et al. 1991), and especially with dinoflagellates (e.g. Eppley et al. 1968, Heaney & Furnass 1980, Heaney & Talling 1980, Cullen & Horrigan 1981, Frempong 1981, Heaney & Eppley 1981, Cullen 1985, Heaney & Butterwick 1985, Taylor et al. 1988), little attention has been paid to quantify the importance of this behaviour in production ecology. Eppley et al. (1968), Salonen et al. (1984) and Watanabe et al. (1988) have shown that such a behaviour can act as a nutrient pump and

Jones (1991) has studied the relative importance of DVM on loss processes, but very few data have so far been published on the effects of DVM on growth rates of algae. Heaney & Eppley (1981) and Kohata & Watanabe (1986) have published some sporadic experimental records on growth rates of migrating flagellates and Sommer (1985) has made an attempt to measure *in situ* growth rates of migrating cryptophytes, but none of these studies included comparisons with non–migrating populations. Raven & Richardson (1984) showed by cost–benefit analysis of dinophyte flagella that in some habitats DVM could increase the growth rate of dinoflagellates, but evidence supporting this hypothesis is yet to be published.

Here, based on studies conducted in laboratory columns which simulated a natural temperature stratification pattern, growth rates of migrating and non–migrating populations of cryptophytes under different light– and nutrient regimes were calculated. The growth measurement technique applied in these experiments was based on *in vivo* chlorophyll fluorescence analysis as first described by Eppley et al. (1968) and since used widely (e.g. Kamykowski & Zentara 1977, Cullen & Horrigan 1981, Heaney & Eppley 1981, Kamykowski 1981, Taylor et al. 1988). As the algal strains in this mesocosm study were the same as used in the previous batch culture experiments (Chapter 2), comparison of the results with the estimated growth potential of the very same strains was possible. Since motility does not increase algal growth *per se*, any detected effects of DVM on growth would be due to reduction of nutrient and/or light limitation by means of movements, as sinking of motile flagellates can be regarded as neglible (Burns & Rosa 1981) and losses by hydraulic washout and predation were eliminated in the laboratory columns.

5.2 METHODS

Experiments were carried out with cryptophytes L485 and L315 (see Chapters 2,3 and 4) in two opaque polyvinyl chloride (PVC) tubes (Fig. 5.1) built into an experimental system which enables the control of physical and chemical stratification (Heaney et al.
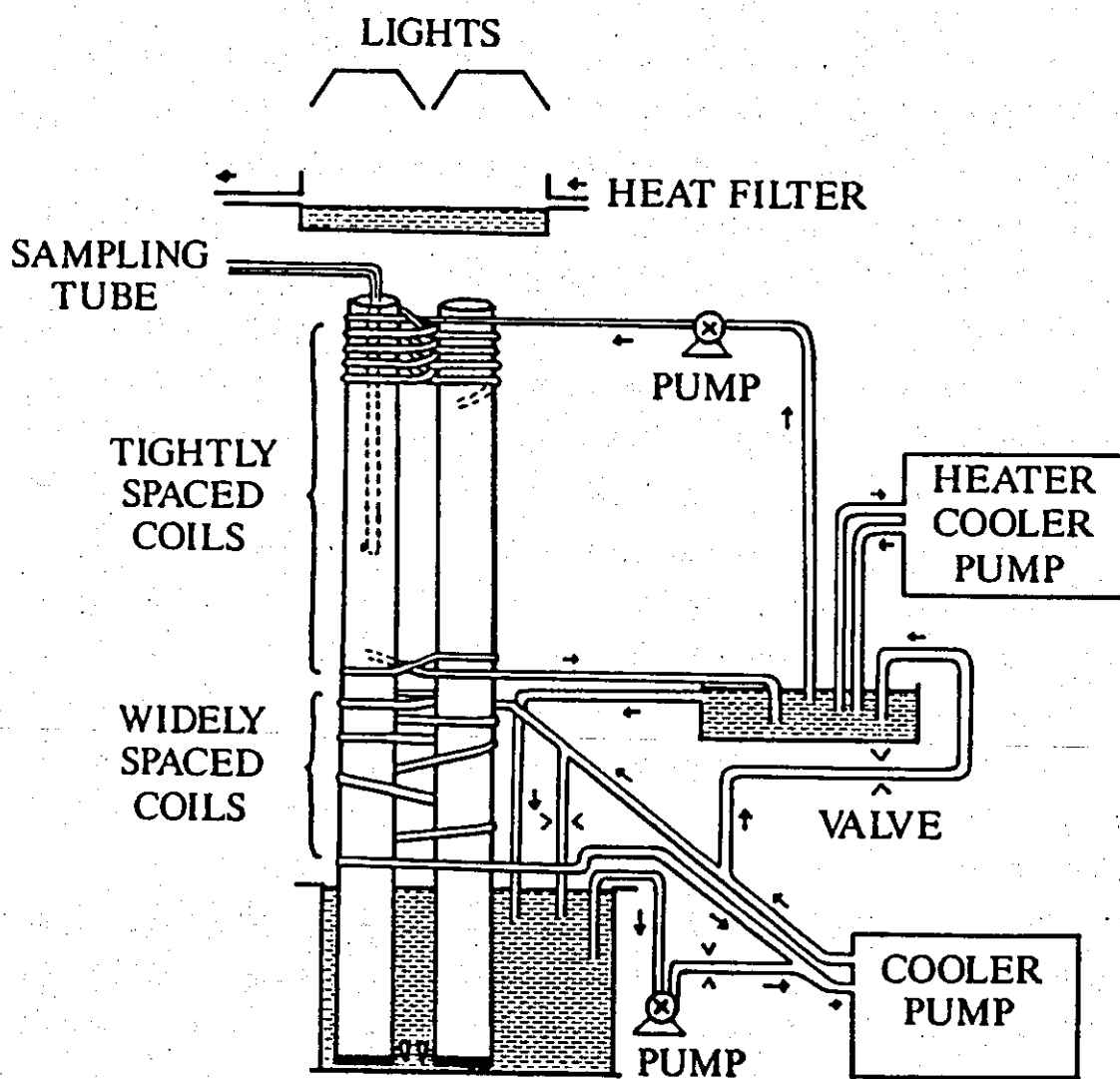
Fig. 5.1. Diagram of 4 m tall tubes and associated systems for maintaining the physical and chemical stratification as presented in Heaney et al. (1989).

1989). The tubes were 4 m tall with an internal diameter 0.25 m giving a total volume of 180 l for each. The columns were placed side by side in a 1 m deep tank of water which was connected to a cooler and kept at 7 °C. The middle layer, between 2 and 3 m from the top of the columns, was slightly cooled by widely spaced coils of plastic tubing that were supplied with water from a tube of the lower cooling system. The middle layer was heavily insulated to prevent atmospheric warming. A second tube from the lower cooling system fed an intermediate water bath that supplied water, maintained at *ca*. 14 °C by a heater circulator, to the upper 2 m layer of the columns through tightly coiled plastic tubing. A constant-level control from the intermediate bath returned water to the lower cooling system. The thermal stratification pattern achieved with this apparatus is presented in Fig. 5.2.

Illumination was provided by a 1000 W tungsten-halogen lamp above each tube. A heat filter, constructed from a Perspex-sided tank through which running water flowed, was placed between the lamps and the tubes. Irradiance levels at the tube surfaces were varied by raising or lowering the lamps or by using neutral density screening. A 12:12 light-dark cycle was controlled by a timer so that the light came on at 10.15h. Vertical profiles of underwater irradiance were obtained using a flat-plate (2π) underwater quantum sensor with non-selective response to quantum flux between 400 and 700 nm (Biggs et al. 1971), and calculated in terms of μmoles m^{-2} s^{-1}.

Vertical profiles of water temperature (± 0.1 °C) were determined using a submersible thermistor (Precision Scientific Company, Chicago, U.S.A). Profiles of *in vivo* fluorescence of chlorophyll *a* were obtained by slowly lowering a weighted silicon rubber tube (internal diameter 25 mm) into an experimental tube and pumping water through a Turner Designs Model 10 fluorometer fitted with a continuous-flow attachment. The pumping rate was kept low so that no appreciable disturbance to algal distribution in the tube was caused. The effluent from the fluorometer was returned to the level from which it was pumped by another silicon rubber tube. Water samples for cell counts and chemical and biochemical analyses were obtained from appropriate depths (usually from the cell maximum) using a three-way valve in the effluent tube. Cell counts were made by the Utermöhl's (1958) technique or by the Lund chamber

depth (cm)
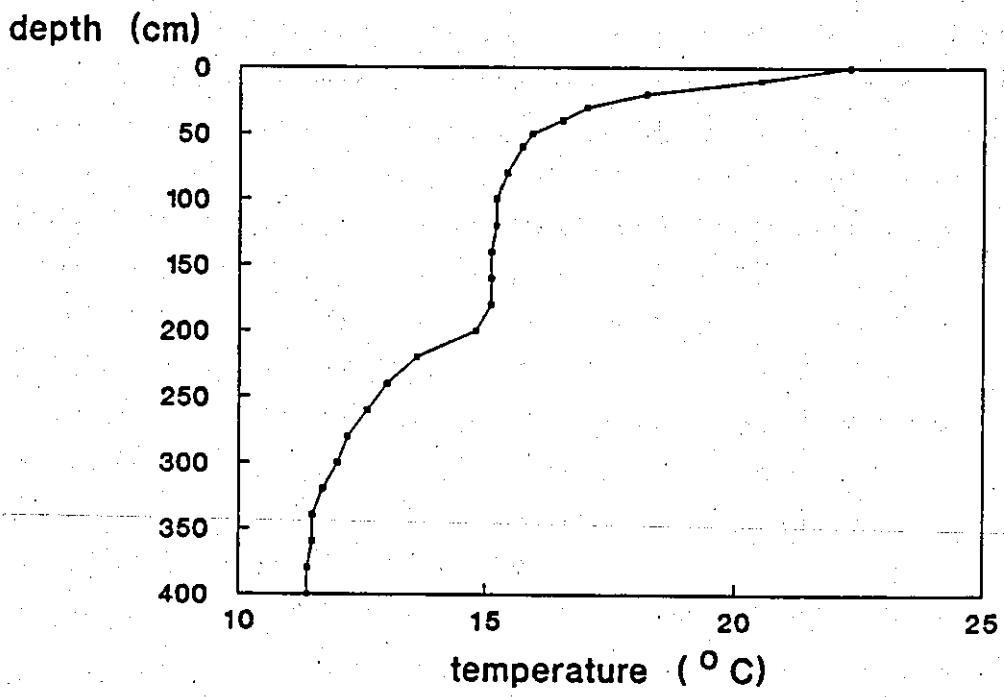
Fig. 5.2. Temperature (°C) profile maintained in experimental columns.

technique (Lund 1959). The correlation between cell numbers and values of fluorescence *in vivo* was statistically very significant ($r > 0.90$, $p < 0.001$) in each experiment. Samples for correlations were taken at different times of the light–dark cycle in order to take into account diurnal changes in fluorescence yield per cell (Kamykowski 1981). Estimates of algal populations were obtained by numerical integration of fluorescence profiles from the surface to 390–400 cm (background fluorescence subtracted) using the trapezoid rule and the application of regression equations between fluorescence and cell number. The log values of cell integrals were used for plotting increase in algal material against time. Growth rates were obtained as the slope of the least square regressions fit to these curves (Guillard 1973).

At the beginning of an experiment, the tube was filled with a modified DM medium (Thompson et al. 1988, Chapter 2) without phosphorus (in phosphorus limitation experiments) or without nitrate (in nitrogen limitation experiments). In the latter experiments $Ca(NO_3)_2.4H_2O$ in DM was replaced with $CaCl_2.2H_2O$ having an equivalent concentration of Ca^{++}. K_2SiO_3 was omitted in order to avoid contamination with diatoms. Only in the P limitation experiment with L315 was K_2SiO_3 replaced with KCl having an equivalent amount of K^+ ions. In all experiments with L485 pH of the medium was adjusted to 4.2 with 0.1 N HCl.

At the start of an experiment, an inoculum of algae grown under a 12:12 light–dark cycle at an irradiance ca 200 μmoles m^{-2} s^{-1}, temperature 19 °C and preconditioned to reduced nutrient concentration (ca. 1–5 l of DM, where PO_4 or NO_3 concentration was 10 % of normal) was added and the column gently mixed by bubbling with sterilized air. The experiments lasted 3–5 weeks of each. No algal contamination was found during the experiments. However, with L315 there was always a small number of *Bodo*–like cells present (cf. Ettl & Moestrup 1980), but these never attained significant biomass, and as colourless flagellates they did not interfere with fluorescence measurements.

During the experiments, cellular carbon, nitrogen, phosphorus, carbohydrate and protein were analyzed to provide information on the nutritional and physiological state of cell populations. For analyses, duplicate aliquots of known volume (10–300 ml) were filtered

through pre-washed and pre-combusted Whatman GF/F or GF/C glassfibre filters. Carbon and nitrogen were analyzed by an Erba Science 1106 Elemental analyser according to Hilton et al. (1986). Particulate phosphorus was analyzed by a modification of the method of Murphy & Riley (1962) using persulphate digestion (Wetzel & Likens 1979). Carbohydrate was analyzed according to the phenol method of Dubois et al. (1956) in Herbert et al. (1971) and protein by a modification (Oliver & Walsby 1984) of the Folin-Ciocalteau reagent method of Lowry et al. (1951) in Herbert et al. (1971). Dissolved inorganic phosphorus was analyzed using the method of Murphy & Riley (1962), nitrate as described by Morris & Riley (1963) and ammonium as described by Chaney & Marbach (1962).

5.3 RESULTS

For the sake of simplicity the four experiments carried out are hereafter classified as phosphorus and nitrogen experiments with L485 and L315, respectively, as these were the nutrients under scrutiny. However, it is fully appreciated that this classification greatly simplifies the complicated nature of the experiments. The migration mode of populations varied in respect of environmental conditions, but L485 always showed DVM whereas L315 in the phosphorus experiment did not show migrations until after two weeks and in the nitrogen experiment migrations did not take place at all. DVM patterns and their response to environmental changes in each experiment are fully dscribed in Arvola et al. (1991).

5.3.1 Phosphorus experiment with L485

Results from the phosphorus experiment with L485 are presented in Fig. 5.3, which depicts the 27-day experiment on a population of L485 under phosphorus depletion. The amount of inorganic phosphorus added into the hypolimnion of the tube at the onset of
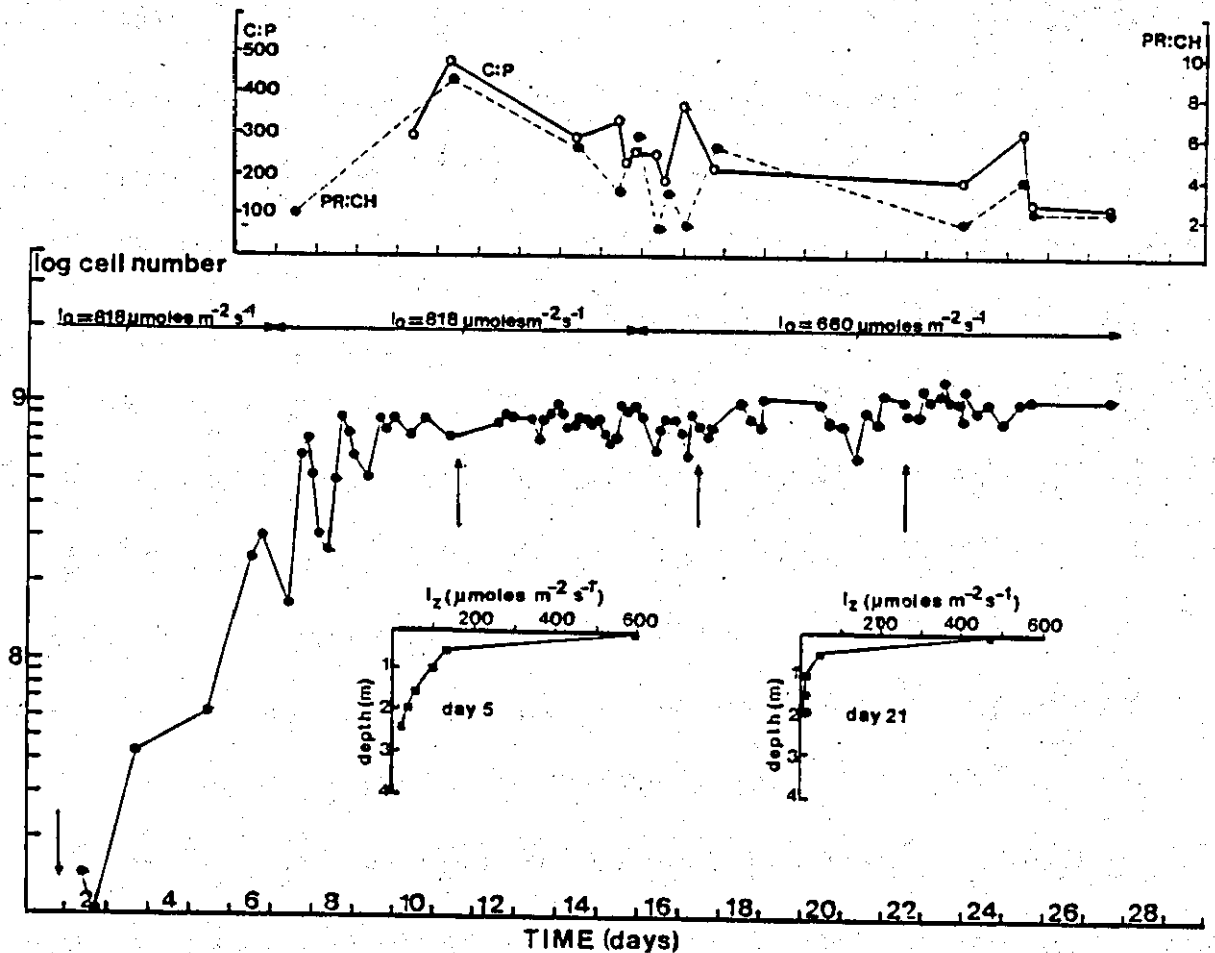
Fig. 5.3. The growth of *Cryptomonas* LA85 in the phosphorus experiment shown as the log values of column integrals. The upper insert shows protein to carbohydrate (PR:CH) and atomic carbon to phosphorus (C:P) ratios. The lower inserts display vertical light attenuation in the column on the 5th and 21st days of the experiment. Vertical arrows indicate the timing of nutrient additions. Changes in photon flux densities (μmoles m^{-2} s^{-1}) at the column surface are shown with horizontal arrows above the curve.

the experiment was enough for *ca.* 5 population divisions, assuming that the average cellular phosphorus content of L485 was 2.83 pg (Table 5.1). The population growth curve in Fig. 5.3 shows a period of rapid growth starting on the second day of the experiment and finishing on the 8th day. As the estimated growth rate was *ca.* 0.9 div. day^{-1} (Table 5.2a), it is probable that at the end of this growth burst L485 was phosphorus depleted. This cannot be confirmed by analysis of cellular composition due to unsufficient number of cells until the 10th day of the experiment. Measurements of cellular C and P on days 10 and 11 gave atomic ratios of C:P of 280 and 470, respectively. This indicated phosphorus starvation, as the "normal" atomic ratio (the so-called Redfield ratio) of C:P is 106:1 (Reynolds 1984). Phosphorus enough for one population division was added on 11th day and was taken up by algae as shown by the decline in C:P ratio from 474 to 270 and low concentrations of SRP (<1.0 µg PO$_4$ l^{-1}, not displayed in Fig. 5.3) throughout the water column, but it was not enough for a distinct burst of growth and the growth rate remained very low (Table 5.2a).

Lowering the surface irradiance from 880 to 660 µmoles m^{-2} s^{-1} did not change the migration pattern (Arvola et al. 1991) nor the growth of the population. Phosphorus added into the hypolimnion at the onset of the 17th day was taken up by the algae thus causing a slight increase in cell number and drop in C:P ratio to 216. The third addition of phosphorus on 22nd day further decreased the C:P ratio but was once again too small to result in a higher growth rate.

Considering the atomic C:N ratios, the L485 population was only occasionally nitrogen limited as just 4 out of 18 measurements resulted in ratios higher than the Redfield ratio of 6.625 (Reynolds 1984). All these four samples indicating nitrogen limitation were taken during the last week of the experiment and originated from a metalimnetic population. Sufficiency of nitrogen was also demonstrated by protein to carbohydrate ratios, which never dropped below 1.4 (Fig. 5.3).

At the beginning of the rapid growth period cells did not form distinct vertical maxima, but by the end of the growth period such maxima became more visible, bloom-formation was recorded and the population seemed to become tightly synchronized (Table 5.3). The

123

Table 5.1. Cellular phosphorus and nitrogen content (pg cell^{-1}) of cryptophytes L485 and L315 in phosphorus and nitrogen experiments.

Strain/Experiment	Phosphorus		Nitrogen	
	P cell^{-1}	N cell^{-1}	P cell^{-1}	N cell^{-1}
L485	2.83	42.49	–	35.11
N	33	18		31
S.D	2.11	37.33		22.05
L315	20.61	255.1	46.20	366.0
N	41	12	4	6
S.D	13.20	50.56	26.27	269.8

Table 5.2a. Growth rates of L485 in the phosphorus experiment. Photon flux densities in μmoles m^{-2} s^{-1} and growth rates in div. day^{-1}. 'All points' column displays results based on all data points and 'Daily maxima' column results based on highest integrated fluorescence readings. PFD refers to experimental periods displayed in Fig. 5.3. *)

PFD	All points			Daily maxima		
	μ	r	N	μ	r	N
818	0.86	0.95	16	0.96	0.98	6
818	0.03	0.21	25	0.06	0.47	6
660	0.11	0.64	42	0.08	0.75	10

Table 5.2b. Growth rates of L485 in the nitrogen experiment. PFD refers to experimental periods displayed in Fig. 5.4. For further explanation, see Table 5.2a.

PFD	All points			Daily maxima		
	μ	r	N	μ	r	N
590	0.81	0.70	9	0.88	0.99	3
Variable	0.16	0.72	26	0.14	0.98	5
430	0.19	0.53	20	0.16	0.86	4

*) μ = growth rate, r = correlation coefficient, N = number of points included in calculations

Table 5.2c. Growth rates of L315 in the phosphorus experiment. PFD refers to experimental periods displayed in Fig. 5.5. For further explanation, see Table 5.2$\overset{a}{c}$.

PFD	All points			Daily maxima		
	μ	r	N	μ	r	N
Variable	0.03	0.32	34	0.07	0.74	15
46$\overset{a}{0}$	0.89	0.85	17	0.68*)	0.99	4
Variable	0.20	0.91	55	0.18	0.95	11

*) low morning readings at the beginning of the period excluded in calculations

Table 5.2d. Growth rates of L315 in the nitrogen experiment. PFD refers to experimental periods displayed in Fig. 5.6. For further explanation, see Table 5.2a.

PFD	All points			Daily maxima		
	μ	r	N	μ	r	N
640	0.27	0.94	14	0.30	0.98	4
640	0.10	0.94	19	0.10	0.96	10

Table 5.3. Maximum cell densities of L485 in the course of the phosphorus experiment. Results are expressed as number of cells ml^{-1}.

Day	Cell density
2	2 560
5	5 661
7	64 117
8	108 412
9	22 354
12	38 806
13	41 970
14	38 774
15	60 289
16	48 298
17	27 416 *)
18	70 445
20	71 711
21	48 930
22	106 513
23	108 412

*) low density caused from the behavioural experiments (cf. Arvola et al. 1991)

maximum cell density of 108,000 ml^{-1} observed on the 8th day closely resembles maximum yields (*ca.* 100,000 cells ml^{-1}) measured in batch cultures with the same species (cf. Chapter 2). When growth ceased after the 8th day, the population – still under the same light regime – seemed to lose its synchrony and remained more dispersed throughout the day (Table 5.3). The synchrony – in terms of vertical maxima – was slowly restored and densities > 100,000 cells ml^{-1} were recorded on the 22nd day, i.e restoration took *ca.* 14 days.

5.3.2 Nitrogen experiment with L485

In the nitrogen experiment with L485, inoculation of cells into the tube was followed by a lag phase of growth despite the simultaneous addition of nitrogen sufficient for 1–2 population divisions (Fig. 5.4). Growth of L485 could not be induced until an extra quantity of nitrogen was added which, together with the initial addition, was enough for 3 divisions; these estimates are founded upon the cellular nitrogen content of 35.11 pg (Table 5.1). The following burst of growth under irradiance of 590 μmoles m^{-2} s^{-1} was of brief duration, lasting only for 2–3 days, but resulted in a fairly high growth rate of *ca.* 0.85 div. day^{-1} (Table 5.2).

After the 8th day, an increase in cellular C:N ratio from 5.8 to 12.5 was determined indicating that the population was nitrogen limited (cf. Cullen & Horrigan 1981). This nitrogen limitation was substantiated with the simultaneous drop of the cellular protein to carbohydrate ratio from 3.0 to 0.6. The population was revived – in terms of nitrogen sufficiency – with an addition of nitrogen on the 10th day enough for one population division. No appreciable growth was obvious and a growth rate of only 0.15 div day^{-1} was recorded (Table 5.2b). The population again became more nitrogen limited, as seen in higher C:N ratios and stable, low protein to carbohydrate ratios. Because this part of the experiment was also used for a behavioural investigation (Arvola et al. 1991), light intensities impinging the water surface were regularly varied from 65 to 430 or 565 μmoles m^{-2} s^{-1}. The light penetration pattern on the 14th day compared to that on the 7th
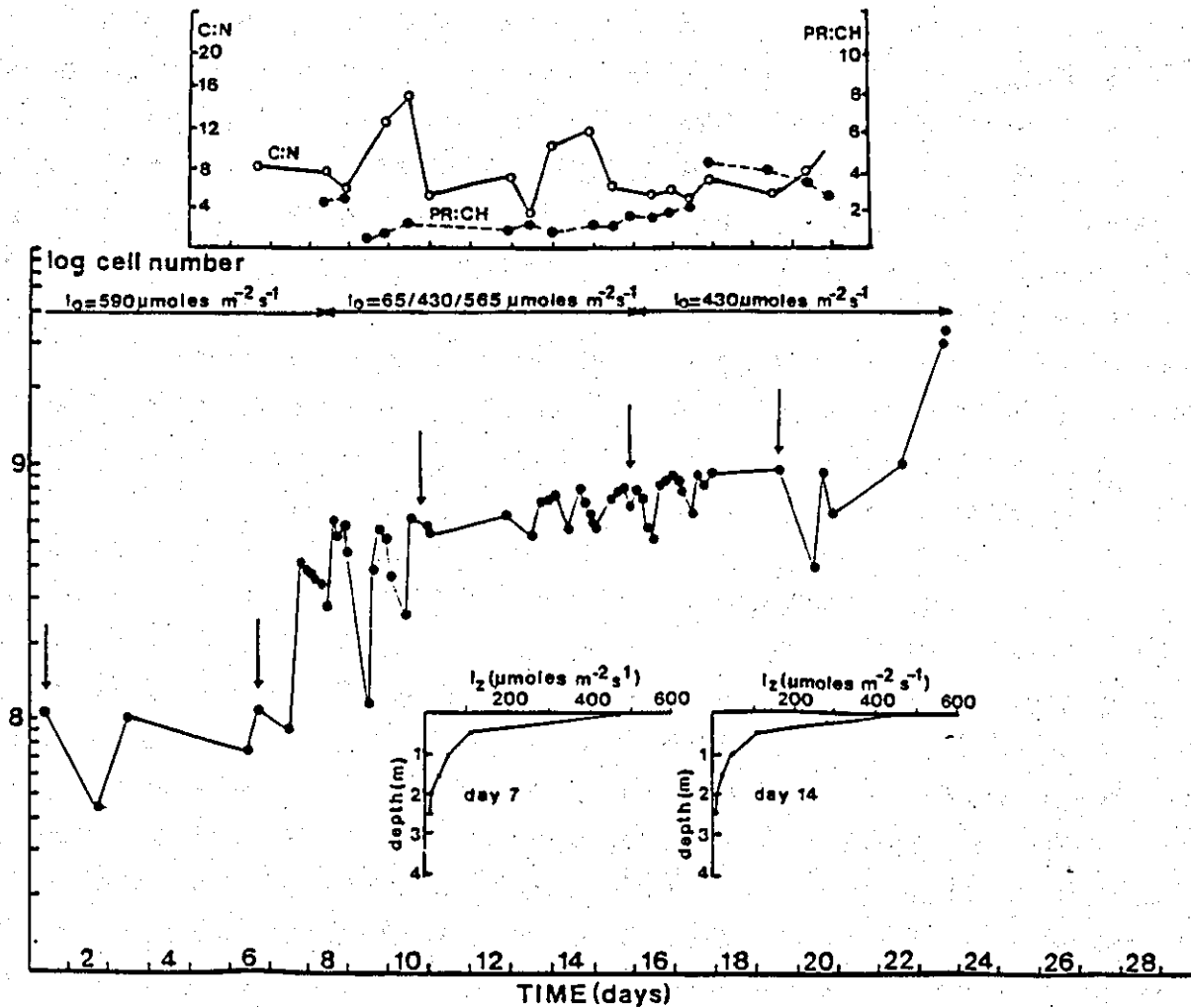
Fig. 5.4. The growth of *Cryptomonas* L485 in the nitrogen experiment shown as the log values of column integrals. The upper insert shows protein to carbohydrate (PR:CH) and atomic carbon to nitrogen (C:N) ratios. The lower inserts display vertical light attenuation (I_z) in the column on the 7th and 14th days of experiment. Vertical arrows indicate the timing of nutrient additions. Changes in photon flux densities (μmoles m^{-2} s^{-1}) at the column surface are shown with horizontal arrows above the curve.

day is shown in Fig. 5.4 and, despite the previous growth burst, no change in the pattern could be detected.

Further additions of nitrogen on the 16th and 20th days resulted in lowered C:N ratios and increased protein to carbohydrate ratios, but no clear period of growth could be seen until the very last days of the experiment (Fig. 5.4).

Besides DVM, algae in this experiment performed distinct horizontal movements. Cells concentrated onto the tube walls late in the afternoon so that fluorescence profiles were *ca.* 50 % higher in late afternoon than in the morning (Table 5.4). Special attention was paid to confirm that differences in fluorescence integrals were not caused from cells lying on the bottom of the tube.

5.3.3 Phosphorus experiment with L315

In this experiment cryptophytes showed an unusual behaviour. Despite generous phosphorus additions – sufficient for 5-6 divisions for cells requiring 20.61 pg phosphorus per cell (Table 5.1) – near the start of the experiment, it took *ca.* 16 days before population started to display DVM. Until then cells stayed on the bottom of the tube where phosphorus was also added. In order to invoke migrations surface irradiance was changed from high to low and vice versa but as light attenuation in the tube showed a sharp profile this did not have the desired impact on the bottom–lying population (Fig. 5.5). During this period of dormancy the growth rate was well below 0.1 div. day^{-1} (Table 5.2c) and between days 16 and 18 the population actually declined at a rate of −0.636 div. day^{-1}.

On the 18th experimental day the population finally commenced DVM (Arvola et al. 1991) and this change in behaviour coincided with a drastic change in growth rate as the dormant population began to grow quickly with a growth rate close to 1.0 division

Table 5.4. Fluorescence integrals of L485 in the nitrogen experiment taken in the morning and in the afternoon. Last column displays how much (%) higher afternoon readings are.

Day	Time (h)	Fluorescence integral	Time (h)	Fluorescence integral	%
6	10	426	15	920	53.7
7	10	589	17	1 981	70.3
8	10	1 464	14	3 017	51.5
9	10	1 027	15	1 907	46.2
10	9	1 410	15	3 209	56.1
13	10	2 590	16	3 992	35.1
14	9	2 732	14	4 938	44.7
15	9	4 058	15	4 630	12.4
16	9	2 520	17	5 380	53.2
17	10	3 403	16	5 349	36.4
20	9	1 500	16	6 659	77.5

Fig. 5.5. The growth of Cryptomonas L315 in the phosphorus experiment shown as the log values of cell integrals. The lower insert shows protein to carbohydrate (PR:CH) and atomic carbon to phosphorus (C:P) ratios. The upper inserts display vertical light attenuation (I_z) in the column on the 2nd and 27th day of experiment. Vertical arrows indicate the timing of nutrient additions. Changes in photon flux densities (μmoles m^{-2} s^{-1}) at the column surface are shown with horizontal arrows above the curve.

day^{-1} (Table 5.2c). However, this period of rapid growth lasted only for 3–4 days. Because no biochemical samples were taken at this stage of the experiment nothing definite can be said about the nutritional state of the cells, but as the initial phosphorus addition was enough for 5–6 cellular divisions and on the 16th day most of it could still be traced in the tube water, it is likely that cells were not phosphorus depleted.

After the burst of rapid cellular division growth slowed down to a rate *ca.* 0.190 div. day^{-1} from the 22nd day onwards. Despite some phosphorus additions the C:P ratio was continuously well above 106 indicating that cells were phosphorus depleted. On the basis of the low C:N ratio (5.6–6.8, not shown in Fig. 5.5) cells were not nitrogen depleted, even though the protein to carbohydrate ratio occasionally dropped below 1.0 (Fig. 5.5).

Throughout the experiment cells of L315 were quite dispersed and peak cell densities were much lower than the maximum cell densities of *ca.* 10,000 cells ml^{-1} recorded for this strain in batch culture (Chapter 2). While growing rapidly, the population reached a density of only 140 cells ml^{-1}, which then increased to *ca.* 700 cells ml^{-1} by the 27th day and further to 1,400 cells ml^{-1} by the end of the experiment. After the experiment was finished the population was kept in the tube and occasional sampling continued. These observations revealed that L315 kept growing slowly and maximum cell densities steadily increased reaching values of 3,300 and 3,800 cells ml^{-1} on the 42th and 45th days, respectively. As sampling was then discontinued, it cannot be said whether L315 would eventually have been able to reach a density of 10,000 cells ml^{-1}.

5.3.4 Nitrogen experiment with L315

After inoculation and initial nutrient additions the population of L315 in the nitrogen experiment entered a lag phase of growth which lasted for approximately 4 days and was followed by a period of growth at *ca.* 0.28 div. day^{-1} (Fig. 5.6, Table 5.2d). Initial nitrogen and phosphorus additions were sufficient for 2–3 and 6 population divisions
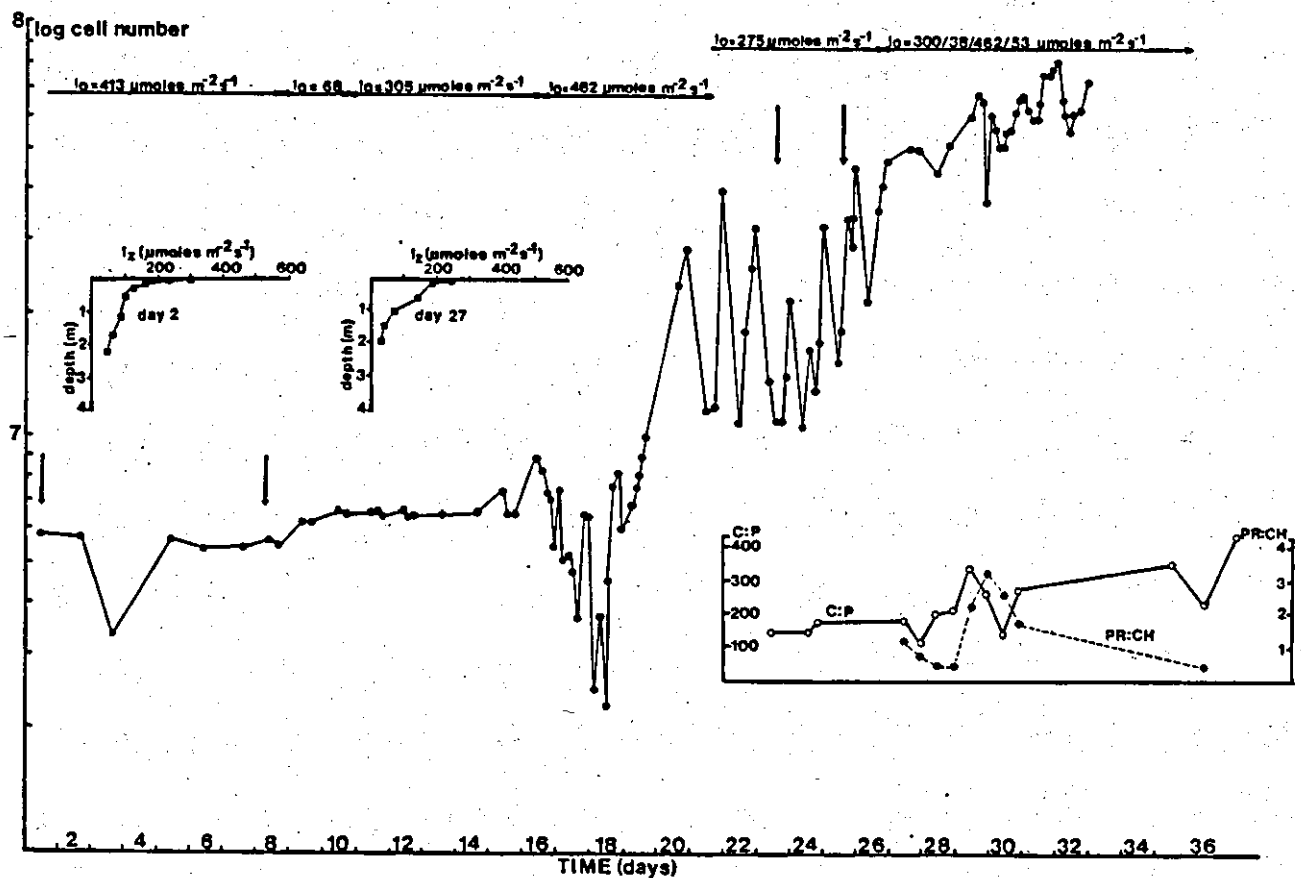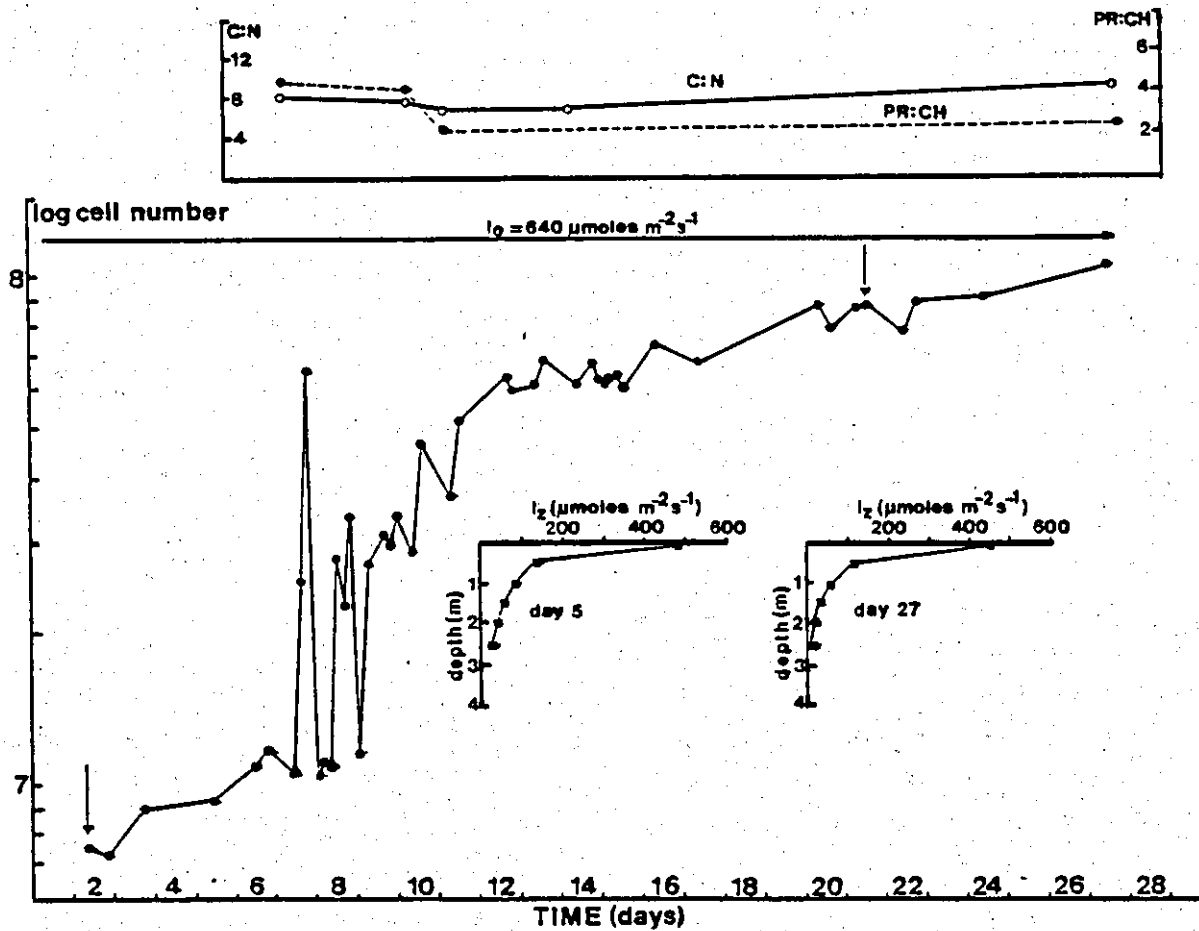
Fig. 5.6. The growth of *Cryptomonas* L315 in the nitrogen experiment shown as the log values of cell integrals. The upper insert shows protein to carbohydrate (PR:CH) and atomic carbon to nitrogen (C:N) ratios. The lower inserts display vertical light attenuation (I_z) in the column on the 5th and 27th days of experiment. Vertical arrows indicate the timing of nutrient additions. Photon flux density (μmoles m^{-2} s^{-1}) at the column surface is shown above the curve.

respectively, assuming that the cellular nitrogen content of L315 cells is 366.0 pg and phosphorus content 46.20 pg (Table 5.1). Since the nitrogen addition on the 2nd day was injected into the hypolimnion, it was unavailable to the non-migrating population, which stayed permanently close to the surface (Arvola et al. 1991), and nitrogen starvation started to show up in high C:N ratios (7.4–8.4) (Fig. 5.6). Phosphorus in the epilimnion was also rapidly taken up. Phosphorus depletion was then seen in high (170–500) cellular C:P ratios between the 7th and 11th days of the experiment. After the second week growth slowed down and for the remaining period a growth rate of only *ca.* 0.10 div. day^{-1} was determined despite the unchanged light environment (Fig. 5.6, Table 5.2d). In spite of the decreased growth, cells were probably not severely nutrient depleted as dissolved NO$_3$–nitrogen as well as PO$_4$– phosphorus was clearly detectable throughout the water column. Phosphorus was always added into the tube when it was topped up with nitrogen–free culture medium which contained 2.83 mg phosphorus per ~~liter~~ litre. Severe nutrient depletion was also ruled out by the high protein:carbohydrate ratios (2.4–4.7), although C:N ratios remained rather high (6.3–9.2) throughout the experiment.

Even though the non–migrating population stayed continuously close to the surface, formation of vertical maxima of cells was not obvious and cell density in indistinct peaks tended to vary throughout the experiment. This variation was partly caused by difficulties in satisfactory sampling from narrow surface peaks. The highest maximum of 6,500 cells ml^{-1} closely corresponding to the batch culture maximum 10,000 cells ml^{-1} of L315, was already recorded at an early stage of the experiment.

5.4 DISCUSSION

Raven & Richardson (1984) argued that the benefits of migrations, i.e increased acquisition of photons and nutrients relative to non–migratory cells, can very substantially exceed the costs to produce and operate the flagellar apparatus or any additional nutrient or photon–harvesting machinery. By means of migrations, slow–growing dinoflagellates can then increase their growth by 30 % or even 50 %.

With L485 the growth comparison between the migrating and non-migrating populations was impossible as regardless the experimental conditions the population always migrated. However, it can be argued that migrations probably were beneficial to this strain as it could achieve a growth rate of *ca.* 0.90 divisions day^{-1} which is only 35 % lower than the maximum growth rate of 1.38 div. day^{-1} recorded for this strain in batch culture experiments (Chapter 2). Benefits of DVM on algal growth could better be discerned in L315 as the highest growth rate of 0.89 div. day^{-1} in the tube was only achieved after migrations commenced. This rate also closely resembles the maximum potential growth rate of 0.87 div. day^{-1} estimated for this very same species on the basis of batch experiments (Chapter 2). Results similar to this were obtained by Kohata & Watanabe (1986) with the alga *Heterosigma akashiwo* Hada (Raphidophyceae) which, during complete mixing conditions (i.e conditions similar to batch culture) and in a migrating state, grew at a growth rate 0.62 div. day^{-1} and 0.69 div. day^{-1}, respectively. There is no similar type of reference data available on cryptophytes, but compared to *in situ* growth rates of migrating and non-migrating *Rhodomonas* and *Cryptomonas* populations in Lake Constance, L485 and L315 achieved fairly high growth rates as the maximum rate observed in Lake Constance was only 0.620 div. day^{-1} (Sommer 1985). It is also remarkable that L315 which is *ca.* 10 times larger than L485 (Chapter 2) was able to reach the same growth rate as its smaller counterpart.

During migrations L315 was probably capable of utilizing low light intensities deeper down in the tube as on the basis of the batch culture experiments (Chapter 2) this strain has a compensation irradiance for growth well below 10 μmoles m^{-2} s^{-1}. The low compensation irradiance may explain the capacity of L315 to maintain its viability whilst on the bottom of the tube or widely dispersed throughout the tube. For L485 the compensation irradiance levels are higher, generally 20–30 μmoles m^{-2} s^{-1}, thus making it more prone to self-shading effects. By precise location of vertical maxima L485 might have tried to overcome light limitation. The importance of light utilization was also recorded by Sommer (1982) who stated that the different niches of migrating *Rho-domonas lens* and *Rhodomonas v. nannoplanctica* in Lake Constance were characterized by light availability. Later Sommer (1985) postulated that for *Cryptomonas marssonii* and *C. rostratiformis* migration behaviour is a necessary compensation for specialized

light requirements, i.e migrating species have growth vs. irradiance curves of sharp and narrow shape, whereas the non–migrating species like *C. ovata* are then more generalized light utilizers. These observations are in agreement with the present results, as the readiness of L485 to migrate coincides with its more specialized light requirements (Chapter 2), and the reluctance of L315 to migrate coincides with its broader growth vs. irradiance curve, even though morphologically L315 resembles *C. rostratiformis*. Lack of migrations in flagellate populations is not as such an unusual observation and has been suggested to be caused by nutrient depletion (Eppley et al. 1968, Cullen & Horrigan 1981, Uematsu–Kaneda & Furuya 1982a, Taylor et al. 1988) and unfavourable light conditions (Samuelsson & Richardson 1982, Häder & Häder 1989, 1990, Häder et al. 1987).

Besides the effective low light utilization, favourable thermal conditions may have contributed to the enhanced growth of L315, as the epilimnetic temperatures of 17–18 °C were close to the estimated optimum temperature of 19 °C for this strain and even at the hypolimnetic temperatures of 12–13 °C it is able to achieve a relatively high growth rate (Chapter 2). It was also shown in batch culture experiments with L315 that by lowering the night time temperature it is possible to get slightly higher growth rates, which could be of use in populations displaying positively phototactic DVM. On the other hand, unfavourable thermal conditions may have contributed to the peculiar behaviour and lack of migrations of L315 in nitrogen experiment, as the surface temperatures were close to the lethal temperature (*ca.* 23 °C) recorded for this strain in the growth experiments (Chapter 2). However, the thermal conditions in phosphorus and nitrogen experiments were similar and therefore there must have been an unknown additional factor affecting algal cells and preventing them from swimming down to more favourable environment. For L485 the overall temperature conditions in the tubes were less favourable as its optimum temperature is 24.5 °C (Chapter 2). By staying continuously at the surface it could have optimized the thermal environment, but on the contrary it migrated vigorously.

As the cryptophyte populations in tubes were not axenic, it could be argued that growth was affected by phagotrophic bacterivory. However, even though cryptophytes may

possess some morphological features like the 'gullet' and 'Maupas ovalis' which make them look like ideal particle feeders, evidence for particle uptake by photosynthetic freshwater cryptophytes is very limited. Tranvik et al. (1989) have estimated that freshwater cryptophytes receive less than 2 % of their daily carbon through bacterivory thus making it quantitatively unimportant. There is no reason to believe L485 and L315 being different in this respect and some preliminary trials with fluorescent latex beads have confirmed this (Arvola, personal communication).

Finally, it can be stated that some migrating cryptophytes under favourable conditions can attain high growth rates and this study is then one of the first ones to support the hypothesis of Raven & Richardson (1984). These growth periods are of short duration and their ecological importance still needs further verification. The next step of this research should be to construct an experimental column on a smaller laboratory scale, which would ease manipulations and facilitate experimental repetition, necessary for quantitative modelling.

Chapter 6

SPRING DEVELOPMENT AND MITOTIC DIVISION PATTERN OF A *CRYPTOMONAS* SP. POPULATION IN AN ACIDIFIED LAKE

6.1 INTRODUCTION

One of the continuing challenges facing phytoplankton ecologists has been measuring intrinsic species–specific growth rates *in situ*. Traditional methods for productivity measurements (e.g. methods based on oxygen production and ^{14}C incorporation) can provide insight into the growth of an entire phytoplankton assemblage, but they have many drawbacks which complicate the interpretation of results. These methods involve incubation of water samples in closed vessels giving rise to problems with unknown bottle effects. If zooplankton grazers are included in incubations the results given by these methods are closer to the net response of algal growth than population–specific growth rate. Grazers can be largely eliminated by prefiltration and samples size–fractionated to get closer to species–specific estimates, but all preincubation manipulations may alter availability of nutrients and thus change the growth conditions of algae (Furgeson et al. 1984). Delicate algal cells like cryptophytes can also be affected (Barbosa, personal communication). An alternative approach is to use the observed increase of cell numbers in a lake as a measure of growth *in situ*, but these estimates are also affected by grazing, sinking and import and export of cells, all factors which are extremely difficult to quantify.

To avoid methods that require incubations or any experimental manipulations, phytoplankton ecologists have brought into use the mitotic index technique whereby proportions of cells in mitosis and cytokinesis are determined. Usually the stages identified are cells with double nuclei and paired cells. Two stages are needed for the determination of the duration of mitosis, essential in growth rate calculations. The method has mainly been applied to dinoflagellates, as with these algae the required stages are better discernible and it is possible to distinguish between just divided and older cells (Elbrächter 1973, Swift et al. 1976, Weiler & Chisholm 1976, Heller 1977, Weiler 1980). Other groups of algae to which the method has been applied are diatoms and, quite recently, desmids, cryptophytes and blue–green algae (Smayda 1975, Braunwarth & Sommer 1985, Campbell & Carpenter 1986, Carpenter & Campbell 1988, Cobelas et al. 1988).

To calculate growth rates from mitotic index data, three assumptions have to be made: (1) the duration of the division stage chosen is constant with respect to changing environmental conditions; (2) this duration is identical for all cells in a population; and (3) all cells in a population are active. Undoubtedly the weakest point of the mitotic index technique is the first assumption, as little has been done to verify it and there is actually some evidence that this assumption may not always be valid (Olson et al. 1983, Olson & Chisholm 1986, Campbell & Carpenter 1986, Weiler & Eppley 1979).

The primary goal of this study was to determine the pattern and timing of nuclear and cellular division in one *Cryptomonas* species and, if possible, to use the data for the calculations of species–specific potential growth rate *in situ*. A secondary goal was to establish the environmental conditions under which this species starts its vernal growth, as cryptophytes have been claimed to be characteristic of the spring phytoplankton in small north temperate and subarctic lakes (Skuja 1956, Arvola 1986). The species chosen for this study was *Cryptomonas* L485, that had already been used in the previous extensive laboratory experiments (Chapters 2,3,4 and 5). Growth rate calculations were based on the three assumptions given above. Instead of the staining with the often used acetocarmine stain, the method used in this work to visualize the nucleus was fluorochrome 4'6–diamidino–2–phenylindole (DAPI) widely used by microbial ecologists (e.g. Coleman 1980, Porter & Feig 1980). DAPI is a highly sensitive stain for DNA combining with adenine–thymine base pairs (Kapuscinski & Skozylas 1977). This DAPI–DNA complex gives a strong blue fluorescence when excited with UV–light. The use of DAPI is practical as samples can be preserved in the field and no heating or soaking of filters is needed.

6.2 DESCRIPTION OF SITE AND SPECIES

The lake chosen for this study was Vähä–Valkjärvi, situated in the Evo forest district in Lammi commune, southern Finland. The lake is 2.3 ha in area and has a maximum depth of 4.0 m (Fig. 6.1). This small headwater lake is surrounded by conifers and birches (Fig. 6.2). It is a clearwater lake with water colour of 15 mg Pt L^{-1}
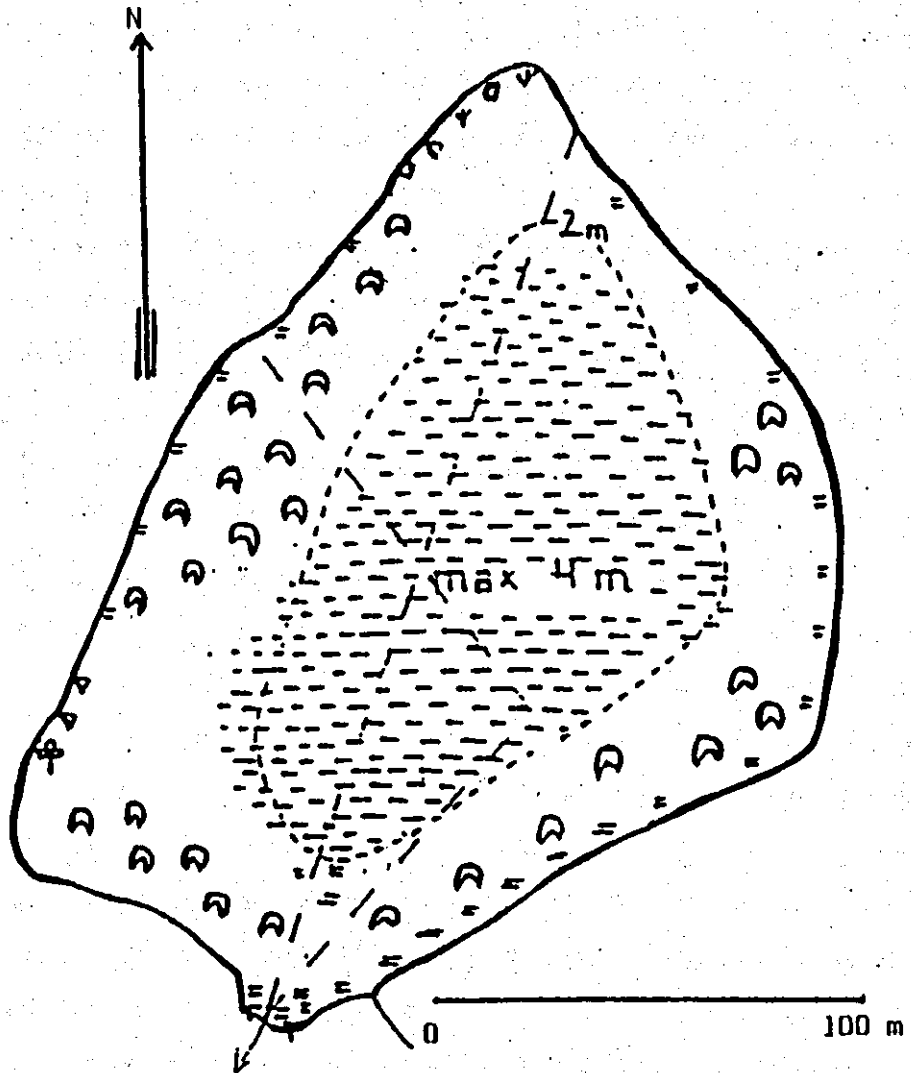
Fig. 6.1. Lake Vähä–Valkjärvi and its vegetation (Kairesalo et al., unpublished data)

↓	Carex lasiocarpa
▽	Carex rostrata
⊕	Menyanthes trifoliata
⌂	Nuphar lutea
⊸	Warnstorfia (Drepanocladus) trichophyllum
≈	Sphagnum sp.

Fig. 6.2. Lake Vähä–Valkjärvi and the surrounding forest.

(Arvola & Kankaala 1989). The present pH is 4.5 so that fish are no longer capable of reproduction in the lake (Lappalainen et al. 1988). However, the very low pH of the lake is a result of recent anthropogenic acidification and there are some old perch and pike hatched before this acidification still living in the lake (Rask , unpublished data, Salonen et al., unpublished data). Effects of the extreme acidity can also be seen in other links of the food chain. The zooplankton comprises only a couple of cladoceran species, *Bosmina longispina obtusirostris* being the dominant species. Probably the most important primary producer in this simplified ecosystem is an aquatic moss, *Warnstorfia (Drepanocladus) trichophyllum*, which covers the central part of the lake bottom (Kairesalo et al. 1987) (Fig. 6.1). The phytoplankton species of greatest importance is *Cryptomonas* L485 living amongst and just above the moss vegetation. In lake Vähä–Valkjärvi it is most abundant in early spring and late summer when densities of cladocerans are lowest (Kairesalo et al. 1987). Figure 6.3 illustrates the species as it is seen in samples taken from the field.

6.3 MATERIAL AND METHODS

6.3.1 Field sampling

Breakup of ice in lake Vähä–Valkjärvi took place on 27. April 1989. Changes of algal population densities were determined from 30. April to 25. May. In order to avoid problems from the possible phasing of cell division, samples were always taken at the same time of the day, at approximately 11.30h standard time. Four integrated samples from the surface to 3.5 m were taken with a flexible tube sampler, pooled and a 100 ml aliquot was withdrawn and preserved immediately with acid Lugol's iodine. Three such samples were taken on every occasion from the central part of the lake.

Samples for a study of phased cell division were taken over a period of 24 hours on 20. May – 21. May 1989, when the time of local sunrise was 3.17 h and sunset 21.12 h. Sampling was started and finished at 9.30 h local standard time. Integrated
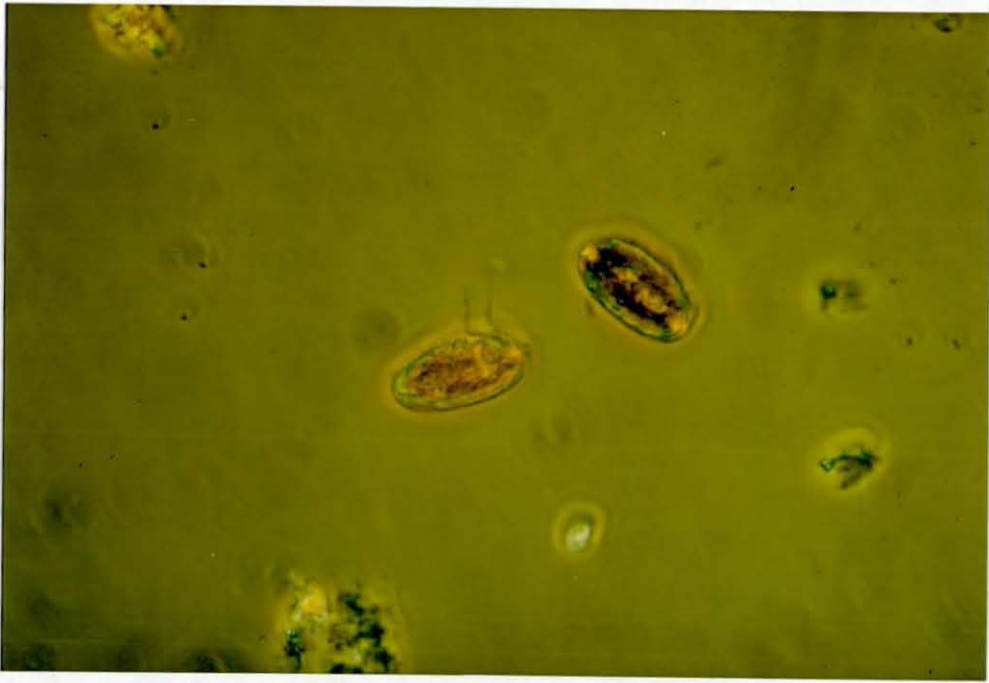
144

Fig. 6.3. *Cryptomonas* L485 in a field sample under phase contrast illuminàtion. Photograph taken on Agfachrome CT 100 film with a Nikon M–35 camera connected to a Nikon Diaphot– TMD inverted microscope. Magnification 400x.

samples from 0–3.5m at time intervals of 30 min were taken with a flexible plastic tube sampler from the central part of the lake where the lake bed was covered by moss. Previous experience (Kairesalo, unpublished data) had shown that samples taken only from the water column might not contain enough cells for microscopical examination, so this time the tube sampler was lowered so deep that part of it penetrated the upper layers of the moss vegetation. Samples taken this way were immediately preserved with acid Lugol's iodine.

Temperature and oxygen concentration were measured after every population sampling with a temperature compensated dissolved oxygen probe, model YSI 57 (Yellow Springs Instruments Co., Yellow Springs, Ohio). During the diel sampling period measurements were made at 9.30, 13.00, 18.00, 21.00 (on 20. May), 1.00, 5.00 and 9.00 (on 21. May).

Samples for pH measurements and for dissolved inorganic nutrients were taken on 3.5., 8.5., 12.5., 16.5. and 21.5. with a Ruttner sampler (volume 2.7 dm^3).

Integrated samples from 0–3.5 m for particulate organic carbon (POC) analyses were taken on 23.5. with the flexible tube sampler. Samples were filtered through a net with 75 μm mesh size.

Solar radiation and vertical attenuation of light were measured twice (20. May and 23. May) during the sampling period with a LI–COR light meter equipped with LI–1000 data logger system and 4π spherical quantum sensor. The 4π design permits an estimation of both incident and scattered light from above and reflected and scattered light from below. Readings taken were means of values measured over 10 minutes.

6.3.2 Laboratory analyses

Samples for population growth rate determination were counted with a Nikon Diaphot–TMD inverted microscope using a 40x objective and Utermöhl's (1958) technique. A subsample of 50 ml was sedimented and the number of L485 cells from

50 fields was counted under phase contrast illumination. The technique used for other dominant species was to count 500 cells from various numbers of random fields of view. Microphotographs of the species (Fig. 6.3) were taken on Agfachrome CT 100 film with a Nikon M–35 camera.

Samples for phased cell division analysis were concentrated from 100 ml to 10 ml by sedimenting the cells in measuring cylinders and siphoning off the overlying water. Samples concentrated in this way were decolorized with 1–2 drops of 1 N sodium thiosulfate and DAPI fluorescent stain (Sigma Co.) was added to a final concentration of 0.5 μg ml^{-1}. Samples were then filtered on 0.2 μm membrane filters (Nuclepore) using a vacuum pump. The filters were placed on glass slides, cleared with a drop of immersion oil and covered with a cover slip. At least 700 cells from each sample were examined under UV light with a Nikon OPTIPHOT microscope equipped with episcopic–fluorescence attachment (EF–D), mercury lamp and 100x oil immersion UV–objective. The filter block used consisted of an excitation filter UV330–380 (main wave length 365nm), a dichroic mirror DM 40 and an eyepiece-side absorption filter 420 K. Cells were counted in three categories: 1) cells with dividing nucleus; 2) dividing cells; and 3) cells with a single interphase nucleus. Specimens of all these categories were documented on photographs using a Nikon M–35 S microscope camera and Kodak Ektachrome 400 film. In order to avoid an overall reddish backgound on the photographs, an auxiliary filter (–5501F) was used to cut off the far–red emission light not observed visually but registered by the film.

Dissolved inorganic nutrient samples were filtered through Whatman GF/C glassfibre filters. Phosphorus was analysed as ortho–phosphate using the colorimetric method of Murphy & Riley (1962). Nitrate analysis was based on nitrate reduction and colorimetric determination of nitrite produced in reaction, as described by Morris & Riley (1963). pH was measured with an Orion model SA 720 pH meter equipped with electrode 9162 SC. Samples for particulate organic carbon (POC) were filtered onto a pre–combusted 4.7 cm Whatman GF/C glassfibre filter and stored in a desiccator before analysis with a Unicarb Universal Carbon Analyzer. In this method POC was determined as CO_2 with an infrared gas analyser after high temperature (900 °C) combustion (Salonen 1979, 1981). From one GF/C filter five replicates

were punched out and analysed in this way. These data were used to estimate the relative importance of L485 in the plankton community.

6.3.3 Calculations of growth rate and production

Potential growth rates of L485 were calculated using the following equation recommended by McDuff & Chisholm (1982):

$$K_e = 1/nt_d \sum_{i=1}^{n} \ln (1 + f_i) \ (day^{-1}) \qquad (1)$$

where K_e is the daily averaged specific growth rate for a 24 hour period during which n samples were taken, f_i gives the proportion of cells in mitosis and t_d is the duration of mitosis. Specific growth rate is divided by ln 2 to obtain k in divisions day^{-1}.

The duration of mitosis was estimated in two different ways: 1) by the difference between the median time of the proportion of cells with dividing nucleus and the median time of the proportion of diving cells; and 2) by the time difference between the maxima of the two division stages. The first approach is generally used when peaks of dividing nuclei and dividing cells are not clear enough for the use of the latter approach (Braunwarth & Sommer 1985, Heller 1977).

The observed rate of increase of the population (K) was calculated from the means of the three pooled samples by least–squares fit of a straight line to logarithmically transformed data as described by Guillard (1973).

Loss rate (λ) was calculated as the difference between the potential and observed rates of increase:

$$\lambda = k - K \ (div. \ day^{-1}) \qquad (2)$$

The rate of production (PP) was calculated from the growth rate K_e (day^{-1}), the population density N, and an average carbon content (C $cell^{-1}$):

$$PP = K_e \times N \times C \text{ cell}^{-1} \quad (\text{mg C m}^{-3} \text{ d}^{-1}) \qquad (3)$$

A carbon value of 0.195 ng C cell^{-1}, based on earlier laboratory experiments at 10 °C (Chapter 3), was used in the calculations.

6.4 RESULTS

6.4.1 The lake

After the breakup of the ice, the lake was thermally stratified and the thermocline lay at a depth of 150 cm (Fig. 6.4a). With solar heating the thermocline gradually sank deeper down and finally, in mid–May, the thermal stratification was lost and the lake was in a state of continuous circulation. During the stratification an orthograde oxygen profile with higher concentrations close to the bottom was maintained, but this stratification also disappeared by mid–May and the oxygen concentration decreased as the water temperature increased (Fig. 6.4b). During the stratification the whole water column was saturated with oxygen, but after mixing saturation dropped to 95–98 %. Some diel fluctuation in oxygen concentration could be seen on 20.–21. May. The oxygen concentration dropped from the highest early evening value of 10.2 ppm to 8.4 ppm at 02.00–06.00 h. A parallel increase could also be seen in the saturation deficit.

Unlike with temperature and oxygen, no stratification of dissolved inorganic nutrients could be found at the beginning of May (Fig. 6.5). Concentrations of nutrients confirmed the earlier understanding that Vähä–Valkjärvi is an oligotrophic lake.

Throughout the sampling period the pH distribution in the water column was quite uniform, the greatest difference between surface and bottom values being less than 0.15 units. Differences of this order can be explained by the activity of communities of primary producers living close to and on the bottom. The lowest surface value of
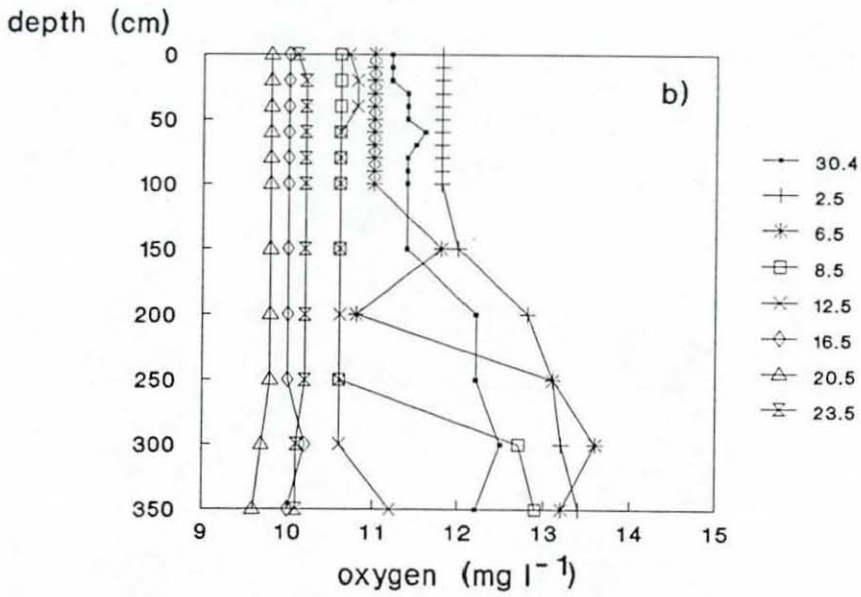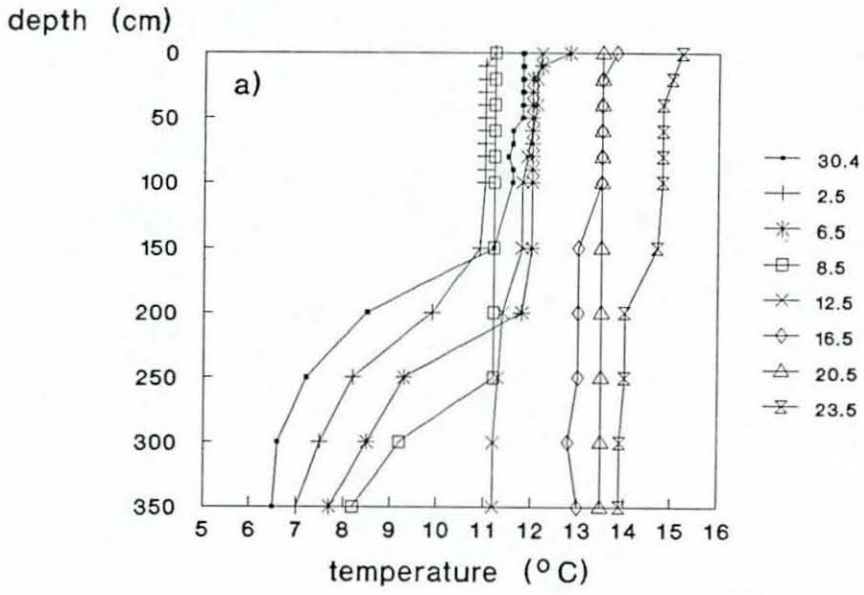
Fig. 6.4. Temperature (a) and oxygen (b) profiles in Vähä–Valkjärvi, at different dates.
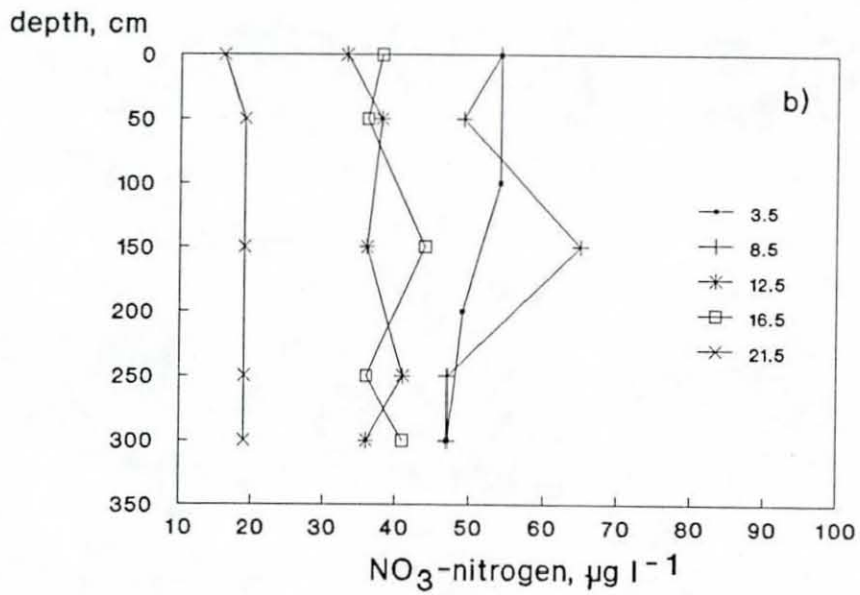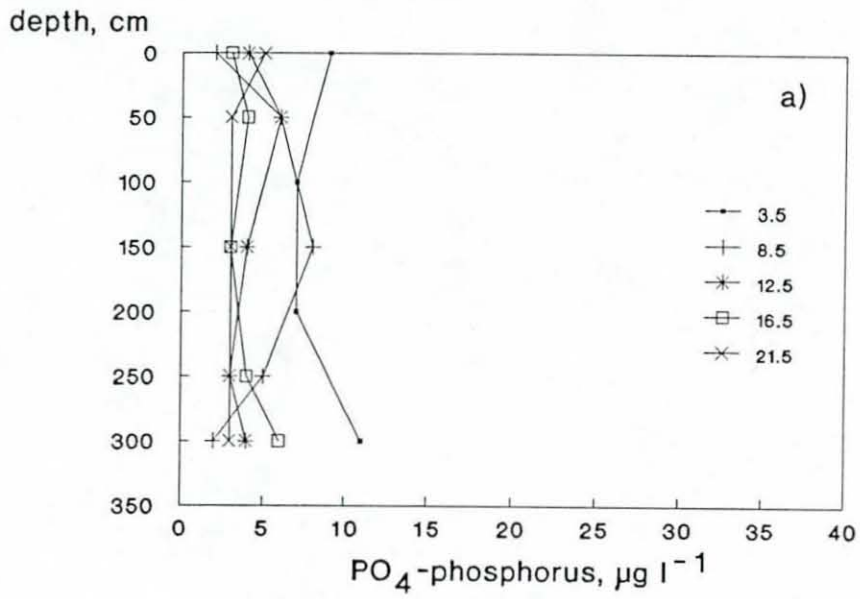
Fig. 6.5. Vertical profiles of PO₄–phosphorus (μg l⁻¹) and NO₃–nitrogen (μg l⁻¹) in Vähä–Valkjärvi in May 1989.

4.45 and the highest bottom value of 4.63 were measured on 8. May and 21. May respectively.

Penetration of solar radiation measured on 23. May is presented in Fig. 6.6. It shows that *ca.* 50 % of the light incident on the surface reached a depth of 3 m. Measurements made on 20. May gave similar results. The vertical attenuation coefficient ε_{PAR} for this lake was 0.30 m^{-1}, which is a normal value for an oligotrophic clearwater lake in this area (Jones & Arvola 1984).

The POC content of water on 23.5. was 293.0 µg C l^{-1} which, combined with the cell density and carbon value data, gives a 63 % contribution of L485 to total carbon. Taking into consideration that the estimate of total POC includes bacteria [(GF/C filter retains *ca.* 50 % of the bacterioplankton (Tulonen et al., unpublished data)] this shows the overwhelming importance of L485 in the phytoplankton assemblage.

6.4.2 Populations of algae

The development of the L485 population together with a small unknown flagellate (diameter < 5 µm) is shown in Fig. 6.7. This small flagellate was practically the only phytoplankton species present in the lake after the breakup of the ice. Occasional sampling had revealed that it was already thriving under the ice cover. Due to its high numbers, the Secchi depth at the beginning of May was smaller than the total depth of the lake and probably this turbidity was partly responsible for the observed thermal stratification pattern of early May.

During the sampling period the population of the unknown flagellate showed a continuous decline that speeded up after 8. May. At the same time L485 started to grow exponentially reaching a net growth rate of 0.75 divisions day^{-1} between 8.5.– 16.5. After that the growth rate dropped to 0.26 div. day^{-1} (16.5.–23.5.). Finally the population reached the stationary phase of growth. The range of cell densities of L485 remained quite high throughout the sampling period. This was assumed to be
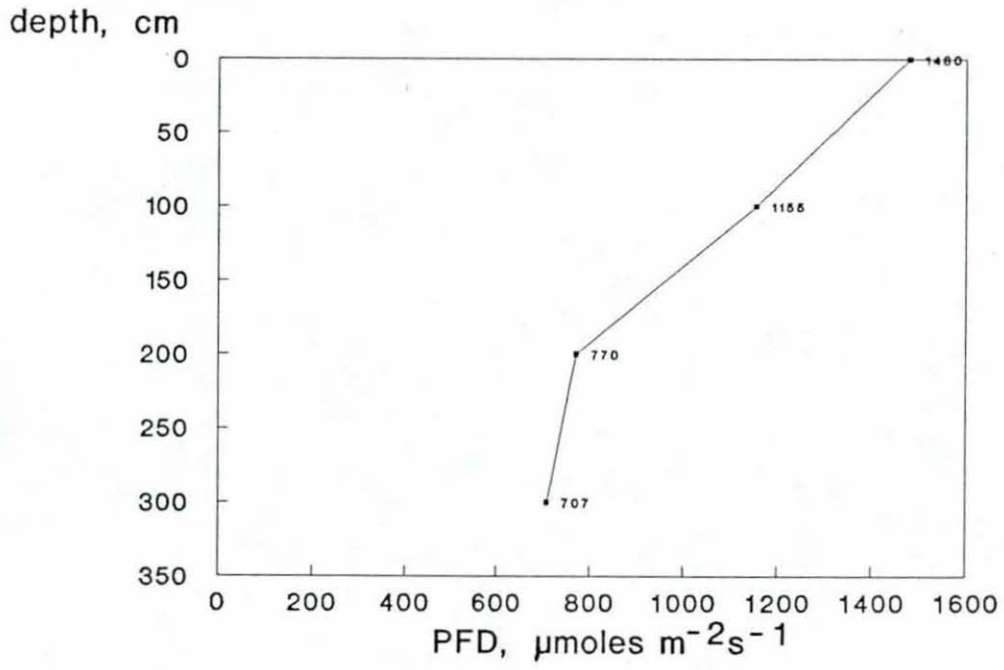
depth, cm

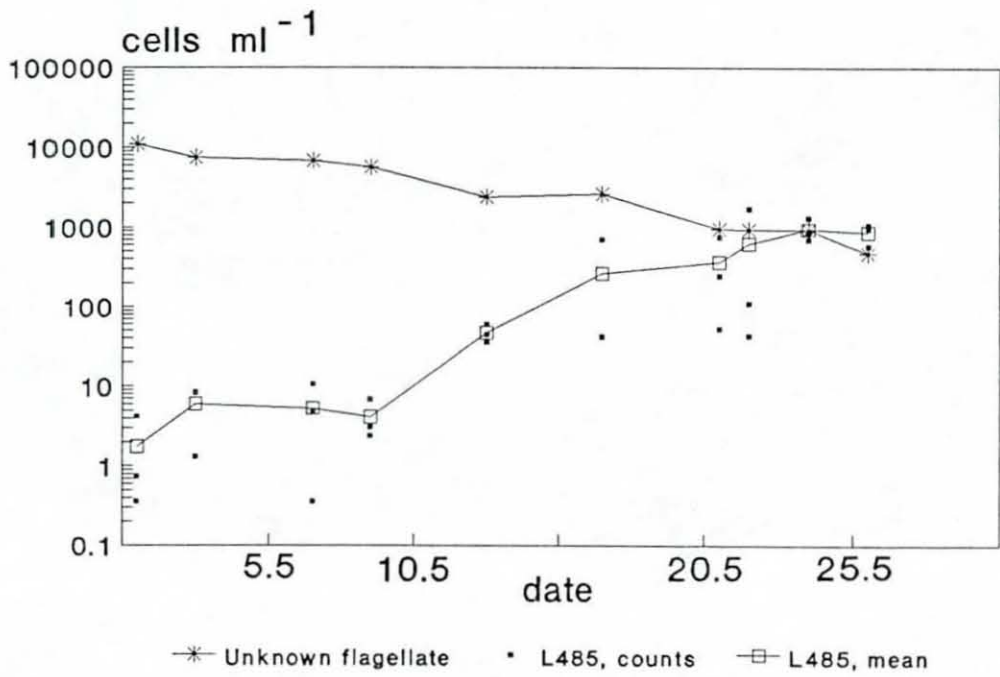**Fig. 6.6.** Light attenuation in Vähä–Valkjärvi on 23.5.1989.

Fig. 6.7. Spring development of the L485 population (• = triplicate samples; □ = mean of counts) together with an unknown flagellate (∗). Population densities are expressed as cells ml⁻¹.

due to the peculiar pattern of vertical distribution as well as the patchiness in horizontal distribution (Kairesalo, personal communication).

6.4.3 Division stages of L485

The division stages of *Cryptomonas* L485 discernible with light microscopy are shown in Fig. 6.8. Despite the staining of DNA only, more than 85 % of which is located in the nucleus (Puiseux–Dao 1981), the whole cell can be easily recognized. At interphase (Fig. 6.8a) cells show the characteristic cryptophycean appearance (Lucas 1970, Oakley & Bisalputra 1977). The nucleus is situated in the posterior end of the cell and it is typically cryptophycean, possessing a large nucleolus – clearly visible under the microscope but impossible to catch on film – and abundant chromatin. The first step of the mitotic sequence distinguishable in the photographs is metaphase (Fig. 6.8b), when the cell rouns up, the nucleus migrates toward the anterior end of the cell and the chromatin is in a disk–shaped mass (Oakley & Bisalputra 1977). At anaphase (Fig. 6.8c) the chromatin separates into two disk–shaped masses, first lying side by side but then parting farther from each other. At telophase (Fig. 6.8d) the two plates stop moving and the nuclei round up. With *Cryptomonas* L485 it was exceptionally easy to distinguish the mitotic cells from interphase cells; only those cells at prophase (i.e. at the phase of flagellar base replication) could not be included in the category of cells with dividing nucleus (cf. Oakley & Bisalputra 1977).

Despite the distinct character of different stages seen in these photographs, in practice it is not always easy to recognize the stages as in light microscopy they seem to form a continuum without clear boundaries.

The first signs of cytokinesis can already be seen by the time the metaphase plate has formed (Fig. 6.8b) and the gradual division process is completed at late telophase (cf. Oakley & Bisalputra 1977). This means that nuclear and cellular division of L485 totally overlap and cells classified as being dividing cells are actually at the telophase of mitosis.

a)

b)

156
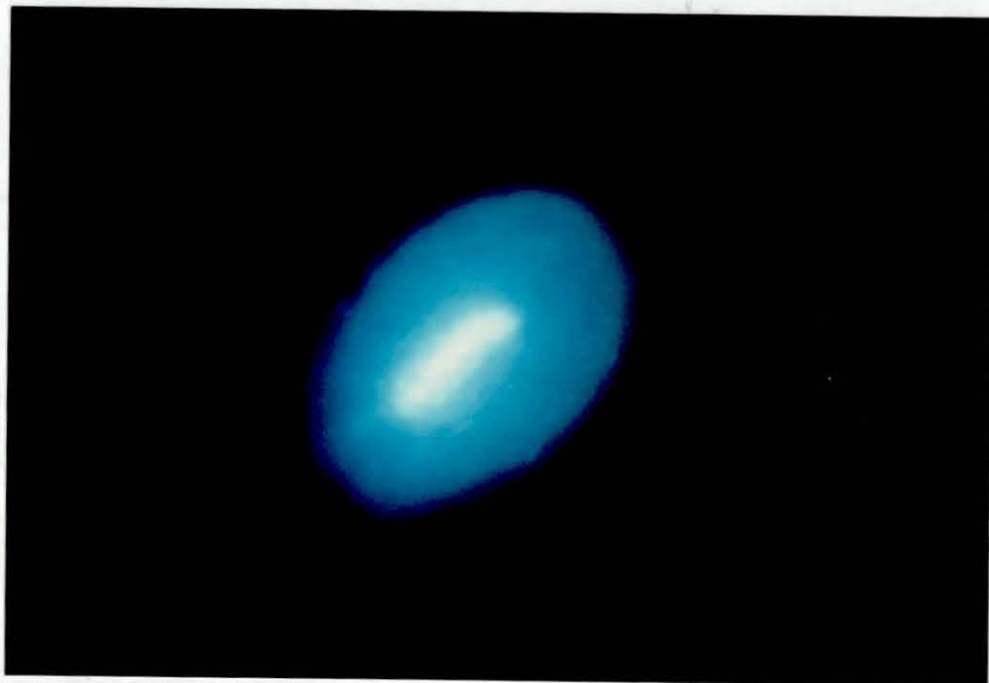
c)
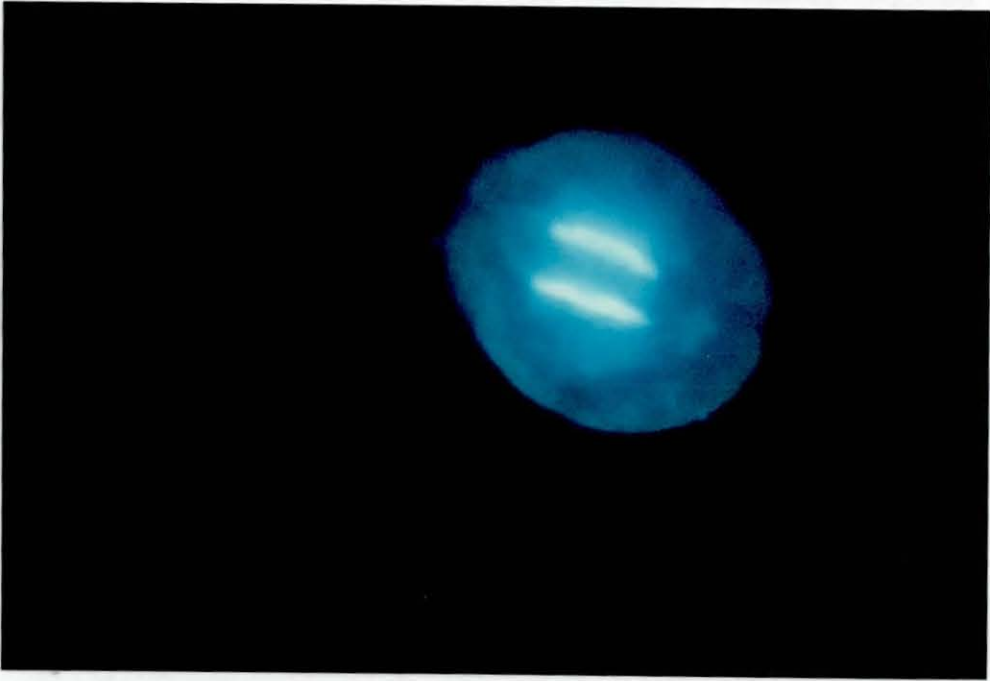
d)

Fig. 6.8. Division stages of *Cryptomonas* L485. A cell at interphase (a), metaphase (b), anaphase (c) and telophase (d). Photographs taken on Ektachrome 400 film with a Nikon M–35 camera connected to a Nikon OPTIPHOT microscope. Magnification 1250x.

The diel pattern of nuclear and cell division of L485 on 20.–21. May is shown in Fig. 6.9. As a consequence of overlapping mitosis and cytokinesis the category "dividing nuclei" includes also the cells identified as "dividing cells". From the figure it can be seen that division processes occured from 18.30 h to 5.30 h, which at these latitudes at that time of the year means twilight conditions instead of darkness. In a lake like Vähä–Valkjärvi, a more substantial increase in incident irradiance is seen approximately from 08.00 h when the sun rises above the surrounding forest so that direct sunlight is then incident on the lake surface (cf. Jones 1988). Practically no dividing nuclei nor dividing cells could be seen outside this time period. The highest peaks of dividing nuclei were observed at 22.30 h and 00.00 h. The two highest maxima of dividing cells occured at 23.00 h and 00.00 h. The percentages of nuclei and cells in division processes remained low even at the highest peaks, the maximum for dividing nuclei and dividing cells being 2.7 % and 1.1 %, respectively. The calculated median time for nuclear division was 22.55 h and 23.00 h for cell division, which means that t_d would have been only 5 minutes. Bearing in mind the peculiarities of the division processes, this estimate of t_d is almost certainly an underestimate. Using the time difference between the highest peaks of cells with dividing nuclei and dividing cells gives a t_d value of 30 minutes.

Potential growth rates calculated using equation (1) and the two estimates of t_d given above are presented in Table 6.1. In addition, growth rates based on the t_d of 10 minutes given by Oakley & Bisalputra (1977) for a smaller *Cryptomonas* sp. with the same kind of nuclear division pattern, as well as generation time T_d and loss rates are shown. The calculated rates of production (PP) are displayed in the last column.

The potential growth rate of 1.49 day^{-1} based on the t_d value of 5 minutes is six times greater than the one based on the value of 30 minutes. With the longest t_d estimated the loss rate drops down to 0.10 div. day^{-1} as the potential growth rate gets close to the observed growth rate of the population. These results indicate the sensitivity of the method to reliable estimates of t_d.
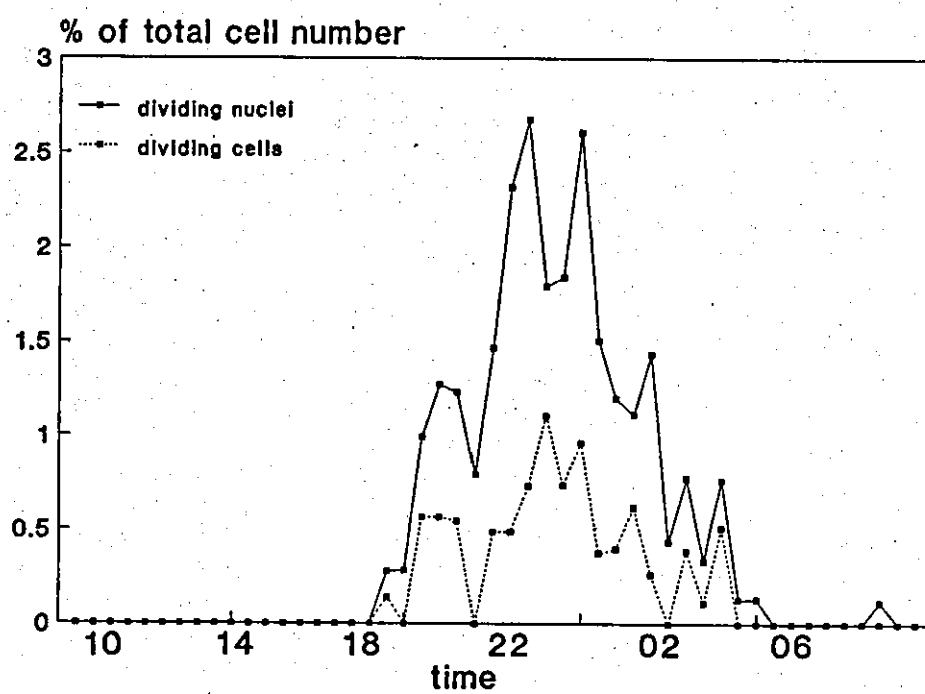
Fig. 6.9. Diel pattern of mitosis and cytokinesis of L485 in Vähä–Valkjärvi on 20.–
21.5.1989.

Table 6.1. Estimates of potential growth rates, generation times, loss rates and rates of production for L485. K_e = specific growth rate, day^{-1}, k = growth rate in divisions day^{-1}, T_d = generation time in days, λ = loss rate, div. day^{-1} (k–K, K = 0.26 div. day^{-1},) PP = rate of production, mg C m^{-3} day^{-1}.

t_d	K_e	k	T_d	λ	PP
5 min	1.49	2.14	0.47	1.88	276.60
10 min	0.74	1.07	0.93	0.81	137.37
30 min	0.25	0.36	2.80	0.10	46.41

6.5 DISCUSSION

The population of L485 started to grow when the bottom temperature in the lake had risen from 8 to 11 °C. Taking into consideration that grazing pressure on cryptophytes in early May must have been extremely low as cladocerans had not yet emerged (the first ones were found in samples on 21. May) and assuming no nutrient limitation or washout in the bottom growing L485 population, the situation resembled those in batch cultures where light and temperature are the variables determining the growth of algae. Thus, the results of the previous laboratory experiments (Chapter 2) can be used for comparison. In batch cultures L485 was estimated to achieve a maximum growth rate of 0.76 div. day^{-1} at 12 °C, which is in good agreement with the growth rate of 0.75 div. day^{-1} observed in this field study. However, at 10 °C in batch culture L485 was estimated to grow only at the maximum growth rate of 0.49 div. day^{-1}. In agreement with this study, Sommer (1981) has reported that at the beginning of spring bloom cryptophytes can grow at a high rate and in this respect they are typical organisms favoured by r–selection.

At low temperatures the saturation of growth of L485 is attained at low irradiances and beyond the saturation point photoinhibition can be observed (Chapter 2); e.g. the laboratory growth rates given above were under light intensities of 100 μmoles m^{-2}s^{-1} and 50 μmoles m^{-2}s^{-1}, respectively. Bearing in mind that on a sunny day in lake Vähä–Valkjärvi the light intensity at the depth of 3 m was 700 μmoles m^{-2}s^{-1}, it must have been advantageous or even necessary for L485 to take refuge amongst the protective *Drepanocladus* vegetation. Since zooplankters were absent at this time, avoidance of grazing pressure could not have been a reason for cryptophytes staying amongst the moss. However, with the methods used in this study it is impossible to say anything definite about the immediate micro environment experienced by the algae. It has been reported that a hot spring alga *Achnantes exigua* lives amongst a thick algal mat in order to reduce exposure to light (Fairchild & Scheridan 1974).

Both the nuclear and cellular division patterns of L485 closely resembled the patterns of a smaller reddish *Cryptomonas* sp. described by Oakley and Bisalputra (1977), but clearly differed from the pattern of *C. ovata, Rhodomonas minuta* and *R. lacustris* (Bailey Ward & Bowen 1977, Braunwarth & Sommer 1985, Barbosa, unpublished

data). The nuclear movement towards the anterior part of the cell and the rounding up of the cell at the beginning of mitosis observed in this work and by Oakley & Bisalputra (1977), has also been recorded in *Chroomonas salina* (Oakley & Dodge 1976). The cell division pattern of L485 and *Cryptomonas* sp. with a cytokinetic furrow formed at early metaphase is rather unusual among the algae and in some respects would appear to resemble that of animal cells (Oakley & Bisalputra 1977).

The nuclear division of L485 was well phased at the time of sampling, as only once were some cells with dividing nuclei found in daylight. This phasing was tighter than that observed in the field populations of *C. ovata* in lake Constance (Braunwarth & Sommer 1985) and *Rhodomonas lacustris* in Esthwaite water (Barbosa, unpublished data). Tightly phased division patterns have been recorded in field populations of *R. minuta* and in cultured *C. ovata* and *Cryptomonas* sp. (Ward & Bowen 1977, Bowen & Ward 1977, Oakley & Bisalputra 1977, Braunwarth & Sommer 1985). Generally, cryptophycean species seem to exhibit night time division, the pattern already established for dinoflagellates (Elbrächter 1973, Pollinger & Serruya 1976, Swift et al. 1976, Weiler & Chisholm 1976).

The degree of phasing has been proposed to be dependent upon short term diurnal fluctuations in nutrients, acting through interspecific competition (Doyle & Poore 1974). Vice versa, phasing of division could possible be used as an indicator of nutrient competition. In lake Vähä-Valkjärvi the only nutrient proven to fluctuate diurnally is inorganic carbon. Its fluctuations are a consequence of daily variations in photosynthetic and respiratory activity of the *Drepanocladus* community (Kairesalo, personal communication), which could also be seen in diel fluctuations in oxygen concentrations. As a macrophyte *Drepanocladus* together with its epiphytic algae is superior in trapping carbon (cf. Kairesalo et al. 1991a, 1991b), leaving nights as the most favourable time for L485 for carbon uptake. Some green algae, diatoms and blue-greens have been shown to possess a capability of accumulating high intracellular concentration of carbon for later use (Colman & Rotatore 1988, Palmqvist et al. 1988, Pierce & Omata 1988). Usually this type of accumulation has been reported to be light dependent, in which case it would not benefit L485 in Vähä-Valkjärvi, but there are also observations of carbon storage in the dark (Church et al. 1983). However, as yet there is no direct evidence of accumulation mechanisms

operating in cryptophytes. Carbon competition between the moss and *Cryptomonas* and possible storage of carbon could in theory explain the timing and tight phasing of the division of L485. After division cells would still have plenty of time for dark uptake and accumulation of inorganic carbon which they could then utilize during the following light period.

The type of division pattern observed, with totally overlapping mitosis and cytokinesis, makes it difficult or even impossible to apply the mitotic index technique for *in situ* growth rate measurements. The vital part of the method is knowing the duration of mitosis, and simultaneous mitosis and cytokinesis prevent its determination, either in the field or in the laboratory. Even a very close interval sampling would not eliminate the problem, as in light microscopy, where cells at prophase cannot be distinguished, all the cells identified as cells with dividing nuclei should also be included in the category of dividing cells. The matter is futher complicated by the fact that prophase may be considerable longer than all the rest of the division process together (Oakley & Bisalputra 1977). A rough estimate of t_d can be obtained by using the technique of Oakley & Bisalputra (1977), who observed the length of cytokinesis under a microscope with intermittent illumination to minimize the harmful effects of light on the duration of cytokinesis.

Comparing the calculated potential growth rates *in situ* to measured growth rates in batch cultures allows some conclusions about which t_d is closest to reality. In batch cultures (cf. Chapter 2) the growth rate of L485 never approached 2.0 div. day^{-1}, an indication that 5 minutes is surely an underestimate of t_d. This is reasonable, as the t_d of 5 minutes is only the time difference between the combined metaphase-anaphase and telophase and not the duration of whole mitosis. The duration of t_d must also be longer than 10 minutes as a growth rate of the same magnitude given by this estimate was only obtained in batch cultures when the temperature was 21 °C and the temperature in the lake was only 13–14 °C. Consequently, the estimate of 30 minutes seems most realistic as it does not leave discrepancies between laboratory and field results. Potential growth rate based on this estimate is also in good agreement with the results of Braunwarth & Sommer (1985) and Barbosa (unpublished data), who give 0.35–0.36 div. day^{-1} and 0.35 div. day^{-1} as *in situ* growth rates for *C. ovata* and *R. lacustris*, respectively. With a t_d of 30 minutes, the

sampling interval equals the duration of mitosis, in which case the estimate of the potential growth rate is closest to the exact one (McDuff & Chisholm 1982). The longest t_d also gives a production estimate agreeing well with the results of Arvola & Rask (1984).

In conclusion, these results emphasise the importance of accurate estimation of t_d for the mitotic index technique and show that possible problems concerning t_d and its applications may not only be its variability with growth conditions, but also species-specific differences in division patterns.

Chapter 7

IN SITU DIEL DNA SYNTHESIS IN A SPRING POPULATION
OF A MIGRATORY *CRYPTOMONAS* SP.

7.1. INTRODUCTION

The eukaryotic cell cycle concept, familiar in cell biology and chronobiology, has been applied to phytoplankton ecology in attempts to measure species–specific growth rates *in situ*. As mitosis has most often been the terminal event and hence the centre of interest in these applications, the approach has been refered to as the mitotic index technique (e.g. McDuff & Chisholm 1982, Braunwarth & Sommer 1985). However, the microscopic observation of mitotic and cytokinetic cells can be highly subjective and thus reduce the accuracy and reliability of results. Moreover, mitosis is relatively short as a terminal event (cf. Oakley & Bisalputra 1977, Chapter 6 in this study) making sampling and analysis extremely laborious. More reliable and objective results could be obtained by using a terminal event of longer duration and a quantitative measuring system. By using this approach the sampling interval for determining algal growth rates could also be lengthened from 20–30 minutes (cf. Braunwarth & Sommer 1985) to 2–3 hours (Chang & Carpenter 1988).

The objective of this study was to determine the diel pattern of the cell cycle of a natural *Cryptomonas* population using a quantitative epifluorescence microscope system, or microfluorometry. The results obtained here are used to verify the suitability of this method for determining species–specific growth rates *in situ* as already applied to DNA quantification and growth measurements in culture conditions (Chang & Carpenter 1988). Compared to the sophisticated flow cytometry technique, microfluorometry, using conventional light microscopy, is a tedious method, but besides being substantially cheaper it is more suitable for field samples containing several phytoplankton species, as each cell can be viewed and identified. In order to compare the intrinsic growth rate to observed growth, the *Cryptomonas* sp. population was monitored over two weeks. The vertical migration pattern of the population was also determined during this period.

The eukaryotic cell cycle on which this study is based, is illustrated in Fig. 7.1. (after Prescott 1976 in Chisholm 1981). The cycle consists of four sequential phases, G_1–
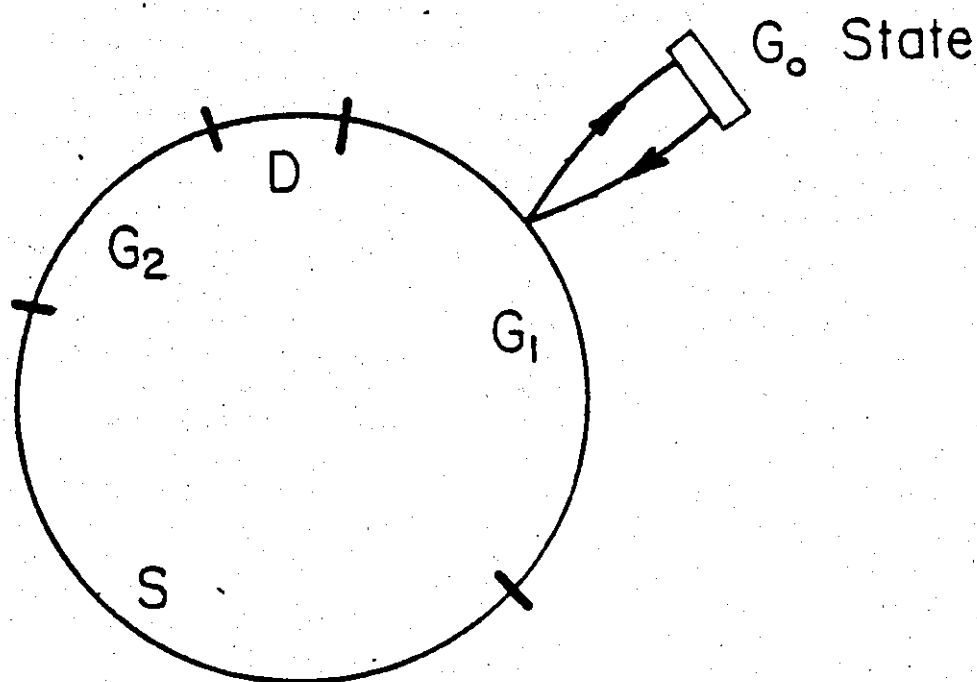
Fig. 7.1. Diagrammatic view of the cell cycle. The cycle begins after division, D (M), with the G_1 (gap) phase and proceeds through DNA synthesis, S, through another gap (G_2), after which division occurs. Some cells can be withdrawn from the cell division cycle and enter a reversible cell cycle arrest (G_0) while in G_1. (After Prescott 1976 in Chisholm 1981).

S–G_2–M (or cell division D). G_1 and G_2 are the gaps separating DNA synthesis, S, and mitosis, M, (or D). Some G_1 cells can be withdrawn from the cell cycle and go into a reversible cell cycle arrest state G_o. It has been hypothesized that in algae this G_o state represents dormant cysts and resource limited vegetative cells (Chisholm 1981). DNA synthesis and division stages are usually well defined for most cell types.

7.2. DESCRIPTION OF SITE

Samples for this study were taken from Priest Pot, a sheltered hypereutrophic tarn in north–west England (54° 22' 31" N, 2° 58' 55" W). It is approximately 1 ha in area and its mean and maximum depths are 2.3 m and 3.9 m, respectively (Fig. 7.2). The tarn is chemically and physically stratified throughout the summer and it regularly develops an anoxic hypolimnion. Its high productivity is based on a large input of nutrients from the surrounding cultivated land (Vincent 1980). Both the abiotic environment and the biota in Priest Pot have been extensively studied and further details of this tarn can be found in Goulder (1971, 1972, 1975), Davison & Finlay (1986) and Stewart & George (1987).

7.3. DESCRIPTION OF SPECIES

The organism chosen for study of diel DNA synthesis was a medium sized (15 μm x 30 μm) form of *Cryptomonas* (Fig. 7.3). The species has not yet been positively identified. Although this was by far the most abundant species of the genus at the time of sampling, two or three other species of cryptophytes were present in the lake. Cells of all *Cryptomonas* taxa provided only a small proportion of the phytoplankton which was dominated by species of *Peridinium*, *Dinobryon* and *Synura* and, towards the end of the study period species of blue–green algae.
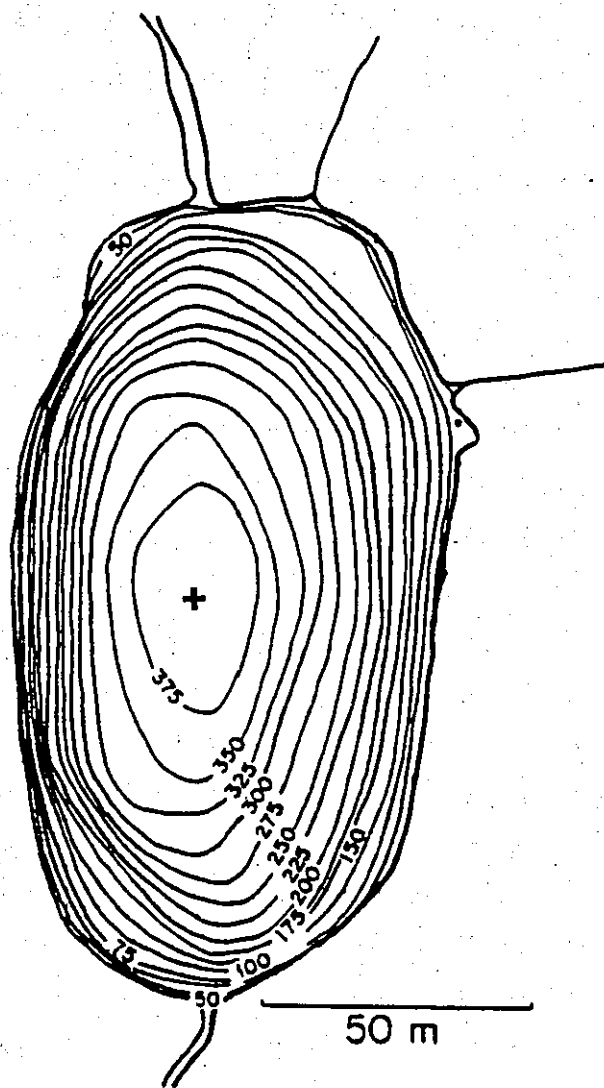
Fig. 7.2. Bathymetric map (depths in cm) of Priest Pot (Davison & Finlay 1986). The sampling location is indicated with a cross.
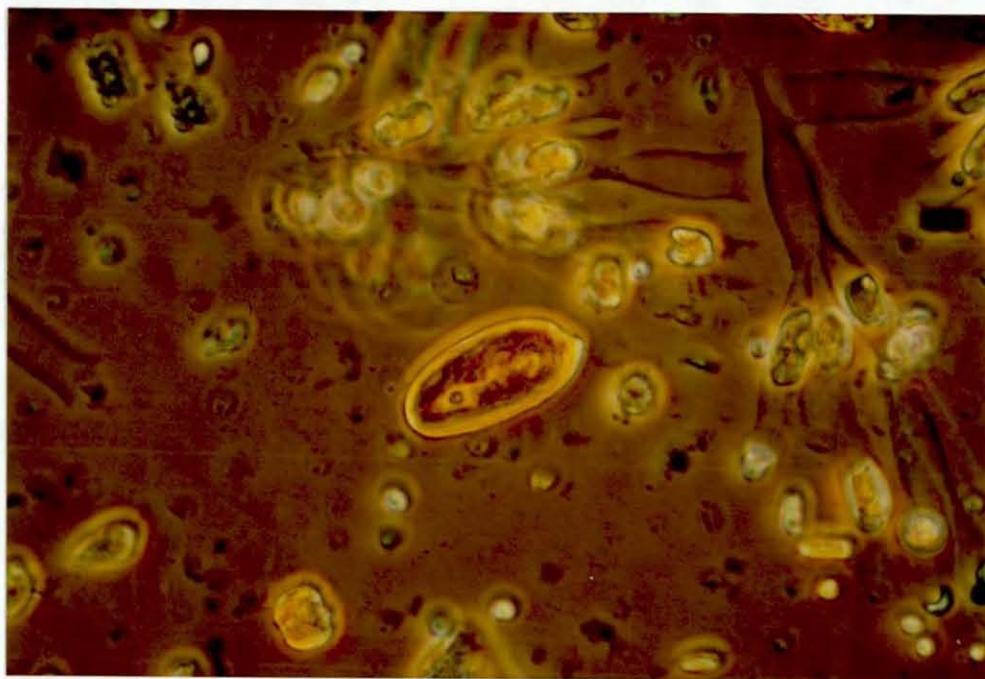
Fig. 7.3. *Cryptomonas* sp. in a field sample under phase contrast illumination. Photograph taken on Agfachrome CT 100 film with a Nikon M–35 camera connected to a Nikon Diaphot–TMD inverted microscope. Magnification 400x.

7.4. MATERIAL AND METHODS

7.4.1. Field sampling

For analysis of diel DNA synthesis samples were collected on 31st May – 1st June 1988 starting at 09.00h GMT. Local sunset was at 20.35h GMT and local sunrise at 3.45h GMT. Sampling was carried out hourly (with some exceptions) at a position over the deepest part of the lake. Two integrated samples from 0–2.5 m taken with a flexible tube sampler were pooled and an aliquot of 250 ml was fixed immediately with acid Lugol's iodine, which was used as a preservative throughout this study. Lugol's iodine was chosen as, according to Booth (1987), it is the best preservative to keep the size and shape of delicate *Cryptomonas* cells.

In order to avoid problems from possible phasing of cell division, samples for measurements of population growth were always taken at approximately 10.30h GMT. Samples were collected as described above between 24th May and 3rd June 1988. A sample consisted of the combined contents of three integrated tube sub-samples over the 0–3 m layer. At the time of sampling temperature (°C) and oxygen (mg l^{-1}) were also monitored with a temperature–compensated dissolved oxygen probe (Yellow Springs Instrument Co., Yellow Springs, Ohio).

Diel vertical movements of *Cryptomonas* sp. were determined over a 24 hour period at four hourly intervals on the day of DNA sampling. Sampling started at 09.00h GMT and finished at 09.00h GMT next morning. Unfortunately, the last set of samples was lost due to fatigue of sampling personnel. Samples were collected using a pneumatically–operated close interval sampler with 10 ml syringes at 20 cm intervals over 2 m (Heaney 1974) and special attention was paid to ensure that samples were taken from positions not yet crossed by the slowly moving rowing boat used for sampling. From the surface to 2 m the sampling depth interval was 20 cm and from 2 m down to 3.6 m the interval was 40 cm. For one sample four 10 ml subsamples were combined and fixed with acid Lugol's iodine. Oxygen was measured simultaneously as described above.

Samples for dissolved inorganic nutrient analysis were collected twice (24th May and 2nd June) at 50 cm intervals from surface to 300-350 cm with a Friedinger bottle of 50 cm in length. The pH in the tarn was measured on 24th May.

The total incident solar radiation (cal cm^{-2} d^{-1}) was measured daily on the roof of the Windermere Laboratory, situated about 4 km from Priest Pot, by a Kipp CM 6 thermopile solarimeter and integrator. The relative penetration of light underwater was measured as a percentage of transmission through red, blue and green filters using a selenium rectifier. An underwater quantum sensor (Lambda Li 192S) connected to a universal meter (Precision Scientific Company, Chicago) and giving readings as mV was used to measure photosynthetically available radiation (PAR, 400-700 nm) underwater.

7.4.2. Laboratory analyses

After returning to the laboratory, 10 ml aliquots were taken for analyses of DNA content and decolorized with a drop of 1 N sodium thiosulfate. Samples were then stained with the fluorochrome 4'-6-diamidino-2-phenylindole (DAPI) (Sigma Co.) (Kapuscinski & Skozylas 1977). The final DAPI concentration in samples was 0.5 µg ml^{-1} (Chang & Carpenter 1988). Concentrations of 0.25 µg ml^{-1} and 1.0 µg ml^{-1} were also tried and no difference in fluorescence yield was recorded compared to 0.5 µg ml^{-1}.

Before quantitative measurements of fluorescence with an epifluorescence microscope (Leitz Fluovert equipped with an MPV compact photometer system) were made, samples were concentrated using a modification of Utermöhl's (1958) technique. An excitation filter block system A was used for measurements and consisted of an excitation filter BP 340-380, dichromatic mirror RKP 400 and suppression filter LP 340. The effective size of the photometer measuring rectangle was kept at 12.7 µm x 12.7 µm throughout the procedure. At least 150 cells from each sample were measured for DNA content using a 40x objective and corrected for background fluorescence by

subtracting the mean value of measurements of approximately 10 fields of view where there were no cells or any other visible material.

Samples for diel vertical profiles and for population growth rate measurements were counted with a Nikon Diaphot–TMD inverted microscope using a 40x objective and Utermöhl's (1958) technique. A 10 ml subsample was sedimented and all the *Cryptomonas* sp. cells in the chamber were counted using phase contrast illumination. Microphotographs of the cells were taken on Agfachrome CT 100 film with a Nikon M–35 S camera.

Samples for dissolved inorganic nutrients were filtered through Whatman GF/F glass fibre filters. Dissolved inorganic phosphorus was analysed using the method of Murphy & Riley (1962), nitrate as described by Morris & Riley (1963) and ammonium as described by Chaney & Marbach (1962). pH was measured using a Radiometer PHM 62 standard pH meter.

7.4.3. Analysis of DNA distributions

The distributions of DNA per cell were analyzed by a simple graphical method which is based on the assumptions that (1) the mean fluorescence value of the G_2+M peak is twice the mean fluorescence value of the G_1 peak; (2) the broadening of the G_1 and G_2+M peaks is random from cell to cell and thus G_1 and G_2+M subpopulations can be described by normal curves; (3) the coefficient of variation (standard deviation/mean) for G_1 is approximately the same as for G_2+M (Dean & Jett 1974, Olson et al. 1983, Chang & Carpenter 1988). The third assumption makes it possible to obtain the proportions of cells in different phases in spite of the presence of S cells.

Mathematically the proportions of cells in G_1, G_2+M and S phases were obtained as in Slater et al. (1977):

$$P(G_1) = N(G_1)/total \qquad (1)$$

$$P(G_2+M) = N(G_2+M)/total \qquad (2)$$

$$P(S) = 1 - [P(G_1) + P(G_2 + M)] \qquad (3)$$

7.4.4. Calculation of population growth rate

Population growth rate was calculated from the means of the three pooled samples by least–squares fit of a straight line to the logarithmically transformed data as described by Guillard (1973) and expressed as divisions per day.

7.5. RESULTS

7.5.1 The tarn

Priest Pot was both chemically and thermally stratified at the time of sampling and chemical stratification was especially steep. The epilimnion was saturated with oxygen down to 1–1.5 m while the hypolimnion was anoxic below 2–2.5 m (Fig. 7.4). The temperature difference between bottom and surface layer was about 5 °C, but stratification was not obvious and no steep thermocline could be found.

As with oxygen, stratification of dissolved inorganic nutrients was also distinct (Fig. 7.5). Highest concentrations of soluble reactive phosphorus (SRP) were found below 1.75 m. However, these are probably underestimates due to adsorption of phosphorus on ferric hydroxide on oxidation of the high concentration ferrous iron also present (Davison & Finlay 1986).

Concentrations of ammonium in the surface waters were usually low, but in the hypolimnion concentrations exceeded 700 μg l^{-1} (Fig. 7.6). In most cases nitrate concentrations were below the detection limit (< 14 μg l^{-1}) throughout the water
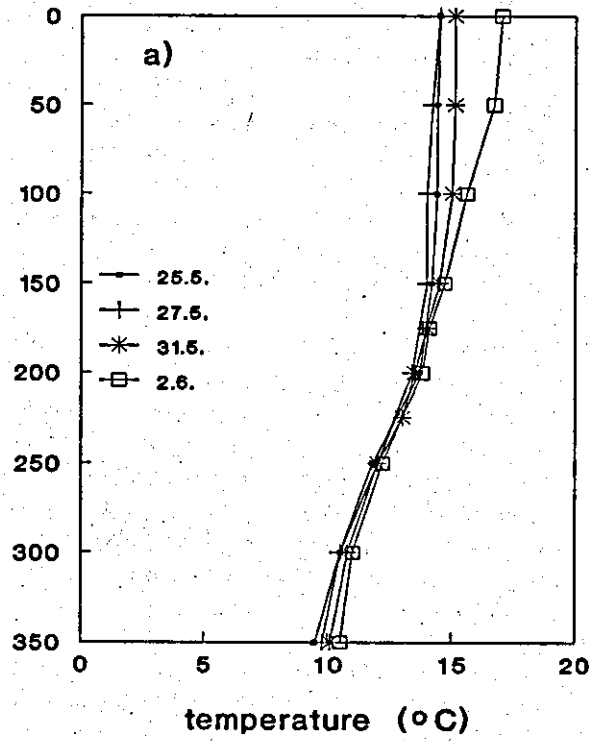
Fig. 7.4. Temperature (°C) (a) and oxygen (mg l⁻¹) (b) profiles in Priest Pot in spring 1988.

Fig. 7.5. Soluble reactive phosphorus (SRP) (μg l^{-1}) in Priest Pot on 24.5.1988 (a) and 2.6.1988 (b).
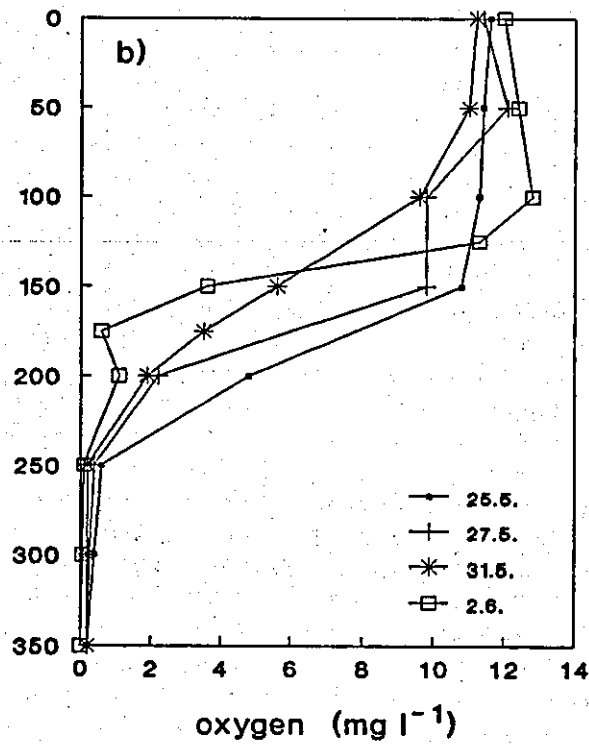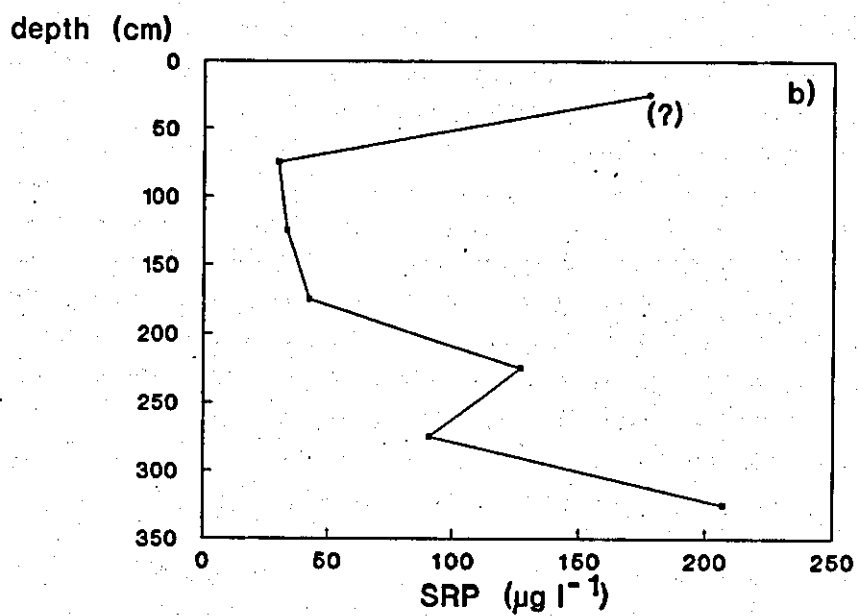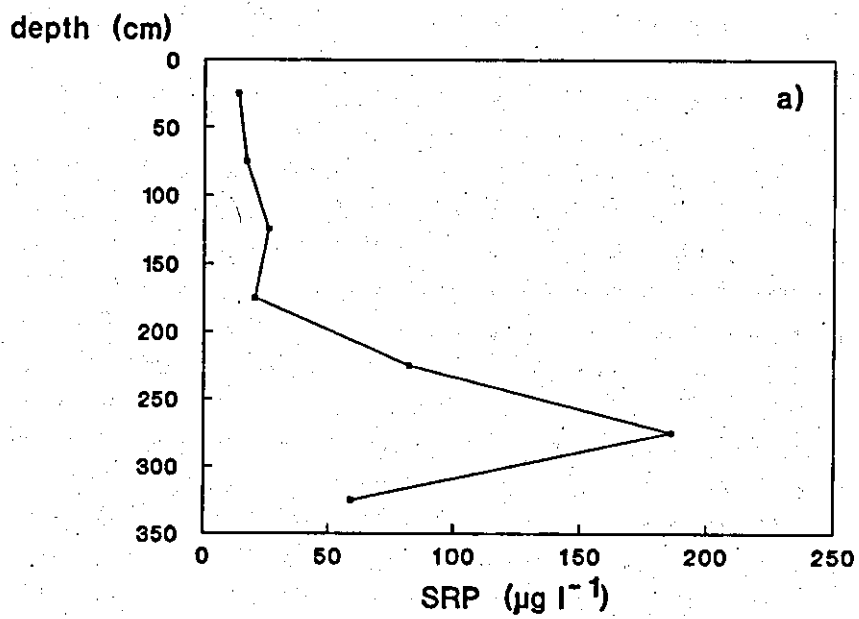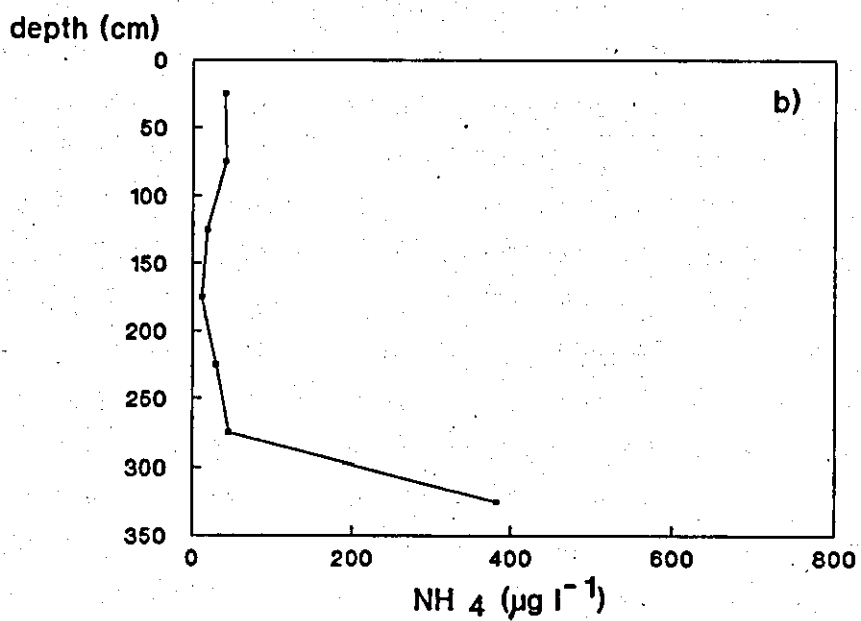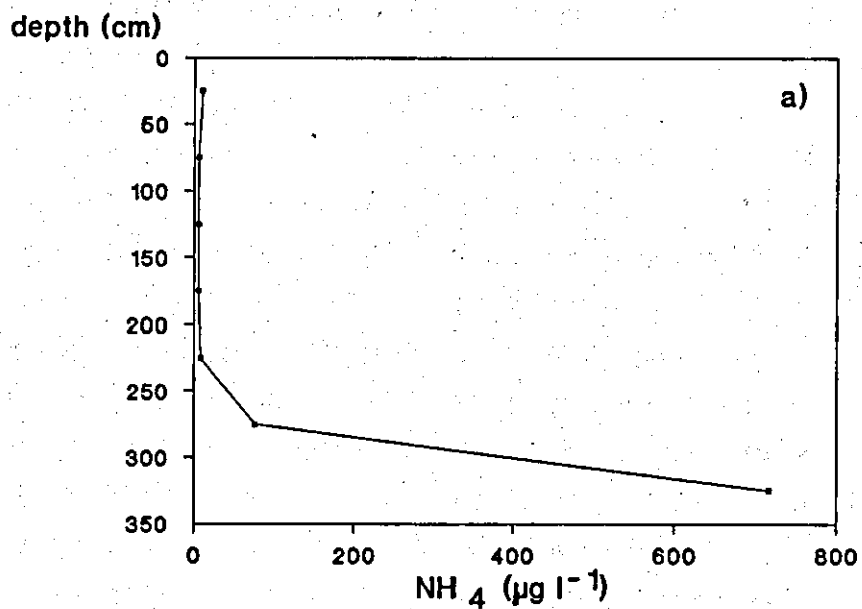
Fig. 7.6. NH$_4$–nitrogen (µg l^{-1}) in Priest Pot on 24.5.1988 (a) and 2.6.1988 (b).

column. Small detectable amounts (20–40 μg l^{-1}) were found on 2nd June in both the epilimnion and hypolimnion, but not in the metalimnion. pH at the surface was 7.6 dropping to 6.3 between 1–2 m (Fig. 7.7).

During diel sampling, the weather was cool and cloudy. The amount of incident solar radiation on 31st May was 249.0 cal cm^{-2} d^{-1} and on 1st June 347.0 cal cm^{-2} d^{-1}.

In the turbid water of Priest Pot blue light decreased more rapidly than red and green light (Fig. 7.8), which both penetrated to 2.0 m. This underwater light environment was probably especially suitable for blue–green algae and some cryptophytes which, with phycobiliproteins as accessory pigments, are possibly best able to exploit low irradiances of green and red light (cf. Chapter 4).

7.5.2 Development of the *Cryptomonas* sp. population

Throughout the period of study the *Cryptomonas* sp. population was declining (Fig. 7.9). There were two discernible phases of decreasing population. First, from 24th May to 1st June there was a period of low rate of decrease when 'growth' rate was −0.24 div. day^{-1} (N=6). This period ended at the time of the diel DNA sampling and was followed by a rapid population collapse. The calculated rate of decrease during this phase was 1.95 cell halvings day^{-1} (N=3). Thereafter, it was not possible to follow population changes due to the low numbers of cells of *Cryptomonas* sp.

7.5.3 Vertical distribution of *Cryptomonas* sp.

Despite its rapid decline, the population of *Cryptomonas* sp. had maintained the ability to undergo diel vertical migrations (Fig. 7.10). These migrations were not as clear as those found by Jones (1988) and Arvola et al. (1991), but could still be distinguished. At midday the majority of the population stayed just beneath the surface, but by late afternoon the sub–surface maximum had moved to the surface. Part of the population
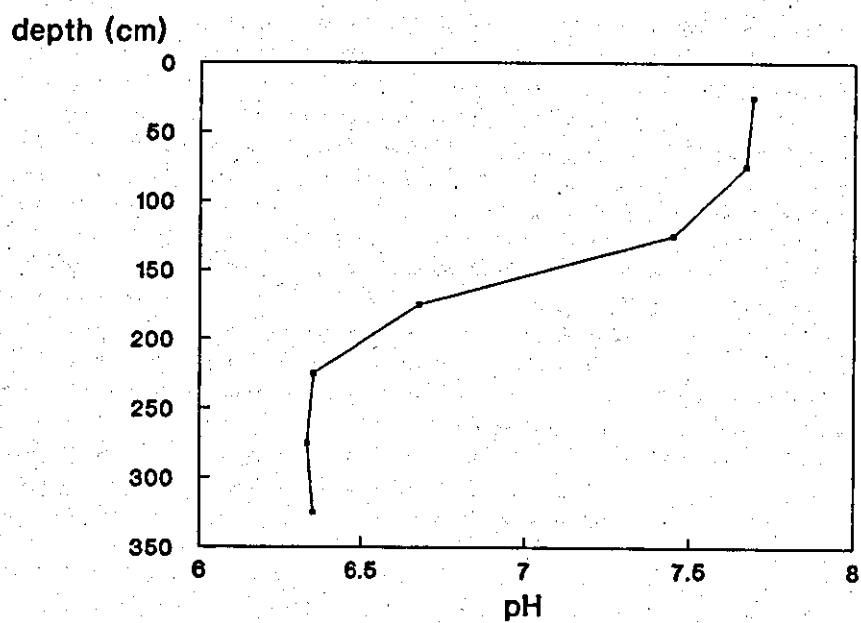
Fig. 7.7. pH in Priest Pot on 24.5.1988
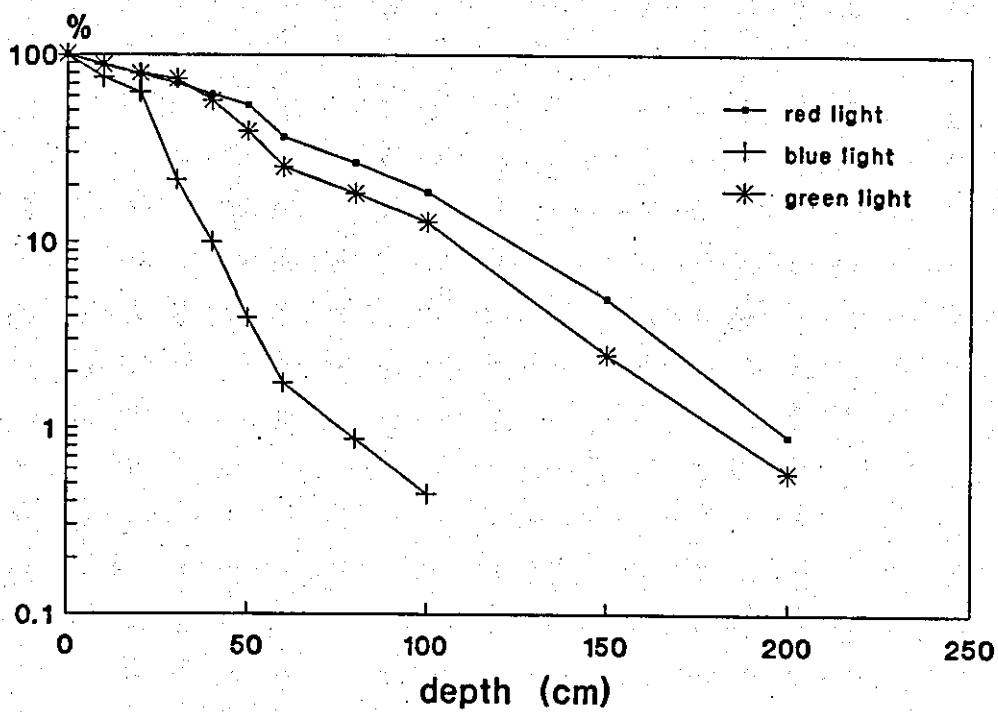
Fig. 7.8. The relative penetration of red, blue and green light underwater in Priest Pot.
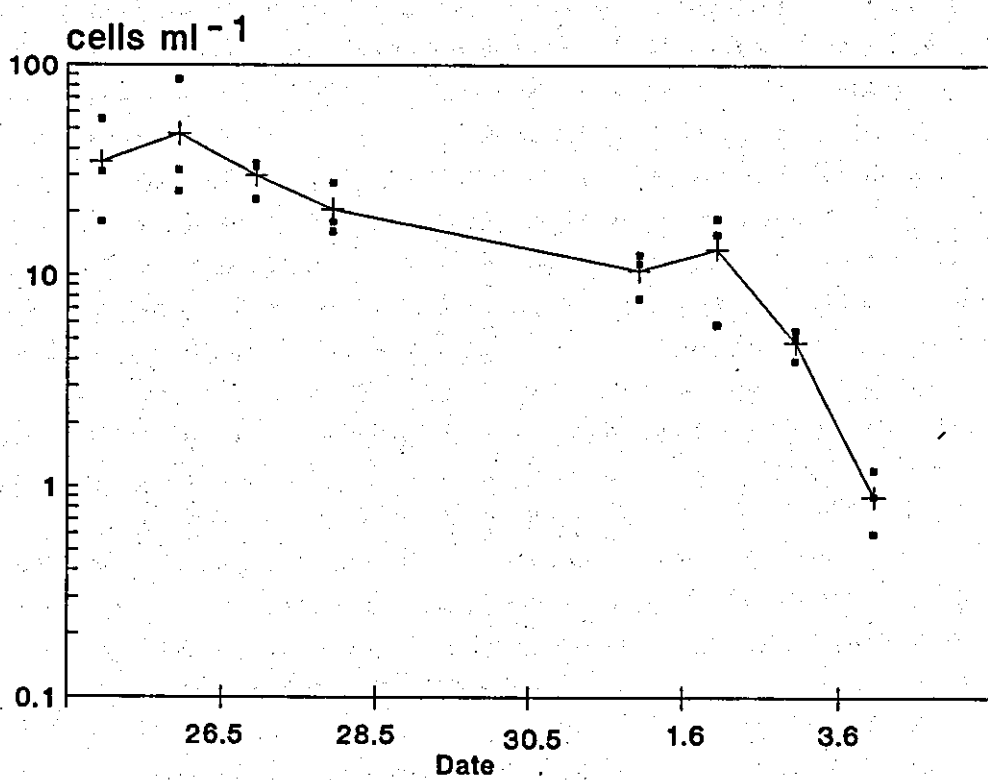
Fig. 7.9. Population changes of *Cryptomonas* sp. (cells ml^{-1}) in Priest Pot between 24. May and 3. June 1988.

depth (cm)

09.00h
31.5.1988

cells ml^{-1}

depth (cm)

13.00h
31.5.1988

cells ml^{-1}

depth (cm)

17.00h
31.5.1988

cells ml^{-1}

depth (cm)

21.00h
31.5.1988

cells ml^{-1}

depth (cm)

cells ml^{-1}

01.00h
1.6.1988

depth (cm)

cells ml^{-1}

05.00h
1.6.1988
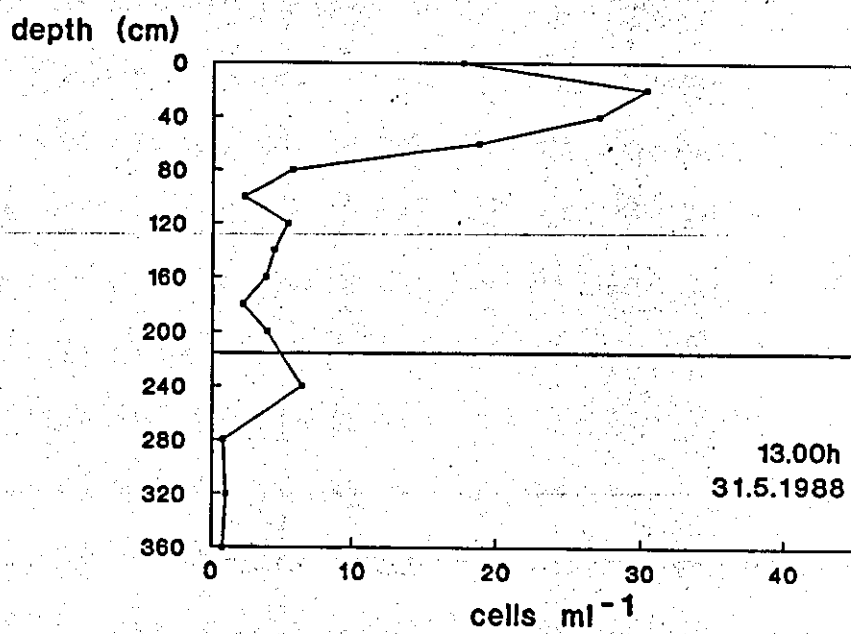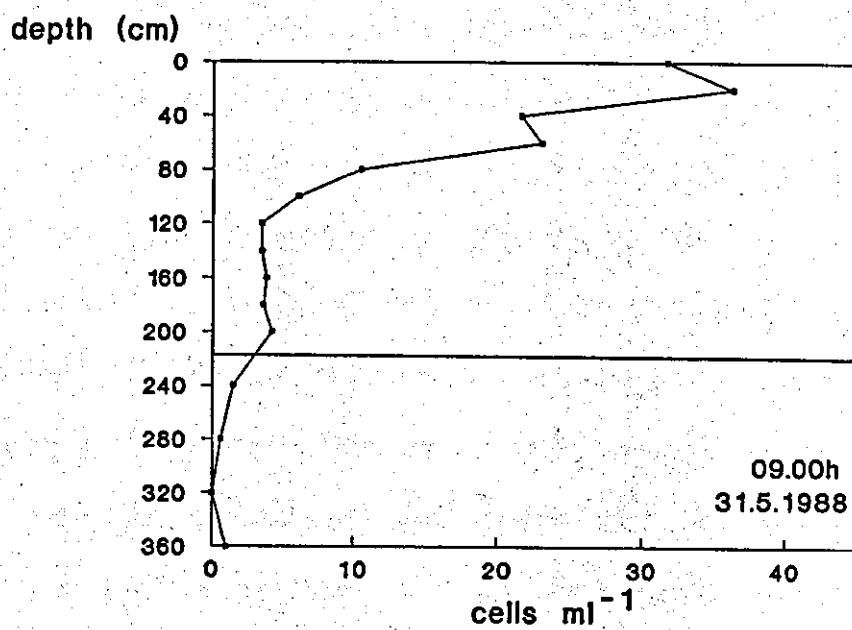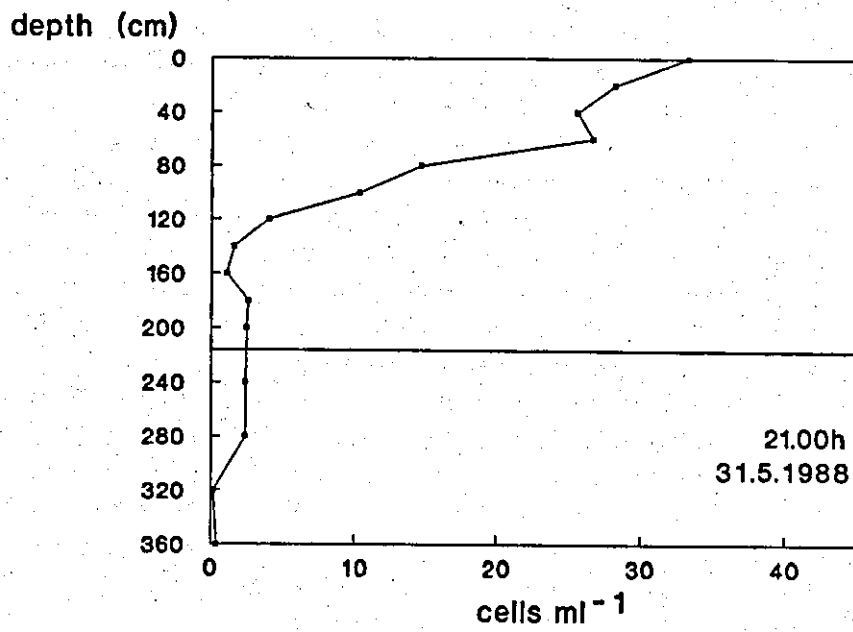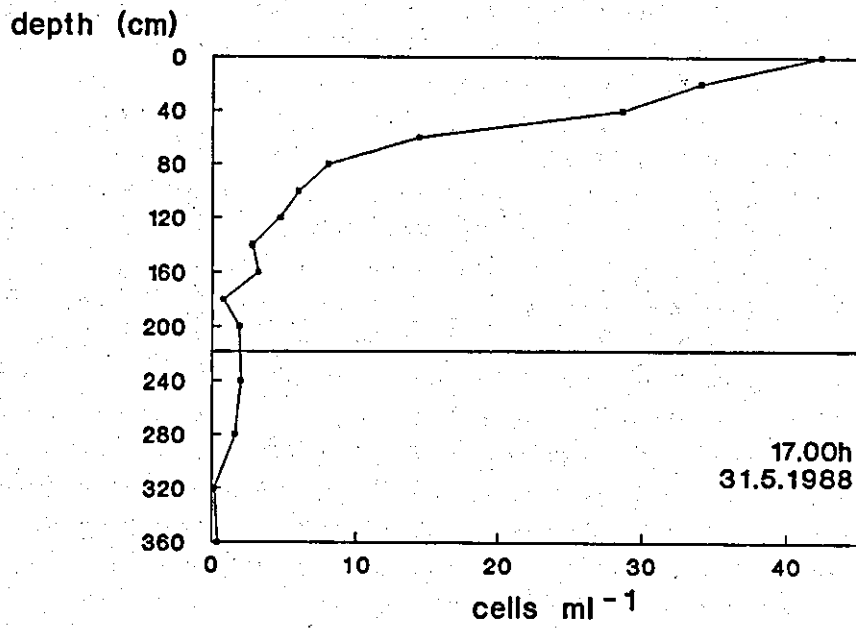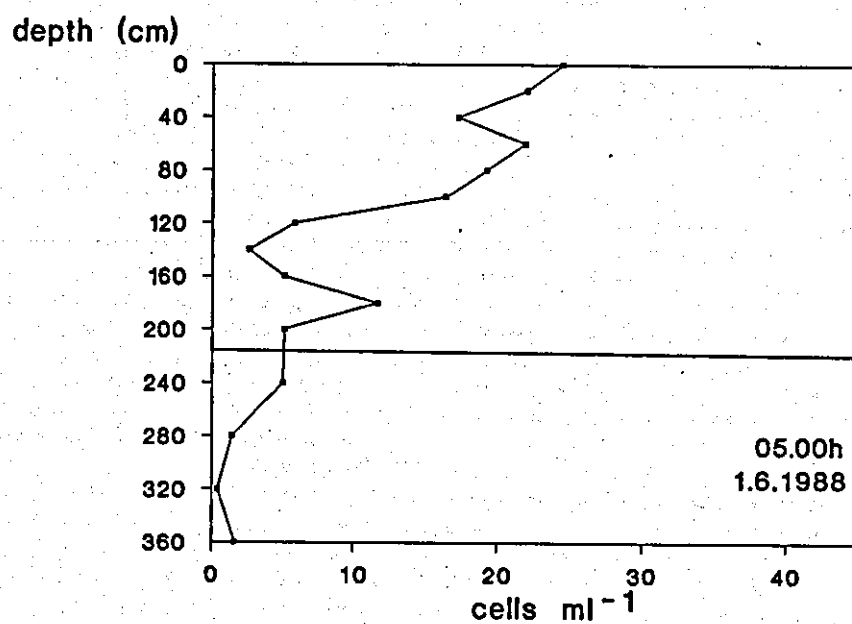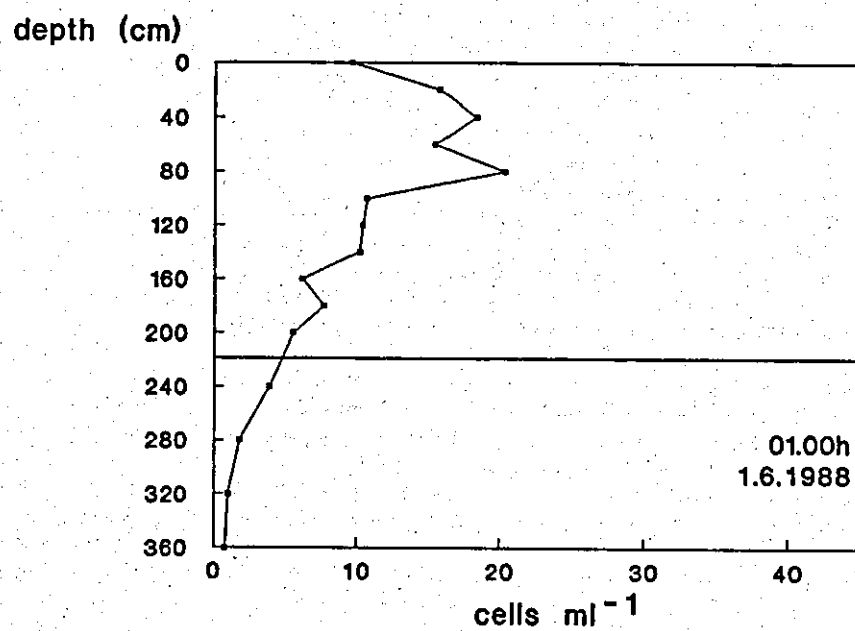
Fig. 7.10. Diel vertical distribution of *Cryptomonas* sp. at the times indicated. Horizontal line shows the boundary of anoxic layer.

started to descend after sunset and formed a peak at the depth of 80 cm at 01.00 GMT. At 05.00 – an hour after sunrise – the population had already started to ascend and form a maximum at the surface. Most of the population remained in water layers where the temperature was 15–16 °C.

In early morning, just above the anoxic layer, there was also a metalimentic peak of *Cryptomonas* sp. which had started to form after midnight. Cells appeared capable of swimming to the anoxic layer, as throughout the sampling period some cells could be found deeper than 2–2.2 m which was the oxic–anoxic boundary. This movement into anoxic water was most prominent at night.

7.5.4 DNA synthesis cycle

Fig. 7.11 shows an example of curves of cellular DNA content drawn from the data and constructed according to the principles described above (7.4.3). It has the same general appearance as Armbrust et al. (1989) have proposed for *Synechococcus* sp. and Helmstetter & Cooper (1968) for *Escherichia coli*. This type of DNA distribution is regarded as typical of slowly growing cells with generation times longer than the time needed for DNA synthesis and cell division. In fast-growing procaryotic populations, all cells are in the S phase since DNA synthesis occurs throughout the cell cycle. For this type of population the mean DNA content per cell is higher than in the slowly growing population and no peaks of G_1 and G_2+M cells can be distinguished. For the final analysis the results from some of the cells were discarded, as they were considered to belong to other species judging from their unusually high fluorescence values.

During the diel cycle the proportions of cells in different phases of the DNA cycle changed. Phase fractions (%) of G_1, S and G_2+M cells against time are shown in Fig. 7.12. Such a distinct phasing as that described by Chang & Carpenter (1988) for cultured dinoflagellates cannot be seen in these results. *Cryptomonas* sp. cells in all three phases could be found throughout the 24 hour sampling cycle and most of the time the majority of the cells seemed to be in S phase synthesizing DNA.
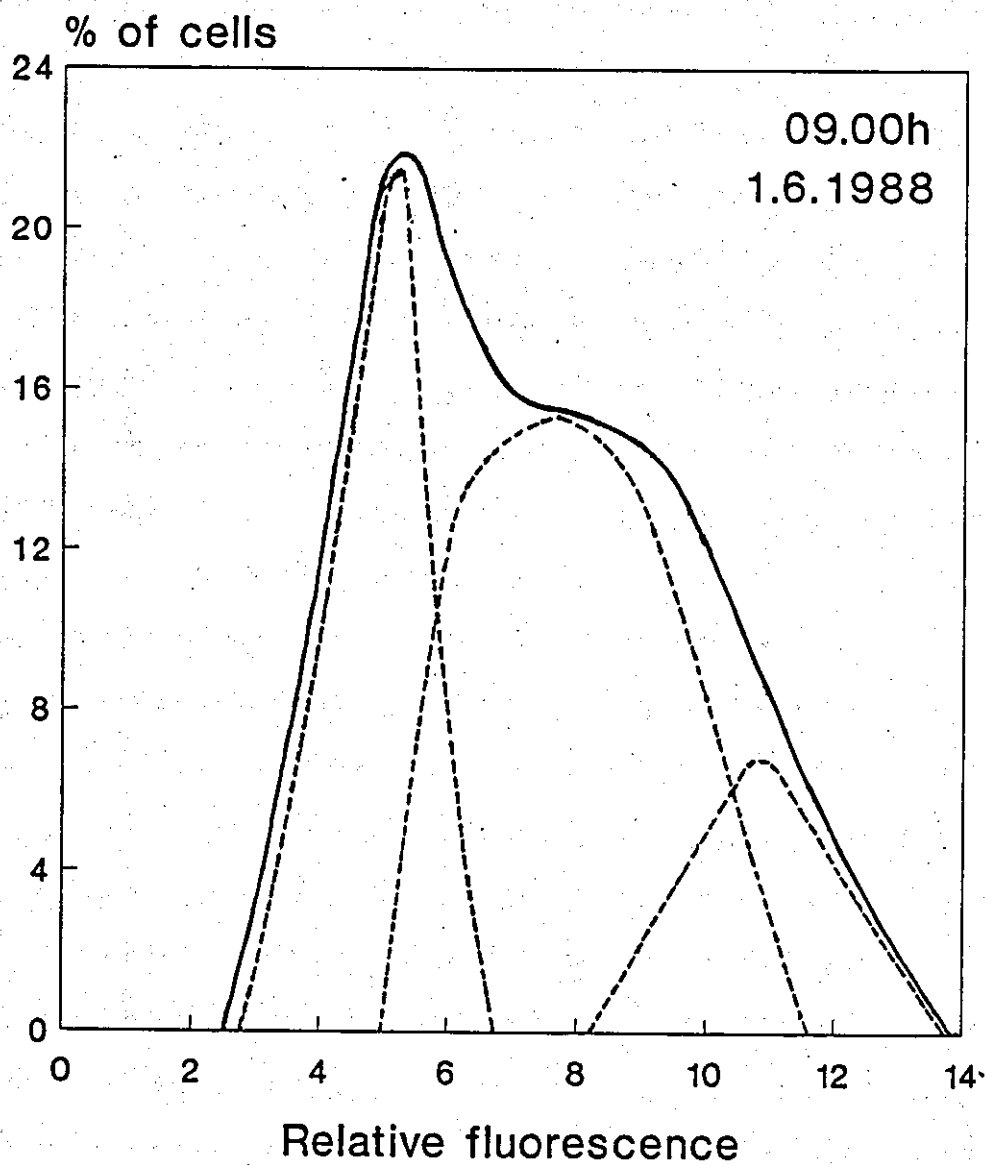
Fig. 7.11. An example of DNA distribution for *Cryptomonas* sp. measured as relative fluorescence. The solid line is the fit to the data, the dashed lines from left to right represent cells in G_1, S and G_2+M phase, respectively. Curves fitted by eye.

a)

b)
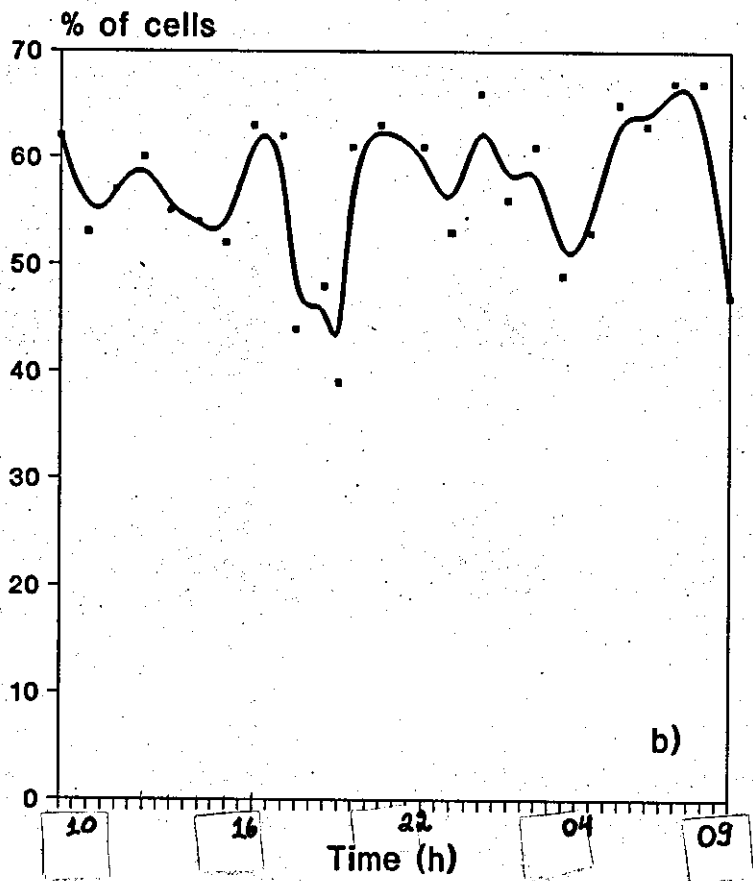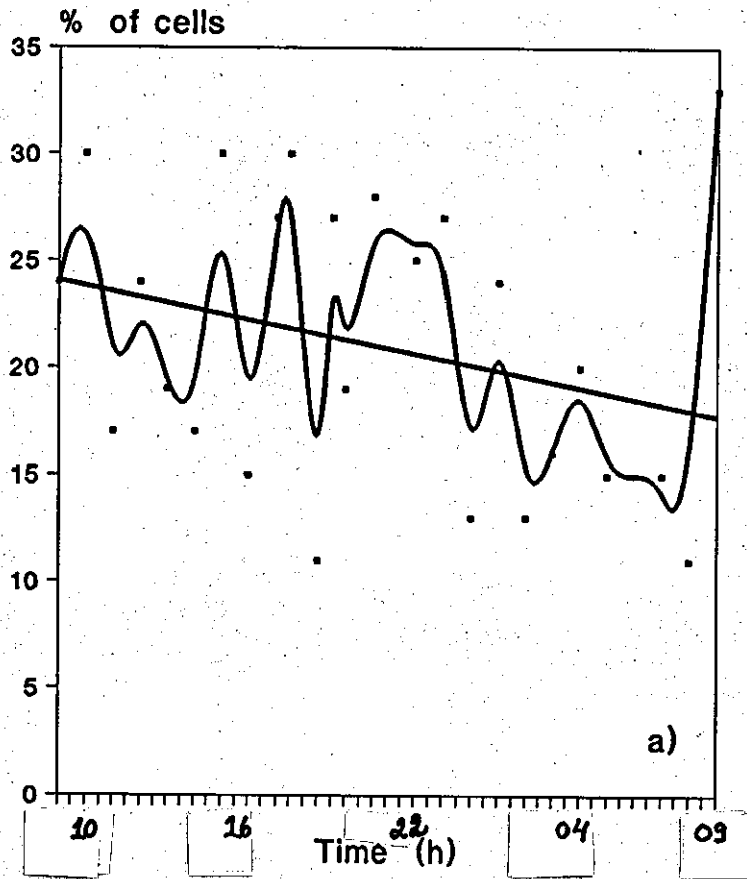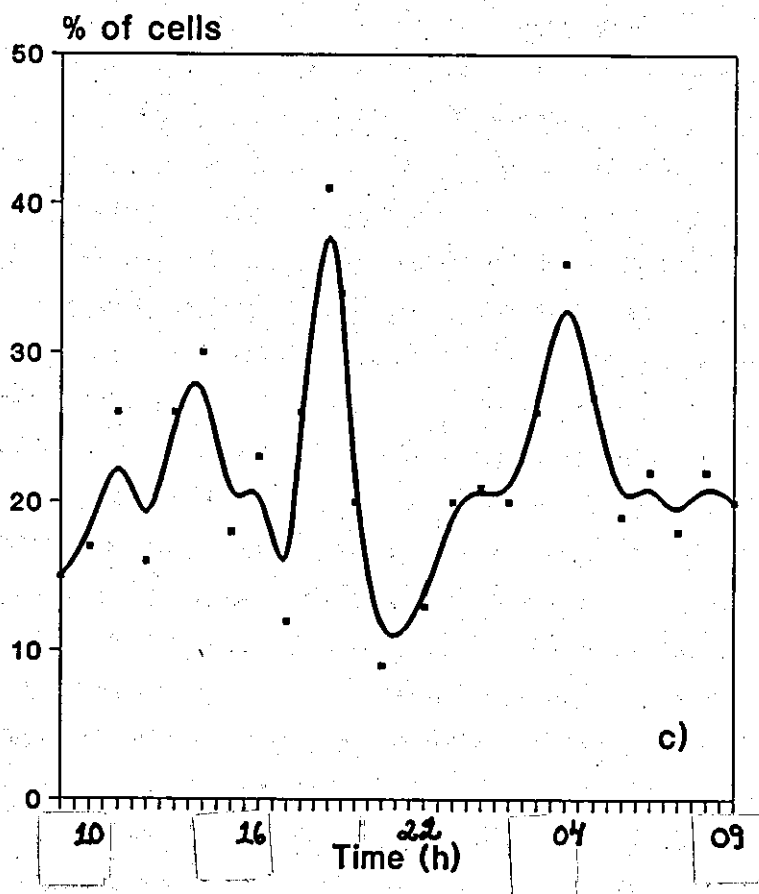
Fig. 7.12. Phase fractions of G_1 (a), S (b) and G_2+M (c) cells. Curves have been interpolated with cubic spline routine. For G_1 cells a trend line is also shown.

However, there was an obvious diel rhytm in each phase fraction. The G_2+M reached its highest peak at 19.30 GMT and at 03.00 GMT, indicating that mitosis of this *Cryptomonas* sp. took place just before sunset and sunrise. In the first increase of G_2+M cells, 41 % of the population were in this phase. During the second increase, the fraction of cells ready for mitosis was slightly less at 36 %.

The highest numbers of cells undergoing the DNA synthesis phase were recorded at 16.00 GMT and 00.00 GMT, i.e. 3–3.5 hours before G_2+M peaks. There was a third peak of S cells at 08.00 GMT on 1st June, but because monitoring of the cell cycle was finished at 09.00 GMT, it was not possible to confirm whether a G_2+M peak followed three hours afterwards at 11.00 GMT. The number of cells in this phase was never lower than 45 % and at times 60–65 % of the population were found synthesizing DNA.

The pattern of the G_1 cells was not obvious, but consisted of several smaller and higher maxima, and even in maxima less than 1/3 of the cells were in this phase. There was a slight declining trend in the proportion of G_1 cells during the sampling period. The last samples, taken on 1st June at 09.00 GMT, again showed a higher proportion of cells in G_1 phase.

7.6 DISCUSSION

The rapid decline of cryptophyte populations in early summer in lakes is not unusual. The appearance of cryptophytes is known to be intermittent and sporadic with rapid increases and declines in abundance (e.g. Dokulil 1988). The decline described here in Priest Pot was probably the result of an interaction of losses and impaired growth potential under nutrient depletion. As *Cryptomonas* sp. was not a dominant species in Priest Pot, it was impossible to confirm its nutritional status, but NO_3–nitrogen could have been the limiting nutrient as its concentrations were below the detection limit and a week after the sampling was finished there was a blue–green algal bloom in the lake. However, Cloern (1977) has concluded that, at least for *Cryptomonas ovata*, ammonium is the primary source of inorganic nitrogen, and this being true with *Cryptomonas* sp., it might not have been short of nitrogen as ammonium was present

in detectable amounts all the time. Part of the population might have obtained extra nutrients by migrating through oxic–anoxic boundary to the nutrient rich hypolimnion (cf. Salonen et al. 1984).

Grazing is said to be the loss factor of greatest importance amongst the cryptophytes (Cloern 1978, Reynolds et al. 1982), but little can be said with certainty about grazing pressure in Priest Pot. The abundance of large ciliates in Priest Pot, reported by Finlay & Berninger (1984) and Finlay et al. (1988), indicates that grazing could greatly affect the population development of *Cryptomonas* sp. Besides grazing, decomposition, sedimentation and even inhibition of growth induced by blue–green algae could have contributed to the decline of the population. Pedrós–Alió et al. (1987) noticed that decomposition was the most important loss factor amongst a metalimnetic population of *Cryptomonas phaseolus* and the decomposition ratio could be as high as -0.130 to -0.22 div. day^{-1}. They also recorded that, especially in spring, sedimentation is an important loss factor, a result different from the traditional idea of cryptophytes being unusually resistant to sedimentation (e.g. Burns & Rosa 1981, Sommer 1984). Vance (1965) has reported that *Microcystis* inhibits the growth of *C. ovata*.

The pattern of vertical migration of *Cryptomonas* sp. in Priest Pot, consisting of an evening descent and a morning ascent, is widely observed for cryptophytes (e.g. Happey–Wood 1976, Salonen et al. 1984, Jones 1988). The reason for this kind of behaviour remains unexplained but it may confer metabolic advantages on those algae which are able to fulfill their nutritional requirements by retrieving inorganic phosphorus or nitrogen from the nutrient–rich hypolimnion (cf. Arvola et al. 1991). In small sheltered lakes like Priest Pot with intense chemical stratification, this often entails migrations into anoxic layers rich in sulfide. Besides the *Cryptomonas* sp. of this study, *C. marssonii* and *C. phaseolus* have been reported to be able to grow in lakes whose deeper layers are anoxic and rich in sulfide (Pedrós–Alió et al. 1987, Jones 1988, Rott 1988). There is also a possibility that by entering anoxic water layers algae ~~phytoplankters~~ avoid predation by grazing animals. In Priest Pot the ciliates *Loxodes striatus* and *L. magnus*, which are both capable of feeding on *Cryptomonas* sp., have sharp population maxima close to the oxic–anoxic boundary (Finlay & Berninger 1984, Finlay et al. 1988).

The original aim of this study was to determine the diel changes of cellular DNA content of *Cryptomonas* sp. from field data and use this information for calculations of species-specific intrinsic growth rate. Unfortunately, the results do not enable more than some speculations, as in order to get plausible growth rate estimates, a population showing only one distinct period of division per day is needed. If there is more than one maximum of division – as in this case – it is uncertain whether some cells divide more than once per day or whether the population consists of more than one subpopulations or subspecies dividing at different times. This problem is accentuated with cryptophytes because of the real difficulty of distinguishing between species; the only practical parameter for identifying species by light microscopy is cell size, but it is known that size variations can be great even in clonal cultures (Klaveness 1988, Chapter 2 in this study). This is partly due to the cell size changes before and during the course of cell division (Oakley & Bisalputra 1977).

The cell cycle results obtained from Priest Pot can be explained using the model of Vaulot & Chisholm (1987). This model is based on the idea of a so called transition point in the cell cycle before which the length of the cycle is dependent on external environmental factors, usually light. The time to complete the second part of the cycle is independent of external conditions. For species with a late transition point a long light period weakens the phasing of cell division and creates a major peak of division during the day and a second smaller peak in the dark. These predictions of the model are in good agreement with the results presented here, especially if considering that the sampling took place just three weeks before summer solstice and the light:dark cycle was then roughly 17:7. Diatoms are algae already known to have multiple bursts of divisions per day and cell cycle phasing dependent on the length of day (Chisholm 1981), but there is further evidence that some cryptophytes might have similarities to diatoms in their cell cycle pattern. Braunwarth & Sommer (1985) noticed that phasing of a summer population of *C. ovata* in lake Constance was not very tight and paired cells and cells with double nuclei could be seen almost throughout the day. The same kind of results were obtained for *Rhodomonas minuta* in Esthwaite Water adjacent to Priest Pot (Barbosa, personal communication).

The duration of various phases of the cell cycle varies with cell type, but for those dinoflagellates and blue-green algae for which there are some data available, G_1 is

usually the longest phase (Olson & Chisholm 1986, Armbrust et al. 1989). G_1 is also the phase prolonged when the growth rate of cells is declining. In this respect the results presented here are different. However, in some algae G_1 can be so short that it cannot be discerned and the cell cycle is dominated by the S phase (Galleron & Durrand 1979). There is also evidence that in some algae nitrogen limitation can cause an increase in duration of the S phase (Olson & Chisholm 1986). This may be the case for *Cryptomonas* populations in Priest Pot where concentrations of nitrate nitrogen were below the detection limit. However, even a rough estimate of *in situ* growth rate of *Cryptomonas* sp. – based on equations by McDuff & Chisholm (1982) and Carpenter & Chang (1988) and on an assumption that cells did not divide more than once per day and on an estimate of duration of mitosis of 3.5 hours –gives a value of 0.7 div. day^{-1}, a rate which is not consistent with nutrient limitation.

It is possible that the blue fluorescence emitted from the DAPI stained nuclei was partly absorbed by the chlorophyll still present in cells, as this has been observed with Hoechst 33342 fluorescent stain (Olson et al. 1983). In this case G_1 and G_2+M peaks can be more indistinct and the fraction of cells in S phase might be overestimated. However, it was already known before this study was started that cryptophytes quickly lose their ability to fluoresce when preserved in Lugol's iodine (Booth 1987, Heaney, personal communication) and to be sure that this also holds for absorption, the absorbtion spectrum of intact cells of cultured *Cryptomonas* L485 (cf. previous Chapters) was compared to the spectrum of cells preserved in Lugol's iodine and decolorized with sodium thiosulfate. The results revealed that even decolorization immediately after preservation reduced the absorbance of the chlorophyll band (max 430 nm) by up to 75 % (Fig. 7.13). With fragile cells like cryptophytes, application of the common procedure of alcohol extraction to remove chlorophyll (e.g. Yentsch et al. 1983) can cause severe damage to the cell membrane and make it impossible to distinguish the *Cryptomonas* under study from other species of cryptophytes present in the Priest Pot samples.

Thus, the results presented here revealed that microfluorometry and DAPI staining can be used in measuring relative DNA contents of individual cells in field samples, but because of the peculiarities in the cell cycle of *Cryptomonas* sp. it was not possible to confirm the suitability of this approach to species–specific growth rate measurements *in situ*.
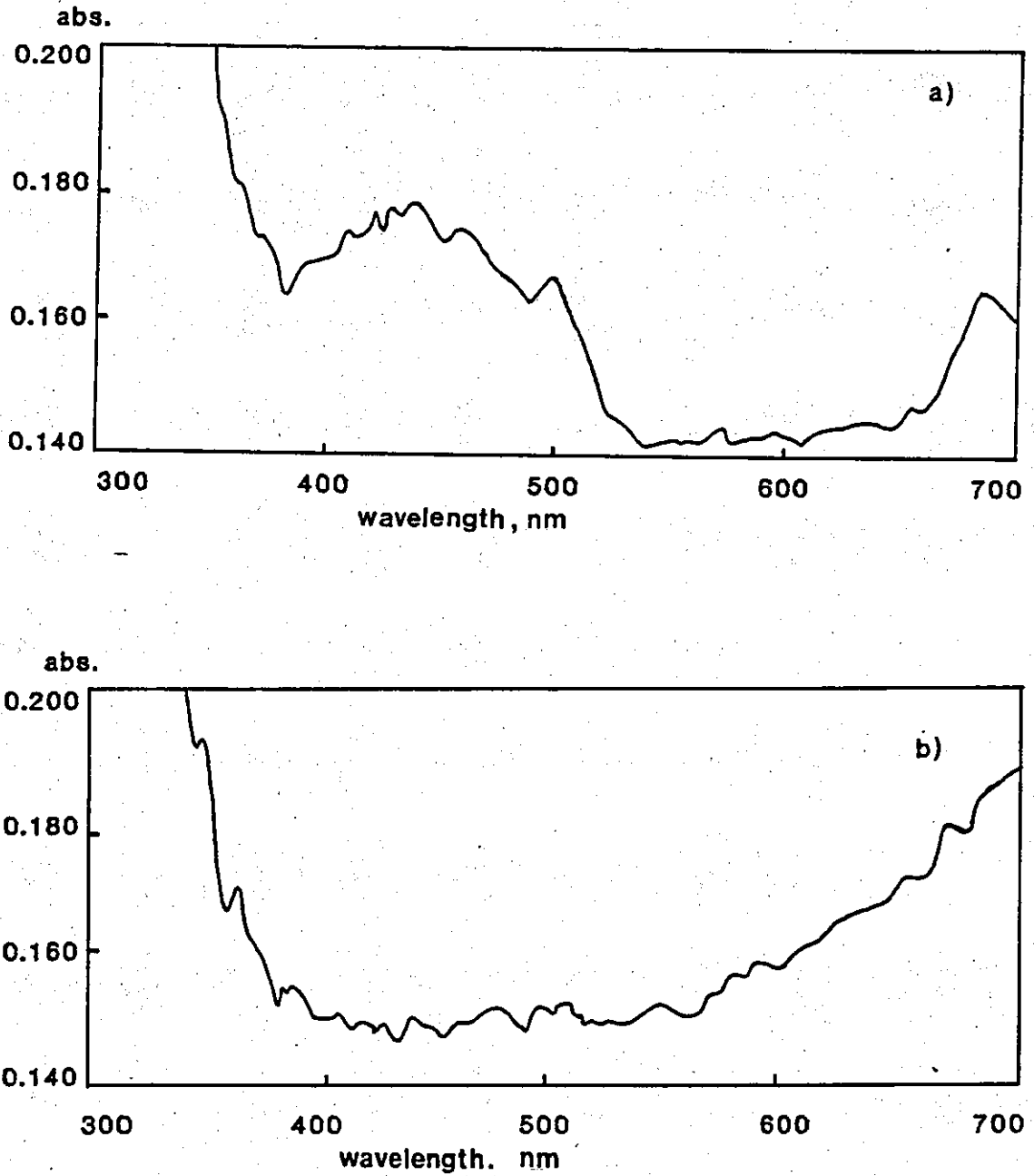
Fig. 7.13. Absorbance spectrum of a) intact and b) preserved cells of *Cryptomonas* L485 measured by Shimadzu UV-2100 UV-VIS recording spectrophotometer with 10 mm optical length. Lugol's iodine was used as a preservative and cells were decolorized with sodium thiosulfate.

Chapter 8

GENERAL DISCUSSION

8. GENERAL DISCUSSION

Stewart & Wetzel (1986) proposed, on the basis of their studies of Lawrence Lake (Michigan) that cryptophytes and other microflagellates frequently increase in numbers immediately following declines of other dominant algal species, and can thus be regarded as opportunistic species. The cryptophyte dominance in spring and late summer communities of phytoplankton has also been demonstrated by several other authors (e.g. Likens 1985, Sommer et al. 1986, Sommer 1987). The concept of an opportunistic species raises a more general discussion of survival strategies of different algae and a question of r- and K-selection. This concept is widely used in general ecological theory (e.g. May 1976) and in phytoplankton ecology it has been applied e.g. by Sommer (1981) and Harris (1986). However, it can surely be argued that some principles of the model are irrelevant for phytoplankton ecology. In particular, this model emphasizes the importance of reproductive strategies, which in apparently asexual organisms (or in organisms with still unknown sexual stages) is not appropriate. Despite this criticism, the theory should not be rejected in phytoplankton ecology as it provides a useful tool to classify and analyse species-specific survival strategies.

According to the model originally developed by MacArthur & Wilson (1967) and based on the logistic equation of growth, K-selection is associated with a relatively predictable environment and a complex, biologically crowded community, whereas r-selection is associated with a relatively unpredictable environment and a simple ecosystem (Pianka 1978). Thus, r-selection prevails in the early stages of succession whereas K-selection is typical of more mature stages. This concept does not only hold for long-term succession patterns, but is also evident in annual phytoplankton succession patterns and times when r-selection and K-selection are predominant can be distinguished (Fig. 8.1, cf. Fig. 1.2). According to Sommer (1981) this coincides with a shift from biological control to physical control. 'r-strategists', i.e. species favoured by r-selection are usually short-lived, fast-growing and capable of rapid colonization of unoccupied habitats that are in abundant supply of resources. 'K-strategists' are more resistant to losses and possess high competitive abilities and high efficiencies in utilization of resources in short supply.
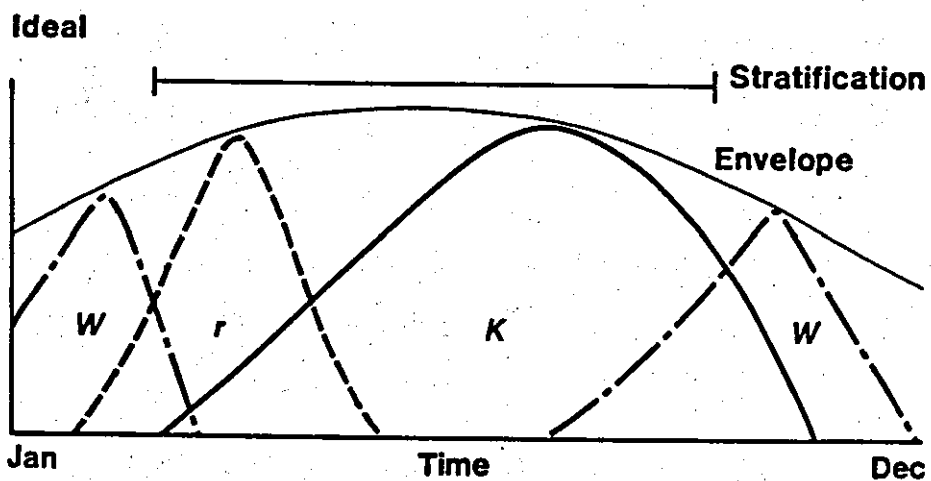
Fig. 8.1. The seasonal succession of phytoplankton in temperate waters as expressed in Harris (1986). Winter diatoms W are replaced by r flagellates as stratification sets in spring. Large K species succeed the r types in summer. W species may recur in autumn.

True r– and K–strategist are uncommon and most organisms, including algae, are in intermediate positions on the r–K continuum. However, cryptophytes L485 and L315 and their habitats possess some features typical either of r– or K–strategists and they can thus roughly be classified as members of one of these groups. The habitat of L485 shares features characteristic to r–selective environment as the recently acidified Vähä–Valkjärvi can be regarded as an unstable environment with an extremely simplified food web structure. As an r–strategist, L485 is most abundant early in the spring when zooplankton is virtually absent; as soon as herbivores appear, the population density of L485 collapses due to high grazing pressure. Competition by other microalgae in Vähä–Valkjärvi is insignificant. L485 can be regarded as a pioneer species which can take advantage of an environmental 'vacuum' where resources were not limiting; light in this oligotrophic lake is clearly in excess and nutrients are probably not in short supply amongst the thick *Drepanocladus* vegetation. L485 appears a true r–strategist also in respect of its small size and short generation time, enabling a relatively high growth rate already early in the spring.

The hypertrophic Priest Pot, like Vähä–Valkjärvi, is strongly affected by human activities, but is more typically an environment suitable for K–strategists. Its mature community structure is more complex, making interspecific competition an important selective feature. On the basis of the batch culture experiments it is obvious that in this habitat L315, which is *ca.* 10 times larger than L485, displays slow growth. In the food web in Priest Pot crustacean grazers have largely been replaced by abundant ciliates. Apart from the largest species these are not capable of feeding on algae of the size of L315.

Thus, the observations of L485 and L315 occupying extreme ends of the r–K continuum confirmed the earlier remarks on cosmopolitanism and great adaptability of cryptophytes, although caution must be exercised when drawing conclusions from data based on such a limited number of species. However, the extensive ecophysiological experiments carried out in this study could not uncover any characteristics typical of cryptophytes which can fully explain the success of these algae. In the batch experiments they did not emerge as species with high efficiency in resource (i.e. light) utilization, as would be expected from species in a highly

competitive environment such as Priest Pot. L485 proved to be more efficient than L315 in energy capture and utilization, but even this strain is rather a mediocre organism amongst other algae. Both strains respired large portion of their gross production and were not able to reach such high growth rates as expected from cells of their size. Accessory pigments which in theory could provide ecological advantages in terms of enhanced growth in chromatic light proved to be rather uneffective. In respect of under-achievement in growth cryptophytes are comparable with dinoflagellates.

The discrepancy between the correlates of r- and K-selection and the results of this study can be due to the parameters (i.e. light and temperature) scrutinized in this study. They are probably not the selective factors of greatest importance experienced by cryptophytes in nature. Especially in Priest Pot, nutrients may play an important role in competition and in the present study no attempt was made to determine the importance of this factor. When faced by competition cryptophytes may improve their status by means of diurnal vertical migrations and increase their growth rate. Although the growth enhancement gained by DVM can be of short duration, it can be crucial in a highly competitive environment such as in Priest Pot. Thus, DVM provides one further successful strategy for countering grazing pressure and nutrient limitation. These aspects needs more *in situ* investigations before decisive conclusions from the ecological importance of migrations can be drawn. Future studies should also focus on nutrient uptake kinetics and its competitive role in cryptophytes.

REFERENCES

Ahlgren, G. 1987. Temperature functions in biology and their application to algal growth constants. Oikos 49: 177– 190.

Ahtiainen, M., Holopainen, A.-L. & Hovi, A. 1985. Phytoplankton, primary production and dark fixation in a polyhumic lake in eastern Finland. Aqua Fennica 1591: 77–88.

Alberte, R.S., Wood, A.M., Kursar, T.A. & Guillard, R.R.L. 1984. Novel phycoerythrins in marine *Synecococcus* spp. Plant Physiol. 75: 732–739.

Anton, A. & Duthie, H.C. 1981. Use of cluster analysis in the systematics of the algal genus *Cryptomonas*. Can. J. Bot. 59: 992–1002.

Armbrust, E.V., Bowen, J.D., Olson, R.J. & Chisholm, S.W.1989. Effect of light on the cell cycle of a marine *Synechococcus* strain. Appl. Environ. Microbiol. 55: 425–432.

Arvola, L. 1984. Vertical distribution of primary production and phytoplankton in two small lakes with different humus concentration in southern Finland. Holarct. Ecol. 7: 390–398.

Arvola, L. 1986. Spring phytoplanton of 54 small lakes in southern Finland. Hydrobiologia 137: 125–134.

Arvola, L. & Kankaala, P. 1989. Winter and spring variability in phyto- and bacterioplankton in lakes with different water colour. Aqua Fennica 19: 29–39.

Arvola, L., Ojala, A., Barbosa, F. & Heaney, S.I. 1991. Migration behaviour of three Cryptophytes in relation to environmental gradients: an experimental approach. Manuscript.

Arvola, L. & Rask, M. 1984. Relations between phytoplankton and environmental factors in a small, spring, meromictic lake in southern Finland. Aqua Fennica 14: 129–138.

Arvola, L., Salonen, K., Bergström, I., Heinänen, A. & Ojala, A. 1986. Effects of experimental acidification on phyto–, bacterio– and zooplankton in enclosures of a highly humic lake. Int. Revue ges. Hydrobiol. 71: 737– 758.

Arvola, L., Salonen, K., Jones, R.I., Heinänen, A. & Bergström, I. 1987. A three day study of the diel behaviour of plankton in a highly humic and steeply stratified lake. Arch. Hydrobiol. 109: 89–106.

Bannister, T.R. 1979. Quantitative description of steady– state nutrient–saturated algal growth, including adaptation. Limnol. Oceanogr. 24: 76–96.

Banse, K. 1976. Rates of growth, respiration and photosynthesis of unicellular algae as related to cell size –a review. J. Phycol. 12: 135–140.

Banse, K. 1982. Cell volumes, maximal growth rates of unicellular algae and ciliates, and the role of ciliates in the marine pelagial. Limnol. Oceanogr. 27: 1059–1071.

Beakes, G., Canter, H.M. & Jaworski, G.H.M. 1988. Zoospores ultrastructure of *Zygorhizidium affluens* Canter and *Z. planktonicum* Canter, two chytrids parasitizing the diatom *Asterionella formosa* Hassall. Can. J. Bot. 66: 1054–1067.

Bergström, I. & Salonen, K. 1984. Measurement of respiration and primary production by CO_2 exchange method. Arch. Hydrobiol. Beih. Ergebn. Limnol. 19: 151–155.

Biggs, W.W., Edison, A.R., Eastin, J.D., Brown, K.W., Maranville, T.W. & Clegg, M.D. 1971. Photosynthesis light sensor and meter. Ecology 52: 125–131.

Bogorad, L. 1975. Phycobiliproteins and complementary chromatic adaptation. Ann. Rev. Plant Physiol. 26: 369– 401.

Booth, B.C. 1987. The use of autofluorescence for analyzing oceanic phytoplankton communities. Botanica Marina 30: 101–108.

Booth, B.C., Lewin, J. & Lorenzen, C.J. 1988. Spring and summer growth rates of subarctic Pasific phytoplankton assemblages determined from carbon uptake and cell volumes estimated using epifluorescence microscopy. Mar. Biol. 98: 287–298.

Borowitzka, M.A. & Borowitzka, L.J. 1988. Microalgal Biotechnology. Cambridge University Press.

Bowen, M.S. & Ward, H.B. 1977. Laboratory culture of *Cryptomonas ovata* and *Chroomonas* sp. (Cryptophyceae). Microbios Letters 6: 77–84.

Braunwarth, C. & Sommer, U. 1985. Analyses of the *in situ* growth rates of Cryptophyceae by use of the mitotic indextechnique. Limnol. Oceanogr. 30: 893–897.

Brown, T.E. & Richardson, F.L. 1968. The effect of growth environment on the physiology of algae: light intensity. J. Phycol. 4: 38–54.

Burns, N,M, & Rosa, F. 1980. *In situ* measurements of the settling velocity of organic particles and ten species of phytoplankton. Limnol. Oceanogr. 25: 855–864.

Burris, J.E. 1977. Photosynthesis, photorespiration, and dark respiration in eight species of algae. Mar. Biol. 39: 371–379.

Burris, J.E. 1981. Effects of oxygen and inorganic carbon concentrations on the photosynthetic quotients of marine algae. Mar. Biol. 65: 215–219.

Burris, J.E., Wedge, R. & Lane, A. 1981. Carbon dioxide limitation of photosynthesis of freshwater phytoplankton. J. Freshwat. Ecol. 1: 81–96.

Caeci, M.S. & Cacheris, W.P. 1984. Fitting curves to data. The Simplex algorithm is the answer. Byte, May(1984): 340– 362.

Campbell, L. & Carpenter, E.J. 1986. Diel patterns of cell division in marine *Synechococcus* spp. (Cyanobacteria): use of the frequency of dividing cells technique to measure growth rate. Mar. Ecol. Prog. Ser. 32: 139–148.

Carpenter, E.J. & Campbell, L. 1988. Diel patterns of cell division and growth rates of *Synechococcus* spp. in Long Island Sound. Mar. Ecol. Prog. Ser. 47: 179–183.

Carpenter, E.J. & Chang, J. 1988. Species–specific phytoplankton growth rates via diel DNA synthesis cycles. I. Concept of the method. Mar. Ecol. Prog. Ser. 43: 105–111.

Chaney, A.L. & Marbach, E.P. 1962. Modified reagents for the determination of urea and ammonia. Clin. Chem. 8: 130–132.

Chang, J. & Carpenter, E.J. 1988. Species–specific phytoplankton growth rates via diel DNA synthesis cycles. II. DNA quantification and model verification in the dinoflagellate *Heterocapsa triquetra*. Mar. Ecol. Prog. Ser. 44: 287–296.

Chisholm, S.W. 1981. Temporal patterns of cell division in unicellular algae. In: Platt, T. (ed.) Physiological bases of phytoplankton ecology. Can. Bull. Fish. Aquat. Sci. 210:150–181.

Church, M.R., Cohen, R.R.H., Galleros, C.L. & Kelly, M.G. 1983. Evidence for carbon uptake and storage in the dark with subsequent photosynthesis fixation by cultures of mixed Chlorophyceae. Arch. Hydrobiol. 98: 509–522.

Claustre, H. & Gostan, J. 1987. Adaptation of biochemical composition and cell size to irradiance in two microalgae: possible ecological implications. Mar. Ecol. Prog. Ser. 40: 167–174.

Cloern, J.E. 1977. Effects of light intensity and temperature on *Cryptomonas ovata* (Cryptophyceae) growth and nutrient uptake rates. J. Phycol. 13: 389–395.

Cloern, J.E. 1978. Simulation model of *Cryptomonas ovata* population dynamics in southern Kootenay Lake, British Columbia. Ecol. Modelling 4: 133–149.

Cobelas, M.A., Velasco, J.L., Rubio, A. & Brook, A.J. 1988. Phased cell division by field population of *Staurastrum longiradiatum* (Conjugatophyceae, Desmidiaceae). Arch. Hydrobiol. 112: 1–20.

Coleman, A.W. 1980. Enhanced detection of bacteria in natural environments by fluorochrome staining of DNA. Limnol. Oceanogr. 25: 948–951.

Coleman, B. & Rotatore, C. 1988. Uptake and accumulation of inorganic carbon by a freshwater diatom. J. Exp. Bot. 39: 1025–1032.

Cook, J.R. 1963. Adaptations in growth and division in *Euglena* effected by energy supply. J. Protozool. 10: 436–444.

Cosby, B.J., Hornberger, G.M. & Kelly, M.G. 1984. Identification of photosynthesis–light models for aquatic systems. II. Application to a macrophyte dominated stream. Ecol. Modelling 23: 25–51.

Coté, B. & Platt, T. 1984. Utility of the light–saturation curve as an operational model for quantifying the effects of environmental conditions on phytoplankton photosynthesis. Mar. Ecol. Prog. Ser. 18: 57–66.

Cullen, J.J. 1985. Diel vertical migrations by dinoflagellates: roles of carbohydrate metabolism and behavioral flexibility. In: Rankin, M.A. (ed.) Migration: mechanisms and adaptive significance. Contributions in Marine Science Supplement Vol. 27: 135–152.

Cullen, J.J. & Horrigan, S.G. 1981. Effects of nitrate on the diurnal vertical migration, carbon to nitrogen ratio, and the photosynthetic capacity of the dinoflagellate *Gymnodinium splendens*. Mar. Biol. 62: 81–89.

Davison, W. & Finlay, B.J. 1986. Ferrous iron and phototrophy as alternative sinks for sulphide in the anoxic hypolimnia of two adjacent lakes. J. Ecol. 74: 663–673.

Dean, P.N. & Jett, J.H. 1974. Mathematical analysis of DNA distributions derived from flow microfluorometry. J. Cell Biol. 60: 523–527.

Devol, A.H. & Packard, T.T. 1978. Seasonal changes in respiratory enzyme activity and productivity in Lake Washington microplankton. Limnol. Oceanogr. 23: 104–111.

Dokulil, M. 1988. Seasonal and spatial distribution of cryptophycean species in the deep, stratifying, alpine lake Mondsee and their role in the food web. Hydrobiologia 161: 185–201.

Doyle, R.W. & Poore, R.V. 1974. Nutrient competition and division synchrony in phytoplankton. J. Exp. Mar. Biol. Ecol. 14: 201–210.

Dring, M.J. 1988. Photocontrol of development in algae. Ann. Rev. Plant Physiol. Plant Mol. Biol. 39: 157–174.

Dubois, M., Gilles, K.A., Hamilton, J.K., Rebers, P.A. & Smith, F. 1956. Colorimetric method for determination of sugars and related substances. Anal. Chem. 28: 350–356.

Dunstan, W.M. 1973. A comparison of the photosynthesis–light intensity relationship in phylogenetically different marine microalgae. J. exp. mar. Biol. Ecol. 13: 181–187.

Elbrächter, M. 1973. Population dynamics of *Ceratium* in coastal waters of the Kiel Bay. Oikos Suppl. 15: 43–48.

Elomaa, E. 1977. A comparison of the penetration of global short wave radiation into four Finnish lakes. Publications of the University of Joensuu. Series BII, no 7.

Eloranta, P. 1978. Light penetration in different types of lakes in Central Finland. Holarct. Ecol. 1: 362– 366.

Eloranta, P. 1986. Phytoplankton structure in different lake types in central Finland. Holarct. Ecol. 9: 214–224.

Eppley, R.W. 1972. Temperature and phytoplankton growth in the sea. Fishery Bulletin 70: 1063–1085.

Eppley, R.W., Holm–Hansen, O. & Strickland, J.D.H. 1968. Some observations on the vertical migration of dinoflagellates. J. Phycol. 4: 330–340.

Eppley, R.W. & Sloan, P.R. 1966. Growth rates of marine phytoplankton: correlation with light absorption by cell chlorophyll *a*. Physiol. Plant. 19: 47–59.

Ettl, H. & Moestrup, Ø. 1980. Über einen intrazellulären Parasiten bei *Cryptomonas (Cryptophyceae)*, I. Pl. Syst. Evol. 135: 211–226.

Fairchild, E. & Sheridan, R.P. 1974. A physiological investigastion of the hot spring diatom, *Achnanthes exigua* Grun. J. Phycol. 10: 1–4.

Falkowski, P.G., Dubinski, Z. & Santostefano, G. 1985a. Light–enhanced dark respiration in phytoplankton. Verh. Internat. Verein. Limnol. 22: 2830–2833.

Falkowski, P.G., Dubinski, Z. & Wyman, K. 1985b. Growth – irradiance relationships in phytoplankton. Limnol. Oceanogr. 30: 311–321.

Falkowski, P.G. & Owens, T.G. 1978. Effects of light intensity on photosynthesis and dark respiration in six species of marine phytoplankton. Mar. Biol. 45: 289–295.

Falkowski, P.G. & Owens, T.G. 1980. Light–shade adaptation. Two strategies in marine phytoplankton. Plant. Physiol. 66: 592–595.

Faust, M.A. 1974. Structure of the periplast of *Cryptomonas ovata* var. *palustris*. J. Phycol. 10: 121– 124.

Feuillade, J.B. & Feuillade, M. 1987. Modelling steady–state growth and photosynthesis rates of *Oscillatoria rubescens* continuous cultures in relation to temperature and irradiance. J. Plankton Res. 9: 445–457.

Finlay, B.J. & Berninger, U.-G. 1984. Coexistence of congeneric ciliates (Karyorelictida: *Loxodes*) in relation to food resources in two freshwater lakes. J. Anim. Ecol. 53: 929–943.

Finlay, B.J., Clarke, K.J., Cowling, A.J., Hindle, R.M. & Rogerson, A. 1988. On the abundance and distribution of Protozoa and their food in a productive freshwater pond. Europ. J. Protistol. 23: 205–217.

Fogg, G.E. 1975. Algal Cultures and Phytoplankton Ecology. Second edition. The University of Wisconsin Press.

Fogg, G.E. 1977. Excretion of organic matter by phytoplankton. Limnol. Oceanogr. 22: 576– 577.

Fogg, G.E. 1983. The ecological significance of extracellular products of phytoplankton photosynthesis. Botanica Marina 26: 3–14.

Frempong, E. 1981. Diel variation in the abundance, vertical distribution, and species composition of phytoplankton in a eutrophic English lake. J. Ecol. 69: 919–939.

Furgeson, R.L., Buckley, E.N. & Palumbo, A.V. 1984. Response of marine bacterioplankton to differential filtration and confinement. Appl. Environm. Microbiol. 47: 49–55.

Galleron, C. & Durrand, A.M. 1979. Cell cycle and DNA synthesis in a marine dinoflagellate *Amphidinium carterae*. Protoplasma 100: 155–165.

Ganf, G.G., Heaney, S.I. & Corry, J.E. 1991. Light absorption and pigment content in natural populations and cultures of a non gas–vacuolate cyanobacterium *Oscillatoria bourellyi*. Manuscript.

Gantt, E. 1980. Photosynthetic cryptophytes. In: Cox, E.R.(ed.) Phytoflagellates. Elsevier North Holland. p. 381–405.

Gavrieli, J. 1984. Studies on the autoecology of the freshwater algae flagellate *Rhodomonas lacustris* Pascher et Ruttner. A dissertation. Swiss Federal Institute of Technology of Zurich (ETH) (Diss. ETH Nr. 7595).

Geider, R.J. & Osborne, B.A. 1989. Respiration and microalgal growth: a review of the quantitative relationship between dark respiration and growth. New Phytol. 112: 327–341.

Geider, R.J., Osborne, B.A. & Raven, J.A. 1986. Growth, photosynthesis and maintenance metabolic cost in the diatom *Phaedactylum tricornutum* at very low light levels. J. Phycol. 22: 39–48

Gibson, C.E. 1985. Growth rate, maintenance energy and pigmentation of planktonic Cyanophyta during one–hour light:dark cycles. Br. phycol. J. 20: 155–161.

Glover, H.E., Keller, M.D. & Spinrad, R.W. 1987. The effects of light quality and intensity on photosynthesis and growth of marine eukaryotic and prokaryotic phytoplankton clones. J. Exp. Mar. Biol. Ecol. 105: 137– 159.

Goldman, J.C., McCarthy, J.J. & Peavey, D.G. 1979. Growth rate influence on the chemical composition of phytoplankton in oceanic waters. Nature 279: 210–215.

Goulder, R. 1971. Vertical distribution of some ciliated protozoa in two freshwater sediments. Oikos 22: 199–203.

Goulder, R. 1972. The vertical distribution of some ciliated Protozoa in the plankton of a eutrophic pond during summer stratification. Freshwat. Biol. 2: 163–176.

Goulder, R. 1975. The effects of photosynthetically raised pH and light on some ciliated Protozoa in a eutrophic pond. Freshwat. Biol. 5: 313–322.

Grobbelaar, J.U. & Soeder, C.J. 1985. Respiration losses in planktonic green algae cultivated in raceway ponds. J. Plankton Res. 7(4): 497–506.

Grotjohann, N. & Kowallik, W. 1989. Influence of blue light on the activity of phosphofructokinase in *Chlorella kessleri*. Physiol. Plant. 75: 43–46.

Guillard, R.R.L. 1973. Division rates. In: Stein, J.R. (ed.) Handbook of Phycological Methods. Culture Methods and Growth Measurements. Cambridge University Press. p. 289– 311.

Häder, D.-P. 1987. The relation of photosynthesis to blue light effects. In: Senger, H. (ed.) Blue Light Responses: Phenomena and Occurrence in Plants and Microorganisms, Volume I, CRC Press Inc., Boca Raton, Florida. p. 145– 160.

Häder, D.-P. & Häder, M. 1989. Effects of solar radiation on photoorientation, motility and pigmentation in a freshwater *Cryptomonas*. Botanica Acta 102: 236–240.

Häder, D.-P. & Häder, M. 1990. Effects of UV radiation on motility, photo–orientation and pigmentation in a freshwater *Cryptomonas*. J. Photochem. Photobiol., B: Biology 5: 105–114.

Häder, D.-P., Rhiel, E. & Wehrmeyer, W. 1987. Phototaxis in the marine flagellate *Cryptomonas maculata*. J. Photochem. Photobiol., B: Biology 1: 115–122.

Happey-Wood, C.M. 1976. Vertical migration patterns in phytoplankton of mixed species composition. Br. phycol. J. 11: 355–369.

Harris, G.P. 1978. Photosynthesis, productivity and growth: the physiological ecology of phytoplankton. Ergebn. Limnol. (Arch. Hydrobiol.) 10: 1–171.

Harris, G.P. 1986. Phytoplankton Ecology. Structure, function and fluctuation. University Press. Cambridge.

Harris, G.P. & Piccinin, B.B. 1983. Phosphorus limitation and carbon metabolism in a unicellular alga: interaction between growth rate and the measurement of net and gross photosynthesis. J. Phycol. 19: 185–192.

Healey, F.P. 1975. Physiological indicators of nutrient deficiency in algae. Fush. Mar. Ser. Res. Dev. Tech. rep. 585: 30 p.

Heaney, S.I. 1974. A pneumatically–operated water sampler for close intervals of depth. Freshwat. Biol. 4: 103–106.

Heaney, S.I. & Butterwick, C. 1985. Comparative mechanisms of algal movement in relation to phytoplankton production. In: Rankin, M.A. (ed.) Migration: mechanisms and adaptive significance. Contributions in Marine Science. Supplement Vol. 27: 114–134.

Heaney, S.I., Davey, M.C. & Brooks, A.S. 1989. Formation of sub–surface maxima of a diatom within a stratified lake and in a laboratory column. J. Plankton Res. 11: 1169–1184.

Heaney, S.I. & Eppley, R.W. 1981. Light, temperature and nitrogen as interacting factors affecting diel vertical migrations of dinoflagellates in culture. J. Plankton Res. 3: 331–344.

Heaney, S.I. & Furnass, T.I. 1980. Laboratory models of diel vertical migration in the dinoflagellate *Ceratium hirundinella*. Freshwat. Biol. 10: 163–170.

Heaney, S.I. & Talling, J.F. 1980. Dynamic aspects of dinoflagellate distribution patterns in a small productive lake. J. Ecol. 68: 75–94.

Heller, M.D. 1977. The phased division of the freshwater dinoflagellate *Ceratium hirundinella* and its use as a method of assessing growth in natural populations. Freshwat. Biol. 7: 527–533.

Helmstetter, C.E. & Cooper, S. 1968. DNA synthesis during the division cycle of a rapidly growing *Escherichia coli*. Br. J. Mol. Biol. 31: 507–518.

Herbert, D., Phipps, P.J. & Strange, R.E. 1971. Chemical analysis of microbial cells. In: Norris, J. & Ribbons, D.W. (eds.) Methods in Microbiology. Vol.5B: 209–344.

Heynig, H. 1976. Beobachtungen an zwei Cryptomonaden. Arch. Protistenk. Bd. 118: 92–97.

Hibberd, D.J., Greenwood, A.D. & Bronwen Griffiths, H. 1971. Observations on the ultrastructure of the flagella and periplast in the Cryptophyceae. Br. phycol. J. 6: 61–72.

Hill, D.R.A. & Wetherbee, R. 1989. A reappraisal of the genus *Rhodomonas* (Cryptophyceae). Phycologia 28: 143–158.

Hilton, J., Lishman, J.P., Mackness, S. & Heaney, S.I. 1986. An automated method for the analysis of particulate carbon and nitrogen in natural waters. Hydrobiologia 141: 269–271.

Hilton, J., Rigg, E. & Jaworski, G. 1989. *In vivo* algal fluorescence, spectral change due to light intensity changes and the automatic characterization of algae. Freshwat. Biol. 21: 375–382.

Holtan, H. 1979. The Lake Mjøsa story. Arch. Hydrobiol. Beih. Ergebn. Limnol. 13: 242–258.

Huber–Pestalozzi, G. 1968. Das Phytoplankton des Süsswassers. Systematik und Bilogie. 3. Teil. 2. Auflage. In: Elster, H.–J. & Ohle, W. Die Binnengewässer. Band

XVI. 3 Teil. 2. Auflage. E. Schweitzerbart'sche Verlagsbuchhandlung (Nägele u. Obermiller).

Humphrey, G.F. 1975. The photosynthesis:respiration ratio of some unicellular marine algae. J. Exp. Mar. Biol. Ecol. 18: 111–119.

Ilmavirta, K. & Kotimaa, A.-L. 1974. Spatial and seasonal variations in phytoplanktonic primary production and biomass in the oligotrophic lake Pääjärvi, southern Finland. Ann. Bot. Fennici 11: 112–120.

Ilmavirta, V. 1983. The role of flagellated phytoplankton in chains of small brown-water lakes in southern Finland. Ann. Bot. Fennici 20: 187–195.

Iwakuma, T. & Yasuno, M. 1983. A comparison of several mathematical equations describing photosynthesis–light curve for natural phytoplankton populations. Arch. Hydrobiol. 97: 208–226.

Jassby, A.D. & Platt, T. 1976. Mathematical formulation of the relationship between photosynthesis and light for phytoplankton. Limnol. Oceanogr. 21: 540–547.

Javornicky, P. 1970. On the utilization of light by freshwater phytoplankton. Arch. Hydrobiol./Suppl. 39. Algological Studies 2/3: 68–85.

Jeffrey, S.W. 1984. Responses of unicellular marine plants to natural blue–green light environments. In: Senger, H. (ed.). Blue Light Effects in Biological Systems. Springer Verlag Berlin Heidelberg. p. 497–508.

Jeffrey, S.W. & Vesk, M. 1977. Effect of blue–green light on photosynthetic pigments and chloroplast structure in the marine diatom Stephanodiscus turris. J. Phycol. 13: 271–279.

Johnson, M.G., Michalski, M.F.P. & Christie, A.E. 1970. Effects of acid mine wastes on phytoplankton communities of two nothern Ontario lakes. J. Fish. Res. Board Canada 27: 425–444.

Jones, R.I. 1977. The importance of temperature conditioning to the respiration of natural phytoplankton communities. Br. phycol. J. 12: 277–285.

Jones, R.I. 1988. Vertical distribution and diel migration of flagellated phytoplankton in a small humic lake. Hydrobiologia 161: 75–87.

Jones, R.I. 1991. Advantages of diurnal vertical migrations to phytoplankton in sharply stratified, humic forest lakes. Arch. Hydrobiol. 120: 257–266.

Jones, R.I. & Arvola, L. 1984. Light penetration and some related characteristics in small forest lakes in southern Finland. Verh. Internat. Verein. Limnol. 22: 811–816.

Jones, R.I. & Ilmavirta, V. 1988. Flagellates in freshwater ecosystems – Concluding remarks. Hydrobiologia 161: 271–274.

Kairesalo, T., Jónsson, G.St., Gunnarsson, K., Lindegaard, C. & Jónasson, P.M. 1991a. Metabolism and community dynamics within Nitella opaca (Charophyceae) beds in Thingvallavatn. Manuscript. Accepted in Oikos.

Kairesalo, T. Heikkonen, K. & Similä, A. 1987. Dynamics and succession of benthic moss vegetation in an acid lake: the contribution of algae and grazers. Lammi Notes 14:10.

Kairesalo, T., Lehtovaara, A. & Saukkonen, P. 1991b. Littoral-pelagial interchange and the decompsition of dissolved organic matter. Manuscript.

Kamiya, A. & Miyachi, S. 1984a. Blue–green and green light adaptations on photosynthetic activity in some algae collected from subsurface chlorophyll layer in the western Pacific Ocean. In: Senger, H. (ed.) Blue Light Effects in Biological Systems. Springer Verlag Berlin Heidelberg. p. 517–528.

Kamiya, A. & Miyachi, S. 1984b. Effects of light quality on formation of 5-aminolevulinic acid, phycoerythrin and chlorophyll in *Cryptomonas* sp. cells collected from the subsurface chlorophyll layer. Plant & Cell Physiol. 25: 831–839.

Kamykowski, D. 1981. Laboratory experiments on the diurnal vertical migration of marine dinoflagellates through temperature gradients. Mar. Biol. 62: 57–64.

Kamykowski, D. & Zentara, S.J. 1977. The diurnal vertical migration of motile phytoplankton through temperature gradients. Limnol. Oceanogr. 22: 148–151.

Kapuscinski, J. & Skozylas, B. 1977. Simple and rapid fluorimetric method for DNA microassay. Analyt. Biochem. 83: 252–257.

Kirk, J.T.O. 1983. Light and Photosynthesis in Aquatic Ecosystems. Cambridge University Press.

Klaveness, D. 1981. *Rhodomonas lacustris* (Pascher et Ruttner) Javornicky (Cryptomonadida): Ultrastructure of the vegetative cell. J. Protozool. 28: 83–90.

Klaveness, D. 1985. Classical and modern criteria for determining species of Cryptophyceae. Bulletin of Plankton Society of Japan 32: 111–123.

Klaveness, D. 1988. Ecology of the Cryptomonadida: A first review. In: Sandgren, C.D. (ed.) Growth and Reproductive Strategies of Freshwater Phytoplankton. Cambridge University Press. p. 105–133.

Klemer, A.R. 1985. Nutrient-induced migrations of blue-green algae (Cyanophyceae). In: Rankin, M.A. (ed.) Migrations: Mechanisms and Adaptive Significance. Contributions in Marine Science. Supplement Vol.27: 153– 165.

Knoechel, R. & Kalff, J. 1978. An in situ study of the productivity and population dynamics of five freshwater planktonic species. Limnol. Oceanogr. 23: 195–218.

Kohata, K. & Watanabe, M. 1986. Synchronous division and the pattern of diel vertical migration of *Heterosigma akashiwo* (Hada) Hada (Raphidophyceae) in a laboratory culture tank. J. Exp. Mar. Biol. Ecol. 100: 209–224.

Kowallik, W. 1987. Blue light effects on carbohydrate and protein metabolism. In: Senger, H. (ed.) Blue Light Responses: Phenomena and Occurrence in Plants and Microorganisms. Volume I, CRC Press, Inc. Boca Raton, Florida. p. 7–16.

Langdon, C. 1987. On the causes of interspecific differences in the growth – irradiance relationship for phytoplankton. Part I. A comparative study of the growth – irradiance relationship of three marine phytoplankton species: *Skeletoenema costatum*, *Olisthodiscus luteus* and *Gonyaulax tamarensis*. J. Plankton res. 9: 459–482.

Langdon, C. 1988. On the causes of interspecific differences in the growth – irradiance relationship for phytoplankton. II. A general review. J. Plankton Res. 10: 1291–1312.

Lappalainen, A., Rask, M. & Vuorinen, P.J. 1988. Acidification affects the perch, *Perca fluviatilis*, populations in small lakes in southern Finland. Environmental Biology of Fishes 21: 231–239.

Laws, E.A. 1975. The importance of respiration losses in controlling the size distribution of marine phytoplankton. Ecology 56: 419–426.

Levy, I. & Gantt, E. 1988. Light acclimation in *Porphyridium purpureum* (Rhodophyta): growth, photosynthesis, and phycobilisomes. J. Phycol. 24: 452–458.

Lewitus, A.J. & Caron, D.A. 1990. Relative effects of nitrogen or phosphorus depletion and light intensity on the pigmentation, chemical composition, and volume of *Pyrenomonas salina* (Cryptophyceae). Mar. Ecol. Prog. Ser. 61: 171–181.

Lichtlé, C. 1979. Effects of nitrogen deficiency and light of high intensity on *Cryptomonas rufescens* (Cryptophyceae) I. Cell and photosynthetic apparatus transformations and encystment. Protoplasma 101: 283–299.

Lichtlé, C. 1980. Effects of nitrogen deficiency and light of high intensity on *Cryptomonas rufescens* (Cryptophyceae). II. Excystment. Protoplasma 102: 11–19.

Lichtlé, C. & Dubacq, J.P. 1984. Lipid modifications related to encystment and excystment of *Cryptomonas rufescens* SKUJA (Cryptophyceae). J. Phycol. 20: 8–12.

Lichtlé, C., Duval, J.C. & Lemoine, Y. 1987. Comparative biochemical, functional and ultrastructural studies of photosystem particles from a Cryptophyceae: *Cryptomonas rufescens*; isolation of an active phycoerythrin particle. Biochim. Biophys. Acta 894: 76–90.

Likens, G.E. 1985. An ecosystem approach to aquatic ecology. Mirror Lake and Its Environment. Springer Verlag New York.

Logan, J.A., Wollkind, D.J., Hoyt, S.C. & Tanigoshi, L.K. 1976. An analytical model for description of temperature dependent rate phenomena in arthropods. Env. Entomol. 5: 1133–1140.

Lucas, I.A.N. 1970. Observations on the fine structure of the Cryptophyceae. I. The genus *Cryptomonas*. J. Phycol. 6: 30–38.

Lund, J.W.G. 1959. A simple counting chamber for nannoplankton. Limnol. Oceanogr. 4: 57–65.

MacArthur, R.H. & Wilson, E.O. 1967. The Theory of Island Biogeography. Princeton University Press.

MacColl, R. 1982. Phycobilisomes and biliproteins. J. Photochem. Photobiol. 35: 899–904.

MacColl, R., Berns, D.S. & Ribbons, O. 1976. Characterization of cryptomonad phycoerythrin and phycocyanin. Archiv. Biochem. Biophys. 177: 265–275.

Mackereth, F.J.H. 1963. Water analysis. Freshwater Biological Association. Scientific publication No. 21.

Mague, T.H., Friberg, E., Hughes, D.J. & Morris, I. 1980. Extracellular release of carbon by marine phytoplankton; a physiological approach. Limnol. Oceanogr. 25: 262–279.

Marra, J. & Heinemann, K. 1987. Primary production in the North Pacific Central Gyre: Some new measurements based on 14C. Deep-Sea Res. 34: 1821–1829.

May, R.M. 1976. Theoretical Ecology. Principles and Applications. Blackwell Scientific Publication.

McDuff, R.E. & Chisholm, S.W. 1982. The calculation of *in situ* growth rates of phytoplankton populations from fractions of cells undergoing mitosis: a clarification. Limnol.Oceanogr. 27: 783–788

Megard, R.O., Tonkyn, D.W. & Senft, W.H., II. 1984. Kinetics of oxygenic photosynthesis in planktonic algae. J. Plankton Res. 6: 325–337.

Morgan, K.C. & Kalff, J. 1975. The winter dark survival of an algal flagellate *Cryptomonas erosa* (Skuja). Verh. Internat. Verein. Limnol. 19: 2734–2740.

Morgan, K.C. & Kalff, J. 1979. Effect of light and temperature interactions on growth of *Cryptomonas erosa* (Cryptophyceae). J. Phycol. 15: 127–134.

Morimoto, H. & James, T.W. 1969. Effects of growth rate on the DNA content of *Astasia longa* cells. Expt. Cell Res. 58: 55–61.

Morris, I. 1981. Photosynthetic products, physiological state, and phytoplankton growth. In: Platt, T. (ed). Physiological Bases of Phytoplankton Ecology. Can. Bull. Fish. Aquat. Sci. 210: 83–102.

Morris, A.W. & Riley, J.P. 1963. The determination of nitrate in sea water. Anal. Chim. Acta 29: 272–279.

Munavar, M. & Bistricki, T. 1979. Scanning electron microscopy of some nannoplankton cryptomonads. Scannning Electron Microsc. 3: 247–252.

Murphy, J. & Riley, J.P. 1962. A modified single solution method for the determination of phosphate in natural waters. Anal. Chim. Acta 27: 31–36.

Myklestad, S. 1974. Production of carbohydrates by marine planktonic diatoms. I. Comparison of nine different species in culture. J. Exp. Mar. Biol. Ecol. 15: 261–274.

Myklestad, S. 1977. Production of carbohydrates by marine planktonic diatoms. II. Influence of the N/P ratio in the growth medium on the assimilation ratio, growth rate and production of the cellular and extracellular carbohydrate by *Chaetoceros affinis var Willei* (Gran) Hustedt and *Skeletonema costatum* (Grev.) Cleve. J. Exp. Mar. Biol. Ecol. 29: 161–179.

Neale, P.J. & Richerson, P.J. 1987. Photoinhibition and diurnal variation of phytoplankton photosynthesis – I. Development of a photosynthesis–irradiance model from studies of *in situ* responses. J. Plankton Res. 9: 167– 193.

Nicklish, A. & Kohl, J.-G. 1983. Growth kinetics of *Microcystis aeruginosa* (Kutz) Kutz as a basis for modelling its population dynamics. Int. Revue ges. Hydrobiol. 68: 317–326.

Oakley, B.R. & Bisalputra, T. 1977. Mitosis and cell division in *Cryptomonas* (Cryptophyceae). Can. J. Bot. 55: 2789–2800.

Oakley, B.R. & Dodge, J.D. 1976. The ultrastructure of mitosis in *Chroomonas salina* (Cryptophyceae). Protoplasma 88: 241–254.

Olaveson, M.M. & Stokes, P.M. 1989. Responses of the acidophilic alga *Euglena mutabilis* (Euglenophyceae) to carbon enrichment at pH 3. J. Phycol. 25: 529–539.

Oliver, R.L. & Walsby, A.E. 1984. Direct evidence for the role of light–mediated gas vesicle collapse in the buoyance regulation of *Anabaena flos–aqua* (cyanobacteria). Limnol. Oceanogr. 29: 879–886.

Olson, R.J. & Chisholm, S.W. 1986. Effects of light and nitrogen limitation on the cell cycle of the dinoflagellate *Amphidinium carteri*. J. Plankton Res. 8:785–793.

Olson, R.J., Frankel, S.L. & Chisholm, S.W. 1983. An inexpensive flow cytometer for the analysis of fluorescence signals in phytoplankton: chlorophyll and DNA distributions. J. Exp. Mar. Biol. Ecol. 68: 129–144.

Palmqvist, K., Sjöberg, S. & Samuelsson, G, 1988. Introduction of inorganic carbon accumulation in the unicellular green algae *Scenedesmus obliquus* and *Chlamydomonas reinhardtii*. Plant Physiol. 87: 437–442.

Parker, R.A. 1973. Some problems associated with computer simulation of an ecological system. In: Bartlett, M.S. & Hiorns, R.W. (eds.) The Mathematical Theory of the Dynamics of Biological Populations. Academic Press, New York–San Fransisco–London, p. 269–288.

Pedrós-Alió, C., Gasol, J.M. & Guerrero, R. 1987. On the ecology of a *Cryptomonas phaseolus* population forming a metalimnetic bloom in Lake Ciso', Spain: Annual distribution and loss factors. Limnol. Oceanogr. 32: 285–298.

Penning de Vries, F.M.T. 1975. The cost of maintenance processes in plant cells. Annals of Botany 39: 77–92 .

Pennington, F.C., Haxo, F.T., Borch, G. & Liaaen- Jensen, S. 1985. Carotenoids of Cryptophyceae. Biochem. Syst. Ecol. 13: 215–219.

Perry, M.J., Larsen, M.C. & Albeerte, R.S. 1981. Photoadaptation in marine phytoplankton: responses of the photosynthetic unit. Mar. Biol. 62: 91–101.

Pianka, E.R. 1978. Evolutionary Ecology. 2nd edition. Harper and Row, New York.

Pierce, J. & Omata, T. 1988. Uptake and utilization of inorganic carbon by cyanobacteria. Photosynthesis Research 16: 141–154.

Platt, T. & Jassby, A.D. 1976. The relationship between photosynthesis and light for natural assemblages of coastal marine phytoplankton. J. Phycol. 12: 421–430.

Pollinger, U. & Serruya, C. 1976. Phased division of *Peridinium cinctum* f. *westii* (Dinophyceae) and development of the lake Kinneret (Israel) bloom. J. Phycol. 12: 163–170.

Porter, K.G. & Feig, Y.S. 1980. The use of DAPI for identifying and counting aquatic microflora. Limnol. Oceanogr. 25: 943–948.

Post, A.F., de Wit, R. & Mur, L.R. 1985. Interactions between temperature and light intensity on growth and photsynthesis of the cyanobacterium *Oscillatoria agardhii*. J. Plankton Res. 7: 487–495.

Prezelin, B.B. & Sweeney, B.M. 1979. Photoadaptation of photosynthesis in two bloom-forming dinoflagellates. In: Taylor, D. & Seliger, H. (ed.). Toxic Dinoflagellate Blooms. Elsevier North Holland, Inc. p. 101–106.

*)

Puiseux-Dao, S. 1981. Cell cycle events in unicellular algae. In: Platt, T. (ed.) Physiological Bases of Phytoplankton Ecology. Can. Bull. Fish. Aquat. Sci. 210: 130–149.

*) Pringsheim, E.g. 1968. Zur Kenntnis der Cryptomonaden des Süßwassers. Nova Hedwigia 16: 367-401.

Rask, M., Heinänen, A., Salonen, K., Arvola, L., Bergström, I., Liukkonen, M. & Ojala, A. 1986. The limnology of a small, naturally acidic, highly humic forest lake. Arch. Hydrobiol. 106: 351–371.

Raven, J.A. 1980. Nutrient transport in microalgae. Advances in Microbial Physiology 21: 47–226.

Raven, J.A. 1984. A cost–benefit analysis of photon absorption by photosynthetic unicells. New Phytol. 98: 593–625.

Raven, J.A. & Beardall, J. 1981. Respiration and photorespiration. In: Platt, T. (ed.) Physiological Bases of Phytoplankton Ecology. Can. Bull. Fish. Aquat. Sci. 210: 55–82.

Raven, J.A. & Geider, R.J. 1988. Temperature and algal growth. New Phytol. 110: 441–461.

Raven, J.A. & Richardson, K. 1984. Dinophyte flagella: a cost–benefit analysis. New Phytol. 98: 259–276.

Reinertsen, H. 1982. The effect of nutrient addition on the phytoplankton community of an oligotrophic lake. Holarct. Ecol. 5: 225–252.

Reynolds, C.S 1984. The Ecology of Freshwater Phytoplankton. Cambridge University Press. Cambridge.

Reynolds, C.S., Thompson, J.M., Ferguson, A.J.D. & Wiseman, S.W. 1982. Loss processes in the population dynamics of phytoplankton maintained in closed systems. J. Plankton Res. 4: 561–600.

Rhiel, E., Häder, D.-P. & Wehrmeyer, W. 1988. Diaphototaxis and gravitaxis in a freshwater *Cryptomonas*. Plant Cell Physiol. 29: 755–760.

Rhiel, E., Kunz, J. & Wehrmyer, W. 1989. Immunocytochemical localization of phycoerythrin-545 and of a chlorophyll *a/c* light harvesting complex in *Cryptomonas maculata* (Cryptophyceae). Botanica Acta 192: 46-53.

Richardson, K, Beardall, J. & Raven, J.A. 1983. Adaptation of unicellular algae to irradiance: an analysis of strategies. New Phytol. 93: 157-191.

Rivkin, R.B. 1989. Influence of irradiance and spectral quality on the carbon metabolism of phytoplankton. I. Photosynthesis, chemical composition and growth. Mar. Ecol. Prog. Ser. 55: 291-304.

Rott, E. 1988. Some aspects of the seasonal distribution of flagellates in mountain lakes. Hydrobiologia 161: 159-170.

Roukhijajnen, M.I. 1977. Rate of cell division in the Black Sea Pyrrophyte Alga *Cryptomonas vulgaris* in culture. Hydrobiological Journal 13: 53-56.

Ruyters, G. 1987. Control of enzyme capacity and enzyme activity. In: Senger, H. (ed.) Blue Light Responses: Phenomena and Occurrence in Plants and Microorganisms, volume II CRC Press, Inc. Boca Raton, Florida. p. 71-88.

Ruyters, G., Hirosawa, T. & Miyachi, S. 1984. Blue light effects on carbon metabolism in *Dunaliella*. In: Senger, H. (ed.) Blue Light Effects in Biological Systems. Springer-Verlag, Berlin Heidelberg, p. 317-322.

Ryther, J.H. 1954. The ratio of photosynthesis to respiration in marine plankton algae and its effect upon the measurement of productivity. Deep-Sea Res. 2: 134-139.

Sakshaug, E. & Andersen, K. 1986. Effect of light regime upon growth rate and chemical composition of a clone of *Skeletonema costatum* from the Trondheimsfjord, Norway. J. Plankton Res. 8: 619-637.

Salonen, K. 1979. A versatile method for the rapid and accurate determination of carbon by high temperature combustion. Limnol. Oceanogr. 24: 177–183.

Salonen, K. 1981. Rapid and precise determination of total inorganic carbon and some gases in aqueous solutions. Water Res. 15: 403–406.

Salonen, K., Jones, R.I. & Arvola, L. 1984. Hypolimnetic phophorus retrieval by diel vertical migrations of lake phytoplankton. Freshwat. Biol. 14: 431–438.

Samuelsson, G. & Richardson, K. 1982. Photoinhibition at low quantum flux densities in a marine dinoflagellate (*Amphidinium carterae*). Mar. Biol. 70: 21–26.

Santore, U.J. 1977. Scanning electron microscopy and comparative micromorphology of the periplast of *Hemiselmis rufescens*, *Chroomonas* sp., *Chroomonas salina* and members of the genus *Cryptomonas* (Cryptophyceae). Br. phycol. J. 12: 255–270.

Santore, U.J. 1978. Light microscopic and electron microscopic observations of the palmelloid phase in members of the genus *Cryptomonas* Cryptophyceae. Archiv für Protistenkunde 120: 420–435.

Santore, U.J. 1984. Some aspects of taxonomy in the Cryptophyceae. New Phytol. 98: 627–646.

Schindler, D.W. & Fee, E.J. 1973. Diurnal variation of dissolved inorganic carbon and its use in estimating primary production and CO_2 invasion in lake 227. J. Fish. Res. Board Can. 30: 1501–1510.

Schnee, H. 1976. Beitrag zur Limnologie von Braunwässern unterschidlicher Typen. Limnologica (Berlin) 11: 57–100.

Senger, H. 1987. Sun and shade effects of blue light on plants. In: Senger, H. (ed.) Blue Light Responses: Phenomena and Occurrence in Plants and Microorganisms. Volume II. CRC Press, Inc. Boca Raton, Florida, p. 141– 149.

Sharp, J.H. 1977. Excretion of organic matter by marine phytoplankton: Do healthy cells do it? Limnol. Oceanogr. 22: 381–399.

Sicko–Goad, L., Stoermer, E.F. Ladewski, B.G. 1977. A morphometric method for correcting phytoplankton cell volume estimates. Protoplasma 93: 147–163.

Skogstad, A., Granskog, L. & Klaveness, D. 1987. Growth of freshwater ciliates offered planktonic algae as food. J. Plankton Res. 9: 503–512.

Skuja, H. 1956. Taxonomische und biologische Studien über das Phytoplankton schwedischer Binnengewässer. Nova Acta r. Soc. scient. upsal. Ser. 4,16,3: 1–404.

Skulberg, O.M. 1978. Some observations on red–coloured species of *Oscillatoria* (Cyanophycea) in nutrient– enriched lakes of southern Norway. Verh. Internat. Verein. Limnol. 20: 776–787.

Slater, M.L., Sharrow, S.O. & Gart, J.J. 1977. Cell cycle of *Saccharomyces cerevisiae* in populations growing at different rates. Proc. Natl. Acad. Sci. U.S.A. 74: 3850–3854.

Smayda,T.J. 1975. Phased cell division in natural populations of the marine diatom *Ditylum brightwelli* and the potential significance of the diel phytoplankton behaviour in the sea. Deep–Sea Res. 22: 151–165.

Smolander, U. & Arvola, L. 1988. Seasonal variation in the diel vertical distribution of the migratory alga *Cryptomonas marssonii* (Cryptophyceae) in a small, highly humic lake. Hydrobiologia 161: 89–98.

Sommer, U, 1981. The role of r– and K–selection in the succession of phytoplankton in Lake Constance. Acta Oecologica Oecol. Gener. 2: 327–334.

Sommer, U. 1982. Vertical niche separation between two closely related planktonic flagellate species (*Rhodomonas lens* and *Rhodomonas minuta* v. *nannoplanctica*). J. Plankton Res. 4: 137–142.

Sommer, U. 1983. Nutrient competition between phytoplankton species in multispecies chemostat experiements. Arch. Hydrobiol. 96: 399–416.

Sommer, U. 1984. Sedimentation of principal phytoplankton species in Lake Constance. J. Plankton Res. 6: 1–14.

Sommer, U. 1985. Differential migration of Cryptophyceae in Lake Constance. In: Rankin, M.A. (ed.) Migration: Mechanisms and Adaptative Significance. Contributions in Marine Science. Supplement Vol. 27:166–175.

Sommer, U. 1987. Factors controlling the seasonal variation in phytoplankton species composition – A case study for a deep, nutrient rich lake. In: Round, F.E. & Chapman, D.J. (ed.) Progress in Phycological Research vol. 5. Biopress Ltd. England. p. 123–178.

Sommer, U. , Gliwicz, Z.M., Lampert, W. & Duncan, A. 1986. The PEG*–model of seasonal succession of planktonic events in fresh waters. Arch. Hydrobiol. 106: 433–471.

Starmach, K. 1974. Cryptophycea – Kryptofity, Dinophyceae – Dinofity, Rapidophyceae – Rafidofity. In: Starmach, K. & Sieminska, J. (ed.). Flora Slodkowodna Polski. Polska Akademia Nauk. Instytut Botaniki.

Steele, J.H. 1965. Notes on some theoretical problems in production ecology. In: Goldman, C.R. (ed.) Primary Productivity in Aquatic Environments (Mem. Ist. Ital. Idrobiol., 18 Suppl.). University of California Press, Berkeley, 383–398.

Steemann Nielsen, E. 1960. Productivity of the oceans. Ann. Rev. Plant Physiol. 1: 341–362.

Steemann Nielsen, E. & Hansen, V.K. 1959. Measurements with the carbon–14 technique of the respiration rates in natural populations of phytoplankton. Deep Sea Res. 5: 222–233.

Steup, M. 1975. Die Wirkung von blauem und rotem licht auf die Synthese ribosomaler RNA bei *Chlorella*. Arch. Microbiol. 105: 143–151.

Steup, M. 1977. Blue light–dependent regulation of cytoplasmic ribosomal RNA synthesis in *Chlorella*. Arch. Microbiol. 112: 277–282.

Stewart, L.J. & George, D.G. 1987. Environmental factors influencing the vertical migration of planktonic rotifers in a hypereutrophic tarn. Hydrobiologia 147: 203–208.

Stewart, A.J. & Wetzel, R.G. 1986. Cryptophytes and other microflagellates as couplers in planktonic community dynamics. Arch. Hydrobiol. 106: 1–19.

Strathmann, R. 1967. Estimating the organic carbon content of phytoplankton from cell volume or plasma volume. Limnol. Oceanogr. 12: 411–418.

Strickland, J.D.H. & Parsons, T.R. 1968. A Practical Handbook of Seawater Analysis. Bull. Fish. Res. Bd. Canada 167. 311 pp.

Suttle, C.A., Stockner, J.G., Shortreed, K.S. & Harrison, P.J. 1988. Time–course of size–fractionated phosphate uptake: are larger cells better competitors for pulses of phosphate than smaller cells? Oecologia 74: 571–576.

Swift, E., Stuart, M. & Meunier, V. 1976. The *in situ* growth rates of some deep-living oceanic dinoflagellates: *Pyrocystis fusiformis* and *Pyrocystis noctiluca*. Limnol. Oceanogr. 21: 418–426.

Taguchi, S. 1976. Relationship between photosynthesis and cell size of marine diatoms. J. Phycol. 12: 185–189.

Takahashi, M., Fuji, K. & Parsons, T.R. 1973. Simulation study of phytoplankton photosynthesis and growth in the Fraser River Estuary. Mar. Biol. 19: 102–116.

Talling, J.F. 1971. The underwater light climate as a controlling factor in the production ecology of freshwater phytoplankton. Mitt. Internat. Verein. Limnol. 19: 214–243.

Taylor, W.D., Barko, J.W. & James, W.F. 1988. Contrasting diel patterns of vertical migration in the dinoflagellate *Ceratium hirundinella* in relation to phosphorus supply in a north temperate reservoir. Can. J. Fish. Aquat. Sci. 45: 1093–1098.

Tett, P., Heaney, S.I. & Droop, M.R. 1985. The Redfield ratio and phytoplankton growth rate. J. mar. biol. Ass. U.K. 65: 487–504.

Thinh, L.-V. 1983. Effect of irradiance on the physiology and ultrastructure of the marine cryptomonad, *Cryptomonas* strain Lis (Cryptophyceae). Phycologia 22: 7–11.

Thompson, A.S., Rhodes, J.C. & Pettman, I. (eds.) 1988. Culture Collection of Algae and Protozoa. Catalogue of Strains. 5th edition.

Tilzer, M.M. 1973. Diurnal productivity in the phytoplankton assemblage of a high mountain lake. Limnol. Oceanogr. 18: 15–30.

Tranvik, L.J., Porter, K.G. & Sieburth, J.McN. 1989. Occurence of bacterivory in *Cryptomonas*, a common freshwater phytoplankter. Oecologia 78: 473–476.

Tsuji, T., Ohki, K. & Fujita, Y. 1986. Determination of photosynthetic pigment composition in an individual phytoplankton cell in seas and lakes using fluorescence microscopy; properties of the fluorescence emitted from picophytoplankton cells. Mar. Biol. 93: 343–349.

Uematsu-Kaneda, H. & Furuya, M. 1982a. Effects of calcium and potassium ions on phototaxis in *Cryptomonas*. Plant & Cell Physiol. 23: 1377–1382.

Uematsu-Kaneda, H. & Furuya, M. 1982b. Effects of viscosity on phototactic movement and period of cell rotation in *Cryptomonas* sp. Physiol. Plant. 56: 194–198.

Utermöhl, H. 1958. Zur Vervollkommnung der quantitativen Phytoplankton Methodik. Mitt. Internat. Verein. Limnol. 9: 1–38.

Vance, B.D. 1965. Composition and succession of cyanophycean water blooms. J. Phycol. 1: 81–86.

Vaulot, D. & Chisholm, S.W. 1987. A simple model of the growth of phytoplankton populations in light/dark cycles. J. Plankton Res. 9: 345–366.

Vehr, J.D., Brown, L.M. & Vanderelst, I.E. 1986. Hydrogen ion buffering of culture media for algae from moderately acidic, oligotrophic waters. J. Phycol. 22: 88–94.

Verity, P.G. 1982. Effects of temperature, irradiance, and daylength on the marine diatom *Leptocylindrus danicus* Cleve. IV. Growth. J. Exp. Mar. Biol. Ecol. 60: 209–222.

Vernet, M., Mitchell, B.G. & Holm–Hansen, O. 1990. Adaptation of *Synechococcus in situ* determined by variability in intracellular phycoerythrin–543 at a coastal station off the southern California coast, USA. Mar. Ecol. Prog. Ser. 63: 9–16.

Vesk, M. & Jeffrey, S.W. 1977. Effect of blue–green light on photosynthetic pigments and chloroplast structure in unicellular marine algae from six classes. J. Phycol. 13: 280–288.

Vincent, W.F. 1980. The physiological ecology of a *Scenedesmus* population in the hypolimnion of a hypertrophic pond. I. Photoautotrophy. Br. phycol. J. 15: 27–34.

Wall, D. & Briand, F. 1979. Response of lake phytoplankton communities to in situ manipulations of light intensity and colour. J. Plankton Res. 1: 103–111.

Wallen, D.G. & Geen, G.H. 1971a. Light quality in relation to growth, photosynthetic rates and carbon metabolism in two species of marine plankton algae. Mar. Biol. 10: 34–43.

Wallen, D.G. & Geen, G.H. 1971b. Light quality and concentration of proteins, RNA, DNA and photosynthetic pigments in two species of marine plankton algae. Mar. Biol. 10: 44–51.

Ward, B. & Bowen, M. 1979. Cytokinesis in *Cryptomonas ovata* (Cryptophyceae). Protoplasma 98: 275–277.

Watanabe, Y, 1980. A study of the excretion and extracellular products of natural phytoplankton in Lake Nakanuma, Japan. Int. Revue ges. Hydrobiol. 65: 809–834.

Watanabe, M. & Furuya, M. 1974. Action spectrum of phototaxis in a cryptomonad alga, *Cryptomonas* sp. Plant & Cell Physiol. 15: 413–420.

Watanabe, M. & Furuya, M. 1982. Phototactic behavior of individual cells of *Cryptomonas* sp. in response to continuous and intermittent light stimuli. Photochem. Photobiol. 35: 559–563.

Watanabe, M., Kohata, K. & Kunugi, M. 1988. Phosphate accumulation and metabolism by *Heterosigma akashiwo* (Raphidophyceae) during diel vertical migration in a stratified microcosm. J. Phycol. 24: 22–28.

Watanabe, M., Miyoshi, Y. & Furuya, M. 1976. Phototaxis in *Cryptomonas* sp. under condition suppressing photosynthesis. Plant & Cell Physiol. 17: 683–690.
Wawrik, F. 1980. Über sexuelle Reproduction bei *Dinobryon suecicum* Lemm. var *longispinum* Lemm. und Beobachtungen bei *Mallomonas reginae* Teil., *Cryptomonas cylindracea* Skj. und *Dichtyosphaerium elegans* Bachm. Arch. Protistenk. 123: 439–445.

Weger, H.G., Herzig, R., Falkowski, P.G. & Turpin, D.H. 1989. Respiratory losses in the light in a marine diatom: Measurements by short–term mass spectrometry. Limnol. Oceanogr. 34: 1153–1161.

Wehr, J.D., Brown, L.M. & Vanderelst, I.E. 1986. Hydrogen ion buffering of culture media for algae from moderately acidic, oligotrophic waters. J. Phycol. 22: 88–94.

Weiler, C.S. 1980. Population structure and *in situ* division rates of *Ceratium* in oligotrophic water of the North Pacific central gyre. Limnol. Oceanogr. 25: 610–619.

Weiler, C.S. & Chisholm, S.W. 1976. Phased cell division in natural populations of marine dinoflagellates from shipboard cultures. J. Exp. Mar. Biol. Ecol. 25: 239–247.

Weiler, C.S. & Eppley, R.W. 1979. Temporal pattern of division in the dinoflagellate genus *Ceratium* and its application to the determination of growth rate. J. exp. mar. Biol. Ecol. 39: 1–24.

Wetzel, R.G. & Likens, G.E. 1979. Limnological Analyses. W.B. Saunders.

Winkler, L.W. 1888. Die Bestimmumg des im Wasser gelösten Sauerstoffs. Ber. dtsch. chem. Ges. 21: 2843–2854.

Wright, R.T. 1964. Dynamics of a phytoplankton community in an ice–covered lake. Limnol.Oceanogr. 9: 163–178.

Wyman, M. & Fay, P. 1986a. Underwater light climate and the growth and pigmentation of planktonic blue–green algae (Cyanobacteria) I. The influence of light quantity. Proc. R. Soc. Lond. B 227: 367–380.

Wyman, M. & Fay, P. 1986b. Underwater light climate and the growth and pigmentation of planktonic blue–green algae (Cyanobacteria) II. The influence of light quality. Proc. R. Soc. Lond. B 227: 381–393.

Wyman, M., Gregory, R.P.F. & Carr, N.G. 1985. Novel role for phycoerythrin in the marine cyanobacterium *Synechococcus* strain DC2. Science, Wash. 230: 818–820.

Yentsch, C.M., Magul, F.C., Horan, P.K. & Muirhead, K. 1983. Flow cytometric DNA determinations of individual cells of the dinoflagellate *Gonyaulax tamarensis* var. *excavata*. J. Exp. Mar. Biol. Ecol. 67: 175–183.

Yentsch, C.S. & Phinney, D.A. 1985. Spectral fluorescence: an ataxonomic tool for studying the structure of phytoplankton populations. J. Plankton Res. 7: 617–632.

Yoder, J.A. 1979. Effect of temperature on light–limited growth and chemical composition of *Skeletonema costatum* (Bacillariophyceae). J. Phycol. 15: 362–370.

Zlotnik, I. & Dubinsky, Z. 1989. The effect of light and temperature on DOC excretion by phytoplankton. Limnol. Oceanogr. 34: 831–839.

APPENDIX I. List of symbols used in the thesis

Symbol	Explanation	Unit
I	light intensity, photon flux density (PFD)	μmoles m^{-2}s^{-1}
I_{opt}	optimum I	μmoles m^{-2}s^{-1}
I_c	compensation light intensity	μmoles m^{-2}s^{-1}
I_k	saturation onset parameter	μmoles m^{-2}s^{-1}
ε_{PAR}	vertical light attenuation coefficient	m^{-1}
T	temperature	$^{\circ}$ C
μ, k	growth rate	divisions day^{-1}
μ_{max}	maximum growth rate	divisions day^{-1}
K_e	daily averaged specific growth rate	day^{-1}
K	observed rate of population increase	divisions day^{-1}
λ	loss rate	divisions day^{-1}
PP	rate of production	mgCm^{-3} day^{-1}
t_d	duration of mitosis	min
T_d	generation time	days
αg	growth efficiency	div. day^{-1}(μmoles m^{-2}s^{-1})$^{-1}$
α_p	photosynthetic efficiency	mg O$_2$h^{-1}mg^{-1}chl$a$(μmolesm^{-2}s^{-1})$^{-1}$ mg O$_2$h^{-1}gC(μmolesm^{-2}s^{-1})$^{-1}$
P_{max}	maximum rate of gross photosynthesis	mg O$_2$h^{-1}mg^{-1}chl$a$ mg O$_2$h^{-1}g^{-1}C

APPENDIX II. Cell breadth (μm) and length (μm) of *Cryptomonas* L485 in different temperature/PFD treatments. Values shown are means and standard errors of means (S.E).

T=26 °C/PFD, μmoles m^{-2} s^{-1}	280/265	195/185	120/110	74/56	30/26
breadth ±S.E	9.03±0.09	8.48±0.37	9.85±0.24	8.52±0.25	8.38±0.12
length ±S.E	16.76±0.26	16.04±0.50	17.87±0.25	16.45±0.36	15.98±0.23
T=21 °C/PFD, μmoles m^{-2} s^{-1}					
breadth ±S.E	8.30±0.18	7.55±0.10	8.02±0.13	7.83±0.10	7.69±0.11
length ±S.E	16.78±0.61	15.64±0.22	17.04±0.25	16.75±0.11	15.53±0.17
T=16 °C/PFS, μmoles m^{-2} s^{-1}					
breadth ±S.E	7.51±0.14	8.13±0.27	8.13±0.28	5.64±0.54	5.79±0.12
length ±S.E	17.79±0.32	18.32±0.23	17.87±0.26	13.30±0.79	12.42±0.16
T=12 °C/PFD, μmoles m^{-2} s^{-1}					
breadth ±S.E	8.20±0.25	8.63±0.11	9.63±0.30	9.15±0.11	7.69±0.26
length ±S.E	18.14±0.30	18.55±0.18	19.96±0.48	19.01±0.38	15.88±0.39
T=10 °C/PFD, μmoles m^{-2} s^{-1}					
breadth ±S.E	8.41±0.11	7.70±0.29	7.72±0.07	7.78±0.13	6.96±0.11
length ±S.E	16.16±0.33	16.21±0.26	16.06±0.37	15.56±0.18	15.00±0.15
T=8 °C/PFD, μmoles m^{-2} s^{-1}					
breadth ±S.E	8.78±0.16	8.24±0.21	8.41±0.12	8.12±0.15	8.00±0.17
length ±S.E	17.68±0.12	17.17±0.18	17.28±0.33	16.79±0.18	16.39±0.33
T=5 °C/PFD, μmoles m^{-2} s^{-1}					
breadth ±S.E	–	8.88±0.20	9.21±0.12	8.45±0.08	7.74±0.20
length ±S.E	–	17.16±0.05	17.43±0.14	16.66±0.19	15.62±0.15

APPENDIX III. Cell breadth (μm) and length (μm) of *Cryptomonas* L315 in different temperature/PFD treatments. Values shown are means and standard errors of means (S.E).

T=21 °C/ PFD, μmoles m^{-2} s^{-1}	290/280	197/195	110	74/52	30/24
breadth ± S.E	20.90±0.24	18.22±0.45	19.09±0.23	20.68±0.14	21.62±0.26
length ± S.E	45.94±1.02	41.96±1.35	40.52±1.02	45.58±0.40	47.23±2.88

T=16 °C/PFD, μmoles m^{-2} s^{-1}					
breadth ± S.E	18.50±0.29	18.96±0.27	18.60±0.30	19.41±0.36	19.77±0.43
length ± S.E	45.08±0.57	44.15±0.50	43.48±0.54	45.60±0.32	46.54±0.47

T=12 °C/PFD, μmoles m^{-2} s^{-1}					
beadth ± S.E	18.50±0.43	17.01±0.30	18.05±0.40	–	–
length ± S.E	45.15±1.49	46.37±0.20	44.27±0.26	–	–

T=10 °C/PFD, μmoles m^{-2} s^{-1}					
breadth ± S.E	15.39±0.32	16.00±0.21	15.65±0.23	15.56±0.22	14.45±0.37
length ± S.E	41.55±0.72	42.75±0.86	41.18±0.71	43.04±0.78	38.91±0.66

T=5 °C/PFD, μmoles m^{-2} s^{-1}					
breadth ± S.E	16.17±0.23	16.52±0.16	16.04±0.18	15.60±0.12	15.39±0.27
length ± S.E	43.93±0.92	44.41±0.44	45.38±0.17	43.82±0.47	44.29±0.69

APPENDIX IV. Summary of cell volume data of *Cryptomonas* L485 and L315. Volumes expressed as μm³.

	L485	L315
Mean	616	7622
Max	1020	12450
Min	232	4306